NATIONAL ACADEMY
OF SCIENCES OF UKRAINE
A. PIDHORNYI INSTITUTE
OF MECHANICAL ENGINEERING PROBLEMS
OF THE NAS OF UKRAINE

НАЦІОНАЛЬНА
АКАДЕМІЯ НАУК УКРАЇНИ
ІНСТИТУТ ПРОБЛЕМ МАШИНОБУДУВАННЯ
ім. А.М. ПІДГОРНОГО НАН УКРАЇНИ

І.А. БАРАНОВ, О.В. КРАВЧЕНКО,
І.Г. СУВОРОВА, В.О. ГОМАН,
Д.О. ВЕЛІГОЦЬКИЙ

КОНСТРУКТИВНІ ЗАСОБИ ДЛЯ МАТЕМАТИЧНОГО ТА КОМП'ЮТЕРНОГО МОДЕЛЮВАННЯ ФІЗИКО-МЕХАНІЧНИХ ПОЛІВ У ОБЛАСТЯХ СКЛАДНОЇ ФОРМИ

ПРОЄКТ
«УКРАЇНСЬКА НАУКОВА КНИГА
ІНОЗЕМНОЮ МОВОЮ»

КИЇВ
АКАДЕМПЕРІОДИКА
2023

I.A. BARANOV, O.V. KRAVCHENKO,
I.G. SUVOROVA, V.O. GOMAN,
D.O.VELIGOTSKIY

CONSTRUCTIVE TOOLS FOR MATHEMATICAL AND COMPUTER MODELING OF PHYSICAL AND MECHANICAL FIELDS IN THE AREAS OF COMPLEX SHAPE

PROJECT
«UKRAINIAN SCIENTIFIC BOOK
IN A FOREIGN LANGUAGE»

KYIV
AKADEMPERIODYKA
2023

https://doi.org/10.15407/akademperiodyka.489.156
UDC 519.6+517.95
C74

Authors:

I.A. BARANOV, O.V. KRAVCHENKO,
I.G. SUVOROVA, V.O. GOMAN, D.O. VELIGOTSKIY

Reviewers:

O.M. KHIMICH, Academician of NAS of Ukraine,
Doctor of Physical and Mathematical Sciences, Professor

Y.G. STOYAN, Corresponding member of NAS of Ukraine,
Doctor of Physical and Mathematical Sciences, Professor

Approved for publication by scientific council of A. Pidhornyi Institute of Mechanical Engineering Problems NAS of Ukraine (July, 14, 2022, Protocol No. 4)

The publication was funded within the framework of the Targeted Complex Program of the NAS of Ukraine "Scientific Bases of Functioning and Providing for Conditions for the Development of the Scientific and Publishing Complex of the NAS of Ukraine"

C74 **Constructive** tools for mathematical and computer modeling of physical and mechanical fields in the areas of complex shape: [monograph] / I.A. Baranov, O.V. Kravchenko, I.G. Suvorova, V.O. Goman, D.O. Veligotskiy. — Kyiv: Akademperiodyka, 2023. — 156 p.

ISBN 978-966-360-489-3

The monograph presents the development of structural methods to increase the approximation capacity of basis functions in the vicinity of the corner points of the area to solve boundary value problems and also the development of local structures that take into account boundary conditions at the area border and docking with standard basis within the area. The development of structural methods based on the approaches listed above significantly expands the possibilities of physical and mechanical processes modeling in the areas of complex shapes to create environmental and economic devices in various industries.

UDC 519.6+517.95

ISBN 978-966-360-489-3

CHAPTER 4

PROBLEMS OF APPROXIMATION WITH THE USE OF DEVELOPED STRUCTURES OF BORDER PROBLEMS SOLUTIONS

CHAPTER 5

MATHEMATICAL AND COMPUTER MODELING OF HYDRODYNAMIC FIELDS

PREFACE

The current global trend is the constant increase in requirements for energy efficiency and environmental friendliness of the used technologies.

Nowadays it is impossible to imagine the development of basic processes of these technologies and modern equipment that implements these processes without the use of mathematical and computer modeling.

Applied mathematics and computational methods play a very important role.

Among the methods of applied mathematics, special attention should be paid to the methods of solving boundary value problems for differential equations in partial derivatives, which model fields of different physical natures (deformation, force, hydrodynamic, temperature, and others). Knowledge of the fields allows one to create highly efficient devices in various industries.

The problem of field research is multi-component and therefore very complex. The physical and geometric parameters that are part of the sought solution algorithm must be taken into account when setting the problems of the field calculation. Additional difficulties may arise due to the complexity of the laws of field distribution, which in some cases have large gradient differences and peculiarities at the corner points of the borders and in multiconnected areas. The calculation of fields for such areas has significant difficulties of algorithmic and computational nature.

The development of many technologies and devices that implement them is based on the study of basic technological processes that are characterized by physical and mechanical fields of different natures. Currently, due to the rapid progress of computer technology and software, during the study of various processes in science-intensive areas, preference is given to mathematical modeling and computational experiment. However, for the results of modeling to correspond to the real process, correct mathematical models and effective methods of solving problems that are based on them are needed. There is a need to solve boundary value problems of mathematical physics in the areas of complex shapes when calculating physical and mechanical fields in real technical devices. Adequate mathematical description of the shape of the problem solution domain is very important, especially in the vicinity of corner points. The implementation of this description is carried out in different computational methods with different degrees of efficiency.

Variational methods of mathematical physics are an effective mathematical apparatus for solving boundary value problems for differential equations. These include the least squares method, the Ritz method, the Bubnov—Galerkin method, and others. In these methods, the solution of the boundary value problem for differential equations is reduced to the minimization of a certain function. However, meeting the problem boundary conditions is often a serious challenge and is usually done by choosing coordinate functions.

To solve this problem, Academician of the NAS of Ukraine V.L. Rvachev developed a structural R-function method, which consists in constructing solution structures that transform functions from certain classes into functions that satisfy the boundary conditions of the problem.

This method allows us to take into account the shape of areas at the analytical level and to build complete coordinate sequences that satisfy the boundary conditions. Thus, geometric information about the area shape and boundary conditions are taken into account precisely, which removes certain problems that exist in other methods.

However, functions constructed using standard systems of R-operations are non-smooth at corner points of the area and may have a low approximation capacity in the vicinity of corner points, especially in the case of approximation of smooth functions. In addition, the peculiarity of the R-function method is that the structure of the boundary value problem solution based on this method transforms all the basic elements, which requires certain machine time consumption. Moreover, the more complex the domain of problem solving is, the more complex the functions included in the basic conversion operator are, which significantly increases the calculation time.

As ensuring fast and accurate calculations is an extremely important problem, it is important to:

- develop structural methods to increase the approximation capacity of basic functions in the vicinity of the corner points of the boundary value problems solution domain;
- develop local structures that take into account the boundary conditions at the area border and docking with the standard basis within the area.

The development of structural methods based on the approaches listed above significantly expands the possibilities of physical and mechanical processes modeling in the areas of complex shapes to create energy-efficient and environmentally friendly technological processes and devices that implement them.

CHAPTER 1

IMPLICATION OF STRUCTURAL METHODS FOR MATHEMATICAL AND COMPUTER MODELING OF PHYSICAL AND MECHANICAL FIELDS

1.1. R-function method

The R-function method (RFM) [41, 48] lies in the usage of functions that accurately satisfy the boundary conditions of the problem when constructing structures for solving various boundary value problems of mathematical physics. The boundary value problem in general can be written as follows

$$\begin{cases} Au(x) = f(x), x \in \Omega, \\ L_i u(x)\big|_{\partial\Omega_j} = \varphi_i(x),\ i = 1, \ldots, N,\ j = 1, \ldots, M, \end{cases} \tag{1.1}$$

where A and L_i — some operators operating in the middle of the area Ω and in regions of its border $\partial\Omega_j$ respectively, $f(x)$ and $\varphi_i(x)$ — known functions, $u(x)$ — sought function, which can be a scalar, vector or tensor, $x = (x_1, x_2, ..., x_n)$.

The solution structure that takes into account the boundary conditions of the problem (1.1) is the formula $u = B(\Phi)$, if $L_i B(\Phi)\big|_{\partial\Omega_i} = \varphi_i(x)$, $i = 1, ..., N, j = 1, ..., M$, where Φ — element of some functional set $\mathbf{M}$, B — some operator: B: $\mathbf{M} \to \mathbf{X}(\Omega)$, $\mathbf{X}(\Omega)$ — functions set defined in the area Ω.

Historically, the first boundary value problem structure is the Dirichlet problem, which is called the Kantorovich structure [19, 48].

This structure satisfies this condition,

$$u(x)\big|_{\partial\Omega} = \varphi(x) \tag{1.2}$$

and has the form $u(x) = \omega(x)\,\Phi(x) + \varphi(x)$, where $x = (x_1, \ldots x_n)$, $\omega(x)$: $\omega(x)=0$, $x \in \delta\Omega$, $\omega(x)>0$, $x \in \Omega$, $\Phi(x)$ — indefinite component of the structure, which is selected from the condition of accurate or approximate satisfaction of the equation $Au(x) = f(x)$. The undefined component is usually presented as a series $\Phi(x) = \sum_{i=1}^{\infty} c_i \varphi_i(x)$, where $\{\varphi_i(x)\}$ — a complete

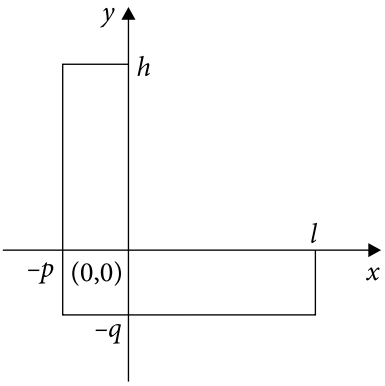

Fig. 1.1. Area in the angular form

system of basic functions, $\{c_i\}$ — uncertain coefficients that have to be determined.

For convex polygons, LV. Kantorovich proposed a method for the construction of $\omega(x, y)$ function as follows: $\omega(x, y) = \pm(a_1x + b_1y + c_1)\cdot\ldots\cdot(a_mx + b_my + c_m)$, where $a_ix + b_iy + c_i = 0$, i= 1, 2, ... m — equation of the polygon sides. The equations of some other areas were constructed similarly. Also, L.V. Kantorovich proposed options of the $\omega(x, y)$ function to describe the non-convex area in the angular form, which is shown in Fig. 1.1. These functions have the form:

$$\omega_1(x, y) = (|x| + |y| - x - y)(x + p)(y + q)(l - x)(h - y),$$

$$\omega_2(x, y) = (x^2 + y^2 - x|x| - y|y|)(x + p)(y + q)(l - x)(h - y).$$

The general ideology of construction of the $\omega(x)$ function for arbitrary areas was proposed by V.L. Rvachev [48] based on Boolean algebra. R-operations are used for these purposes. Denote

$$S_2(t) = \begin{cases} 0, t < 0 \\ 1, t > 0 \end{cases}. \tag{1.3}$$

Definition. The function $f(x_1,...,x_m): E^m \to E$ is called an R-function if such a Boolean function $F(X_1,...,X_m)$ exists that $S_2(f(x_1,...,x_m)) \equiv F(S_2(x_1),...,S_2(x_m))$.

If $E = (-\infty, \infty)$ then R-functions can be called R-operations.

Since the system $H = \{X \wedge Y, X \vee Y, \overline{X}\}$ is the most convenient and widely used complete system of Boolean functions [41, 48], then in the R-function theory the R-operations that correspond to the said Boolean functions are the main ones.

The most used in the literature is the R_0 system of R-operations, which has the form:

$$\begin{cases} x \wedge_0 y = x + y - \sqrt{x^2 + y^2}, \\ x \vee_0 y = x + y + \sqrt{x^2 + y^2}. \\ \overline{x} = -x. \end{cases} \tag{1.4}$$

In the general case, the inhomogeneous Dirichlet condition can be represented as follows:

$$u(x)\Big|_{\partial\Omega_i} = \varphi_i(x). \tag{1.5}$$

For a boundary value problem with inhomogeneous Dirichlet conditions, the solution structure has the form $u(x)=\omega(x)\Phi(x)+\varphi_0(x)$, where $\varphi_0(x)$ — a function that satisfies the inhomogeneous Dirichlet conditions $\varphi_0(x)\big|_{\partial\Omega_i}=\varphi_i(x)$ [41, 48]. Neumann's condition is considered

$$\left.\frac{\partial u(x)}{\partial \nu}\right|_{\partial\Omega}=\varphi(x). \tag{1.6}$$

For a boundary value problem with the Neumann condition, the solution structure has the form $u(x)=\Phi_1(x)+\omega(x)(-D_1\Phi_1(x)-\varphi(x)-\omega(x)\Phi_2(x))$, where $\omega(x)$ — normalized function that satisfies the homogeneous Dirichlet condition, D_1 — operator: $D_1 f=\frac{\partial f}{\partial x}\frac{\partial \omega}{\partial x}+\frac{\partial f}{\partial y}\frac{\partial \omega}{\partial y}$.

When in the boundary value problem derivatives of normal in different regions of the border are given by some functions, the boundary conditions have the form:

$$\left.\frac{\partial u(x)}{\partial \nu}\right|_{\partial\Omega_i}=\varphi_i(x). \tag{1.7}$$

In this case, the solution structure has the form $u(x)=\Phi_1(x)+$ $+\omega(x)\left(-D_1\Phi_1(x)-\varphi_0(x)-\omega(x)\Phi_2(x)\right)$, where $\varphi_0(x)$ satisfies the conditions $\varphi_0(x)\big|_{\partial\Omega_i}=\varphi_i(x)$.

When constructing structures of boundary value problem solutions, there are functions that turn into zero in some border regions of the boundary value problem solution, as well as on the borders of the entire solution domain [22, 24, 41, 47, 48]. Such functions can be built in different ways and also with the implication of R-functions [17, 19, 21, 25, 53, 56, 59]. The R-function method allows us to take into account additional information about the symmetry of the solution domain [39, 52]. Using this method, important practical problems of geometric design [39—41, 55], mechanics [50, 51], electrostatics [41, 48], electrodynamics [48], hydrodynamics [64, 66—69], heat transfer [47], rods torsion [45, 63, 65], plate theory [48], elasticity and plasticity theory [48], etc. are solved.

1.2. Analysis of some constructive means of R-function theory

The R_α system is a more general R-operations system compared to the R_o system [41, 48], and it has the form:

$$\begin{cases} x\wedge_a y=\dfrac{1}{1+a}\left(x+y-\sqrt{x^2+y^2-2\alpha xy}\right), \\ x\vee_a y=\dfrac{1}{1+a}\left(x+y+\sqrt{x^2+y^2-2axy}\right), \\ \overline{x}=-x, \end{cases} \quad \text{where } -1<a(x,y)\le 1. \tag{1.8}$$

When α =1, the R_1 system of R-operations is obtained

$$\begin{cases} x \wedge_1 y = \dfrac{1}{2}\left(x + y - |x - y|\right), \\ x \vee_1 y = \dfrac{1}{2}\left(x + y + |x - y|\right), \\ \overline{x} = -x \end{cases} \tag{1.9}$$

R-conjunctions and R-disjunctions from the system (1.8) at $-1 < a(x, y) < 1$ belong to the class C^∞ in all points of R^2, except for point (0,0), where they are continuous. R-conjunctions and R-disjunctions from the system (1.9) belong to the class C^∞ in all points of R^2, except for the line $y = x$, where these functions are continuous.

There also is the R_0^m system of R-operations [41, 57]

$$\begin{cases} x \underset{0}{\overset{m}{\wedge}} y = \left(x + y - \sqrt{x^2 + y^2}\right)\left(x^2 + y^2\right)^{\frac{m}{2}}, \\ x \underset{0}{\overset{m}{\vee}} y = \left(x + y - \sqrt{x^2 + y^2}\right)\left(x^2 + y^2\right)^{\frac{m}{2}}, \\ \overline{x} = -x. \end{cases} \tag{1.10}$$

R-conjunctions and R-disjunctions from the system (1.10) belong to the class $C^m\left(R^2\right)$.

System

$$\begin{cases} x \wedge_p y = x + y - \sqrt[2p]{x^{2p} + y^{2p}}, \\ x \vee_p y = x + y + \sqrt[2p]{x^{2p} + y^{2p}}, \\ \overline{x} = -x \end{cases} \tag{1.11}$$

is a system of R-operations PS [47, 48], in which R-conjunctions and R-disjunctions at point (0,0) are not differential. These functions have the property of normalization to p order.

System R_C^m [41, 48] has the form:

$$\begin{cases} x \underset{C}{\overset{m}{\wedge}} y = \left(\dfrac{x + y}{2}\right)^m sign(x + y)^{m+1} - \left(\dfrac{x - y}{2}\right)^m sign(x - y)^m, \\ x \underset{C}{\overset{m}{\vee}} y = \left(\dfrac{x + y}{2}\right)^m sign(x + y)^{m+1} + \left(\dfrac{x - y}{2}\right)^m sign(x - y)^m, \\ \overline{x} = -x. \end{cases} \tag{1.12}$$

R-conjunctions and R-disjunctions from this system are polynomial splines of degree m, defect 1. This suggests that these functions belong to the class $C^{m-1}(R^2)$.

There also is the R_p system of R-operations [41]:

$$\begin{cases} x \wedge_\rho y = x + y - \sqrt{x^2 + y^2 + \dfrac{SR}{8\rho^2}(SR + |SR|)}, \\ x \vee_\rho y = x + y + \sqrt{x^2 + y^2 + \dfrac{SR}{8\rho^2}(SR + |SR|)}, \\ \overline{x} = -x. \end{cases} \tag{1.13}$$

where $SR = \rho^2 - x^2 - y^2$.

R-conjunctions and R-disjunctions from this system are not R-operations in the classical sense. These functions are R-operations with rounding. There are also R-operations with rounding, which are called S-functions [58—61] of 1, 2, 3, and 4 classes.

The system of S-functions of the 1st class has the form:

$$\begin{cases} \omega_1 \underset{S}{\wedge} \omega_2 = -b + e^{\omega_1} + e^{\omega_2} - \sqrt[2k]{e^{2k_{\omega_1}} + e^{2k_{\omega_2}}}, \\ \omega_1 \underset{S}{\vee} \omega_2 = b - e^{-\omega_1} - e^{-\omega_2} + \sqrt[2k]{e^{-2k_{\omega_1}} + e^{-2k_{\omega_2}}}, \\ \overline{\omega} = -\omega. \end{cases} \tag{1.14}$$

The system of S-functions of the 2nd class has the form:

$$\begin{cases} \omega_1 \underset{S}{\wedge} \omega_2 = 1 - \sqrt[2k]{e^{2k_{\omega_1}} + e^{2k_{\omega_2}}}, \\ \omega_1 \underset{S}{\vee} \omega_2 = -1 + \sqrt[2k]{e^{-2k_{\omega_1}} + e^{-2k_{\omega_2}}}, \\ \overline{\omega} = -\omega. \end{cases} \tag{1.15}$$

The system of S-functions of the 3rd class has the form:

$$\begin{cases} \omega_1 \underset{S}{\wedge} \omega_2 = -1 + e^{\omega_1} + e^{\omega_2} - 2e^{\omega_2 + \omega_1} + \sqrt[2k]{e^{2k_{\omega_1}} - e^{2k_{\omega_2}}}, \\ \omega_1 \underset{S}{\vee} \omega_2 = 1 - e^{-\omega_1} - e^{-\omega_2} + 2e^{-\omega_2 - \omega_1} - \sqrt[2k]{e^{-2k_{\omega_1}} - e^{-2k_{\omega_2}}}, \\ \overline{\omega} = -\omega. \end{cases} \tag{1.16}$$

The system of S-functions of the 4th class has the form:

$$\begin{cases} \omega_1 \underset{S}{\wedge} \omega_2 = \omega_1 + \omega_2 - \sqrt[2k]{\omega_1^{2k} + \omega_2^{2k} + \beta_1 \cdot \exp\left[-\beta_2 \cdot \left(\omega_1^{2k} + \omega_2^{2k}\right)\right]}, \\ \omega_1 \underset{S}{\vee} \omega_2 = \omega_1 + \omega_2 + \sqrt[2k]{\omega_1^{2k} + \omega_2^{2k} + \beta_1 \cdot \exp\left[-\beta_2 \cdot \left(\omega_1^{2k} + \omega_2^{2k}\right)\right]}, \\ \overline{\omega} = -\omega. \end{cases} \tag{1.17}$$

It is proved that the systems (1.14 — 1.17) are quite complete and the functions of these systems belong to the class $C^{\infty}\left(R^2\right)$.

In the papers of O.M. Litvin [36—38] the system of R-operations of a class $C^{n-1}\left(R^2\right)$ is considered. It has the form

$$\begin{cases} x \wedge_n y = |x|^{n-1} x + |y|^{n-1} y - |x-y|^n, \\ x \vee_n y = |x|^{n-1} x + |y|^{n-1} y + |x-y|^n, \\ \overline{x} = -x. \end{cases} \tag{1.18}$$

These R-operations are piecewise polynomial splines of degree $n, n \geq 1$ defect 1 and are recurrent solutions of the Poisson equation system:

$$\begin{cases} \Delta \wedge (x,y,q+2) = (q+3)(q+2) \wedge (x,y,q), \ (x,y) \in R^2, \quad q = 0,1..., \\ \Delta \vee (x,y,q+2) = (q+3)(q+2) \wedge (x,y,q), \ (x,y) \in R^2, \quad q = 0,1..., \end{cases} \tag{1.19}$$

where

$$\Delta = \frac{\partial^2}{\partial x^2} + \frac{\partial^2}{\partial y^2}\ ,\ \wedge(x,y,q) = x \wedge_{q+1} y\ ,\ \vee(x,y,q) = x \vee_{q+1} y\ .$$

1.3. Normalization of R-operations

An important feature of R-operations is the preservation of normalization [41, 48].

Definition. The equation $\omega(x,y) = 0$ of border Γ and area Ω is normalized up to *m*-th order when the following conditions are met:

$$\omega(x,y)\big|_{\Gamma} = 0, \frac{\partial \omega(x,y)}{\partial n}\bigg|_{\Gamma} = 1, \frac{\partial^k \omega(x,y)}{\partial n^k}\bigg|_{\Gamma} = 0, k = 2,3,...,m,$$

where $\overline{n}$ — normal vector to Γ.

The property of normalization preservation means that if R-operations that preserve normalization are applied to normalized equations of border regions, the resulting equation will be normalized.

For all R-conjunctions $r_{\wedge}(x,y)$, which preserve normalization, the following conditions are met:

$$\begin{cases} \dfrac{\partial r_{\wedge}(x,y)}{\partial x} = 1, \ (x=0) \wedge (y>0), \\ \dfrac{\partial r_{\wedge}(x,y)}{\partial y} = 1, \ (x>0) \wedge (y=0). \end{cases} \tag{1.20}$$

For all R-disjunctions $r_{\vee}(x,y)$, which preserve normalization, the following conditions are met:

$$\begin{cases} \dfrac{\partial r_{\wedge}(x,y)}{\partial x}=1, & (x=0)\wedge(y<0), \\ \dfrac{\partial r_{\wedge}(x,y)}{\partial y}=1, & (x<0)\wedge(y=0). \end{cases} \tag{1.21}$$

The following systems of R-operations have the property of normalization:

$$\begin{cases} x\wedge_0 y = x+y-\sqrt{x^2-y^2}, \\ x\vee_0 y = x+y+\sqrt[2p]{x^2+y^2}, \\ \overline{x}=-x. \end{cases} \quad \begin{cases} x\wedge_1 y = \dfrac{1}{2}\left(x+y-\left|x-y\right|\right), \\ x\vee_1 y = \dfrac{1}{2}\left(x+y+\left|x-y\right|\right), \\ \overline{x}=-x. \end{cases}$$

$$\begin{cases} x\wedge_p y = x+y-\sqrt[2p]{x^{2p}+y^{2p}}, \\ x\vee_p y = x+y+\sqrt[2p]{x^{2p}+y^{2p}}, \\ \overline{x}=-x. \end{cases}$$

Functions from the R-operations system (1.11) have stronger conditions that ensure the normalization preservation up to $2p-1$-th order. These conditions have the form:

$$\begin{cases} \dfrac{\partial\left(x\wedge_p y\right)}{\partial x}=1, & (x=0)\wedge(y>0), \\ \dfrac{\partial^2\left(x\wedge_p y\right)}{\partial x^2}=0, & (x=0)\wedge(y>0), \\ \ldots & \\ \dfrac{\partial^p\left(x\wedge_p y\right)}{\partial x^p}=0, & (x=0)\wedge(y>0), \\ \dfrac{\partial\left(x\wedge_p y\right)}{\partial x^p}=1, & (x>0)\wedge(y=0), \\ \dfrac{\partial^2\left(x\wedge_p y\right)}{\partial y^2}=0, & (x>0)\wedge(y=0), \\ \ldots & \\ \dfrac{\partial^p\left(x\wedge_p y\right)}{\partial y^p}=0, & (x>0)\wedge(y=0), \end{cases} \quad \begin{cases} \dfrac{\partial\left(x\vee_p y\right)}{\partial x}=1, & (x=0)\wedge(y<0), \\ \dfrac{\partial^2\left(x\vee_p y\right)}{\partial x^2}=0, & (x=0)\wedge(y<0), \\ \ldots & \\ \dfrac{\partial^p\left(x\vee_p y\right)}{\partial x^{p-1}}=0, & (x=0)\wedge(y<0), \\ \dfrac{\partial\left(x\vee_p y\right)}{\partial y}=1, & (x<0)\wedge(y=0), \\ \dfrac{\partial^2\left(x\vee_p y\right)}{\partial y^2}=0, & (x<0)\wedge(y=0), \\ \ldots & \\ \dfrac{\partial^p\left(x\vee_p y\right)}{\partial y^p}=0, & (x<0)\wedge(y=0). \end{cases}$$

All smooth systems of R-operations (1.10, 1.12, 1.18) do not have the property of normalization preservation. Functions that are constructed involving non-smooth R-operations may have peculiarities in the corner points of the area and have a low approximation capacity when approximating smooth functions [56].

The question is, are there smooth R-conjunctions and R-disjunctions that preserve normalization? In addition, it is important to study the behavior of smooth R-conjunctions and R-disjunctions in the vicinity of the point (0,0) and the behavior of smooth functions that acquire constant values on non-smooth curves. Based on these studies, it will be possible to answer the question of the completeness of some structures when using smooth R-operations.

R-operations with R_p rounding are considered in more detail:

$$\begin{cases} x \wedge_\rho y = x + y - \sqrt{x^2 + y^2 + \dfrac{SR}{8\rho^2}\left(SR + \left|SR\right|\right)}; \\ x \vee_\rho y = x + y + \sqrt{x^2 + y^2 + \dfrac{SR}{8\rho^2}\left(SR + \left|SR\right|\right)}; \\ \overline{x} = -x. \end{cases} \tag{1.22}$$

These functions coincide with the system of R-operations R_0 for all $(x, y): x^2 + y^2 \geq \rho^2$.

In fact, $\dfrac{SR}{8\rho^2}\left(SR + \left|SR\right|\right) = \dfrac{\left(\rho^2 - x^2 - y^2\right)}{8\rho^2}\left(\rho^2 - x^2 - y^2 + \left|\rho^2 - x^2 - y^2\right|\right)$. When $\rho^2 - x^2 - y^2 \leq 0$, then $\dfrac{SR}{8\rho^2}\left(SR + \left|SR\right|\right) = 0$. Of course, this system is normalized outside the vicinity of point (0,0). Lines x and y connect in the vicinity of the point $(0,0)$ by at arc of the circle, which equation is normalized. For arbitrary functions, the connection will not be made along the circular arc.

The differential properties of the given system (1.22) are considered in the example of a function $x \wedge_\rho y = x + y - \sqrt{x^2 + y^2 + \dfrac{SR}{8\rho^2}\left(SR + \left|SR\right|\right)}$.

Expression is written as $SR = \rho^2 - x^2 - y^2$, then

$$x \wedge_\rho y = x + y - \sqrt{x^2 + y^2 + \frac{\left(\rho^2 - x^2 - y^2\right)}{8\rho^2}\left(\rho^2 - x^2 - y^2 + \left|\rho^2 - x^2 - y^2\right|\right)}.$$

The following labeling is introduced $f_\rho(x, y) = x \wedge_\rho y$. The following function is considered

$$\frac{\partial\left(f_\rho(x,y)\right)}{\partial x}=1-\frac{2x+\frac{1}{8\rho^2}\left(-4\left(\rho^2-x^2-y^2\right)x\left(1+sign(\rho^2-x^2-y^2)\right)\right)}{2\sqrt{x^2+y^2+\frac{(\rho^2-x^2-y^2)}{8\rho^2}\left(\rho^2-x^2-y^2+\left|\rho^2-x^2-y^2\right|\right)}}=$$

$$=1-\frac{x-\frac{x}{4\rho^2}\left(\left(\rho^2-x^2-y^2\right)+\left|\rho^2-x^2-y^2\right|\right)}{\sqrt{x^2+y^2+\frac{(\rho^2-x^2-y^2)}{8\rho^2}\left(\rho^2-x^2-y^2+\left|\rho^2-x^2-y^2\right|\right)}}.$$

This function is continuous. Similarly, the function

$$\frac{\partial\left(f_\rho(x,y)\right)}{\partial y}=1-\frac{2y+\frac{1}{8\rho^2}\left(-4\left(\rho^2-x^2-y^2\right)y\left(1+sign(\rho^2-x^2-y^2)\right)\right)}{2\sqrt{x^2+y^2+\frac{(\rho^2-x^2-y^2)}{8\rho^2}\left(\rho^2-x^2-y^2+\left|\rho^2-x^2-y^2\right|\right)}}=$$

$$=1-\frac{y-\frac{y}{4\rho^2}\left(\left(\rho^2-x^2-y^2\right)+\left|\rho^2-x^2-y^2\right|\right)}{\sqrt{x^2+y^2+\frac{\left(\rho^2-x^2-y^2\right)}{8\rho^2}\left(\rho^2-x^2-y^2+\left|\rho^2-x^2-y^2\right|\right)}}$$

is continuous as well.

The second derivative of the function $f_\rho(x,y)$ with respect to x has the form:

$$\frac{\partial^2\left(f_\rho(x,y)\right)}{\partial x^2}=-\frac{1-\frac{1}{4\rho^2}\left(\left(\rho^2-x^2-y^2\right)+\left|\rho^2-x^2-y^2\right|\right)-\frac{x^2}{2\rho^2}\left(1+sign(\rho^2-x^2-y^2)\right)}{\sqrt{x^2+y^2+\frac{(\rho^2-x^2-y^2)}{8\rho^2}\left(\rho^2-x^2-y^2+\left|\rho^2-x^2-y^2\right|\right)}}+$$

$$+\frac{\left(x-\frac{x}{4\rho^2}\left(\left(\rho^2-x^2-y^2\right)+\left|\rho^2-x^2-y^2\right|\right)\right)^2}{\left(x^2+y^2+\frac{(\rho^2-x^2-y^2)}{8\rho^2}\left(\rho^2-x^2-y^2+\left|\rho^2-x^2-y^2\right|\right)\right)^{\frac{3}{2}}}.$$

This function is discontinuous at points $x^2+y^2=\rho^2$. Similarly, the function

$$\frac{\partial^2\left(f_\rho(x,y)\right)}{\partial y^2}=-\frac{1-\frac{1}{4\rho^2}\left(\left(\rho^2-x^2-y^2\right)+\left|\rho^2-x^2-y^2\right|\right)-\frac{y^2}{2\rho^2}\left(1+sign(\rho^2-x^2-y^2)\right)}{\sqrt{x^2+y^2+\frac{(\rho^2-x^2-y^2)}{8\rho^2}\left(\rho^2-x^2-y^2+\left|\rho^2-x^2-y^2\right|\right)}}+$$

$$+\frac{\left(y-\frac{y}{4\rho^2}\left(\left(\rho^2-x^2-y^2\right)+\left|\rho^2-x^2-y^2\right|\right)\right)^2}{\left(x^2+y^2+\frac{(\rho^2-x^2-y^2)}{8\rho^2}\left(\rho^2-x^2-y^2+\left|\rho^2-x^2-y^2\right|\right)\right)^{\frac{3}{2}}}$$

is also discontinuous at points $x^2+y^2=\rho^2$. Thus, system (1.22) is a system of R-operations with class rounding $C^1\left(R^2\right)$.

Based on the above, it is very important to build R-operations with rounding of different smoothness classes, which are not R-operations only in the vicinity of the point $(0,0)$.

The problem with inhomogeneous Dirichlet boundary conditions is considered. Suppose that in some area Ω it is necessary to find a solution to the boundary value problem

$$\begin{cases} Au(x,y)=f(x,y), & (x,y)\in\Omega, \\ u(x,y)\big|_{\partial\Omega}=u_0(x,y). \end{cases}$$

This problem for a linear operator A can be reduced to a boundary value problem with a homogeneous Dirichlet condition by replacing $u(x,y)=u_1(x,y)+u_0(x,y)$ [19, 41, 48]

$$\begin{cases} Au_1(x,y)=f(x,u)-Au_0(x,y), & (x,y)\in\Omega, \\ u_1(x,y)\big|_{\partial\Omega}=0. \end{cases}$$

Thus, the initial boundary value problem will be reduced to the construction of the function $u_0(x,y)$, which takes the specified values at the area border.

Suppose that $\partial\Omega=\gamma_1\cup\gamma_2\cup\ldots\cup\gamma_n$, where γ_i — regions of the area border, which are described by the equation $\omega_i(x,y)=0$. The area $\Omega\subset R^2$ with $n=3$ is shown in Fig. 1.2.

It is necessary to construct a function that takes some values $f_i(x,y)$ on the border fractions — curves γ_i. The function that satisfies these properties will be built using gluing formulas [41, 48]

$$u_0(x,y)=\frac{\sum_{i=1}^{n}\frac{f_i(x,y)}{\omega_i^k(x,y)}}{\sum_{i=1}^{n}\frac{1}{\omega_i^k(x,y)}}. \qquad (1.23)$$

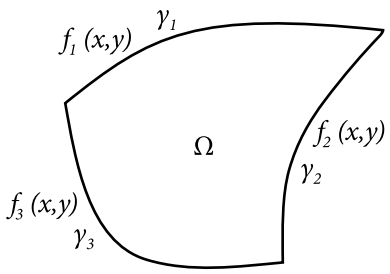

Fig. 1.2. Area Ω, within which the functions $f_i(x,y)$ are set

It should be noted that when using function $u_0(x,y)$ as a component of the solution structure, it must belong to some class of

smoothness. In the general case, the functions of the form (1.23) are not differentiated at the corner points of the area.

Thus, there is a need to build smooth functions that take given values at given borders. Such functions can be applied to different solution structures [41, 48].

The problem of constructing a function that takes the given conditions in the border regions belongs to the problems of interlination [36, 41]. Interlination is an approximation of the functions of two variables using information about their traces and traces of their derivatives on a fixed system of lines. The generalization of this theory to a higher dimension is called interfletation. These theories were developed in the papers of Professor O.M. Litvin [36—38]. The theory of interlination is used for many engineering problems, for example, modeling in computed tomography, cartography of the ocean floor according to sonar, construction of the surface of a space body according to radar on a system of lines, design of the bodies of cars, aircrafts, experiment planning, etc.

1.4. Computational scheme of R-function method

To solve the problems of mathematical physics by the R-function method, a general solution structure that satisfies all or some boundary conditions is constructed [37, 43]. Then, one of the methods of solution is used. Different variational methods can be used here: the least squares method, the Ritz method, the Bubnov — Galerkin method, etc. The finite difference method, the finite element method, and other methods can be used as well [15, 26, 27, 37, 48, 73]. The construction of the solution structure is considered as the simplest example of a homogeneous boundary value problem with the Dirichlet condition. The structure of the solution for this problem is written in the form $u(x) = \omega(x)\Phi(x)$, where $\omega(x) : \omega(x) = 0, x \in \partial\Omega :,\ \omega(x) > 0, x \in \Omega;\ \Phi(x)$ — indefinite component of the structure that has the form, $\Phi(x) = \sum_{i=1}^{k} c_i \varphi_i(x)$, $\{c_i\}$ — unknown coefficients, $\{\varphi_i(x)\}$ — a complete system of basic functions, such as algebraic polynomials [3, 48], trigonometric polynomials [3, 14], splines [1, 28, 48, 73], Chebyshev polynomials [3, 14], atomic functions [49, 61] or others.

Algebraic polynomials of degrees not higher than n in the two-dimensional case are taken as an example. Then $\Phi(x, y) = \sum_{i=0}^{n} \sum_{j=0}^{i} a_{i,j} x^{i-j} y^j$.

After applying the solution structure operator to the standard basis $\{x^{i-j} y^j\}$, $i = 0,...,n, j = 0,...,i$, a new basis for the homogeneous Dirichlet problem is obtained: $\{\omega(x, y) x^{i-j} y^j\}$, $i = 0,...,n,\ j = 0,...,i$.

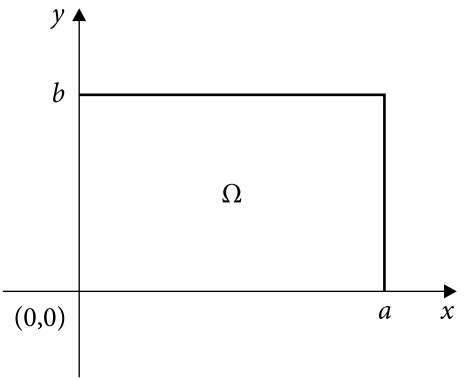

Fig. 1.3. Area $\Omega = (0,a)\times(0,b)$

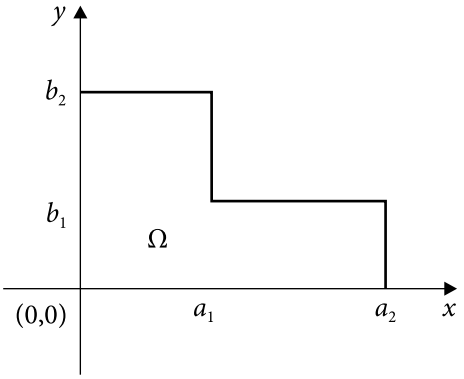

Fig. 1.4. Corner area

The function $\omega(x,y)$ is considered for some areas and built using the R-operations system R_0.

For the first example, a rectangular area (Fig. 1.3) with sides a and b is considered.

The function $\omega(x,y)$ of this area is $\omega(x,y) = x(a-x) + y(b-y) - \sqrt{x^2(a-x)^2 + y^2(b-y)^2}$. The basis of a homogeneous boundary value problem for a given area has the form:

$$\left\{\left(x(a-x)+y(b-y)-\sqrt{x^2(a-x)^2+y^2(b-y)^2}\right)x^{i-j}y^j\right\},\ i=0,...,n,\ j=0,...,i.$$

The area in the form of a corner is considered in the second example (Fig. 1.4).

Function $\omega(x,y)$ for this area:

$$\omega(x,y) = \left(x(a_1-x)+y(b_2-y)-\sqrt{x^2(a_1-x)^2+y^2(b_2-y)^2}\right)+$$
$$+\left(x(a_2-x)+y(b_1-y)-\sqrt{x^2(a_1-x)^2+y^2(b_1-y)^2}\right)^2+$$
$$+\sqrt{\left(x(a_1-x)+y(b_2-y)-\sqrt{x^2(a_1-x)^2+y^2(b_2-y)^2}\right)^2+ \cdots \rightarrow}$$
$$\leftarrow \cdots \overline{+\left(x(a_2-x)+y(b_1-y)-\sqrt{x^2(a_2-x)^2+y^2(b_1-y)^2}\right)^2}.$$

The basis of the homogeneous Dirichlet boundary value problem for this area has the form:

$$\left\{\left(\left(x(a_1-x)+y(b_2-y)-\sqrt{x^2(a_1-x)^2+y^2(b_2-y)^2}\right)+\right.\right.$$
$$\left.\left.+\left(x(a_2-x)+y(b_1-y)-\sqrt{x^2(a_2-x)^2+y^2(b_1-y)^2}\right)+\right.\right.$$

$$+\sqrt{\left(x(a_1-x)+y(b_2-y)-\sqrt{x^2(a_1-x)^2+y^2(b_2-y)^2}\right)^2+}\ \ldots\rightarrow$$

$$\leftarrow\ldots\ \overline{+\left(x(a_2-x)+y(b_1-y)-\sqrt{x^2(a_2-x)^2+y^2(b_1-y)^2}\right)^2}\Bigg)x^{i-j}y^j\Bigg\},$$

$$i=0,\ldots,n,\ j=0,\ldots,i.$$

R-operations were used in the second example, and 1 was used in the first one. When using each subsequent R-operation, the function $\omega(x,y)$ increases several times. Thus, the function $\omega(x,y)$ increases by an exponential law and has a very complex view even for fairly simple areas. When applying variational methods, it is necessary to calculate the integrals of functions that depend on the basic elements of the system. The complexity of the function $\omega(x,y)$ in such calculations leads to a significant increase in calculation time. Thus, an important problem is the development of local structures that take into account the boundary conditions at the borders of the area and the connection with the basic elements that have the simplest structure within the area.

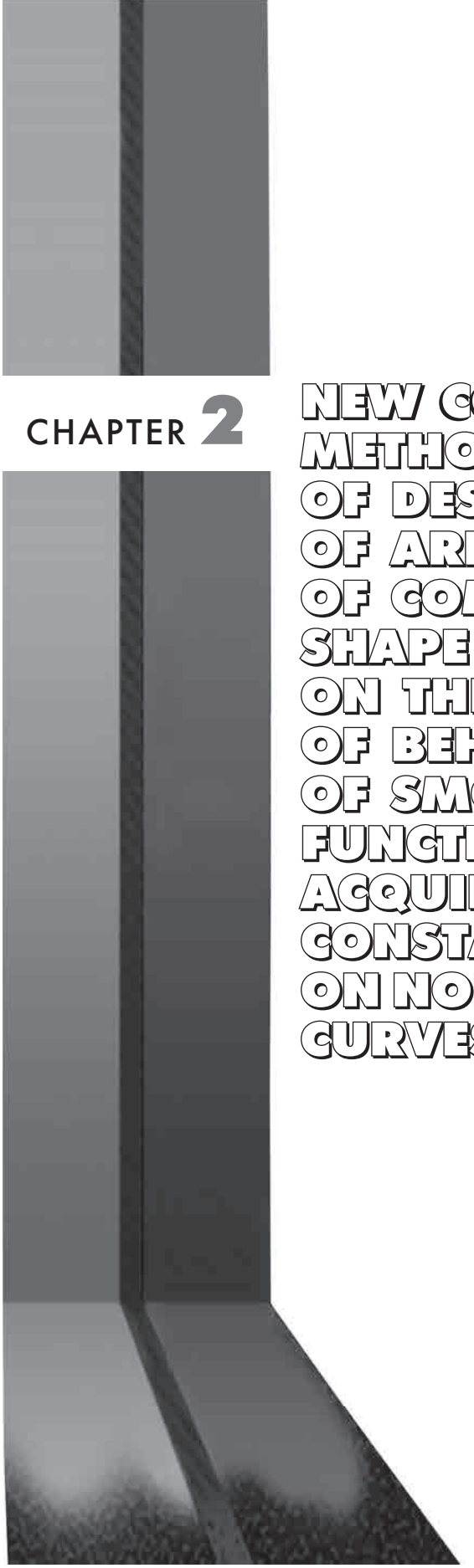

CHAPTER 2

NEW CONSTRUCTIVE METHODS OF DESCRIPTION OF AREAS OF COMPLEX SHAPE BASED ON THE STUDY OF BEHAVIOR OF SMOOTH FUNCTIONS ACQUIRING CONSTANT VALUES ON NON-SMOOTH CURVES

2.1. Corners rounding when describing areas with a non-smooth border

The following system of R-operations is most often used when solving problems of calculation of physical and mechanical fields by the R-function method [41, 48]

$$\begin{cases} x \wedge_0 y = x + y - \sqrt{x^2 + y^2}, \\ x \vee_0 y = x + y + \sqrt{x^2 + y^2}, \\ \overline{x} = -x. \end{cases} \qquad (2.1)$$

Functions $x \wedge_0 y$, $x \vee_0 y$ belong to the class C^∞ at all points R^2 where they are continuous, except for point (0,0).

The differential properties of a system (2.1) are considered. The system is determined by the differential properties of the function $f_1(x,y) = \sqrt{x^2 + y^2}$. Function $f_1(x,y)$ describes half of the cone and is undifferentiated at point (0,0). Function $f_2(x,y) = \sqrt{x^2 + y^2 + \alpha}$, where α is some positive constant, is introduced. This function describes the hyperboloid of rotation and is a function of class $\tilde{N}^\infty\left(R^2\right)$, moreover $f_2(x,y) \underset{\alpha \to 0}{\to} f_1(x,y)$.

The functions $f^{\pm}(x,y,\alpha) = x + y \pm \sqrt{x^2 + y^2 + \alpha}$ are considered. These functions belong to the class $C^\infty\left(R^2\right)$, moreover

$$\begin{cases} f^{-}(x,y,\alpha) \underset{\alpha \to 0}{\longrightarrow} x \wedge_0 y, \\ f^{+}(x,y,\alpha) \underset{\alpha \to 0}{\longrightarrow} x \vee_0 y. \end{cases}$$

Suppose that α is some positive function. For the functions $f^{\pm}(x,y,\alpha(x,y)) = x + y \pm \sqrt{x^2 + y^2 + \alpha(x,y)}$ to

coincide with the functions $x \vee_0 y$ and $x \wedge_0 y$ everywhere, in particular in the vicinity of point (0,0), it is necessary for the function $\alpha(x, y)$ to be equal to zero everywhere except the vicinity of point (0,0), i.e. to be finite. In addition, the function $\alpha(x, y)$ must belong to some class of smoothness.

Then the system of R-operations with rounding R_0^α will have the form:

$$\begin{cases} x \overset{\alpha}{\wedge_0} y = x + y - \sqrt{x^2 + y^2 + \alpha(x, y)}, \\ x \overset{\alpha}{\vee_0} y = x + y + \sqrt{x^2 + y^2 + \alpha(x, y)}, \\ \overline{x} = -x. \end{cases} \tag{2.2}$$

The function $\alpha(x, y)$ can be diverse, for example

$$\alpha_k(x, y) = \begin{cases} b\left(1 - \left(\frac{x}{a}\right)^2 - \left(\frac{y}{a}\right)^2\right)^{k+1}, & x^2 + y^2 < a^2, \\ 0, & x^2 + y^2 \geq a^2, \end{cases} \tag{2.3}$$

$$\alpha_\infty(x, y) = \begin{cases} be^{\frac{x^2+y^2}{x^2+y^2-a^2}}, & x^2 + y^2 < a^2, \\ 0, & x^2 + y^2 \geq a^2, \end{cases} \tag{2.4}$$

where α and b — rounding parameters: α — half the diameter of the carrier, b — maximum value of functions $\alpha_k(x, y)$ and $\alpha_\infty(x, y)$.

The choice of rounding parameter is considered on the example of a rounded R-conjunction. Fig. 2.1 shows a graph of the zero line of the R-conjunction level with rounding. In Fig. 2.1. quantities d_1 and d_2 are set as rounding parameters. The values of the parameters α and b for functions (2.3) and (2.4) at given values d_1 and d_2 are determined. Obviously $a = d_1$. The value of the parameter b is found.

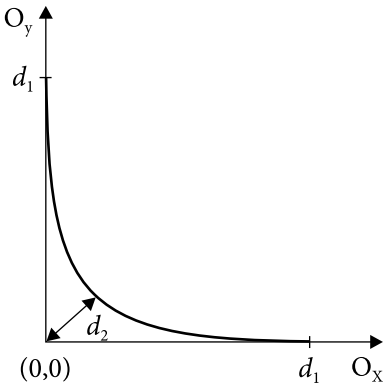

Fig. 2.1. Graph of the zero line of the R-conjunction level with rounding

The coordinates of the intersection of the zero line of the R-conjunction level with rounding and line $y = x$ are determined as

$$2x - \sqrt{2x^2 + \alpha(x, x)} = 0,$$

$$2x^2 = \alpha(x, x). \tag{2.5}$$

A point (x^*, x^*) will be the coordinate of the intersection zero line of the R-conjunction level with rounding and line $y = x$ at x^*, which satisfies the equation (2.5).

On the other hand, $x^* = \frac{d_2}{\sqrt{2}}$. Substituting this value in equation (2.5), we obtain

$$d_2^2 = \alpha\left(\frac{d_2}{\sqrt{2}}, \frac{d_2}{\sqrt{2}}\right).$$

This equation is considered for the function $\alpha_k(x, y)$

$$d_2{}^2 = b\left(1 - \left(\frac{d_2}{d_1\sqrt{2}}\right)^2 - \left(\frac{d_2}{d_1\sqrt{2}}\right)^2\right)^{k+1}, \quad d_2 < d_1.$$

Then, $b = d_2{}^2\left(\frac{d_1{}^2}{d_1{}^2 - d_2{}^2}\right)^{k+1}$, $d_2 < d_1$. The equation $d_2^2 = \alpha\left(\frac{d_2}{\sqrt{2}}, \frac{d_2}{\sqrt{2}}\right)$ is considered for the function $\alpha_\infty(x, y)$ $d_2^2 = be^{\frac{d_2{}^2}{d_2{}^2 - d_1{}^2}}$, $d_2 < d_1$. Then, $b = d_2^2\, e^{\frac{d_2{}^2}{d_1{}^2 - d_2{}^2}}$, $d_2 < d_1$.

Assertion 2.1.

It is needed to prove that function $\alpha_k(x, y) \in C^k\left(R^2\right)$.

Proof.

Function $\alpha_k(x, y) = \begin{cases} b\left(1 - \left(\frac{x}{a}\right)^2 - \left(\frac{y}{a}\right)^2\right)^{k+1}, & x^2 + y^2 < a^2 \\ 0, \quad x^2 + y^2 \geq a^2 \end{cases}$ belongs to the class C^∞ at all points of R^2, except points $\{(x, y)\}: x^2 + y^2 = a^2$. Since $\alpha_k(x, y) = 0, x^2 + y^2 \geq a^2$, then all partial derivatives of any order of the function $\alpha_k(x, y)$ at approximation $x^2 + y^2 \to a^2 + 0$ are equal to zero. Therefore, for functions, $\alpha_k(x, y) \in C^k\left(R^2\right)$ it is sufficient to prove that all partial derivatives of the *k*-th order of the function $\alpha_k(x, y)$ at approximation $x^2 + y^2 \to a^2 - 0$ are equal to zero.

The proof is performed by the mathematical induction method. This statement is proved when *k*=1. We have

$$\alpha_1(x, y) = b\left(1 - \left(\frac{x}{a}\right)^2 - \left(\frac{y}{a}\right)^2\right)^2, \quad x^2 + y^2 < a^2,$$

$$\lim_{x^2 + y^2 \to a^2 - 0} \frac{\partial \alpha_1(x, y)}{\partial x} = 2b\left(1 - \left(\frac{x}{a}\right)^2 - \left(\frac{y}{a}\right)^2\right)\left(\frac{-2x}{a}\right) = 0,$$

$$\lim_{x^2 + y^2 \to a^2 - 0} \frac{\partial \alpha_1(x, y)}{\partial y} = 2b\left(1 - \left(\frac{x}{a}\right)^2 - \left(\frac{y}{a}\right)^2\right)\left(\frac{-2y}{a}\right) = 0.$$

It is assumed that this statement is realized for k-1, i.e. $\frac{\partial^i \alpha_{k-1}(x,y)}{\partial x^j \partial y^{i-j}} = 0$, $i \le k-1$, $j \le i$. We have

$$\alpha_k(x,y) = \alpha_{k-1}(x,y)\left(1 - \left(\frac{x}{a}\right)^2 - \left(\frac{y}{a}\right)^2\right), \quad x^2 + y^2 < a^2,$$

$$\frac{\partial^i \alpha_k(x,y)}{\partial x^j \partial y^{i-j}} = \frac{1}{a^2}\left(\frac{\partial^i \alpha_{k-1}(x,y)}{\partial x^j \partial y^{i-j}}\left(a^2 - x^2 - y^2\right) - 2(i-j)y\frac{\partial^{i-1}\alpha_{k-1}(x,y)}{\partial x^j \partial y^{i-j-1}} - \right.$$

$$\left. - (i-j)(i-j-1)\frac{\partial^{i-2}\alpha_{k-1}(x,y)}{\partial x^j \partial y^{i-j-2}} - 2jx\frac{\partial^{i-1}\alpha_{k-1}(x,y)}{\partial x^{j-1}\partial y^{i-j}} - j(j-1)\frac{\partial^{i-2}\alpha_{k-1}(x,y)}{\partial x^{j-2}\partial y^{i-j}}\right),$$

$$x^2 + y^2 < a^2, \quad \lim_{x^2+y^2 \to a^2 - 0} \frac{\partial^i \alpha_k(x,y)}{\partial x^j y^{i-j}} = 0, \quad i < k.$$

This expression is considered for $i = k$ and proved to be equal to 0.

$$\lim_{x^2+y^2 \to a^2 - 0} \frac{\partial^k \alpha_k(x,y)}{\partial x^j y^{k-j}} = \frac{1}{a^2}\left(\frac{\partial^k \alpha_{k-1}(x,y)}{\partial x^j \partial y^{k-j}}\left(a^2 - x^2 - y^2\right)\right).$$

A function $\alpha_{k-1}(x,y)$ is a polynomial of $2k$ degree, so $\frac{\partial^k \alpha_{k-1}(x,y)}{\partial x^j \partial y^{k-j}}$ is a polynomial of k degree, i.e. $\frac{\partial^k \alpha_{k-1}(x,y)}{\partial x^j \partial y^{k-j}}$ is limited at the endpoints R^2. Since $\left(a^2 - x^2 - y^2\right) \underset{x^2+y^2 \to a^2 - 0}{\to} 0$, then $\lim_{x^2+y^2 \to a^2 - 0} \frac{\partial^k \alpha_k(x,y)}{\partial x^j y^{k-j}} = 0$. *The assertion is proved.*

Assertion 2.2.

It is needed to prove that function $\alpha_\infty(x,y) \in C^\infty\left(R^2\right)$.

Proof.

Function $\alpha_\infty(x,y) = \begin{cases} be^{\frac{x^2+y^2}{x^2+y^2-a^2}}, & x^2 + y^2 < a^2, \\ 0, & x^2 + y^2 \ge a^2 \end{cases}$ belongs to the class C^∞ at all points of R^2 except for, perhaps, points $\{(x,y)\}: \; x^2 + y^2 = a^2$. Therefore, it is necessary to check that $\alpha_\infty(x,y) \in C^\infty\left(\{(x,y)\}: x^2 + y^2 = a^2\right)$. Since $\alpha_\infty(x,y) = 0, \quad x^2 + y^2 \ge a^2$, then all partial derivatives of any order of the function $\alpha_\infty(x,y)$ at $x^2 + y^2 \to a^2 + 0$ are equal to zero. Therefore, for the functions to be $\alpha_\infty(x,y) \in C^\infty\left(R^2\right)$, it is sufficient to prove that all partial derivatives of any order of the function $\alpha_\infty(x,y)$ at points $\{(x,y)\}: \; x^2 + y^2 = a^2$ are equal to zero at approximation $x^2 + y^2 \to a^2 - 0$. Consider

$$\alpha_\infty(x,y) = be^{\frac{x^2+y^2}{x^2+y^2-a^2}},\ x^2+y^2<a^2,\ \frac{\partial^i \alpha_\infty(x,y)}{\partial x^j \partial y^{i-j}} = be^{\frac{x^2+y^2}{x^2+y^2-a^2}} Q(x,y),\quad x^2+y^2<a^2,$$

where $Q(x,y)$ is some fractional rational function.

Since the function $e^{\frac{x^2+y^2}{x^2+y^2-a^2}} \underset{x^2+y^2-a^2\to 0}{\to} 0$ is faster than any degree of a polynomial, then $\lim\limits_{x^2+y^2\to a^2-0} \frac{\partial^i \alpha_\infty(x,y)}{\partial x^j y^{i-j}} = 0$.

The assertion is proved.

2.2. R-operation systems for different smoothness classes

An important property of R-operations is the normalization preservation used in the construction of many structures for solving boundary value problems [41, 47, 48]. This property means that if R-operations that preserve normalization are applied to the normalized equations of the border regions, the resulting equation will also be normalized. However, not all known R-operations that preserve normalization are smooth at point (0,0).

A theorem that shows that the non-smoothness property is common to all R-operations that preserve normalization is proved.

Theorem 2.1.

There are no R-conjunctions and R-disjunctions of smoothness class higher than $C\left(R^2\right)$, which preserve the normalization of functions.

Proof.

The proof is considered on the example of R-conjunction (the proof for R-disjunction is similar).

Suppose that there is some R-conjunction $r_\wedge(x,y)$ that preserves the normalization of functions. Assume that $r_\wedge(x,y)$ belongs to the class $C\left(R^2\right)$.

These functions have the following properties:

$$\begin{cases} r_\wedge(x,y)>0, & (x>0)\wedge(y>0), \\ r_\wedge(x,y)<0, & (x<0)\vee(y<0), \\ r_\wedge(x,y)=0, & ((y=0)\wedge(x\geq 0))\vee((x=0)\wedge(y\geq 0)), \\ r_\wedge(x,y)<0, & ((y=0)\wedge(x<0))\vee((x=0)\wedge(y<0)), \end{cases}$$

$$\begin{cases} \frac{\partial r_\wedge(x,y)}{\partial x}=1, & (x=0)\wedge(y>0), \\ \frac{\partial r_\wedge(x,y)}{\partial y}=1, & (x>0)\wedge(y=0). \end{cases}$$

Consider $\left.\frac{\partial r_{\wedge}(x,y)}{\partial x}\right|_{(0,0)} = \lim_{\varepsilon\to+0}\frac{r_{\wedge}(\varepsilon,0)-r_{\wedge}(0,0)}{\varepsilon} = \lim_{\varepsilon\to+0}\frac{0-0}{\varepsilon} = 0$. On the other hand, $\left.\frac{\partial r_{\wedge}(x,y)}{\partial x}\right|_{(0,0)} = \lim_{\substack{y\to+0\\x\to+0}}\frac{\partial r_{\wedge}(x,y)}{\partial x} = 1$. It follows that the function $\frac{\partial r_{\wedge}(x,y)}{\partial x}$ is discontinuous. Similarly, $\left.\frac{\partial r_{\wedge}(x,y)}{\partial y}\right|_{(0,0)} = \lim_{\varepsilon\to+0}\frac{r_{\wedge}(0,\varepsilon)-r_{\wedge}(0,0)}{\varepsilon} = \lim_{\varepsilon\to+0}\frac{0-0}{\varepsilon} = 0$, $\left.\frac{\partial r_{\wedge}(x,y)}{\partial y}\right|_{(0,0)} = \lim_{\substack{y\to+0\\x\to+0}}\frac{\partial r_{\wedge}(x,y)}{\partial y} = 1$. Thus, the function $\frac{\partial r_{\wedge}(x,y)}{\partial y}$ is discontinuous. This is a contradiction to the theorem assumption, therefore, *the theorem is proved*.

Normalization of functions $\omega_i(x,y)$ that are part of the structures of boundary value problems is not used for all structures.

For example, in Kantorovich's structure [19, 41, 48] for a homogeneous Dirichlet problem $u(x,y)=\omega(x,y)P(x,y)$ there is no need for normalization of the function $\omega(x,y)$. Based on the statement of Theorem 2.1, there are no R-operations of smoothness class higher than $C\left(R^2\right)$ that preserve normalization. However, if one abandons the property of normalization preservation, it is possible to increase the smoothness of R-operations.

The monograph proposes a system of R-operations R^k, which has the form

$$x\overset{k}{\wedge}y=\left(-1\right)^{k+1}\sqrt{x^2+y^2}\left(x+(-1)^{k+1}y\right)^k+\left(-1\right)^k\left(x+(-1)^k y\right)^{k+1},$$

$$x\overset{k}{\vee}y=\sqrt{x^2+y^2}\left(x+(-1)^{k+1}y\right)^k+\left(x+(-1)^k y\right)^{k+1},\ \overline{x}=-x. \qquad (2.6)$$

The proof for the following theorem shows that the functions of this system are R-operations of the class $C\left(R^2\right)$.

Theorem 2.2.

Functions $r_{\wedge}^k(x,y)=x\overset{k}{\wedge}y,\quad k=0,1,2...$ and $r_{\vee}^k(x,y)=x\overset{k}{\vee}y,\quad k=0,1,2...$ are R-conjunctions and R-disjunctions, respectively.

First, the lemma is proved.

Lemma 2.1.

$\forall k=0,1,2,...,\forall x,y\in R$, $\left(|x|+|y|\right)^k\geq\left(\pm|x|\mp|y|\right)^k$, moreover, equality is satisfied when $x=y=0$.

Proof of the lemma 2.1.

Suppose that k is odd, then the function x^k is monotonically increasing. So, $\left(|x|+|y|\right)^k\geq\left(\pm|x|\mp|y|\right)^k$, since $\begin{cases}|x|+|y|\geq|x|-|y|,\\|x|+|y|\geq-|x|+|y|.\end{cases}$

Suppose that k is even. Then $\left(\pm|x|\mp|y|\right)^k = \left|\pm|x|\mp|y|\right|^k = \left||x|-|y|\right|^k$.

Since x^k is monotonically increasing at $x \geq 0$ and $|x|+|y| \geq \left||x|-|y|\right|$, then $\left(|x|+|y|\right)^k \geq \left(\left||x|-|y|\right|\right)^k = \left(\pm|x|\mp|y|\right)^k$. Thus, the following is proven: $\left(|x|+|y|\right)^k \geq$ $\geq \left(\pm|x|\mp|y|\right)^k$.

Suppose that $\left(|x|+|y|\right)^k = \left(\pm|x|\mp|y|\right)^k$, then $|x|+|y| = \left|\pm|x|\mp|y|\right|$. It follows that $\begin{cases} |x|+|y| = |x|-|y| \Rightarrow |y| = 0, \\ |x|+|y| = -|x|+|y| \Rightarrow |x| = 0. \end{cases}$ *Lemma 2.1 is proved.*

Also, to prove Theorem 2.2, the triangle inequality [2] is used in the following form: $\forall x, y \in R$, $\left||x|-|y|\right| \leq \sqrt{x^2+y^2} \leq |x|+|y|$, and equality is satisfied in the case $(x=0) \vee (y=0)$.

Proof of Theorem 2.2.

It is necessary to prove that the following conditions are met:

$$\begin{cases} r_{\wedge}^k(x,y) > 0, & (x>0) \wedge (y>0), \\ r_{\wedge}^k(x,y) < 0, & (x<0) \vee (y<0), \\ r_{\wedge}^k(x,y) = 0, & ((y=0) \wedge (x \geq 0)) \vee ((x=0) \wedge (y \geq 0)), \\ r_{\wedge}^k(x,y) < 0, & ((y=0) \wedge (x<0)) \vee ((x=0) \wedge (y<0)), \end{cases}$$

$$\begin{cases} r_{\vee}^k(x,y) > 0, & (x>0) \vee (y>0), \\ r_{\vee}^k(x,y) < 0, & (x<0) \wedge (y<0), \\ r_{\vee}^k(x,y) > 0, & ((y=0) \wedge (x \geq 0)) \vee ((x=0) \wedge (y \geq 0)), \\ r_{\vee}^k(x,y) = 0, & ((y=0) \wedge (x<0)) \vee ((x=0) \wedge (y<0)). \end{cases}$$

The proof begins with the first statement. The case $x, y > 0$ is considered. We have

$$r_{\wedge}^k(x,y) = (-1)^{k+1}\sqrt{x^2+y^2}\left(x+(-1)^{k+1}y\right)^k + (-1)^k\left(x+(-1)^k y\right)^{k+1} >$$

$$> (-1)^{k+1}\left||x|-|y|\right|\left(|x|+(-1)^{k+1}|y|\right)^k + (-1)^k\left(|x|+(-1)^k|y|\right)^{k+1} =$$

$$= \begin{cases} -\left||x|-|y|\right|\left(|x|-|y|\right)^k + \left(|x|+|y|\right)^{k+1} = \\ = -sign\left(|x|-|y|\right)\left(|x|-|y|\right)^{k+1} + \left(|x|+|y|\right)^{k+1} > 0, \quad k-even \\ \left||x|-|y|\right|\left(|x|+|y|\right)^k - \left(|x|-|y|\right)^{k+1} = \\ = \left||x|-|y|\right|\left(\left(|x|+|y|\right)^k - sign\left(|x|-|y|\right)\left(|x|-|y|\right)^k\right) > 0, \quad k-odd \end{cases}$$

(according to Lemma 2.1 and the triangle inequality).

So $r_{\wedge}^{k}(x,y)>0$. In this case $x>0$, $y<0$, we have

$$r_{\wedge}^{k}(x,y)=(-1)^{k+1}\sqrt{x^2+y^2}\left(x+(-1)^{k+1}y\right)^{k}+(-1)^{k}\left(x+(-1)^{k}y\right)^{k+1}<$$
$$<(-1)^{k+1}\left(|x|+|y|\right)\left(|x|+(-1)^{k}|y|\right)^{k}+(-1)^{k}\left(|x|+(-1)^{k+1}|y|\right)^{k+1}=$$
$$=\begin{cases}-\left(|x|+|y|\right)^{k+1}+\left(|x|-|y|\right)^{k+1}<0,\ k-even\\ \left(|x|+|y|\right)\left(|x|-|y|\right)^{k}-\left(|x|+|y|\right)^{k+1}=\left(|x|+|y|\right)\left(\left(|x|-|y|\right)^{k}-\left(|x|+|y|\right)^{k}\right)<0,\ k-odd\end{cases}$$

(according to Lemma 2.1 and the triangle inequality).

It follows that $r_{\wedge}^{k}(x,y)<0$. In this case $x<0,\quad y>0$, we have

$$r_{\wedge}^{k}(x,y)=(-1)^{k+1}\sqrt{x^2+y^2}\left(x+(-1)^{k+1}y\right)^{k}+(-1)^{k}\left(x+(-1)^{k}y\right)^{k+1}<$$
$$<(-1)^{k+1}\left(|x|+|y|\right)\left(-|x|+(-1)^{k+1}|y|\right)^{k}+(-1)^{k}\left(-|x|+(-1)^{k}|y|\right)^{k+1}=$$
$$=\begin{cases}-\left(|x|+|y|\right)\left(-|x|-|y|\right)^{k}+\left(-|x|+|y|\right)^{k+1}=-\left(|x|+|y|\right)^{k+1}+\left(-|x|+|y|\right)^{k+1}<0,\ k-even\\ \left(|x|+|y|\right)\left(-|x|+|y|\right)^{k}-\left(-|x|-|y|\right)^{k+1}=\left(|x|+|y|\right)\left(\left(-|x|+|y|\right)^{k}-\left(|x|+|y|\right)^{k}\right)<0,\ k-odd\end{cases}$$

(according to Lemma 2.1 and the triangle inequality).

It follows that $r_{\wedge}^{k}(x,y)<0$. In this case $x<0$, $y<0$, we have

$$r_{\wedge}^{k}(x,y)=(-1)^{k+1}\sqrt{x^2+y^2}\left(x+(-1)^{k+1}y\right)^{k}+(-1)^{k}\left(x+(-1)^{k}y\right)^{k+1}<$$
$$<(-1)^{k+1}\left(|x|+|y|\right)\left(-|x|+(-1)^{k}|y|\right)^{k}+(-1)^{k}\left(-|x|+(-1)^{k+1}|y|\right)^{k+1}=$$
$$=\begin{cases}-\left(|x|+|y|\right)\left(-|x|+|y|\right)^{k}+\left(-|x|-|y|\right)^{k+1}=-\left(|x|+|y|\right)\left(\left(-|x|+|y|\right)^{k}+\left(|x|+|y|\right)^{k}\right)<0,\\ k-even\\ \left(|x|+|y|\right)\left(-|x|-|y|\right)^{k}-\left(-|x|+|y|\right)^{k+1}=-\left(|x|+|y|\right)^{k+1}-\left(-|x|+|y|\right)^{k+1}<0,\\ k-odd\end{cases}$$

(according to Lemma 2.1 and the triangle inequality).

Thus, $r_{\wedge}^{k}(x,y)<0$. The following property for the function $r_{\wedge}^{k}(x,y)$ is proved:

$$\begin{cases}r_{\wedge}^{k}(x,y)>0, & (x>0)\wedge(y>0),\\ r_{\wedge}^{k}(x,y)<0, & (x<0)\vee(y<0).\end{cases}$$

It is needed to prove that

$$\begin{cases}r_{\wedge}^{k}(x,y)=0, & ((y=0)\wedge(x\geq 0))\vee((x=0)\wedge(y\geq 0)),\\ r_{\wedge}^{k}(x,y)<0, & ((y=0)\wedge(x<0))\vee((x=0)\wedge(y<0)).\end{cases}$$

The value of the function $r_{\wedge}^{k}(x,y)$ on the coordinate axes is considered. We have the following:

$$r_{\wedge}^{k}(x,0)=(-1)^{k+1}|x|(x)^{k}+(-1)^{k}(x)^{k+1}=(-1)^{k+1}(x)^{k+1}+(-1)^{k}(x)^{k+1}=0,\ x\geq 0;$$

$$r_{\wedge}^{k}(0,y)=(-1)^{k+1}|y|\left((-1)^{k+1}y\right)^{k}+(-1)^{k}\left((-1)^{k}y\right)^{k+1}=(-1)^{(k+1)^{2}}y^{k+1}+(-1)^{k^{2}+2k}y^{k+1}=0,$$
$$y\geq 0;$$

$$r_{\wedge}^{k}(x,0)=(-1)^{k+1}|x|(x)^{k}+(-1)^{k}(x)^{k+1}=-(-1)^{k+1}(x)^{k+1}-(-1)^{k+1}(x)^{k+1}=$$
$$=-2(-x)^{k+1}=-2|x|^{k+1}<0,\ x<0$$

$$r_{\wedge}^{k}(0,y)=(-1)^{k+1}|y|\left((-1)^{k+1}y\right)^{k}+(-1)^{k}\left((-1)^{k}y\right)^{k+1}=(-1)^{k^{2}+2k}y^{k+1}+(-1)^{k^{2}+2k}y^{k+1}=$$
$$=2(-1)^{k^{2}+2k}y^{k+1}=2(-1)^{k^{2}+2k}(-1)^{k+1}|y|^{k+1}=-2(-1)^{k^{2}+2k+1}(-1)^{k+1}|y|^{k+1}=$$
$$=-2(-1)^{(k+1)(k+2)}|y|^{k+1}=-2|y|^{k+1}<0,\ y<0.$$

Thereby,
$$\begin{cases} r_{\wedge}^{k}(x,y)>0, & (x>0)\wedge(y>0),\\ r_{\wedge}^{k}(x,y)<0, & (x<0)\vee(y<0),\\ r_{\wedge}^{k}(x,y)=0, & ((y=0)\wedge(x\geq 0))\vee((x=0)\wedge(y\geq 0)),\\ r_{\wedge}^{k}(x,y)<0, & ((y=0)\wedge(x<0))\vee((x=0)\wedge(y<0)).\end{cases}$$

Since

$$-r_{\wedge}^{k}(-x,-y)=(-1)^{k+2}\sqrt{x^{2}+y^{2}}\left(-x-(-1)^{k+1}y\right)^{k}+(-1)^{k+1}\left(-x-(-1)^{k}y\right)^{k+1}=$$
$$=(-1)^{k+2}(-1)^{k}\sqrt{x^{2}+y^{2}}\left(x+(-1)^{k+1}y\right)^{k}+(-1)^{k+1}(-1)^{k+1}\left(x+(-1)^{k}y\right)^{k+1}=$$
$$=\sqrt{x^{2}+y^{2}}\left(x+(-1)^{k+1}y\right)^{k}+\left(x+(-1)^{k}y\right)^{k+1}=r_{\vee}^{k}(x,y),$$

then the functions $r_{\wedge}^{k}(x,y),\quad k=0,1,2,\ldots$ have the following property:

$$\begin{cases} r_{\vee}^{k}(x,y)>0, & (x>0)\vee(y>0),\\ r_{\vee}^{k}(x,y)<0, & (x<0)\wedge(y<0),\\ r_{\vee}^{k}(x,y)>0, & ((y=0)\wedge(x\geq 0))\vee((x=0)\wedge(y\geq 0)),\\ r_{\vee}^{k}(x,y)=0, & ((y=0)\wedge(x<0))\vee((x=0)\wedge(y<0)).\end{cases}$$

Theorem 2.2 is proved.

Theorem 2.3.

The functions $r_{\wedge}^{k}(x,y), k=0,1,2,\ldots$ and $r_{?}^{k}(x,y), k=0,1,2,...$ belong to the class $C^{k}(R^{2})$.

Proof.

Consider $r_{\wedge}^{k}(x,y)=\left(-1\right)^{k+1}\sqrt{x^2+y^2}\left(x+(-1)^{k+1}y\right)^{k}+\left(-1\right)^{k}\left(x+(-1)^{k}y\right)^{k+1}$.

The second member of the $r_{\wedge}^{k}(x,y)$ functions family belongs to the class $C^{\infty}\left(R^2\right)$, so it is needed to check that $\sqrt{x^2+y^2}\left(x+(-1)^{k+1}y\right)^{k}$ belongs to the class $C^{k}\left(R^2\right)$. It is enough to show that

$$\begin{cases} g_k^1(x,y)=\sqrt{x^2+y^2}\left(x+y\right)^{k}\in C^{k}\left(R^2\right), \\ g_k^2(x,y)=\sqrt{x^2+y^2}\left(x-y\right)^{k}\in C^{k}\left(R^2\right). \end{cases}$$

These functions belong to the class C^{∞} at all points of R^2, except for point (0,0). Thus, it is necessary to check the smoothness of these functions up to the *k*-th order at point (0,0).

The first statement $g_k^1(x,y)=\sqrt{x^2+y^2}\left(x+y\right)^{k}\in C^{k}\left(R^2\right)$ is checked. To do this, it is sufficient to show that all partial derivatives are continuous, and also that

$$\left.\frac{\partial^{i} g_k^1(x,y)}{\partial x^{j}\partial y^{i-j}}\right|_{(0,0)}=0,\quad i\le k.$$

The proof will be carried out with the mathematical induction method. This assertion is proven for $k=1$.

Consider

$$\frac{\partial g_1^1(x,y)}{\partial x}=\frac{x\left(x+y\right)}{\sqrt{x^2+y^2}}+\sqrt{x^2+y^2},\ \frac{\partial g_1^1(x,y)}{\partial y}=\frac{y\left(x+y\right)}{\sqrt{x^2+y^2}}+\sqrt{x^2+y^2}.$$

Then $\lim\limits_{\substack{x\to 0\\ y\to 0}}\frac{\partial g_1^1(x,y)}{\partial x}=\lim\limits_{\substack{x\to 0\\ y\to 0}}\frac{x\left(x+y\right)}{\sqrt{x^2+y^2}}$. To $\lim\limits_{\substack{x\to 0\\ y\to 0}}\frac{x\left(x+y\right)}{\sqrt{x^2+y^2}}=0$, it is necessary and sufficient for $\lim\limits_{\substack{x\to 0\\ y\to 0}}\frac{x^2\left(x+y\right)^2}{x^2+y^2}=0$. Consider this limit

$$\lim_{\substack{x\to 0\\ y\to 0}}\frac{x^2\left(x+y\right)^2}{x^2+y^2}=\lim_{\substack{x\to 0\\ y\to 0}}\frac{x^2\left(x^2+2xy+y^2\right)}{x^2+y^2}=\lim_{\substack{x\to 0\\ y\to 0}}\left(x^2+x^2\frac{2xy}{x^2+y^2}\right)=\lim_{\substack{x\to 0\\ y\to 0}}x^2\frac{2xy}{x^2+y^2}=0,$$

because $\left|\frac{2xy}{x^2+y^2}\right|\le 1$. Thus, $\lim\limits_{\substack{x\to 0\\ y\to 0}}\frac{\partial g_1^1(x,y)}{\partial x}=\lim\limits_{\substack{x\to 0\\ y\to 0}}\frac{x\left(x+y\right)}{\sqrt{x^2+y^2}}=0$.

Consider

$$\lim_{\substack{x\to 0\\ y\to 0}}\frac{\partial g_1^1(x,y)}{\partial y}=\lim_{\substack{x\to 0\\ y\to 0}}\frac{y\left(x+y\right)}{\sqrt{x^2+y^2}},$$

$$\lim_{\substack{x\to 0\\ y\to 0}}\frac{y^2\left(x+y\right)^2}{x^2+y^2}=\lim_{\substack{x\to 0\\ y\to 0}}\frac{y^2\left(x^2+2xy+y^2\right)}{x^2+y^2}=\lim_{\substack{x\to 0\\ y\to 0}}\left(y^2+y^2\frac{2xy}{x^2+y^2}\right)=$$

$$=\lim_{\substack{x\to 0\\ y\to 0}}y^2\frac{2xy}{x^2+y^2}=0\text{, since }\left|\frac{2xy}{x^2+y^2}\right|\le 1.$$

Thus, $\lim\limits_{\substack{x\to 0\\ y\to 0}}\dfrac{\partial g_1^1(x,y)}{\partial y}=\lim\limits_{\substack{x\to 0\\ y\to 0}}\dfrac{y\left(x+y\right)}{\sqrt{x^2+y^2}}=0.$

Based on the proven, $g_1^1(x,y)=\sqrt{x^2+y^2}\left(x+y\right)\in C^1\left(R^2\right)$. Assume that this assertion is executed for $k-1$, i.e.

$$\frac{\partial^i g_{k-1}^1(x,y)}{\partial x^j\partial y^{i-j}}=0,\quad i\le k-1,\quad j\le i.$$

Then

$$g_k^1(x,y)=\sqrt{x^2+y^2}\left(x+y\right)^k=\sqrt{x^2+y^2}\left(x+y\right)^{k-1}\left(x+y\right)=g_{k-1}^1(x,y)\left(x+y\right),$$

$$\left.\frac{\partial^i g_k^1(x,y)}{\partial x^j\partial y^{i-j}}\right|_{(0,0)}=\left.\left(\frac{\partial^i g_{k-1}^1(x,y)}{\partial x^j\partial y^{i-j}}(x+y)+(i-j)\frac{\partial^{i-1}g_{k-1}^1(x,y)}{\partial x^j\partial y^{i-j-1}}+j\frac{\partial^{i-1}g_k^1(x,y)}{\partial x^{j-1}\partial y^{i-j}}\right)\right|_{(0,0)}=$$

$$=0,\quad i<k,\ \left.\frac{\partial^k g_k^1(x,y)}{\partial x^j\partial y^{k-j}}\right|_{(0,0)}=\lim_{\substack{x\to 0\\ y\to 0}}\left(\frac{\partial^k g_{k-1}^1(x,y)}{\partial x^j\partial y^{k-j}}(x+y)\right).$$

Suppose that $\lim\limits_{\substack{x\to 0\\ y\to 0}}\left(\dfrac{\partial^k g_{k-1}^1(x,y)}{\partial x^j\partial y^{k-j}}(x+y)\right)\ne 0.$

Suppose that this limit exists and is finite, $\lim\limits_{\substack{x\to 0\\ y\to 0}}\left(\dfrac{\partial^k g_{k-1}^1(x,y)}{\partial x^j\partial y^{k-j}}(x+y)\right)=C$,

then

$$\frac{\partial^k g_{k-1}^1(x,y)}{\partial x^j\partial y^{k-j}}\sim\frac{C}{(x+y)},\text{ and }\frac{\partial}{\partial x}\left(\frac{\partial^{k-1}g_{k-1}^1(x,y)}{\partial x^{j-1}\partial y^{k-j}}\right)\sim\frac{C}{(x+y)}.$$

Thus, $\frac{\partial^{k-1} g^1_{k-1}(x,y)}{\partial x^{j-1}\partial y^{k-j}} \sim C\ln|x+y|\Big|_{\substack{x=0\\y=0}} = \infty$, and this contradicts the assumption.

Suppose that $\lim\limits_{\substack{x\to 0\\y\to 0}}\left(\frac{\partial^k g^1_{k-1}(x,y)}{\partial x^j\partial y^{k-j}}(x+y)\right) = \infty$. Then $\frac{\partial^k g^1_{k-1}(x,y)}{\partial x^j\partial y^{k-j}} \underset{\substack{x\to 0\\y\to 0}}{\to} 0$ faster than $\frac{C}{(x+y)}$, therefore, $\frac{\partial^{k-1} g^1_{k-1}(x,y)}{\partial x^{j-1}\partial y^{k-j}} \underset{\substack{x\to 0\\y\to 0}}{\to} \infty$ faster than $C\ln|x+y|$, which also contradicts the assumption.

Suppose that this limit does not exist. This means that at different approximations of x and y to zero we have different limits.

Consider the limit $\lim\limits_{\substack{x\to 0\\y\to 0}}\left(\frac{\partial^k g^1_{k-1}(x,y)}{\partial x^j\partial y^{k-j}}(x+y)\right) = C$ for some option of approximation of x and y to zero (in which the limit is not equal to zero), then

$$\frac{\partial^k g^1_{k-1}(x,y)}{\partial x^j\partial y^{k-j}} \sim \frac{C}{(x+y)}, \text{ i.e. } \frac{\partial}{\partial x}\left(\frac{\partial^{k-1} g^1_{k-1}(x,y)}{\partial x^{j-1}\partial y^{k-j}}\right) \sim \frac{C}{(x+y)}.$$

Thus, $\frac{\partial^{k-1} g^1_{k-1}(x,y)}{\partial x^{j-1}\partial y^{k-j}} \sim C\ln|x+y|\Big|_{\substack{x=0\\y=0}} = \infty$ (in this case of the approximation of x and y to zero), which contradicts the assumption.

Based on the above, $\left.\frac{\partial^k g^1_k(x,y)}{\partial x^j\partial y^{k-j}}\right|_{(0,0)} = 0$. It is similarly proved that $g^1_k(x,y) = \sqrt{x^2+y^2}\,(x-y)^k \in C^k_{R^2}$. Thus, $r^k_{\wedge}(x,y) \in C^k\left(R^2\right), k = 0,1,2,\ldots$ Since $r^k_{\vee}(x,y) = -r^k_{\wedge}(-x,-y)$, then

$$\frac{\partial^i r^k_{\vee}(x,y)}{\partial x^j\partial y^{i-j}} = \frac{\partial^i(-r^k_{\wedge}(-x,-y))}{\partial x^j\partial y^{i-j}} = -\frac{\partial^i(r^k_{\wedge}(-x,-y))}{\partial x^j\partial y^{i-j}} = (-1)^{i+1}\frac{\partial^i r^k_{\wedge}(-x,-y)}{\partial x^j\partial y^{i-j}}.$$

Based on the fact that all partial derivatives of function $r^k_{\wedge}(x,y)$ up to the k-th order exist and are continuous, it follows that all partial derivatives of function $r^k_{\vee}(x,y)$ up to the k-th order also exist and are continuous, i.e. $r^k_{\vee}(x,y) \in C^k\left(R^2\right), k = 0,1,2,\ldots$ *The theorem is proved.*

Conclusion. A system of R-operations R^k of smoothness class $C^k(R^2)$, $k = 0, 1, 2, \ldots$ is built. At $k = 0$, this system is transformed into a system of R-operations R_0.

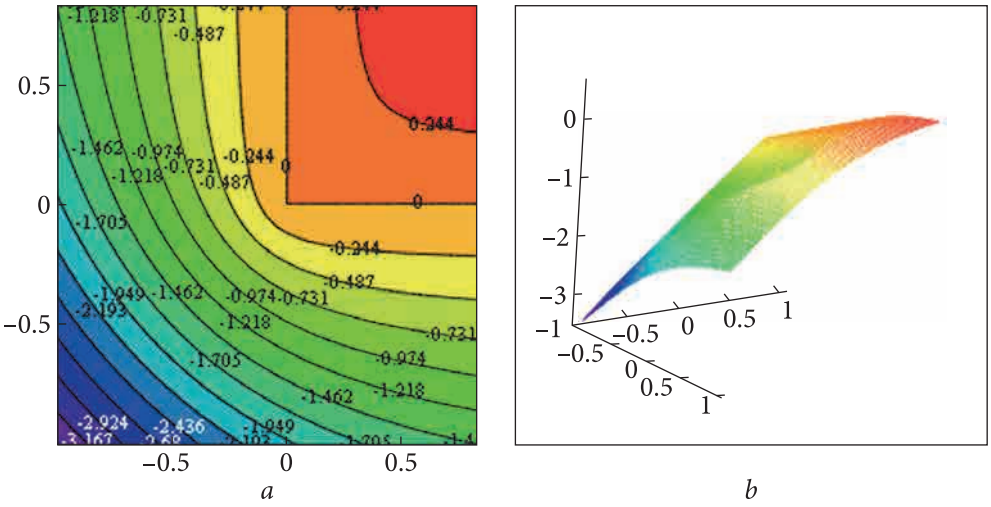

Fig. 2.2. Visualization of the function $f(x,y)=x\wedge y$ graph: *a* — in the form of lines of constant level on the plane xOy; *b* — in the form of a surface in space R^3

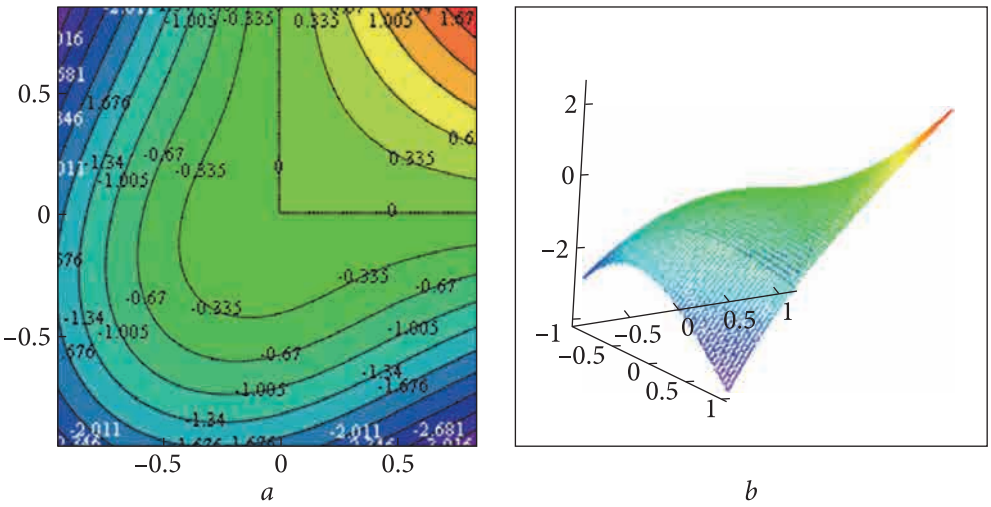

Fig. 2.3. Visualization of the function $f(x,y)=x\overset{1}{\wedge}y$ graph: *a* — in the form of lines of constant level on the plane xOy; *b* — in the form of a surface in space R^3

Fig. 2.2—2.4 show the visualization of graphs of R-conjunction functions from the given system R^k at $k=0$, $k=1$, $k=2$.

The question arises as to whether it is possible to explicitly construct an R-conjunction and an R-disjunction of class $C^\infty(R^2)$. The following system

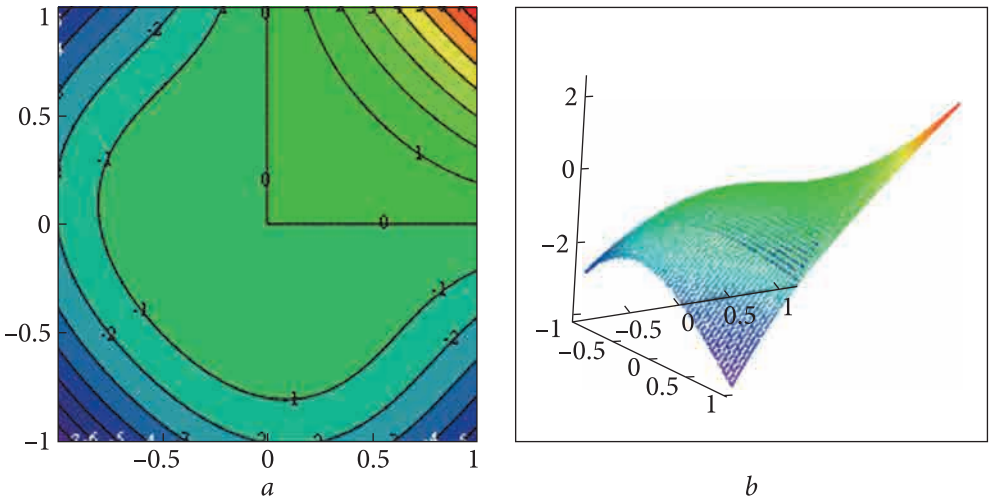

a *b*

Fig. 2.4. Visualization of the function $f(x,y) = x \overset{2}{\wedge} y$ graph: *a* — in the form of lines of constant level on the plane xOy; *b* — in the form of a surface in space R^3

of R-operations R^∞ gives a positive answer to this question:

$$x \overset{\infty}{\wedge} y = \begin{cases} sign(x+y)\, e^{\frac{(x+y)^2-1}{|x+y|}} - e^{\frac{(x-y)^2-1}{|x-y|}}, & (x \neq y) \wedge (x \neq -y), \\ sign(x+y)\, e^{\frac{(x+y)^2-1}{|x+y|}}, & x = y \neq 0, \\ -e^{\frac{(x-y)^2-1}{|x-y|}}, & x = -y \neq 0, \\ 0, & x = y = 0, \end{cases}$$

$$x \overset{\infty}{\vee} y = \begin{cases} sign(x+y)\, e^{\frac{(x+y)^2-1}{|x+y|}} + e^{\frac{(x-y)^2-1}{|x-y|}}, & (x \neq y) \wedge (x \neq -y), \\ sign(x+y)\, e^{\frac{(x+y)^2-1}{|x+y|}}, & x = y \neq 0,\ \overline{x} = -x \\ e^{\frac{(x-y)^2-1}{|x-y|}}, & x = -y \neq 0, \\ 0, & x = y = 0, \end{cases} \qquad (2.7)$$

$$\overline{x} = -x\,.$$

Theorems that show that functions of a given system are R-operations of class $C^\infty\left(R^2\right)$ are proved.

Denote $r^\infty_\wedge(x,y) = x \overset{\infty}{\wedge} y, \quad r^\infty(x,y) = x \overset{\infty}{\vee} y.$

Theorem 2.4.

The functions $r_{\wedge}^{\infty}(x,y) = x \overset{\infty}{\wedge} y$ and $r_{\vee}^{\infty}(x,y) = x \overset{\infty}{\vee} y$ are R-conjunction and R-disjunction, respectively.

Proof.

It is necessary to prove that the following conditions are met:

$$\begin{cases} r_{\wedge}^{\infty}(x,y) > 0, & (x>0)\wedge(y>0), \\ r_{\wedge}^{\infty}(x,y) < 0, & (x<0)\vee(y<0), \\ r_{\wedge}^{\infty}(x,y) = 0, & ((y=0)\wedge(x\geq 0))\vee((x=0)\wedge(y\geq 0)), \\ r_{\wedge}^{\infty}(x,y) < 0, & ((y=0)\wedge(x<0))\vee((x=0)\wedge(y<0)), \end{cases}$$

$$\begin{cases} r_{\vee}^{\infty}(x,y) > 0, & (x>0)\vee(y>0), \\ r_{\vee}^{\infty}(x,y) < 0, & (x<0)\wedge(y<0), \\ r_{\vee}^{\infty}(x,y) > 0, & ((y=0)\wedge(x\geq 0))\vee((x=0)\wedge(y\geq 0)), \\ r_{\vee}^{\infty}(x,y) = 0, & ((y=0)\wedge(x<0))\vee((x=0)\wedge(y<0)). \end{cases}$$

The meeting of conditions for functions $r_{\wedge}^{\infty}(x,y)$ is proved. The case $x, y > 0$ is considered.

Suppose that $x \geq y$, then

$$r_{\wedge}^{\infty}(x,y) = \begin{cases} e^{\frac{(x+y)^2-1}{(x+y)}} - e^{\frac{(x-y)^2-1}{(x-y)}} > 0, & (x\neq y)\wedge(x\neq -y), \\ e^{\frac{(x+y)^2-1}{(x+y)}} > 0, & x = y \neq 0. \end{cases}$$

At $x = y \neq 0$ the inequality is obvious. At $(x\neq y)\wedge(x\neq -y)$ the inequality is realized based on the monotonicity of the function e^x and inequality $\frac{(x+y)^2-1}{(x+y)} > \frac{(x-y)^2-1}{(x-y)}$. This inequality is proved in the assumption $x \geq y > 0$.

Since $(x+y) - \frac{1}{(x+y)} > (x-y) - \frac{1}{(x-y)}$, then $2y > \frac{1}{(x+y)} - \frac{1}{(x-y)} =$

$= \frac{-2y}{x^2-y^2}$. This inequality is realized because the left side is positive and the right side is negative.

Suppose that $x \le y$, then

$$r_{\wedge}^{\infty}(x,y)=\begin{cases} e^{\frac{(x+y)^2-1}{(x+y)}}-e^{-\frac{(x-y)^2-1}{(x-y)}}>0, & (x\neq y)\wedge(x\neq -y),\\ e^{\frac{(x+y)^2-1}{(x+y)}}>0, & x=y\neq 0. \end{cases}$$

At $x=y\neq 0$ the inequality is obvious. At $(x\neq y)\wedge(x\neq -y)$ the inequality is realized based on the monotonicity of the function e^x and inequality $\frac{(x+y)^2-1}{(x+y)}>-\frac{(x-y)^2-1}{(x-y)}$. This inequality is proved in the assumption $y\ge x>0$.

Since

$(x+y)-\frac{1}{(x+y)}>(y-x)+\frac{1}{(x-y)}$, then $2x>\frac{1}{(x+y)}+\frac{1}{(x-y)}=\frac{2x}{x^2-y^2}$.

This inequality is realized because the left side is positive and the right side is negative.

The case $(x<0)\wedge(y>0)$ is considered.

Suppose that $x\ge -y$, then

$$r_{\wedge}^{\infty}(x,y)=\begin{cases} e^{\frac{(x+y)^2-1}{(x+y)}}-e^{-\frac{(x-y)^2-1}{(x-y)}}<0, & (x\neq y)\wedge(x\neq -y),\\ -e^{-\frac{(x-y)^2-1}{(x-y)}}<0, & x=-y\neq 0. \end{cases}$$

At $x=-y\neq 0$, the inequality is obvious. At $(x\neq y)\wedge(x\neq -y)$ the inequality is realized based on the monotonicity of the function e^x and inequality $\frac{(x+y)^2-1}{(x+y)}<-\frac{(x-y)^2-1}{(x-y)}$.

This inequality is proved in the assumption $0>x\ge -y$.

Since $(x+y)-\frac{1}{(x+y)}<(y-x)+\frac{1}{(x-y)}$, then $2x<\frac{1}{(x+y)}+\frac{1}{(x-y)}=$ $=\frac{2x}{x^2-y^2}$. This inequality is realized because the left side is positive and the right side is negative.

Suppose that $x\le -y$, then

$$r_{\wedge}^{\infty}(x,y)=\begin{cases} -e^{\frac{(x+y)^2-1}{(x+y)}}-e^{-\frac{(x-y)^2-1}{(x-y)}}<0, & (x\neq y)\wedge(x\neq -y),\\ -e^{-\frac{(x-y)^2-1}{(x-y)}}<0, & x=-y\neq 0. \end{cases}$$

This inequality is obvious. The case when $(x<0)\wedge(y<0)$ is considered. Suppose that y≥x, then

$$r_{\wedge}^{\infty}(x,y)=\begin{cases}-e^{-\frac{(x+y)^2-1}{(x+y)}}-e^{-\frac{(x-y)^2-1}{(x-y)}}<0, & (x\neq y)\wedge(x\neq -y),\\ -e^{-\frac{(x-y)^2-1}{(x-y)}}<0, & x=-y\neq 0.\end{cases}$$

These inequalities are obvious.

Suppose that $y\le x$, then

$$r_{\wedge}^{\infty}(x,y)=\begin{cases}-e^{-\frac{(x+y)^2-1}{(x+y)}}-e^{\frac{(x-y)^2-1}{(x-y)}}<0, & (x\neq y)\wedge(x\neq -y),\\ -e^{-\frac{(x-y)^2-1}{(x-y)}}<0, & x=-y\neq 0.\end{cases}$$

These inequalities are obvious. The case $(x>0)\wedge(y<0)$ is considered.

Suppose that $x\ge -y$, then

$$r_{\wedge}^{\infty}(x,y)=\begin{cases}e^{\frac{(x+y)^2-1}{(x+y)}}-e^{\frac{(x-y)^2-1}{(x-y)}}<0, & (x\neq y)\wedge(x\neq -y),\\ -e^{\frac{(x-y)^2-1}{(x-y)}}<0, & x=-y\neq 0.\end{cases}$$

At $x=-y\neq 0$ inequality is obvious. At $(x\neq y)\wedge(x\neq -y)$ the inequality is realized based on the monotonicity of the function e^x and inequality $\frac{(x+y)^2-1}{(x+y)}<\frac{(x-y)^2-1}{(x-y)}$.

This inequality is proved in the assumption $0>y\ge -x$.

Since $(x+y)-\frac{1}{(x+y)}<(x-y)-\frac{1}{(x-y)}$, then $2y<\frac{1}{(x+y)}-\frac{1}{(x-y)}=$ $=\frac{-2y}{x^2-y^2}$. This inequality is realized because the left side is positive and the right side is negative.

Suppose that $x\le -y$, then

$$r_{\wedge}^{\infty}(x,y)=\begin{cases}-e^{-\frac{(x+y)^2-1}{(x+y)}}-e^{\frac{(x-y)^2-1}{(x-y)}}<0, & (x\neq y)\wedge(x\neq -y),\\ -e^{\frac{(x-y)^2-1}{(x-y)}}<0, & x=-y\neq 0.\end{cases}$$

These inequalities are obvious.

Thus, the following property of the function $r_{\wedge}^{\infty}(x,y)$ *is proved*

$$\begin{cases} r_{\wedge}^{\infty}(x,y) > 0, & (x>0)\wedge(y>0), \\ r_{\wedge}^{\infty}(x,y) < 0, & (x<0)\vee(y<0). \end{cases}$$

Now it is needed to prove that

$$\begin{cases} r_{\wedge}^{\infty}(x,y) = 0, & \big((y=0)\wedge(x\geq 0)\big)\vee\big((x=0)\wedge(y\geq 0)\big), \\ r_{\wedge}^{\infty}(x,y) < 0, & ((y=0)\wedge(x<0))\vee((x=0)\wedge(y<0)). \end{cases}$$

The function $r_{\wedge}^{\infty}(x,0)$ is considered at $x\geq 0$

$$r_{\wedge}^{\infty}(x,0) = \begin{cases} e^{\frac{x^2-1}{|x|}} - e^{\frac{x^2-1}{|x|}} = 0 & (x\neq y)\wedge(x\neq -y), \\ 0, \ x=y=0. \end{cases}$$

The function $r_{\wedge}^{\infty}(0,y)$ is considered at $y\geq 0$

$$r_{\wedge}^{\infty}(0,y) = \begin{cases} e^{\frac{y^2-1}{|y|}} - e^{\frac{y^2-1}{|y|}}, = 0 & (x\neq y)\wedge(x\neq -y), \\ 0, \ x=y=0. \end{cases}$$

The function $r_{\wedge}^{\infty}(x,0)$ is considered at $x<0$

$$r_{\wedge}^{\infty}(x,0) = -e^{\frac{x^2-1}{|x|}} - e^{\frac{x^2-1}{|x|}} < 0.$$

The function $r_{\wedge}^{\infty}(0,y)$ is considered at $y<0$

$$r_{\wedge}^{\infty}(0,y) = -e^{\frac{y^2-1}{|y|}} - e^{\frac{y^2-1}{|y|}} < 0.$$

The theorem is proved for the function $r_{\wedge}^{\infty}(x,y)$. The proof for the function $r_{\vee}^{\infty}(x,y)$ is considered. Since $r_{\vee}^{\infty}(x,y) = -r_{\wedge}^{\infty}(-x,-y)$, then the function $r_{\vee}^{\infty}(x,y)$, $k=0,1,2\ldots$ has a property

$$\begin{cases} r_{\vee}^{\infty}(x,y) > 0, & (x>0)\vee(y>0), \\ r_{\vee}^{\infty}(x,y) < 0, & (x<0)\wedge(y<0), \\ r_{\vee}^{\infty}(x,y) > 0, & \big((y=0)\wedge(x\geq 0)\big)\vee\big((x=0)\wedge(y\geq 0)\big), \\ r_{\vee}^{\infty}(x,y) = 0, & ((y=0)\wedge(x<0))\vee((x=0)\wedge(y<0)). \end{cases}$$

Thus, *the theorem is proved.*

Theorem 2.5.
The functions $r_{\wedge}^{\infty}(x,y)$ and $r_{\vee}^{\infty}(x,y)$ belong to the class $C^{\infty}=(R^2)$.
Proof.
It is needed to prove that $r_{\wedge}^{\infty}(x,y)\in C^{\infty}\left(R^2\right)$. The function

$$r_{\wedge}^{\infty}(x,y)=\begin{cases} sign(x+y)e^{\frac{(x+y)^2-1}{|x+y|}}-e^{\frac{(x-y)^2-1}{|x-y|}}, & (x\neq y)\wedge(x\neq -y),\\ sign(x+y)e^{\frac{(x+y)^2-1}{|x+y|}}, & x=y\neq 0,\\ -e^{\frac{(x-y)^2-1}{|x-y|}}, & x=-y\neq 0,\\ 0, & x=y=0 \end{cases}$$

is considered.

Obviously, $r_{\wedge}^{\infty}(x,y)\in C^{\infty}\left(R^2\right)$, $\forall x,y:\ (x\neq y)\wedge(x\neq -y)$.

For the case $(y>x)\wedge(y>-x)$ we have $r_{\wedge}^{\infty}(x,y)=e^{\frac{(x+y)^2-1}{(x+y)}}-e^{-\frac{(x-y)^2-1}{(x-y)}}$. It follows that

$$\frac{\partial^i r_{\wedge}^{\infty}(x,y)}{\partial x^j\partial y^{i-j}}=\frac{\partial^i\left(e^{\frac{(x+y)^2-1}{(x+y)}}\right)}{\partial x^j\partial y^{i-j}}-\frac{\partial^i\left(e^{-\frac{(x-y)^2-1}{(x-y)}}\right)}{\partial x^j\partial y^{i-j}}=e^{\frac{(x+y)^2-1}{(x+y)}}P_1(x,y)-e^{-\frac{(x-y)^2-1}{(x-y)}}Q_1(x,y),$$

where $P_1(x,y)$ and $Q_1(x,y)$ — some fractional rational functions.

Since the functions $e^{\frac{(x+y)^2-1}{(x+y)}}$ and $e^{-\frac{(x-y)^2-1}{(x-y)}}$ approach zero faster than any degree of the polynomial at $y\to -x$ and $y\to x$ respectively, then

$$\lim_{y\to -x}\frac{\partial^i r_{\wedge}^{\infty}(x,y)}{\partial x^j\partial y^{i-j}}=-\frac{\partial^i\left(e^{-\frac{(x-y)^2-1}{(x-y)}}\right)}{\partial x^j\partial y^{i-j}},\ \lim_{y\to x}\frac{\partial^i r_{\wedge}^{\infty}(x,y)}{\partial x^j\partial y^{i-j}}=\frac{\partial^i\left(e^{\frac{(x+y)^2-1}{(x+y)}}\right)}{\partial x^j\partial y^{i-j}},$$

$$\lim_{\substack{x\to 0\\ y\to 0}}\frac{\partial^i r_{\wedge}^{\infty}(x,y)}{\partial x^j\partial y^{i-j}}=0.$$

The case $(y<x)\wedge(y>-x)$ is considered. Since $r_{\wedge}^{\infty}(x,y)=e^{\frac{(x+y)^2-1}{(x+y)}}-$ $-e^{\frac{(x-y)^2-1}{(x-y)}}$, then

$$\frac{\partial^i r_{\wedge}^{\infty}(x,y)}{\partial x^j\partial y^{i-j}}=\frac{\partial^i\left(e^{\frac{(x+y)^2-1}{(x+y)}}\right)}{\partial x^j\partial y^{i-j}}-\frac{\partial^i\left(e^{\frac{(x-y)^2-1}{(x-y)}}\right)}{\partial x^j\partial y^{i-j}}=e^{\frac{(x+y)^2-1}{(x+y)}}P_1(x,y)-e^{\frac{(x-y)^2-1}{(x-y)}}Q_2(x,y),$$

where $P_1(x,y)$ and $Q_2(x,y)$ — some fractional rational functions.

Then

$$\lim_{y\to x}\frac{\partial^i r_\wedge^\infty(x,y)}{\partial x^j\partial y^{i-j}}=\frac{\partial^i\left(e^{\frac{(x+y)^2-1}{(x+y)}}\right)}{\partial x^j\partial y^{i-j}},\ \lim_{y\to -x}\frac{\partial^i r_\wedge^\infty(x,y)}{\partial x^j\partial y^{i-j}}=-\frac{\partial^i\left(e^{\frac{(x-y)^2-1}{(x-y)}}\right)}{\partial x^j\partial y^{i-j}},$$

$$\lim_{\substack{x\to 0\\ y\to 0}}\frac{\partial^i r_\wedge^\infty(x,y)}{\partial x^j\partial y^{i-j}}=0.$$

The case $(y<x)\wedge(y<-x)$ is considered. Since $r_\wedge^\infty(x,y)=-e^{-\frac{(x+y)^2-1}{(x+y)}}-e^{\frac{(x-y)^2-1}{(x-y)}}$, then

$$\frac{\partial^i r_\wedge^\infty(x,y)}{\partial x^j\partial y^{i-j}}=-\frac{\partial^i\left(e^{-\frac{(x+y)^2-1}{(x+y)}}\right)}{\partial x^j\partial y^{i-j}}-\frac{\partial^i\left(e^{\frac{(x-y)^2-1}{(x-y)}}\right)}{\partial x^j\partial y^{i-j}}=-e^{-\frac{(x+y)^2-1}{(x+y)}}P_2(x,y)-e^{\frac{(x-y)^2-1}{(x-y)}}Q_2(x,y),$$

where $P_1(x,y)$ and $Q_2(x,y)$ — some fractional rational functions.

Then

$$\lim_{y\to x}\frac{\partial^i r_\wedge^\infty(x,y)}{\partial x^j\partial y^{i-j}}=-\frac{\partial^i\left(e^{-\frac{(x+y)^2-1}{(x+y)}}\right)}{\partial x^j\partial y^{i-j}},\ \lim_{y\to -x}\frac{\partial^i r_\wedge^\infty(x,y)}{\partial x^j\partial y^{i-j}}=-\frac{\partial^i\left(e^{\frac{(x-y)^2-1}{(x-y)}}\right)}{\partial x^j\partial y^{i-j}},$$

$$\lim_{\substack{x\to 0\\ y\to 0}}\frac{\partial^i r_\wedge^\infty(x,y)}{\partial x^j\partial y^{i-j}}=0.$$

The case $(y>x)\wedge(y<-x)$ is considered.

Since $r_\wedge^\infty(x,y)=-e^{-\frac{(x+y)^2-1}{(x+y)}}-e^{-\frac{(x-y)^2-1}{(x-y)}}$, then

$$\frac{\partial^i r_\wedge^\infty(x,y)}{\partial x^j\partial y^{i-j}}=-\frac{\partial^i\left(e^{-\frac{(x+y)^2-1}{(x+y)}}\right)}{\partial x^j\partial y^{i-j}}-\frac{\partial^i\left(e^{\frac{(x-y)^2-1}{(x-y)}}\right)}{\partial x^j\partial y^{i-j}}=-e^{-\frac{(x+y)^2-1}{(x+y)}}P_2(x,y)-e^{\frac{(x-y)^2-1}{(x-y)}}Q_2(x,y),$$

where $P_2(x,y)$ and $Q_1(x,y)$ — some fractional rational functions.

Then

$$\lim_{y\to x}\frac{\partial^i r_\wedge^\infty(x,y)}{\partial x^j\partial y^{i-j}}=-\frac{\partial^i\left(e^{\frac{(x+y)^2-1}{(x+y)}}\right)}{\partial x^j\partial y^{i-j}},\ \lim_{y\to -x}\frac{\partial^i r_\wedge^\infty(x,y)}{\partial x^j\partial y^{i-j}}=-\frac{\partial^i\left(e^{\frac{(x-y)^2-1}{(x-y)}}\right)}{\partial x^j\partial y^{i-j}},$$

$$\lim_{\substack{x\to 0\\ y\to 0}}\frac{\partial^i r_\wedge^\infty(x,y)}{\partial x^j\partial y^{i-j}}=0.$$

Thus, all partial derivatives of functions $r_\wedge^\infty(x,y)$ *of arbitrary order exist and are continuous, therefore* $r_\wedge^\infty(x,y)\in C^\infty\left(R^2\right)$.

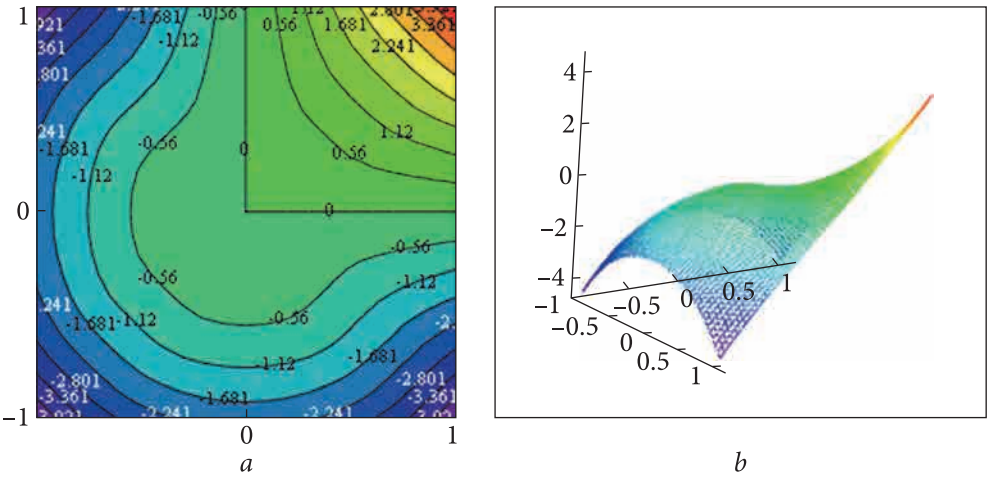

a *b*

Fig. 2.5. Visualization of the function $f(x,y) = x \overset{\infty}{\wedge} y$ graph: *a* — in the form of lines of constant level on the plane xOy; *b* — in the form of a surface in space R^3

It is needed to prove that $r_{\vee}^{\infty}(x,y) \in C^{\infty}\left(R^2\right)$.

Since $r_{\vee}^{\infty}(x,y) = -r_{\vee}^{\infty}(-x,-y)$, then

$$\frac{\partial^i r_{\vee}^{\infty}(x,y)}{\partial x^j \partial y^{i-j}} = \frac{\partial^i (-r_{\wedge}^{\infty}(-x,-y)}{\partial x^j \partial y^{i-j}} = -\frac{\partial^i (r_{\wedge}^{\infty}(-x,-y)}{\partial x^j \partial y^{i-j}} = (-1)^{i+1} \frac{\partial^i r_{\wedge}^{\infty}(-x,-y)}{\partial x^j \partial y^{i-j}}.$$

Based on the fact that all partial derivatives of a function $r_{\wedge}^{\infty}(x,y)$ of arbitrary order exist and are continuous, all partial derivatives of a function $r_{\vee}^{\infty}(x,y)$ of arbitrary order also exist and are continuous. So $r_{\vee}^{\infty}(x,y) \in C^{\infty}\left(R^2\right)$.

The theorem is proved.

Fig. 2.5 shows a visualization of the graph of the R-conjunction function from the system of R-operations R^{∞}.

2.3. Behavior of smooth functions with constant values on non-smooth curves in the vicinity of the corner point

To study the behavior of a smooth function that satisfies the homogeneous Dirichlet boundary value condition at the corner point of the border, the following theorem is proved.

Theorem 2.6.

Suppose that there is a function $f(x,y)$, that is defined in some area $\Omega \subset R^2$, for which the following conditions are met: $f(x,y)\big|_{\gamma} = const$, point (x_0, y_0) — corner point of the curve γ, $0 < \beta < \pi$ — the angle between the semi-tangents [2] to the curve γ at the point (x_0, y_0). Suppose that function $f(x,y)$

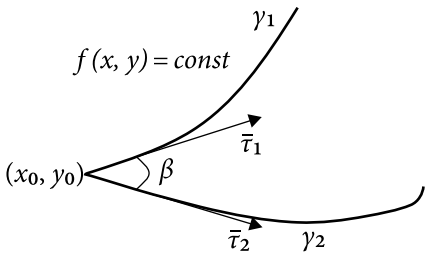

Fig. 2.6. The curve γ, on which $f(x,y)=const$

belongs to a class C^1 in the vicinity of point (x_0,y_0), then $\left.\frac{\partial f(x,y)}{\partial l}\right|_{(x_0,y_0)}=0$,

where l is an arbitrary direction.

Proof.

Suppose that $\gamma=\gamma_1\cup\gamma_2$, $\overline{\tau}_1$ and $\overline{\tau}_2$ are unit vectors relative to the curves γ_1 and γ_2 at point (x_0,y_0) (Fig. 2.6). Suppose that $\overline{\tau}_1\angle\overline{\tau}_2=\beta$, $0<\beta<\pi$.

The derivative of the function $f(x,y)$ is considered at the point (x_0,y_0) in the direction τ_1

$$\frac{\partial f(x_0,y_0)}{\partial\tau_1}=\left(\nabla f(x_0,y_0),\overline{\tau}_1\right)=\frac{\partial f(x_0,y_0)}{\partial x}\tau_{11}+\frac{\partial f(x_0,y_0)}{\partial y}\tau_{12}.$$

Since the function $f(x,y)=0$ at γ_1, then $\frac{\partial f(x_0,y_0)}{\partial\tau_1}=0$. So,

$$\frac{\partial f(x_0,y_0)}{\partial x}\tau_{11}+\frac{\partial f(x_0,y_0)}{\partial y}\tau_{12}=0. \qquad (2.8)$$

Similarly,

$$\frac{\partial f(x_0,y_0)}{\partial x}\tau_{21}+\frac{\partial f(x_0,y_0)}{\partial y}\tau_{22}=0. \qquad (2.9)$$

These equations are a system of linear equations concerning variables $\frac{\partial f(x_0,y_0)}{\partial x}$ and $\frac{\partial f(x_0,y_0)}{\partial y}$.

The determinant of the matrix T of the system (2.8)—(2.9) is written as

$$det\,T=\tau_{11}\tau_{22}-\tau_{12}\tau_{21}=\left(\left(\tau_{11},\tau_{12}\right),\left(\tau_{22},-\tau_{21}\right)\right)=$$

$$=\sqrt{{\tau_{11}}^2+{\tau_{12}}^2}\sqrt{{\tau_{22}}^2+{\tau_{21}}^2}cos\left(\beta+\frac{\pi}{2}\right)=sin\beta\neq 0\ ,\ 0<\beta<\pi\ .$$

Since the determinant of the system is nonzero, the system (2.8—2.9) can be unequivocally solved, and $\begin{cases}\frac{\partial f(x_0,y_0)}{\partial x}=0,\\ \frac{\partial f(x_0,y_0)}{\partial y}=0.\end{cases}$ Some direction l is considered, then $\frac{\partial f(x_0,y_0)}{\partial l}=\frac{1}{\left|\overline{l}\right|}\left(\nabla f(x_0,y_0),\overline{l}\right)=0$.

Thus, **Theorem 2.6** is proved.

During the proof of the R-operations smoothness (2.5—2.6), it was shown that:

$$\left.\frac{\partial^i r_{\wedge}^k(x,y)}{\partial x^j \partial y^{i-j}}\right|_{(0,0)} = \left.\frac{\partial^i r_{\vee}^k(x,y)}{\partial x^j \partial y^{i-j}}\right|_{(0,0)} = 0, \quad \forall i \le k, \quad \forall j \le i.,$$

$$\left.\frac{\partial^i r_{\wedge}^{\infty}(x,y)}{\partial x^j \partial y^{i-j}}\right|_{(0,0)} = \left.\frac{\partial^i r_{\vee}^{\infty}(x,y)}{\partial x^j \partial y^{i-j}}\right|_{(0,0)} = 0, \quad \forall i, \quad \forall j \le i.$$

This property when using R-operations (2.6) to construct the function provides the condition $\frac{\partial^i \left(\omega(x,y)P(x,y)\right)}{\partial x^j \partial y^{i-j}} = 0$ at the corner points of the area, if the function $P(x,y)$ is limited, at $\forall i \le k, \forall j \le i$ for R-operations from the system (2.6) and $\forall i, \forall j \le i$ for R-operations from the system (2.7). This can lead to the incompleteness of basis functions for the structure of a homogeneous Dirichlet problem.

The question arises, is this property common to all smooth R-conjunctions and R-disjunctions or is it a feature of the given systems? To answer this question, a theorem that shows the behavior of a smooth function, which acquires constant values on a non-smooth curve in the vicinity of its corner point, and which changes the sign when passing this curve, is proved.

Theorem 2.7.

Suppose that there is a function $f(x,y)$, that is defined in some area $\Omega \subset R^2$, for which the following condition is met: $f(x,y)\big|_{\gamma} = const$, (x_0, y_0) — corner point of the curve γ $\left(\gamma = \gamma_1 \cup \gamma_2\right)$, $0 < \beta < \pi$ — the angle between the semi-tangents [2] to the curve γ at a point (x_0, y_0), which have a direction from the point (x_0, y_0) along γ. Assume that the function $f(x,y)$ belongs to the class $C^k\left(\Omega\right)$ and passes monotonically through the curve γ (Fig. 2.7). Then

$$\left.\frac{\partial^i f(x,y)}{\partial x^j \partial y^{i-j}}\right|_{(x_0,y_0)} = \left.\frac{\partial^i f(x,y)}{\partial x^j \partial y^{i-j}}\right|_{(x_0,y_0)} = 0, \forall i \le k, \forall j \le i.$$

To prove this theorem, two lemmas are proved (2.2 and 2.3).

Lemma 2.2.

Suppose that $f(x) \in C^k\left(\left[x_0 - h, x_0 + h\right]\right)$ and $f^{(i)}(x_0) = 0, \forall i = 0,1,2,..,k-1.$ Then if $\forall 0 < \varepsilon < h$, $f(x_0 + \varepsilon) > 0$, then $f^{(k)}(x_0) \ge 0$, if $\forall 0 < \varepsilon < h$, $f(x_0 + \varepsilon) < 0$, then $f^{(k)}(x_0) \le 0$.

Proof of the lemma 2.2.

Suppose that for $\forall\, 0 < \varepsilon < h$ the inequality $f(x_0 + \varepsilon) > 0$ is satisfied. Since $f(x_0) = 0$, then $\exists \delta_0$, in which the function $f(x)$ is such that it does not decrease on the segment $\left[x_0, x_0 + \delta_0\right)$.

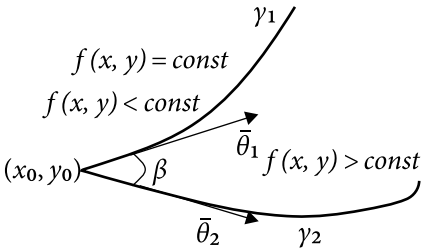

Fig. 2.7. The curve γ, on which $f(x,y)=const$

Consider $\tilde{x}\in\left[x_0, x_0+\delta_0\right)$. Then

$$f'(\tilde{x})=\lim_{\varepsilon\to+0}\frac{f(\tilde{x}+\varepsilon)-f(\tilde{x})}{\varepsilon}\geq 0.$$

Thus, for $\forall 0<\varepsilon<\delta_0$ the inequality $f'(x_0+\varepsilon)\geq 0$ is realized. Since $f(x_0)=0$, then $\exists\delta_1$, at which $f'(x)$ does not decrease in a segment $\left[x_0, x_0+\delta_1\right)$.

Consider $\tilde{x}\in\left[x_0, x_0+\delta_1\right)$. Then

$$f''(\tilde{x})=\lim_{\varepsilon\to+0}\frac{f'(\tilde{x}+\varepsilon)-f'(\tilde{x})}{\varepsilon}\geq 0.$$

The reasoning is continued in the same way. For $\exists\delta_{k-1}$, at which $f^{(k-1)}(x)$ does not decrease on a segment $\left[x_0, x_0+\delta_{k-1}\right)$. Then

$$f^{(k)}(\tilde{x})=\lim_{\varepsilon\to+0}\frac{f^{(k-1)}(\tilde{x}+\varepsilon)-f^{(k-1)}(\tilde{x})}{\varepsilon}\geq 0,\ \forall\tilde{x}\in\left[x_0, x_0+\delta_{k-1}\right).$$

Thus, $f^{(k)}(x_0)\geq 0$.

Suppose $\forall\varepsilon>0\quad f(x_0+\varepsilon)<0$ is satisfied. Then the function $g\left(x\right)=-f\left(x\right)$ $g(x_0+\varepsilon)>0$ is satisfied. Based on the proved above, we have that $g^{(k)}(x_0)\geq 0$. Since $g^{(k)}(x)=-f^{(k)}(x)$, then $f^{(k)}(x_0)\leq 0$.

Lemma 2.2 is proved.

Lemma 2.3.

Assume that there is a function $f(x,y)\in C^k\left(R^2\right)$ and some vector $\overline{\tau}=(\tau_1,\tau_2)$, $\left|\overline{\tau}\right|=1$. Suppose that there is a direction τ along the vector $\overline{\tau}=(\tau_1,\tau_2)$, and suppose that $g(x)=f(\tau_1 x,\tau_2 x)$. Then $\left.\dfrac{\partial^i f(x,y)}{\partial\tau^i}\right|_{(\tau_1 x,\tau_2 x)}=g^{(i)}(x),\quad\forall i\leq k$.

Proof of Lemma 2.3.

Consider

$$\frac{\partial^i f(x,y)}{\partial\tau^i}=\sum_{j=0}^{i}\frac{\partial^i f(x,y)}{\partial x^j\partial y^{i-j}}C_i^j\tau_1^j\tau_2^{i-j},\quad\forall i\leq k.$$

Based on

$$g^{(i)}(x)=\sum_{j=0}^{i}\left.\frac{\partial^i f(x,y)}{\partial x^j\partial y^{i-j}}\right|_{(\tau_1 x,\tau_2 x)}C_i^j\tau_1^j\tau_2^{i-j},\quad\forall i\leq k,$$

we get that

$$\left.\frac{\partial^i f(x,y)}{\partial\tau^i}\right|_{(\tau_1 x,\tau_2 x)}=g^{(i)}(x),\quad\forall i\leq k.$$

Lemma 2.3 is proved.

Proof of theorem 2.7.

Suppose that $\gamma = \gamma_1 \cup \gamma_2$, $\overline{\theta}_1$ and $\overline{\theta}_2$ — unit vectors to curves γ_1 and γ_2 at point (x_0, y_0), such that $\overline{\theta}_1 \angle \overline{\theta}_2 = \beta$, $0 < \beta < \pi$. Suppose for certainty that $f(x,y) > const$ at points corresponding to the angle β (Fig. 2.7). Otherwise, the function $-f(x,y) + 2const$ can be considered. For simplicity, a point $(0,0)$ is taken as a point (x_0, y_0) (for an arbitrary corner point, one can consider the function $f(x - x_0, y - y_0)$) and as a constant, $const = 0$ (for an arbitrary constant, one can consider the function $f(x, y) - const$).

The proof is carried out by the mathematical induction method. This assertion is proved for the case $k = 1$. Two linearly independent vectors $\overline{\tau}_1 = (\tau_{1,1}, \tau_{1,2})$ and $\overline{\tau}_2 = (\tau_{2,1}, \tau_{2,2})$ such that $\overline{\tau}_i = \alpha_i \overline{\theta}_1 + \beta_i \overline{\theta}_2$, $\alpha_i > 0, \beta_i < 0$, $\sqrt{{\tau_{1,1}}^2 + {\tau_{1,2}}^2} = 1$, $\sqrt{{\tau_{2,1}}^2 + {\tau_{2,2}}^2} = 1$ are considered.

The functions $g_1(x) \quad f(\tau_{1,1}x, \tau_{1,2}x)$ and $g_2(x) = f(\tau_{2,1}x, \tau_{2,2}x)$ are considered. Functions $g_1(0) = 0$, $g_2(0) = 0$, $g_1(x) < 0$, $\forall x > 0$, $g_2(x) < 0, \forall x > 0$. Then, according to the lemma 2.2 $g_2'(0) \le 0$. In addition, according to lemma 2.3

$$g_1'(0) = \left.\frac{\partial f(x,y)}{\partial \tau_1}\right|_{(0,0)} \text{ and } g_2'(0) = \left.\frac{\partial f(x,y)}{\partial \tau_2}\right|_{(0,0)}.$$

Thus,

$$\frac{\partial f(0,0)}{\partial \tau_1} = \frac{\partial f(0,0)}{\partial x}\tau_{1,1} + \frac{\partial f(0,0)}{\partial y}\tau_{1,2} \le 0, \tag{2.10}$$

$$\frac{\partial f(0,0)}{\partial \tau_2} = \frac{\partial f(0,0)}{\partial x}\tau_{2,1} + \frac{\partial f(0,0)}{\partial y}\tau_{2,2} \le 0. \tag{2.11}$$

Similarly for vectors $-\overline{\tau}_1 = (-\tau_{1,1}, -\tau_{1,2})$ and $-\overline{\tau}_2 = (-\tau_{2,1}, -\tau_{2,2})$ functions $\tilde{g}_1(x) = f(-\tau_{1,1}x, -\tau_{1,2}x)$ and $g_2(x) = f(-\tau_{2,1}x, -\tau_{2,2}x)$ are considered. Functions $\tilde{g}_1(0) = 0$, $\tilde{g}_2(0) = 0$, $\tilde{g}_1(x) < 0, \quad \forall x > 0$, $\tilde{g}_2(x) < 0, \quad \forall x > 0$. Then, according to lemma 2.2 $\tilde{g}_1'(0) \le 0$, $\tilde{g}_2'(0) \le 0$. In addition, according to lemma 2.3

$$\tilde{g}_1'(0) = \left.\frac{\partial f(x,y)}{\partial(-\tau_1)}\right|_{(0,0)} \text{ and } \tilde{g}_2'(0) = \left.\frac{\partial f(x,y)}{\partial(-\tau_2)}\right|_{(0,0)}.$$

We have

$$\frac{\partial f(0,0)}{\partial(-\tau_1)} = -\frac{\partial f(0,0)}{\partial x}\tau_{1,1} - \frac{\partial f(0,0)}{\partial y}\tau_{1,2} \le 0, \tag{2.12}$$

$$\frac{\partial f(0,0)}{\partial(-\tau_2)} = -\frac{\partial f(0,0)}{\partial x}\tau_{2,1} - \frac{\partial f(0,0)}{\partial y}\tau_{2,2} \le 0. \tag{2.13}$$

So, based on (2.10) — (2.13),

$$\frac{\partial f(0,0)}{\partial x}\tau_{1,1}+\frac{\partial f(0,0)}{\partial y}\tau_{1,2}=0, \tag{2.14}$$

$$\frac{\partial f(0,0)}{\partial x}\tau_{2,1}+\frac{\partial f(0,0)}{\partial y}\tau_{2,2}=0. \tag{2.15}$$

Since the vectors $\overline{\tau}_1=\left(\tau_{1,1},\tau_{1,2}\right)$ and $\overline{\tau}_2=\left(\tau_{2,1},\tau_{2,2}\right)$ — linearly independent, $\det\begin{pmatrix}\tau_{1,1} & \tau_{1,2}\\ \tau_{2,1} & \tau_{2,2}\end{pmatrix}\neq 0$. Therefore, the system (2.14) — (2.15) can be unequivocally solved and $\frac{\partial f(0,0)}{\partial x}=0$, $\frac{\partial f(0,0)}{\partial y}=0$.

Suppose that $\left.\frac{\partial^i f(x,y)}{\partial x^j \partial y^{i-j}}\right|_{(0,0)}=0,\ \forall i\le k-1,\ \forall j\le i$.

Suppose k is even.

$k+1$ pairwise linearly independent vectors $\overline{\tau}_i=\left(\tau_{i,1},\tau_{i,2}\right)$, $i=1,...,k+1$, such that $\overline{\tau}_i=\alpha_i\overline{\theta}_1+\beta_i\overline{\theta}_2$, $\alpha_i>0,\beta_i>0$, $i=1,..,k+1$, $\sqrt{{\tau_{i,1}}^2+{\tau_{i,2}}^2}=1$, $i=1,..,k+1$ are considered.

The functions $g_i(x)=f(\tau_{i,1}x,\tau_{i,2}x)$ are considered. Functions $g_i(0)=0$, $g_i(x)>0,\ \forall x>0$. Also, since $\left.\frac{\partial^l f(x,y)}{\partial x^j \partial y^{l-j}}\right|_{(0,0)}=0,\ \forall l\le k-1,\ \forall j\le l$, then according to lemma 2.3 $g_i^{(l)}(0)=0,\quad \forall i\le k+1,\forall l\le k-1$. Then, according to the lemma 2.2 $g_i^{(k)}(0)\ge 0$. Since, according to lemma 2.3 $g_i^{(k)}(0)=\left.\frac{\partial^k f(x,y)}{\partial \tau_i^k}\right|_{(0,0)}$, then

$$\frac{\partial^k f(0,0)}{\partial \tau_i^k}=\sum_{j=0}^{k}\frac{\partial^k f(0,0)}{\partial x^j \partial y^{k-j}}C_k^j\tau_{i,1}^j\tau_{i,2}^{k-j}\ge 0,\quad \forall i\le k+1. \tag{2.16}$$

Similarly, vectors $-\overline{\tau}_i=\left(-\tau_{i,1},-\tau_{i,2}\right)$, $i=1,...,k+1$ are considered. Thus, functions $\tilde{g}_i(x)=f(-\tau_{i,1}x,-\tau_{i,2}x)$. Functions $\tilde{g}_i(0)=0$, $\tilde{g}_i(x)<0,\ \forall x>0$. Also, since $\left.\frac{\partial^l f(x,y)}{\partial x^j \partial y^{l-j}}\right|_{(0,0)}=0,\quad \forall l\le k-1,\quad \forall j\le l$, then according to lemma 2.3 $\tilde{g}_i^{(l)}(0)=0,\quad \forall i\le k+1,\forall l\le k-1$. Then, according to the lemma 2.2 $\tilde{g}_i^{(k)}(0)\le 0$. Since, according to lemma 2.3 $g_i^{(k)}(0)=\left.\frac{\partial^k f(x,y)}{\partial\left(-\tau_i\right)^k}\right|_{(0,0)}$, then

$$\frac{\partial^k f(0,0)}{\partial\left(-\tau_i\right)^k}=\sum_{j=0}^{k}\frac{\partial^k f(0,0)}{\partial x^j\partial y^{k-j}}C_k^j(-1)^k\tau_{i,1}^j\tau_{i,2}^{k-j}\le 0,\quad \forall i\le k+1. \tag{2.17}$$

Since k is even, based on (2.16) — (2.17) we have

$$\frac{\partial^k f(0,0)}{\partial\tau_i^k}=\sum_{j=0}^{k}\frac{\partial^k f(0,0)}{\partial x^j\partial y^{k-j}}C_k^j\tau_{i,1}^j\tau_{i,2}^{k-j}=0,\quad i=1,...,k+1. \tag{2.18}$$

That is, we have a homogeneous system of linear equations for $\dfrac{\partial^k f(0,0)}{\partial x^j\partial y^{k-j}}$.

The determinant of the matrix T of the corresponding system (2.18):

$$\det \mathrm{T}=\det\begin{pmatrix}
\tau_{1,1}^k & k\tau_{1,1}^{k-1}\tau_{1,2} & \dfrac{k(k-1)}{2}\tau_{1,1}^{k-2}\tau_{1,2}^2 & \dots & C_k^j\tau_{1,1}^{k-j}\tau_{1,2}^j & \dots & k\tau_{1,1}\tau_{1,2}^{k-1} & \tau_{1,2}^k\\
\tau_{2,1}^k & k\tau_{2,1}^{k-1}\tau_{2,2} & \dfrac{k(k-1)}{2}\tau_{2,1}^{k-2}x_{2,2}^2 & \dots & C_k^j\tau_{2,1}^{k-j}\tau_{2,2}^j & \dots & k\tau_{2,1}\tau_{2,2}^{k-1} & \tau_{2,2}^k\\
\tau_{3,1}^k & k\tau_{3,1}^{k-1}\tau_{3,2} & \dfrac{k(k-1)}{2}\tau_{3,1}^{k-2}x_{3,2}^2 & \dots & C_k^j\tau_{3,1}^{k-j}\tau_{3,2}^j & \dots & k\tau_{3,1}\tau_{3,2}^{k-1} & \tau_{3,2}^k\\
\dots & \dots & \dots & & \dots & & \dots & \dots\\
\tau_{k+1,1}^k & k\tau_{k+1,1}^{k-1}\tau_{k+1,2} & \dfrac{k(k-1)}{2}\tau_{k+1,1}^{k-2}\tau_{k+1,2}^2 & \dots & C_k^j\tau_{k+1,1}^{k-j}\tau_{k+1,2}^j & \dots & k\tau_{k+1,1}\tau_{k+1,2}^{k-1} & \tau_{k+1,2}^k
\end{pmatrix}=$$

$$=\left(\prod_{i=0}^{k}C_k^i\right)\det\begin{pmatrix}
\tau_{1,1}^k & \tau_{1,1}^{k-1}\tau_{1,2} & \tau_{1,1}^{k-2}\tau_{1,2}^2 & \dots & \tau_{1,1}\tau_{1,2}^{k-1} & \tau_{1,2}^k\\
\tau_{2,1}^k & \tau_{2,1}^{k-1}\tau_{2,2} & \tau_{2,1}^{k-2}x_{2,2}^2 & \dots & \tau_{2,1}\tau_{2,2}^{k-1} & \tau_{2,2}^k\\
\tau_{3,1}^k & \tau_{3,1}^{k-1}\tau_{3,2} & \tau_{3,1}^{k-2}x_{3,2}^2 & \dots & \tau_{3,1}\tau_{3,2}^{k-1} & \tau_{3,2}^k\\
\dots & \dots & \dots & \dots & \dots & \dots\\
\tau_{k+1,1}^k & \tau_{k+1,1}^{k-1}\tau_{k+1,2} & \tau_{k+1,1}^{k-2}\tau_{k+1,2}^2 & \dots & \tau_{k+1,1}\tau_{k+1,2}^{k-1} & \tau_{k+1,2}^k
\end{pmatrix}=$$

$$=\left(\prod_{i=0}^{k}C_k^i\right)\tau_{1,1}^k\cdot\tau_{2,1}^k\cdot\tau_{3,1}^k\cdot\ldots\cdot\tau_{k+1,1}^k\det\begin{pmatrix}
1 & \dfrac{\tau_{1,2}}{\tau_{1,1}} & \dfrac{\tau_{1,2}^2}{\tau_{1,1}^2} & \dots & \dfrac{\tau_{1,2}^{k-1}}{\tau_{1,1}^{k-1}} & \dfrac{\tau_{1,2}^k}{\tau_{1,1}^k}\\
1 & \dfrac{\tau_{2,2}}{\tau_{2,1}} & \dfrac{\tau_{2,2}^2}{\tau_{2,1}^2} & \dots & \dfrac{\tau_{2,2}^{k-1}}{\tau_{2,1}^{k-1}} & \dfrac{\tau_{2,2}^k}{\tau_{2,1}^k}\\
1 & \dfrac{\tau_{3,2}}{\tau_{3,1}} & \dfrac{\tau_{3,2}^2}{\tau_{3,1}^2} & \dots & \dfrac{\tau_{3,2}^{k-1}}{\tau_{3,1}^{k-1}} & \dfrac{\tau_{3,2}^k}{\tau_{3,1}^k}\\
\dots & \dots & \dots & \dots & \dots & \dots\\
1 & \dfrac{\tau_{k+1,2}}{\tau_{k+1,1}} & \dfrac{\tau_{k+1,2}^2}{\tau_{k+1,1}^2} & \dots & \dfrac{\tau_{k+1,2}^{k-1}}{\tau_{k+1,1}^{k-1}} & \dfrac{\tau_{k+1,2}^k}{\tau_{k+1,1}^k}
\end{pmatrix}.$$

is considered.

The last factor is the Vandermonde determinant [35]. Then

$$\det \mathrm{T} = \left(\prod_{i=0}^{k} C_k^i \right) \tau_{1,1}^k \cdot \tau_{2,1}^k \cdot \tau_{3,1}^k \cdot \ldots \cdot \tau_{k+1,1}^k \prod_{1 \le i < j \le k+1} \left(\frac{\tau_{i,2}}{\tau_{i,1}} - \frac{\tau_{j,2}}{\tau_{j,1}} \right) =$$

$$= \left(\prod_{i=0}^{k} C_k^i \right) \tau_{1,1}^k \cdot \tau_{2,1}^k \cdot \tau_{3,1}^k \cdot \ldots \cdot \tau_{k+1,1}^k \prod_{1 \le i < j \le k+1} \left(\frac{\tau_{i,2}\tau_{j,1} - \tau_{j,2}\tau_{i,1}}{\tau_{i,1}\tau_{j,1}} \right) =$$

$$= \prod_{i=0}^{k} C_k^i \prod_{1 \le i < j \le k+1} \left(\tau_{i,2}\tau_{j,1} - \tau_{j,2}\tau_{i,1} \right).$$

Since vectors $\overline{\tau}_i = \left(\tau_{i,1}, \tau_{i,2} \right)$ — are pairwise linearly independent, then $\det \begin{pmatrix} \tau_{j,1} & \tau_{j,2} \\ \tau_{i,1} & \tau_{i,2} \end{pmatrix} = \tau_{i,2}\tau_{j,1} - \tau_{j,2}\tau_{i,1} \neq 0,\ i \neq j$. Thus, if the determinant of a system) (2.18) is nonzero, then system (2.18) can be unequivocally solved and $\left. \frac{\partial^k f(x,y)}{\partial x^j \partial y^{k-j}} \right|_{(0,0)} =$ $= 0, \quad \forall j \le k$

Suppose that k is odd. Consider $k+1$ pairwise linearly independent vectors $\overline{\tau}_i = \left(\tau_{i,1}, \tau_{i,2} \right), i = 1,...,k+1$, such that $\overline{\tau}_i = \alpha_i \overline{\theta}_1 + \beta_i \overline{\theta}_2,\ \alpha_i > 0, \beta_i < 0,\ i = 1,..,k+1$, $\sqrt{{\tau_{i,1}}^2 + {\tau_{i,2}}^2} = 1, \quad i = 1,..,k+1$ are considered.

Suppose that the functions $g_i(x) = f(\tau_{i,1}x, \tau_{i,2}x)$, and functions $g_i(0) = 0$, $g_i(x) < 0, \forall x > 0$. Also, since $\left. \frac{\partial\, f(x,y)}{\partial x^j \partial y^{l\ j}} \right|_{(0,0)} = 0,\ \forall l \le k-1,\ \forall j \le l$, then according to lemma 2.3 $g_i^{(l)}(0) = 0, \quad \forall i \le k+1, \forall l \le k-1$. Then, according to the lemma 2.2 $g_i^{(k)}(0) \le 0$. Since, according to lemma 2.3 $g_i^{(k)}(0) = \left. \frac{\partial^k f(x,y)}{\partial \tau_i^k} \right|_{(0,0)}$, then

$$\frac{\partial^k f(0,0)}{\partial \tau_i^k} = \sum_{j=0}^{k} \frac{\partial^k f(0,0)}{\partial x^j \partial y^{k-j}} C_k^j \tau_{i,1}^j \tau_{i,2}^{k-j} \le 0, \quad \forall i \le k+1. \qquad (2.19)$$

Similarly, vectors $-\overline{\tau}_i = \left(-\tau_{i,1}, -\tau_{i,2} \right), i = 1,...,k+1$ are considered. Suppose that the functions $\tilde{g}_i(x) = f(\tau_{i,1}x, -\tau_{i,2}x)$, and functions $\tilde{g}_i(0) = 0$, $\tilde{g}_i(x) < 0,$ $\tilde{g}_i(x) < 0, \forall x > 0$. Also, since $\left. \frac{\partial^l f(x,y)}{\partial x^j \partial y^{l-j}} \right|_{(0,0)} = 0,\ \forall l \le k-1, \forall j \le l$, then according

to lemma 2.3 $\tilde{g}_i^{(l)}(0)=0,\ \forall i\le k+1, \forall l\le k-1$. Then, according to the lemma 2.2 $\tilde{g}_i^{(k)}(0)\le 0$. Since according to lemma 2.3

$$g_i^{(k)}(0)=\left.\frac{\partial^k f(x,y)}{\partial\left(-\tau_i\right)^k}\right|_{(0,0)},$$

then

$$\frac{\partial^k f(0,0)}{\partial\left(-\tau_i\right)^k}=\sum_{j=0}^{k}\frac{\partial^k f(0,0)}{\partial x^j\partial y^{k-j}}C_k^j(-1)^k\tau_{i,1}^j\tau_{i,2}^{k-j}\le 0,\quad \forall i\le k+1. \tag{2.20}$$

For odd k, from (2.19)—(2.20) it follows that

$$\frac{\partial^k f(0,0)}{\partial \tau_i^{\,k}}=\sum_{j=0}^{k}\frac{\partial^k f(0,0)}{\partial x^j\partial y^{k-j}}C_k^j\tau_{i,1}^j\tau_{i,2}^{k-j}=0,\quad \forall i\le k+1. \tag{2.21}$$

We have a homogeneous system of linear equations concerning $\frac{\partial^k f(0,0)}{\partial x^j\partial y^{k-j}}$. This system of equations coincides with the system (2.18), so it is solved, and thus $\left.\frac{\partial^k f(x,y)}{\partial x^j\partial y^{k-j}}\right|_{(0,0)}=0,\quad \forall j\le k$.

Thus, it is proved that $\left.\frac{\partial^i f(x,y)}{\partial x^j\partial y^{i-j}}\right|_{(0,0)}=0, \forall i\le k, \forall j\le i$.

Theorem 2.7 is proved.

Based on the proved theorem on the behavior of a smooth function of class C^k, which acquires constant values on a non-smooth curve, it is possible to answer the question on the behavior of C^k-smooth R-conjunctions and R-disjunctions in the vicinity of the point (0, 0).

Theorem 2.8.

For any functions $r_\vee(x,y)$ and $r_{\hat{\wedge}}(x,y)$, which are R-conjunction and R-disjunction and belong to the class $C^{\hat{k}}\left(R^2\right)$, the following conditions are met

$$\left.\frac{\partial^i r_\wedge(x,y)}{\partial x^j\partial y^{i-j}}\right|_{(0,0)}=0,\quad \left.\frac{\partial^i r_\vee(x,y)}{\partial x^j\partial y^{i-j}}\right|_{(0,0)}=0,\quad \forall i\le k,\quad \forall j\le i.$$

Proof.

Suppose that there are some functions $r_\vee(x,y)$ and $r_\wedge(x,y)$, that are C^k-smooth R-conjunction and R-disjunction. The zero-level lines of these functions are considered. They are non-smooth curves at a point $(0,0)$. Functions $r_\vee(x,y)$ and $r_\wedge(x,y)$ when passing their zero level lines change the sign by definition, i.e.

pass them monotonically. Thus, all conditions of the theorem are met.

$$\text{So, } \left.\frac{\partial^i r_{\wedge}(x,y)}{\partial x^j \partial y^{i-j}}\right|_{(0,0)} = 0, \quad \left.\frac{\partial^i r_{\vee}(x,y)}{\partial x^j \partial y^{i-j}}\right|_{(0,0)} = 0, \quad \forall i \le k, \quad \forall j \le i\,.$$

The theorem is proved.

2.4. New system of R-operations

As p increases, the curvature of the given functions along the lines $y = \pm x$ increases (Fig. 2.8).

Normalization preservation is a local property in the vicinity of the R-operations level zero lines, but in the system R_p this property extends into the area, resulting in increased curvature around the lines $y = \pm x$. To overcome this effect, a new system of R-operations, a R_{nk} system, has been proposed. This system has the following form:

$$x \wedge_{nk} y = x + y - \frac{\sum_{i=1}^{n}\left(\left(\sin\left(i\pi/2(n+1)\right)|x|\right)^k + \left(\cos\left(i\pi/2(n+1)\right)|y|\right)^k\right)^{\frac{1}{k}}}{\sum_{i=1}^{n}\cos\left(i\pi/2(n+1)\right)},$$

$$x \vee_{nk} y = x + y + \frac{\sum_{i=1}^{n}\left(\left(\sin\left(i\pi/2(n+1)\right)|x|\right)^k + \left(\cos\left(i\pi/2(n+1)\right)|y|\right)^k\right)^{\frac{1}{k}}}{\sum_{i=1}^{n}\cos\left(i\pi/2(n+1)\right)}, \quad \overline{x} = -x. \tag{2.22}$$

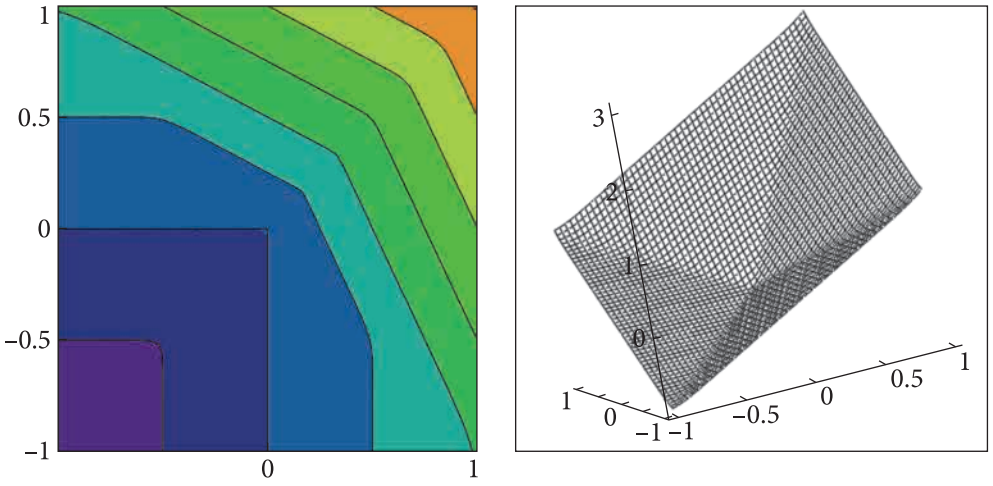

Fig. 2.8. R-disjunction from the system R_p, at $p = 5$

It is needed to prove that these functions are R-operations.

Theorem 2.9. The functions from the system (2.22) are R-operations.

Proof.

It is needed to prove that

$$x \vee_{nk} y = x + y + \frac{\sum_{i=1}^{n}\left(\left(\sin\left(i\pi/2(n+1)\right)|x|\right)^k + \left(\cos\left(i\pi/2(n+1)\right)|y|\right)^k\right)^{\frac{1}{k}}}{\sum_{i=1}^{n}\cos\left(i\pi/2(n+1)\right)}$$

is an R-disjunction. For the R-conjunction, the proof is similar. Denote

$$r_{\vee}^{nk}(x,y) = x \vee_{nk} y = x + y + \frac{\sum_{i=1}^{n}\left(\left(\sin\left(i\pi/2(n+1)\right)|x|\right)^k + \left(\cos\left(i\pi/2(n+1)\right)|y|\right)^k\right)^{\frac{1}{k}}}{\sum_{i=1}^{n}\cos\left(i\pi/2(n+1)\right)}.$$

It is necessary to prove that the following conditions are met:

$$\begin{cases} r_{\vee}^{nk}(x,y) > 0, & (x>0)\vee(y>0), \\ r_{\vee}^{nk}(x,y) < 0, & (x<0)\wedge(y<0), \\ r_{\vee}^{nk}(x,y) > 0, & ((y=0)\wedge(x\geq 0))\vee((x=0)\wedge(y\geq 0)), \\ r_{\vee}^{nk}(x,y) = 0, & ((y=0)\wedge(x<0))\vee((x=0)\wedge(y<0)). \end{cases} \tag{2.23}$$

The case when $(x=0)$ is considered.

$$r_{\vee}^{nk}(0,y) = y + \frac{\sum_{i=1}^{n}\left(\left(\cos\left(i\pi/2(n+1)\right)|y|\right)^k\right)^{\frac{1}{k}}}{\sum_{i=1}^{n}\cos\left(i\pi/2(n+1)\right)} = y + \frac{|y|\sum_{i=1}^{n}\cos\left(i\pi/2(n+1)\right)}{\sum_{i=1}^{n}\cos\left(i\pi/2(n+1)\right)} = y + |y|.$$

Then, $\begin{cases} r_{\vee}^{nk}(0,y) = 0, & y \leq 0; \\ r_{\vee}^{nk}(0,y) > 0, & y > 0. \end{cases}$. The case when $(y=0)$ is considered.

$$r_{\vee}^{nk}(x,0) = x + \frac{\sum_{i=1}^{n}\left(\left(\sin\left(i\pi/2(n+1)\right)|x|\right)^k\right)^{\frac{1}{k}}}{\sum_{i=1}^{n}\cos\left(i\pi/2(n+1)\right)} = y + \frac{|x|\sum_{i=1}^{n}\sin\left(i\pi/2(n+1)\right)}{\sum_{i=1}^{n}\cos\left(i\pi/2(n+1)\right)} = x + |x|.$$

The expression $\dfrac{\sum_{i=1}^{n}\sin\left(i\pi/2(n+1)\right)}{\sum_{i=1}^{n}\cos\left(i\pi/2(n+1)\right)}$ is considered. The reduction formula $\cos(\alpha)=\sin\left(\dfrac{\pi}{2}-\alpha\right)$ is used. Then

$$\frac{\sum_{i=1}^{n}\sin\left(\dfrac{i\pi}{2(n+1)}\right)}{\sum_{i=1}^{n}\sin\left(\dfrac{\pi}{2}-\dfrac{i\pi}{2(n+1)}\right)}=\frac{\sum_{i=1}^{n}\sin\left(\dfrac{i\pi}{2(n+1)}\right)}{\sum_{i=1}^{n}\sin\left(\dfrac{\pi(n+1)-i\pi}{2(n+1)}\right)}=\frac{\sum_{i=1}^{n}\sin\left(\dfrac{i\pi}{2(n+1)}\right)}{\sum_{i=1}^{n}\sin\left(\dfrac{\pi(n+1-i)}{2(n+1)}\right)}.$$

If the index in the denominator gets renumbered in reverse order, we get that

$$\frac{\sum_{i=1}^{n}\sin\left(\dfrac{i\pi}{2(n+1)}\right)}{\sum_{i=1}^{n}\sin\left(\dfrac{\pi(n+1-i)}{2(n+1)}\right)}=\frac{\sum_{i=1}^{n}\sin\left(\dfrac{i\pi}{2(n+1)}\right)}{\sum_{j=1}^{n}\sin\left(\dfrac{j\pi}{2(n+1)}\right)}=1.$$

Then,

$$r_{\vee}^{nk}(x,0)=y+\frac{|x|\sum_{i=1}^{n}\sin\left(i\pi/2(n+1)\right)}{\sum_{i=1}^{n}\cos\left(i\pi/2(n+1)\right)}=x+|x|.$$

That is,

$$\begin{cases} r_{\vee}^{nk}(x,0)=0, & x\le 0;\\ r_{\vee}^{nk}(x,0)>0, & x>0. \end{cases}$$

The case $(x>0)\vee(y>0)$ is considered.

$$r_{\vee}^{nk}(x,y)=x+y+\frac{\sum_{i=1}^{n}\left(\left(\sin\left(i\pi/2(n+1)\right)|x|\right)^{k}+\left(\cos\left(i\pi/2(n+1)\right)|y|\right)^{k}\right)^{\frac{1}{k}}}{\sum_{i=1}^{n}\cos\left(i\pi/2(n+1)\right)}>0.$$

The case $(x<0)\vee(y<0)$ is considered.

$$r_{\vee}{}^{nk}(x,y)=x+y+\frac{\sum_{i=1}^{n}\left(\left(\sin\left(i\pi/2(n+1)\right)|x|\right)^{k}+\left(\cos\left(i\pi/2(n+1)\right)|y|\right)^{k}\right)^{\frac{1}{k}}}{\sum_{i=1}^{n}\cos\left(i\pi/2(n+1)\right)}=$$

$$=-\left(|x|+|y|\right)+\frac{\sum_{i=1}^{n}\left(\left(\sin\left(i\pi/2(n+1)\right)|x|\right)^{k}+\left(\cos\left(i\pi/2(n+1)\right)|y|\right)^{k}\right)^{\frac{1}{k}}}{\sum_{i=1}^{n}\cos\left(i\pi/2(n+1)\right)}.$$

$$\frac{\sum_{i=1}^{n}\left(\left(\sin\left(i\pi/2(n+1)\right)|x|\right)^{k}+\left(\cos\left(i\pi/2(n+1)\right)|y|\right)^{k}\right)^{\frac{1}{k}}}{\sum_{i=1}^{n}\cos\left(i\pi/2(n+1)\right)}\le$$

$$\le\frac{\sum_{i=1}^{n}\left(\left(\sin\left(i\pi/2(n+1)\right)|x|\right)+\left(\cos\left(i\pi/2(n+1)\right)|y|\right)\right)}{\sum_{i=1}^{n}\cos\left(i\pi/2(n+1)\right)}=$$

$$=\frac{\sum_{i=1}^{n}\left(\sin\left(i\pi/2(n+1)\right)|x|\right)+\sum_{i=1}^{n}\left(\cos\left(i\pi/2(n+1)\right)|y|\right)}{\sum_{i=1}^{n}\cos\left(i\pi/2(n+1)\right)}=$$

$$=\frac{\sum_{i=1}^{n}\left(\sin\left(i\pi/2(n+1)\right)|x|\right)}{\sum_{i=1}^{n}\cos\left(i\pi/2(n+1)\right)}+\frac{\sum_{i=1}^{n}\left(\cos\left(i\pi/2(n+1)\right)|y|\right)}{\sum_{i=1}^{n}\cos\left(i\pi/2(n+1)\right)}=$$

$$=\frac{|x|\sum_{i=1}^{n}\sin\left(i\pi/2(n+1)\right)}{\sum_{i=1}^{n}\cos\left(i\pi/2(n+1)\right)}+\frac{|y|\sum_{i=1}^{n}\cos\left(i\pi/2(n+1)\right)}{\sum_{i=1}^{n}\cos\left(i\pi/2(n+1)\right)}=|x|+|y|.$$

Thus,

$$r_{\vee}^{nk}(x,y)=x+y+\frac{\sum_{i=1}^{n}\left(\left(\sin\left(i\pi/2(n+1)\right)|x|\right)^{k}+\left(\cos\left(i\pi/2(n+1)\right)|y|\right)^{k}\right)^{\frac{1}{k}}}{\sum_{i=1}^{n}\cos\left(i\pi/2(n+1)\right)}=$$

$$=-\left(|x|+|y|\right)+\frac{\sum_{i=1}^{n}\left(\left(\sin\left(i\pi/2(n+1)\right)|x|\right)^{k}+\left(\cos\left(i\pi/2(n+1)\right)|y|\right)^{k}\right)^{\frac{1}{k}}}{\sum_{i=1}^{n}\cos\left(i\pi/2(n+1)\right)}\leq$$

$$\leq-\left(|x|+|y|\right)+|x|+|y|=0.$$

The fraction

$$\frac{\sum_{i=1}^{n}\left(\left(\sin\left(i\pi/2(n+1)\right)|x|\right)^{k}+\left(\cos\left(i\pi/2(n+1)\right)|y|\right)^{k}\right)^{\frac{1}{k}}}{\sum_{i=1}^{n}\cos\left(i\pi/2(n+1)\right)}\geq$$

$$\geq\frac{\sum_{i=1}^{n}\left(\left(\sin\left(i\pi/2(n+1)\right)|x|\right)^{k}\right)^{\frac{1}{k}}}{\sum_{i=1}^{n}\cos\left(i\pi/2(n+1)\right)}=\frac{|x|\sum_{i=1}^{n}\sin\left(i\pi/2(n+1)\right)}{\sum_{i=1}^{n}\cos\left(i\pi/2(n+1)\right)}=|x|$$

is considered. Similarly

$$\frac{\sum_{i=1}^{n}\left(\left(\sin\left(i\pi/2(n+1)\right)|x|\right)^{k}+\left(\cos\left(i\pi/2(n+1)\right)|y|\right)^{k}\right)^{\frac{1}{k}}}{\sum_{i=1}^{n}\cos\left(i\pi/2(n+1)\right)}\geq$$

$$\geq\frac{\sum_{i=1}^{n}\left(\left(\cos\left(i\pi/2(n+1)\right)|y|\right)^{k}\right)^{\frac{1}{k}}}{\sum_{i=1}^{n}\cos\left(i\pi/2(n+1)\right)}=\frac{|y|\sum_{i=1}^{n}\cos\left(i\pi/2(n+1)\right)}{\sum_{i=1}^{n}\cos\left(i\pi/2(n+1)\right)}=|y|.$$

So,

$$\frac{\sum_{i=1}^{n}\left(\left(\sin\left(i\pi/2(n+1)\right)|x|\right)^k+\left(\cos\left(i\pi/2(n+1)\right)|y|\right)^k\right)^{\frac{1}{k}}}{\sum_{i=1}^{n}\cos\left(i\pi/2(n+1)\right)}\geq\max\{|x|,|y|\}.$$

The case when $(x<0)\vee(y>0)$ is considered.

$$r_{\vee}{}^{nk}(x,y)=x+y+\frac{\sum_{i=1}^{n}\left(\left(\sin\left(i\pi/2(n+1)\right)|x|\right)^k+\left(\cos\left(i\pi/2(n+1)\right)|y|\right)^k\right)^{\frac{1}{k}}}{\sum_{i=1}^{n}\cos\left(i\pi/2(n+1)\right)}=$$

$$=\left(|y|-|x|\right)+\frac{\sum_{i=1}^{n}\left(\left(\sin\left(i\pi/2(n+1)\right)|x|\right)^k+\left(\cos\left(i\pi/2(n+1)\right)|y|\right)^k\right)^{\frac{1}{k}}}{\sum_{i=1}^{n}\cos\left(i\pi/2(n+1)\right)}\geq$$

$$\geq\left(|y|-|x|\right)+\max\{|x|,|y|\}>0.$$

The case when $(x>0)\vee(y<0)$ is considered.

$$r_{\vee}{}^{nk}(x,y)=x+y+\frac{\sum_{i=1}^{n}\left(\left(\sin\left(i\pi/2(n+1)\right)|x|\right)^k+\left(\cos\left(i\pi/2(n+1)\right)|y|\right)^k\right)^{\frac{1}{k}}}{\sum_{i=1}^{n}\cos\left(i\pi/2(n+1)\right)}=$$

$$=\left(|x|-|y|\right)+\frac{\sum_{i=1}^{n}\left(\left(\sin\left(i\pi/2(n+1)\right)|x|\right)^k+\left(\cos\left(i\pi/2(n+1)\right)|y|\right)^k\right)^{\frac{1}{k}}}{\sum_{i=1}^{n}\cos\left(i\pi/2(n+1)\right)}\geq$$

$$\geq\left(|x|-|y|\right)+\max\{|x|,|y|\}>0.$$

Thus, it is proved that conditions (2.23) are met. That is, functions

$$x\vee_{nk}y=x+y+\frac{\sum_{i=1}^{n}\left(\left(\sin\left(i\pi/2(n+1)\right)|x|\right)^k+\left(\cos\left(i\pi/2(n+1)\right)|y|\right)^k\right)^{\frac{1}{k}}}{\sum_{i=1}^{n}\cos\left(i\pi/2(n+1)\right)}$$

are R-disjunctions, for any n,k.

Theorem 2.9 is proved.

Fig. 2.9—2.18 show graphs of R-operations with different values of *n* and *k*.

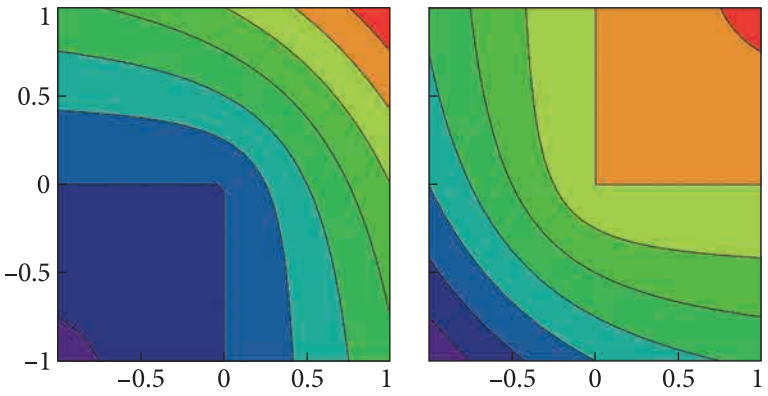

Fig. 2.9. Graphs of R-operations at $n=1$ and $k=2$ (in this case, R-operations coincide with the classical system R_0)

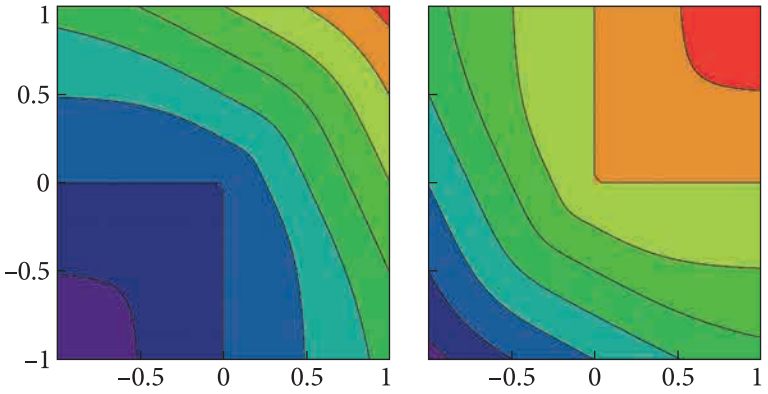

Fig. 2.10. Graphs of R-operations at $n=1$ and $k=4$ (in this case, R-operations coincide with the system R_p, $p=2$)

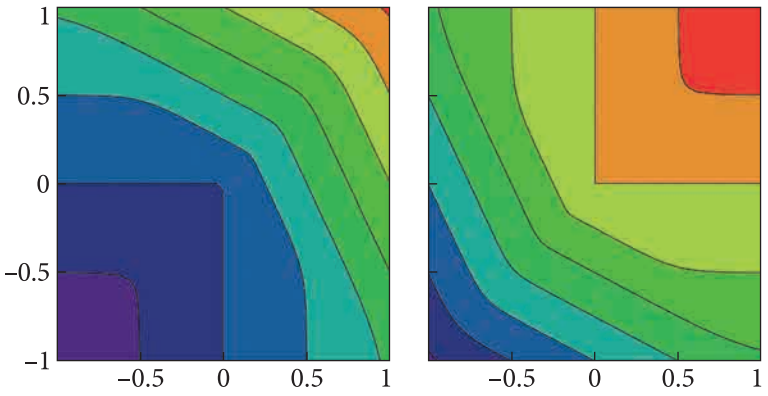

Fig. 2.11. Graphs of R-operations at $n=1$ and $k=8$ (in this case, R-operations coincide with the system R_p, $p=4$)

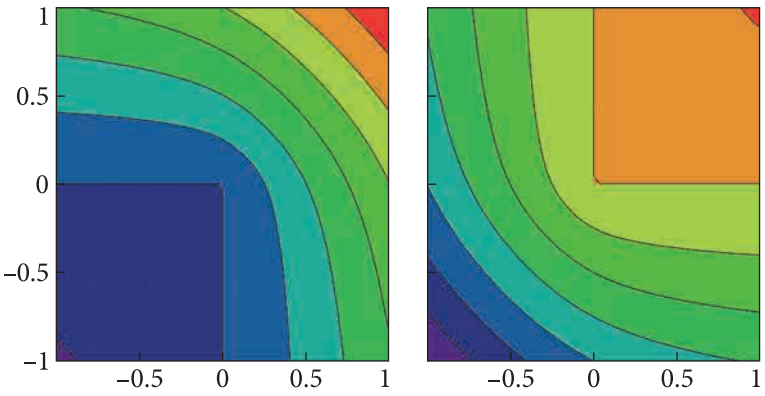

Fig. 2.12. Graphs of R-operations at $n = 2$ and $k = 2$

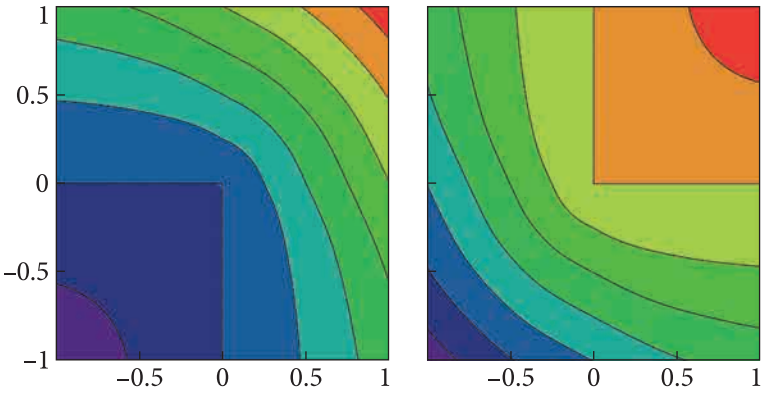

Fig. 2.13. Graphs of R-operations at $n = 2$ and $k = 4$

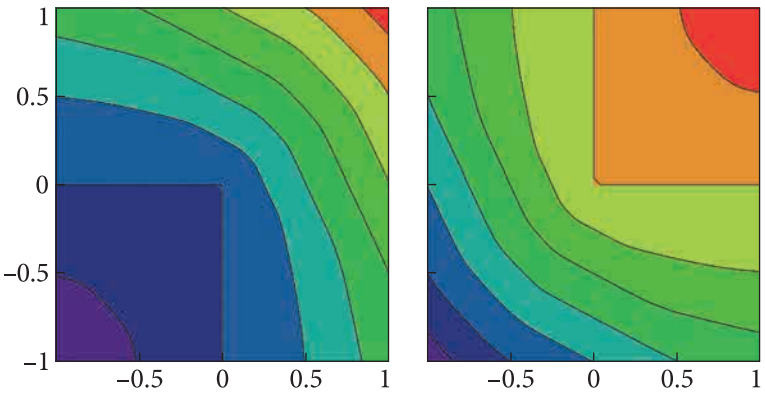

Fig. 2.14. Graphs of R-operations at $n = 2$ and $k = 8$

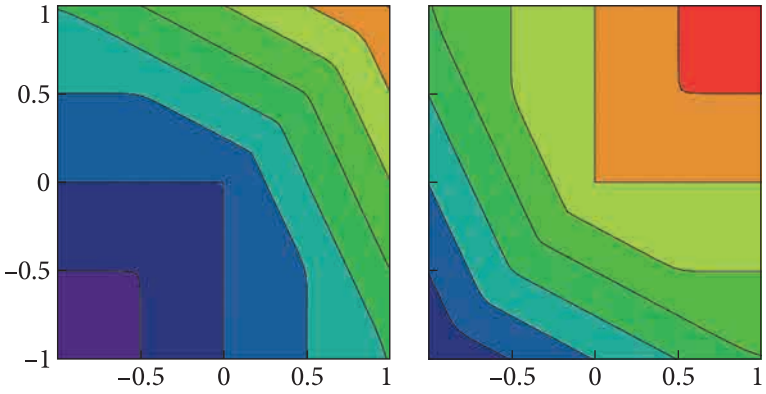

Fig.2.15. Graphs of R-operations at $n=1$ and $k=20$ (in this case, R-operations coincide with the system R_p, $p=10$)

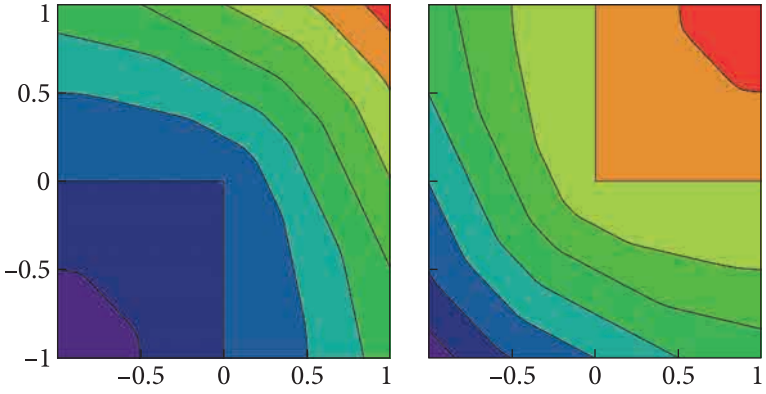

Fig. 2.16. Graphs of R-operations at $n=2$ and $k=20$

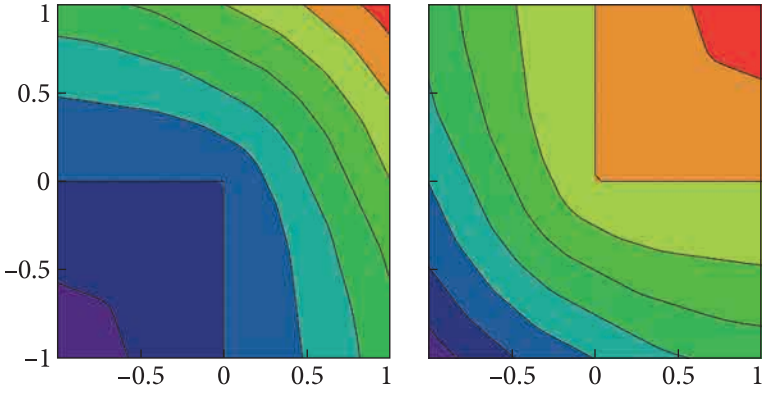

Fig. 2.17. Graphs of R-operations at $n=3$ and $k=20$

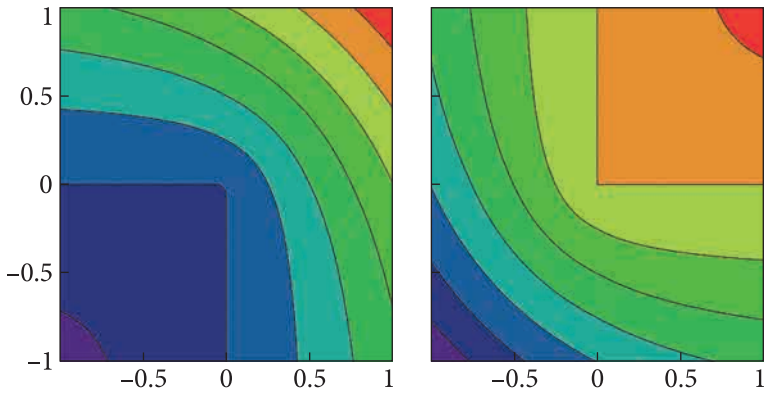

Fig. 2.18. Graphs of R-operations at $n=20$ and $k=20$

It is needed to prove that the given functions are normalized to a given order. So,

$$x\vee_{nk} y = x + y + \frac{\sum_{i=1}^{n}\left(\left(\sin\left(i\pi/2(n+1)\right)|x|\right)^k + \left(\cos\left(i\pi/2(n+1)\right)|y|\right)^k\right)^{\frac{1}{k}}}{\sum_{i=1}^{n}\cos\left(i\pi/2(n+1)\right)}$$

is a normalized function up to *k-1* order. It is necessary to prove that

$$\begin{cases}
\dfrac{\partial\left(x\vee_{nk} y\right)}{\partial x}=1, \quad (x=0)\wedge(y<0),\\
\dfrac{\partial^2\left(x\vee_{nk} y\right)}{\partial x^2}=0, \quad (x=0)\wedge(y<0),\\
\ldots.\\
\dfrac{\partial^{k-1}\left(x\vee_{nk} y\right)}{\partial x^{k-1}}=0, \quad (x=0)\wedge(y<0),\\
\dfrac{\partial\left(x\vee_{nk} y\right)}{\partial y}=1, \quad (x<0)\wedge(y=0),\\
\dfrac{\partial^2\left(x\vee_{nk} y\right)}{\partial y^2}=0, \quad (x<0)\wedge(y=0),\\
\ldots.\\
\dfrac{\partial^{k-1}\left(x\vee_{nk} y\right)}{\partial y^{k-1}}=0, \quad (x<0)\wedge(y=0).
\end{cases}$$

Denote

$$x \vee_{nk} y = f_1(x,y) + f_2(x,y),$$

where

$$f_1(x,y) = x + y,$$

$$f_2(x,y) = \frac{\sum_{i=1}^{n}\left(\left(\sin\left(i\pi/2(n+1)\right)|x|\right)^k + \left(\cos\left(i\pi/2(n+1)\right)|y|\right)^k\right)^{\frac{1}{k}}}{\sum_{i=1}^{n}\cos\left(i\pi/2(n+1)\right)}.$$

$\frac{\partial f_1(x,y)}{\partial x} = 1$, $\frac{\partial f_1(x,y)}{\partial y} = 1$ are considered. That is, for the function $f_1(x,y) = x + y$ the given conditions are met. Therefore, it is necessary to prove that

$$\begin{cases} \frac{\partial f_2(x,y)}{\partial x} = 0, & (x=0)\wedge(y<0), \\ \frac{\partial^2 f_2(x,y)}{\partial x^2} = 0, & (x=0)\wedge(y<0), \\ \ldots. \\ \frac{\partial^{k-1} f_2(x,y)}{\partial x^{k-1}} = 0, & (x=0)\wedge(y<0), \\ \frac{\partial f_2(x,y)}{\partial y} = 0, & (x<0)\wedge(y=0), \\ \frac{\partial^2 f_2(x,y)}{\partial y^2} = 0, & (x<0)\wedge(y=0), \\ \ldots. \\ \frac{\partial^{k-1} f_2(x,y)}{\partial y^{k-1}} = 0, & (x<0)\wedge(y=0). \end{cases}$$

The function $f_2(x,y)$ consists of the sum of terms of the form $\beta\left(\alpha_1|x|^k + \alpha_2|y|^k\right)^{\frac{1}{k}}$. Since each of the terms meets these conditions, the function $f_2(x,y)$ also meets these conditions. That is, it follows that $x \vee_{nk} y$ are normalized up to $k-1$ order.

The functions of the given system of R-operations increase the curvature when increasing the order of normalization, i.e. the parameter k, which can be seen in Fig. 2.15, 2.16, and 2.17. However, as can be seen from Fig. 2.15 —2.18, when increasing the parameter n, the system R_{nk} is close in view to the functions R_0 of the classical system of R-operations. It is needed to prove that this fact is not accidental.

Theorem 2.10. Functions from the system R_{nk} coincide point by point with functions from the system R_0.

Proof.

The proof is carried out on the example of R-disjunction. The functions $x \vee_0 y = x + y + \sqrt{x^2 + y^2}$ and

$$x \vee_{nk} y = x + y + \frac{\sum_{i=1}^{n}\left(\left(\sin\left(i\pi/2(n+1)\right)|x|\right)^k + \left(\cos\left(i\pi/2(n+1)\right)|y|\right)^k\right)^{\frac{1}{k}}}{\sum_{i=1}^{n}\cos\left(i\pi/2(n+1)\right)}$$

are considered.

Move on to the polar coordinate system by replacement:

$$\begin{cases} x = r\cos(\phi), \\ y = r\sin(\phi), \end{cases}$$

$$x \vee_0 y = r\cos(\phi) + r\sin(\phi) + r,$$

$$x \vee_{nk} y = r\cos(\phi) + r\sin(\phi) +$$

$$+\frac{\sum_{i=1}^{n}\left(\left(\sin\left(i\pi/2(n+1)\right)|r\cos(\phi)|\right)^k + \left(\cos\left(i\pi/2(n+1)\right)|r\sin(\phi)|\right)^k\right)^{\frac{1}{k}}}{\sum_{i=1}^{n}\cos\left(i\pi/2(n+1)\right)} =$$

$$= r\cos(\phi) + r\sin(\phi) +$$

$$+\frac{r\sum_{i=1}^{n}\left(\left(\sin\left(i\pi/2(n+1)\right)|\cos(\phi)|\right)^k + \left(\cos\left(i\pi/2(n+1)\right)|\sin(\phi)|\right)^k\right)^{\frac{1}{k}}}{\sum_{i=1}^{n}\cos\left(i\pi/2(n+1)\right)}.$$

It is needed to prove that

$$\frac{\sum_{i=1}^{n}\left(\left(\sin\left(i\pi/2(n+1)\right)\left|\cos(\phi)\right|\right)^{k}+\left(\cos\left(i\pi/2(n+1)\right)\left|\sin(\phi)\right|\right)^{k}\right)^{\frac{1}{k}}}{\sum_{i=1}^{n}\cos\left(i\pi/2(n+1)\right)}\xrightarrow[\substack{n\to\infty\\k\to\infty}]{}1.$$

A limit transition at $k\to\infty$ is made.

$$\lim_{k\to\infty}\frac{\sum_{i=1}^{n}\left(\left(\sin\left(i\pi/2(n+1)\right)\left|\cos(\phi)\right|\right)^{k}+\left(\cos\left(i\pi/2(n+1)\right)\left|\sin(\phi)\right|\right)^{k}\right)^{\frac{1}{k}}}{\sum_{i=1}^{n}\cos\left(i\pi/2(n+1)\right)}=$$

$$=\frac{\sum_{i=1}^{n}\left(\max\left(\left|\sin\left(i\pi/2(n+1)\right)\cos(\phi)\right|,\left|\cos\left(i\pi/2(n+1)\right)\sin(\phi)\right|\right)\right)}{\sum_{i=1}^{n}\cos\left(i\pi/2(n+1)\right)}. \qquad (2.24)$$

Consider

$$\lim_{n\to\infty}\frac{\sum_{i=1}^{n}\cos\left(\frac{i\pi}{2(n+1)}\right)}{\frac{2(n+1)}{\pi}}=\lim_{n\to\infty}\frac{\pi}{2(n+1)}\sum_{i=1}^{n}\cos\left(\frac{i\pi}{2(n+1)}\right)=\int_{0}^{\frac{\pi}{2}}\cos(x)dx=1.$$

We get that

$$\sum_{i=1}^{n}\cos\left(\frac{i\pi}{2(n+1)}\right)\sim\frac{2n}{\pi}. \qquad (2.25)$$

Consider $\max\left(\left|\sin\left(i\pi/2(n+1)\right)\cos(\phi)\right|,\left|\cos\left(i\pi/2(n+1)\right)\sin(\phi)\right|\right)$. The value of *i*, at which

$$\left|\sin\left(i\pi/2(n+1)\right)\cos(\phi)\right|\geq\left|\cos\left(i\pi/2(n+1)\right)\sin(\phi)\right|,$$

$$\left|\sin\left(i\pi/2(n+1)\right)\right|\left|\cos(\phi)\right|\geq\left|\cos\left(i\pi/2(n+1)\right)\right|\left|\sin(\phi)\right|,$$

$$\left|tg\left(i\pi/2(n+1)\right)\right|\geq\left|tg(\phi)\right|$$

is found.

Denote $\phi^* = arctg\left(\left|tg\left(\phi\right)\right|\right)$. Then

$$\frac{i\pi}{2(n+1)} \geq \phi^*,\ i \geq \frac{2(n+1)}{\pi}\phi^*,$$

$$\max\left(\left|\sin\left(i\pi/2(n+1)\right)\cos(\phi)\right|,\left|\cos\left(i\pi/2(n+1)\right)\sin(\phi)\right|\right) =$$

$$= \begin{cases} \left|\sin\left(i\pi/2(n+1)\right)\cos(\phi)\right|, i \geq \dfrac{2(n+1)}{\pi}\phi^*, \\ \left|\cos\left(i\pi/2(n+1)\right)\sin(\phi)\right|, i < \dfrac{2(n+1)}{\pi}\phi^*, \end{cases}$$

$$\sum_{i=1}^{n}\left(\max\left(\left|\sin\left(i\pi/2(n+1)\right)\cos(\phi)\right|,\left|\cos\left(i\pi/2(n+1)\right)\sin(\phi)\right|\right)\right) =$$

$$= \sum_{i=1}^{\left[\frac{2(n+1)}{\pi}\phi^*\right]}\left(\left|\cos\left(i\pi/2(n+1)\right)\sin(\phi)\right|\right) + \sum_{i=\left[\frac{2(n+1)}{\pi}\phi^*\right]}^{n}\left(\left|\sin\left(i\pi/2(n+1)\right)\cos(\phi)\right|\right).$$

$$\lim_{n\to\infty}\frac{\sum_{i=1}^{\left[\frac{2(n+1)}{\pi}\phi^*\right]}\left(\left|\cos\left(i\pi/2(n+1)\right)\sin(\phi)\right|\right) + \sum_{i=\left[\frac{2(n+1)}{\pi}\phi^*\right]}^{n}\left(\left|\sin\left(i\pi/2(n+1)\right)\cos(\phi)\right|\right).}{\frac{2(n+1)}{\pi}} =$$

$$= \lim_{n\to\infty}\left(\left|\sin(\phi)\right|\frac{\pi}{2(n+1)}\sum_{i=1}^{\left[\frac{2(n+1)}{\pi}\phi^*\right]}\left(\left|\cos\left(i\pi/2(n+1)\right)\right|\right) + \right.$$

$$\left. + \left|\cos(\phi)\right|\sum_{i=\left[\frac{2(n+1)}{\pi}\phi^*\right]}^{n}\left(\left|\sin\left(i\pi/2(n+1)\right)\right|\right)\right) =$$

$$= \left|\sin(\phi)\right|\int_0^{\phi^*}\cos(x)dx + \left|\cos(\phi)\right|\int_{\phi^*}^{\frac{\pi}{2}}\sin(x)dx = \left|\sin(\phi)\right|\sin\left(\phi^*\right) + \left|\cos(\phi)\right|\cos\left(\phi^*\right) =$$

$$= \left(\sin(\phi)\right)^2 + \left(\cos(\phi)\right)^2 = 1.$$

Thus (2.25) is met, i.e.

$$\sum_{i=1}^{n}\left(\max\left(\left|\sin\left(i\pi/2(n+1)\right)\cos(\phi)\right|,\left|\cos\left(i\pi/2(n+1)\right)\sin(\phi)\right|\right)\right) \sim \frac{2n}{\pi}. \qquad (2.26)$$

A limit transition in (2.24) is made at $n \to \infty$, and (2.25) and (2.26) are used.

$$\lim_{\substack{k\to\infty \\ n\to\infty}} \frac{\sum_{i=1}^{n}\left(\left(\sin\left(i\pi/2(n+1)\right)\left|\cos(\phi)\right|\right)^{k}+\left(\cos\left(i\pi/2(n+1)\right)\left|\sin(\phi)\right|\right)^{k}\right)^{\frac{1}{k}}}{\sum_{i=1}^{n}\cos\left(i\pi/2(n+1)\right)} =$$

$$\lim_{n\to\infty} \frac{\sum_{i=1}^{n}\left(\max\left(\left|\sin\left(i\pi/2(n+1)\right)\cos(\phi)\right|,\left|\cos\left(i\pi/2(n+1)\right)\sin(\phi)\right|\right)\right)}{\sum_{i=1}^{n}\cos\left(i\pi/2(n+1)\right)} = \frac{\left(\frac{2n}{\pi}\right)}{\left(\frac{2n}{\pi}\right)} = 1.$$

Theorem 2.10 is proved.

Thus, it is possible to conclude that the functions of the new system of R-operations R_{nk} have the following properties: when increasing the order of normalization, i.e. parameter *k*, the curvature increases; they coincide with the functions of the classical R-operations system R_0 point by point.

CHAPTER 3

METHOD OF CONSTRUCTION OF BORDER BASIC ELEMENTS BASED ON CUBIC B-SPLINES

3.1. Construction of boundary basic elements for one-dimensional boundary value problems with different boundary conditions

The problem of approximation in the domain of some function that satisfies certain boundary conditions is considered. For these purposes, a method for constructing a basis based on cubic B-splines has been developed [1, 10, 28, 44]. The new basis consists of B-splines (if their carriers belong to the closure of the domain) and elements that determine the function behavior in the vicinity of the area border, i.e. the boundary basic elements. B-splines, the carriers of which belong to the domain closure, provide an approximation in some region that belongs to the area. Boundary basic elements satisfy the boundary conditions of the problem and also take into account the docking with the basic elements within the area. Thus, the method of construction of the basis is reduced to the construction of boundary basic elements.

The problem of constructing a basis based on cubic B-splines for approximation of functions, which are solutions of one-dimensional boundary value problems for an ordinary differential equation (ODE), is considered.

Possible cases of boundary conditions at a certain point x_1 are considered.

One boundary condition can be written as follows:

$$\left\{ a_0^1 u(x) + a_1^1 u'(x) + a_2^1 u''(x) \Big|_{x=x_1} = b_0 \right. . \tag{3.1}$$

The two boundary conditions can be written as follows:

$$\begin{cases} a_0^1 u(x) + a_1^1 u'(x) + a_2^1 u''(x) \Big|_{x=x_1} = b_1, \\ a_0^2 u(x) + a_1^2 u'(x) + a_2^2 u''(x) \Big|_{x=x_1} = b_2, \end{cases} \tag{3.2}$$

where $\left(a_0^1, a_1^1, a_2^1\right)$ and $\left(a_0^2, a_1^2, a_2^2\right)$ — linearly independent vectors.

Three boundary conditions are written in the form

$$\begin{cases} a_0^1 u(x) + a_1^1 u'(x) + a_2^1 u''(x)\Big|_{x=x_1} = b_1, \\ a_0^2 u(x) + a_1^2 u'(x) + a_2^2 u''(x)\Big|_{x=x_1} = b_2, \\ a_0^3 u(x) + a_1^3 u'(x) + a_2^3 u''(x)\Big|_{x=x_1} = b_3, \end{cases} \tag{3.3}$$

where $\left(a_0^1, a_1^1, a_2^1\right)$, $\left(a_0^2, a_1^2, a_2^2\right)$ i $\left(a_0^3, a_1^3, a_2^3\right)$ — linearly independent vectors.

Boundary conditions of the form (3.2) ($k_2^2 \neq 0, k_0^1 \neq 0$) and (3.3) can be brought to the following form:

$$\begin{cases} \tilde{a}_0^1 u(x) + \tilde{a}_1^1 u'(x)\Big|_{x=x_1} = \tilde{b}_1, \\ \tilde{a}_1^2 u'(x) + \tilde{a}_2^2 u''(x)\Big|_{x=x_1} = \tilde{b}_2; \end{cases} \tag{3.4}$$

$$\begin{cases} u(x)\Big|_{x=x_1} = \tilde{b}_1, \\ u'(x)\Big|_{x=x_1} = \tilde{b}_2, \\ u''(x)\Big|_{x=x_1} = \tilde{b}_3. \end{cases} \tag{3.5}$$

The given conditions can be reduced to homogeneous

$$\left\{k_0^1 u(x) + k_1^1 u'(x) + k_2^1 u''(x)\right\}\Big|_{x=x_1} = 0 \tag{3.6}$$

$$\begin{cases} k_0^1 u(x) + k_1^1 u'(x)\Big|_{x=x_1} = 0, \\ k_1^2 u'(x) + k_2^2 u''(x)\Big|_{x=x_1} = 0; \end{cases} \tag{3.7}$$

$$\begin{cases} u(x)\Big|_{x=x_1} = 0, \\ u'(x)\Big|_{x=x_1} = 0, \\ u''(x)\Big|_{x=x_1} = 0. \end{cases} \tag{3.8}$$

The problem of building a basis based on the cubic B-splines $\{\varphi_i\}$ with a carrier diameter $2h$, to approximate functions that satisfy the boundary condition (3.6), or the boundary conditions (3.7), or (3.8) is considered.

Suppose that there is space for cubic splines of defect 1 $S_{3,1}(\Delta)$, defined on the segment $[x_1, x_2]$, where $\Delta = \left\{x_1, x_1 + \frac{h}{2}, x_1 + h, ..., x_2\right\}$ — uniform segment splitting $[x_1, x_2]$.

B-splines, the carriers of which belong to the closure of the solution domain, remain unchanged (Fig. 3.1, bold lines).

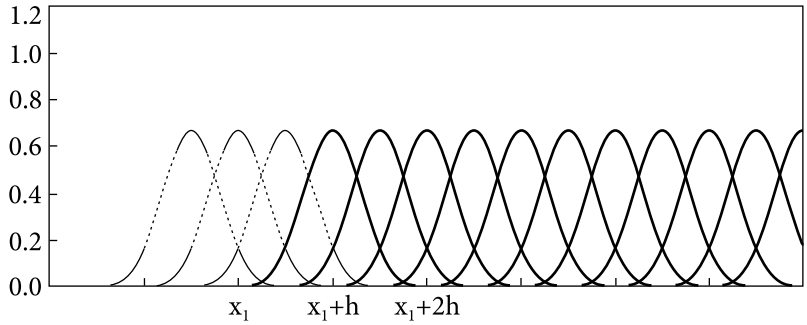

Fig. 3.1. Graphs of cubic B-splines

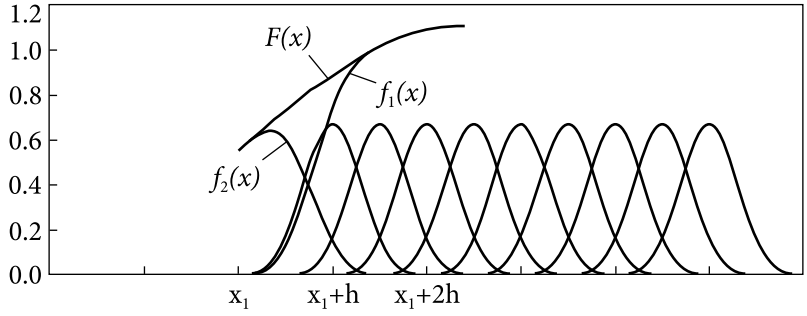

Fig. 3.2. Graphs of functions $f_1(x)$ and $f_2(x)$

The method of constructing boundary basic elements that meet the boundary conditions (3.6—3.8) is considered. To do this, some function $\omega(x) \in C^2\left(\left[x_1, x_2\right]\right)$ such that $\omega(x_1) = 0$, $\omega'(x_1) = \omega_1$, $\omega''(x_1) = \omega_2$ is taken.

Some function $F(x)$ is considered. This function is decomposed in the vicinity of point x_1 as $F(x) = a\omega(x)^2 + b\omega(x) + c + \delta$.

The function $F(x)$ is necessary to decompose on a new basis that satisfies the boundary conditions. The decomposition of the function $F(x)$ on the standard basis of a cubic B-spline $F(x) \approx \sum_{i=0}^{2n} c_i \varphi_i$ is constructed. $F(x) \approx \sum_{i=0}^{2} c_i \varphi_i +$ $+ \sum_{i=3}^{2n} c_i \varphi_i = f_2(x) + f_1(x)$ (Fig. 3.2).

The function $f_1(x)$ remains unchanged. The construction of a function $f_2(x)$ is considered. For this the decomposition of functions $\left\{1, \omega(x), \omega^2(x)\right\}$ in the vicinity of a point $x_1 + \dfrac{3h}{2}$ is constructed:

$$1 = \sum_{i=3}^{5} c_i^0 \varphi_i \,;\, \omega(x) \approx \sum_{i=3}^{5} c_i^1 \varphi_i \,;\, \omega^2(x) \approx \sum_{i=3}^{5} c_i^2 \varphi_i$$

such that

$$\left(\omega^i(x)\right)^{(j)}\Big|_{\frac{3h}{2}} = \sum_{k=3}^{5} c_k^i \varphi^{(j)}{}_k\Big|_{\frac{3h}{2}},\ i, j = 0, 1, 2.$$

Then the boundary basic elements can be taken in the form

$$g_i(x) = \begin{cases} \omega^i(x) - \sum_{k=3}^{5} c_k^i \phi_k, x \in \left[x_1, x_1 + \dfrac{3h}{2}\right], \\ 0, x \overline{\in} \left[x_1, x_1 + \dfrac{3h}{2}\right], \end{cases} \quad i = 0,1,2.$$

Functions $g_i(x) \in C^2\left(\left[x_1, x_2\right]\right)$.

The function $f_2(x)$ is taken in the form $\tilde{f}_2(x) = ag_2(x) + bg_1(x) + cg_0(x)$.

Function $F(x) \approx \tilde{f}_2(x) + f_1(x) = ag_2(x) + bg_1(x) + cg_0(x) + \sum_{i=3}^{2n} c_i \varphi_i$.

The case where the function $F(x)$ satisfies the condition $k_0^1 u(x) + k_1^1 u'(x) + k_2^1 u''(x)\Big|_{x=x_1} = 0$ is considered. Since

$$\left(\sum_{k=3}^{2n} c_k \varphi_k\right)^{(i)}\Bigg|_{x_1} = 0 \text{ and } \left(\sum_{k=3}^{5} c_k^i \varphi_k\right)^{(i)}\Bigg|_{x_1} = 0,\ i = 0, 1, 2,$$

then

$$\left(k_0^1 F(x) + k_1^1 F'(x) + k_2^1 F''(x)\right)\Big|_{x_1} =$$

$$= \left(k_0^1\left(a\omega^2(x) + b\omega(x) + c\right) + k_1^1\left(2a\omega(x)\omega'(x) + b\omega'(x)\right) +\right.$$

$$\left. + k_2^1\left(2a(\omega'(x))^2 + 2a\omega(x)\omega''(x) + b\omega''(x)\right)\right)\Big|_{x_1} = k_0^1 c + k_1^1\omega_1 b + k_2^1(2a(\omega_1)^2 + b\omega_2) = 0.$$

It follows that

$$\begin{cases} c = -\dfrac{k_1^1\omega_1 b + k_2^1(2a(\omega_1)^2 + b\omega_2)}{k_0^1}, \quad k_0^1 \neq 0; \\ a = -\dfrac{b(k_1^1\omega_1 + k_2^1\omega_2)}{2k_2^1(\omega_1)^2}, \quad k_0^1 = 0, k_2^1 \neq 0; \\ b = 0, \quad k_0^1 = 0, k_2^1 = 0. \end{cases}$$

Based on this, we have

$$f_2(x) = ag_2(x) + bg_1(x) - \frac{k_1^1\omega_1 b + k_2^1(2a(\omega_1)^2 + b\omega_2)}{k_0^1} g_0(x) =$$

$$= a\left(g_2(x) - \frac{2k_2^1(\omega_1)^2}{k_0^1} g_0(x)\right) + b\left(g_1(x) - \frac{k_1^1\omega_1 + k_2^1\omega_2}{k_0^1} g_0(x)\right), \quad k_0^1 \neq 0,$$

or

$$f_2(x) = -\frac{b(k_1^1\omega_1 + k_2^1\omega_2)}{2k_2^1(\omega_1)^2} g_2(x) + bg_1(x) + cg_0(x) =$$

$$= b\left(g_1(x) - \frac{(k_1^1\omega_1 + k_2^1\omega_2)}{2k_2^1(\omega_1)^2} g_2(x) \right) + cg_0(x), \quad k_0^1 = 0, \quad k_2^1 \neq 0,$$

or

$$f_2(x) = ag_2(x) + cg_0(x), \quad k_0^1 = 0, \quad k_2^1 = 0.$$

Thus, such set of functions:

$$\begin{cases} \left\{ g_2(x) - \dfrac{2k_2^1(\omega_1)^2}{k_0^1} g_0(x), \quad g_1(x) - \dfrac{k_1^1\omega_1 + k_2^1\omega_2}{k_0^1} g_0(x) \right\}, \quad k_0^1 \neq 0; \\ \left\{ g_1(x) - \dfrac{(k_1^1\omega_1 + k_2^1\omega_2)}{2k_2^1(\omega_1)^2} g_2(x), \quad g_0(x) \right\}, \quad k_0^1 = 0, k_2^1 \neq 0; \\ \left\{ g_2(x), \quad g_0(x) \right\}, \quad k_0^1 = 0, \quad k_2^1 = 0 \end{cases}$$

can be considered as the first two elements of the basis. These functions satisfy the condition $k_0^1 u(x) + k_1^1 u'(x) + k_2^1 u''(x)\Big|_{x=r_1} = 0$.

The case when the conditions

$$\begin{cases} k_0^1 u(x) + k_1^1 u'(x)\Big|_{x=0} = 0, \\ k_1^2 u'(x) + k_2^2 u''(x)\Big|_{x=0} = 0. \end{cases}$$

are satisfied is considered.

The function $F(x)$ is required to meet this boundary condition.

Since $\left(\sum_{k=3}^{2n} c_k \varphi_k \right)^{(i)}\Big|_{x_1} = 0$ and $\left(\sum_{k=3}^{5} c_k^i \varphi_k \right)^{(i)}\Big|_{x_1} = 0$, $i = 0, 1, 2,$ then

$$\left(k_0^1 F(x) + k_1^1 F'(x) \right)\Big|_{x_1} = \left(k_0^1 \left(a\omega^2(x) + b\omega(x) + c \right) + \right.$$

$$= \left. + k_1^1 \left(2a\omega(x)\omega'(x) + b\omega'(x) \right) \right)\Big|_{x_1} = k_0^1 c + k_1^1 \omega_1 b = 0,$$

$$\left(k_1^2 F'(x) + k_2^2 F''(x) \right)\Big|_{x_1} = \left(k_1^2 \left(2a\omega(x)\omega'(x) + b\omega'(x) \right) + \right.$$

$$\left. + k_2^2 \left(2a(\omega'(x))^2 + 2a\omega(x)\omega''(x) + b\omega''(x) \right) \right)\Big|_{x_1} = k_1^2 b\omega_1 + k_2^2 (2a(\omega_1)^2 + b\omega_2) = 0.$$

It follows that

$$\begin{cases} \begin{cases} c = -\dfrac{k_1^1 \omega_1 b}{k_0^1}, & k_0^1 \neq 0; \\ b = 0 \quad k_0^1 = 0; \end{cases} \\ \begin{cases} a = -\dfrac{b(k_1^2 \omega_1 + k_2^2 \omega_2)}{2k_2^2 (\omega_1)^2}, & k_2^2 \neq 0; \\ b = 0, \quad k_2^2 = 0. \end{cases} \end{cases}$$

So,

$$f_2(x) = -\frac{b(k_1^2 \omega_1 + k_2^2 \omega_2)}{2k_2^2 (\omega_1)^2} g_2(x) + b g_1(x) - \frac{k_1^1 \omega_1 b}{k_0^1} g_0(x) =$$

$$= b\left(g_1(x) - \frac{(k_1^2 \omega_1 + k_2^2 \omega_2)}{2k_2^2 (\omega_1)^2} g_2(x) - \frac{k_1^1 \omega_1}{k_0^1} g_0(x) \right), \quad k_0^1 \neq 0, k_2^2 \neq 0,$$

$$f_2(x) = a g_2(x), \quad k_0^1 \neq 0, k_2^2 = 0\,,$$

or

$$f_2(x) = c g_0(x), \; k_0^1 = 0, \; k_2^2 = 0\,.$$

Given functions

$$\begin{cases} \left\{ g_1(x) - \dfrac{(k_1^2 \omega_1 + k_2^2 \omega_2)}{2k_2^2 (\omega_1)^2} g_2(x) - \dfrac{k_1^1 \omega_1}{k_0^1} g_0(x) \right\}, & k_0^1 \neq 0, k_2^2 \neq 0, \\ \left\{ g_2(x) \right\}, & k_0^1 \neq 0, k_2^2 = 0, \\ \left\{ g_0(x) \right\}, & k_0^1 = 0, \quad k_2^2 \neq 0 \end{cases}$$

can be taken as the first elements of the basis. They meet the conditions

$$\begin{cases} k_0^1 u(x) + k_1^1 u'(x)\Big|_{x_1} = 0, \\ k_1^2 u'(x) + k_2^2 u''(x)\Big|_{x_1} = 0. \end{cases}$$

The case when the conditions

$$\begin{cases} u(x)\Big|_{x=0} = 0, \\ u'(x)\Big|_{x=0} = 0, \\ u''(x)\Big|_{x=0} = 0. \end{cases}$$

are met is considered.

The function $F(x)$ is required to meet this boundary condition. Since

$$\left(\sum_{k=3}^{2n} c_k \varphi_k\right)^{(i)}\Bigg|_{x_1} = 0 \text{ and} \left(\sum_{k=3}^{5} c_k^i \varphi_k\right)^{(i)}\Bigg|_{x_1} = 0,\ i = 0,\ 1,\ 2,$$

then

$$F(x)\Big|_{x_1} = \left(a\omega^2(x) + b\omega(x) + c\right)\Big|_{x_1} = c = 0,$$

$$F'(x)\Big|_{x_1} = \left(2a\omega(x)\omega'(x) + b\omega'(x)\right)\Big|_{x_1} = b\omega_1 = 0,$$

$$F''(x)\Big|_{x_1} = \left(2a(\omega'(x))^2 + 2a\omega(x)\omega''(x) + b\omega''(x)\right)\Big|_{x_1} = 2a(\omega_1)^2 + b\omega_2 = 0.$$

It follows that $a = b = c = 0$, that is $f_2(x) = 0$.

The theorem on the completeness of a basis consisting of cubic B-splines and boundary basic elements is proved for the described method of boundary basic elements construction. Without limiting the unification, for the sake of simplicity, we will consider $x_1 = 0$.

Theorem 3.1.

In the case when function $\omega(x) = x$, any function from the spline functions $S_{3,1}(\Delta)$ space, corresponding to the boundary condition (3.6), the boundary conditions (3.7) or (3.8) at point $x_1 = 0$, can be accurately decomposed on a basis consisting of B-splines and boundary basic elements.

Proof.

The following decompositions:

$$1 = \sum_{i=0}^{2n} c_i^0 \varphi_i\ ,\ x = \sum_{i=0}^{2n} c_i^1 \varphi_i\ ,\ x^2 = \sum_{i=0}^{2n} c_i^2 \varphi_i$$

are considered. Then $g_i(x) = \sum_{k=0}^{2} c_k^i \varphi_k,\ i = 0, 1, 2$.

Arbitrary function from the space of spline functions $S_{3,1}(\Delta)$ can be given in the form $\sum_{i=0}^{2n} c_i \varphi_i$. Assume that

$$\sum_{i=0}^{2n} c_i \varphi_i = a\sum_{i=0}^{2} c_i^2 \varphi_i + b\sum_{i=0}^{2} c_i^1 \varphi_i + c\sum_{i=0}^{2} c_i^0 \varphi_i + \sum_{i=3}^{2n} c_i \varphi_i\ .$$

Then

$$\sum_{i=0}^{2} c_i \varphi_i = a\sum_{i=0}^{2} c_i^2 \varphi_i + b\sum_{i=0}^{2} c_i^1 \varphi_i + c\sum_{i=0}^{2} c_i^0 \varphi_i\ .$$

Functions $\varphi_i,\ i = 0, 1, 2$ — linearly independent, then $c_i\varphi_i = ac_i^2\varphi_i + bc_i^1\varphi_i + cc_i^0\varphi_i$, $i = 0, 1, 2$. Once each equation is divided into φ_i, the following system

of linear equations is obtained:

$$\begin{pmatrix} c_0^2 & c_0^1 & c_0^0 \\ c_1^2 & c_1^1 & c_1^0 \\ c_2^2 & c_2^1 & c_2^0 \end{pmatrix} \begin{pmatrix} a \\ b \\ c \end{pmatrix} = \begin{pmatrix} c_0 \\ c_1 \\ c_2 \end{pmatrix}.$$

Denote the matrix of this system as **C**. Matrix columns **C** — are linearly independent because the functions {1, x, x^2} — are linearly independent. Therefore $\det \mathbf{C} \neq 0$, hence, there is $\mathbf{C}^{-1}$. Then

$$\begin{pmatrix} a \\ b \\ c \end{pmatrix} = \mathbf{C}^{-1} \begin{pmatrix} c_0 \\ c_1 \\ c_2 \end{pmatrix}.$$

So it is always possible to introduce

$$\sum_{i=0}^{2n} c_i \varphi_i = a \sum_{i=0}^{2} c_i^2 \varphi_i + b \sum_{i=0}^{2} c_i^1 \varphi_i + c \sum_{i=0}^{2} c_i^0 \varphi_i + \sum_{i=3}^{2n} c_i \varphi_i \ .$$

It is required for the boundary conditions of the form (3.6), (3,7), or (3.8) to be met at a point $x_1 = 0$ from an arbitrary function from the space of spline functions $S_{3,1}(\Delta)$. We have

$$\left\{ k_0^1 \sum_{i=0}^{2n} c_i \varphi_i + k_1^1 \left(\sum_{i=0}^{2n} c_i \varphi_i \right)' + k_2^1 \left(\sum_{i=0}^{2n} c_i \varphi_i \right)'' \right|_{x=0} = 0;$$

$$\begin{cases} k_0^1 \sum_{i=0}^{2n} c_i \varphi_i + k_1^1 \left(\sum_{i=0}^{2n} c_i \varphi_i \right)' \Big|_{x=0} = 0, \\ k_1^2 \left(\sum_{i=0}^{2n} c_i \varphi_i \right)' + k_2^2 \left(\sum_{i=0}^{2n} c_i \varphi_i \right)'' \Big|_{x=0} = 0; \end{cases}$$

$$\begin{cases} \sum_{i=0}^{2n} c_i \varphi_i \Big|_{x=0} = 0, \\ \left(\sum_{i=0}^{2n} c_i \varphi_i \right)' \Big|_{x=0} = 0, \\ \left(\sum_{i=0}^{2n} c_i \varphi_i \right)'' \Big|_{x=0} = 0. \end{cases}$$

Taking into account that $\sum_{i=0}^{2n} c_i\varphi_i = a\sum_{i=0}^{2} c_i^2\varphi_i + b\sum_{i=0}^{2} c_i^1\varphi_i + c\sum_{i=0}^{2} c_i^0\varphi_i + \sum_{i=3}^{2n} c_i\varphi_i$, it is possible to come to the conditions

$$\begin{cases} c = -\dfrac{k_1^1 b + 2k_2^1 a}{k_0^1}, \quad k_0^1 \neq 0, \\ a = -\dfrac{bk_1^1}{2k_2^1}, \quad k_0^1 = 0, k_2^1 \neq 0, \\ b = 0, \quad k_0^1 = 0, k_2^1 = 0; \end{cases} \quad \begin{cases} \begin{cases} c = -\dfrac{k_1^1 b}{k_0^1}, \quad k_0^1 \neq 0, \\ b = 0 \quad k_0^1 = 0; \end{cases} \\ \begin{cases} a = -\dfrac{bk_1^2}{2k_2^2}, \quad k_2^2 \neq 0, \\ b = 0, \quad k_2^2 = 0; \end{cases} \end{cases} \quad \{a = b = c = 0.$$

This coincides with the derived conditions at $\begin{cases} \omega_1 = 1; \\ \omega_2 = 0. \end{cases}$

So, *the theorem is proved*.

3.2. Construction of boundary basic elements for approximation of functions satisfying the homogeneous Dirichlet boundary condition in the two-dimensional case

The problem of constructing a basis based on cubic B-splines for the approximation of functions satisfying the homogeneous Dirichlet boundary condition for the two-dimensional case is considered.

Suppose that the area of the problem approximation is Ω, for which $\partial\Omega$ — smooth border of the area described by the inequality $\omega(x, y) > 0$, where $\omega(x, y) \in C^2(\overline{\Omega})$, $\omega(x, y)\big|_{\partial\Omega} = 0$, $0 < \nabla\omega(x, y)\big|_{\partial\Omega} < \infty$. A basis consisting of cubic B-splines $\{\varphi_i\}$, $i = 0, ..., N$ is considered. Number the basic elements as follows: elements φ_i, i=0, …, n are the elements whose carriers cross the border of the area Ω, and elements φ_i, i=n+1, …, N are the elements, the carriers of which belong to the set $\overline{\Omega}$.

The following expansions of functions $\omega^k(x, y), k = 0, ..., 3$ in the area Ω: $\omega^k(x, y) \approx \sum_{i=0}^{N} c_{i,k}\varphi_i, k = 0, ..., 3$ are considered using, for example, the least squares method. Assume that $\delta_k(x, y) = \sum_{i=0}^{N} c_{i,k}\varphi_i,\ k = 0, ..., 3.$

Suppose that some area $\Omega' \subset \Omega$: $\operatorname{supp}\varphi_i \cap \Omega' = \varnothing, i = 0,.., n$ has an equation $\omega'(x, y) < 0$ for which $\partial\Omega' \in \tilde{N}^2$ is area border Ω', $\omega'(x, y)\big|_{\partial\Omega'} = 0$, $\omega'(x, y) \in C^2(\overline{\Omega}), 0 < \nabla\omega'(x, y)\big|_{\partial\Omega'} < \infty$.

Assume $\omega_2(x,y)=\begin{cases}\omega'(x,y),(x,y)\in(\Omega/\Omega');\\ 0,(x,y)\in\Omega'.\end{cases}$

The functions $\theta_k(x,y)=\dfrac{\omega_2{}^3(x,y)\left(\sum\limits_{i=0}^{N}c_{i,k}\varphi_i-\omega^k(x,y)\right)}{\omega^k(x,y)+\omega_2{}^3(x,y)}$, $k=0...3$ are considered.

Assume that $\delta_k^*(x,y)=\delta_k(x,y)-\theta_k(x,y)$. Then

$$\delta^*{}_k(x,y)=\sum_{i=0}^{n}c_{i,k}\varphi_i-\frac{\omega_2{}^3(x,y)\left(\sum\limits_{i=0}^{N}c_{i,k}\varphi_i-\omega^k(x,y)\right)}{\omega^k(x,y)+\omega_2{}^3(x,y)}=$$

$$=\frac{\left(\omega^k(x,y)+\omega_2{}^3(x,y)\right)\sum\limits_{i=0}^{n}c_{i,k}\varphi_i-\omega_2{}^3(x,y)\left(\sum\limits_{i=0}^{N}c_{i,k}\varphi_i-\omega^k(x,y)\right)}{\omega^k(x,y)+\omega_2{}^3(x,y)}=$$

$$\left(\omega^k(x,y)+\omega_2{}^3(x,y)\right)\sum_{i=0}^{n}c_{i,k}\varphi_i-\omega_2{}^3(x,y)\left(\sum_{i=0}^{n}c_{i,k}\varphi_i\right)-$$

$$=\frac{-\omega_2{}^3(x,y)\left(\sum\limits_{i=n+1}^{N}c_{i,k}\varphi_i\right)+\omega^k(x,y)\omega_2{}^3(x,y)}{\omega^k(x,y)+\omega_2{}^3(x,y)};$$

$$\delta^*{}_k(x,y)=\frac{\omega^k(x,y)\sum\limits_{i=0}^{n}c_{i,k}\varphi_i-\omega_2{}^3(x,y)\sum\limits_{i=n+1}^{N}c_{i,k}\varphi_i+\omega^k(x,y)\omega_2{}^3(x,y)}{\omega^k(x,y)+\omega_2{}^3(x,y)}. \quad (3.9)$$

Functions $\delta^*(x,y)\in C^2(\Omega),\quad =0,...,3.$

Assertion 3.1.

$$\left.\frac{\partial^i\delta_k^*(x,y)}{\partial n^i}\right|_{\partial\Omega}=0,\quad i=0,...,k-1,\quad k=1,...,3.$$

Proof.
Consider

$$\delta^*{}_k(x,y)=\frac{\omega^k(x,y)\sum\limits_{i=0}^{n}c_{i,k}\varphi_i-\omega_2{}^3(x,y)\sum\limits_{i=n+1}^{N}c_{i,k}\varphi_i+\omega^k(x,y)\omega_2{}^3(x,y)}{\omega^k(x,y)+\omega_2{}^3(x,y)}=$$

$$= \frac{\omega^k(x,y)\sum_{i=0}^{n} c_{i,k}\varphi_i}{\omega^k(x,y)+\omega_2{}^3(x,y)} - \frac{\omega_2{}^3(x,y)\sum_{i=n+1}^{N} c_{i,k}\varphi_i}{\omega^k(x,y)+\omega_2{}^3(x,y)} + \frac{\omega^k(x,y)\omega_2{}^3(x,y)}{\omega^k(x,y)+\omega_2{}^3(x,y)}.$$

Then

$$\frac{\partial^i \delta^*_k(x,y)}{\partial n^i} = \frac{\partial^i\left(\frac{\omega^k(x,y)\sum_{i=0}^{n} c_{i,k}\varphi_i}{\omega^k(x,y)+\omega_2{}^3(x,y)}\right)}{\partial n^i} - \frac{\partial^i\left(\frac{\omega_2{}^3(x,y)\sum_{i=n+1}^{N} c_{i,k}\varphi_i}{\omega^k(x,y)+\omega_2{}^3(x,y)}\right)}{\partial n^i} + \frac{\partial^i\left(\frac{\omega^k(x,y)\omega_2{}^3(x,y)}{\omega^k(x,y)+\omega_2{}^3(x,y)}\right)}{\partial n^i}.$$

Each component of the right-hand side of this equation is calculated:

$$\frac{\partial^i\left(\frac{\omega^k(x,y)\omega_2{}^3(x,y)}{\omega^k(x,y)+\omega_2{}^3(x,y)}\right)}{\partial n^i} = 0, \quad i = 0,\ldots,k-1, \quad k = 1,\ldots,3$$

for $(x,y)\in\partial\Omega$, since the the function $\left.\frac{\omega_2{}^3(x,y)}{\omega^k(x,y)+\omega_2{}^3(x,y)}\right|_{\partial\Omega}$ is limited; simi-

lary, $\frac{\partial^i\left(\frac{\omega_2{}^3(x,y)\sum_{i=n+1}^{N} c_{i,k}\varphi_i}{\omega^k(x,y)+\omega_2{}^3(x,y)}\right)}{\partial n^i} = 0, \quad i = 0,\ldots,k-1, k = 1,\ldots,3$ for $(x,y)\in\partial\Omega$,

since the function $\left.\frac{\omega_2{}^3(x,y)}{\omega^k(x,y)+\omega_2{}^3(x,y)}\right|_{\partial\Omega}$ is limited, and $\frac{\partial^i\left(\sum_{i=n+1}^{N} c_{i,k}\varphi_i\right)}{\partial n^i} = 0, \forall i$;

$\frac{\partial^i\left(\frac{\omega^k(x,y)\sum_{i=0}^{n} c_{i,k}\varphi_i}{\omega^k(x,y)+\omega_2{}^3(x,y)}\right)}{\partial n^i} = 0, i = 0,\ldots, k-1, k = 1,\ldots,3$ for $(x,y)\in\partial\Omega$, since

the function $\left.\frac{\sum_{i=0}^{n} c_{i,k}\varphi_i}{\omega^k(x,y)+\omega_2{}^3(x,y)}\right|_{\partial\Omega}$ is limited.

So,

$$\left.\frac{\partial^i \delta^*{}_k(x,y)}{\partial n^i}\right|_{\partial\Omega} = 0, i = 0, ..., k-1,\ k = 1, ..., 3.$$

The assertion is proved.
Assume that

$$\psi^k{}_i(x,y) = \frac{\varphi_i(x,y)\delta^*{}_k(x,y)}{\sum_{i=0}^{n}\varphi_i(x,y)}, \quad i = 0, ..., n, \quad k = 0, ..., 3. \tag{3.10}$$

Functions $\psi^k{}_i(x,y)$ can be taken as elements of the basis.
Suppose that there's a decomposition of some function $F(x,y)$ in the area Ω

$$F(x,y) \approx \sum_{i=0}^{n} c_i\varphi_i + \sum_{i=n+1}^{N} c_i\varphi_i .$$

This function can be decomposed on a new basis

$$F(x,y) \approx \sum_{i=0}^{n}\sum_{k=0}^{3} \tilde{c}_{i,k}\psi^k{}_i + \sum_{i=n+1}^{N} c_i\varphi_i .$$

The function $F(x,y)$ is required to satisfy the homogeneous Dirichlet boundary condition $F(x,y)\big|_{\partial\Omega} \approx \left(\sum_{i=0}^{n}\sum_{k=0}^{3} \tilde{c}_{i,k}\psi^k{}_i + \sum_{i=n+1}^{N} c_i\varphi_i\right)\Big|_{\partial\Omega} = 0$. Elements $\{\varphi_i\}$, $i = n+1,...,N$ satisfy this condition. Function

$$\psi^k{}_i(x,y) = \frac{\varphi_i(x,y)\delta^*{}_k(x,y)}{\sum_{i=0}^{n}\varphi_i(x,y)}, \quad i = 0,...,n$$

is considered.

We have $\psi^k{}_i(x,y)\big|_{\partial\Omega} = \varphi_i(x,y)\delta^*{}_k(x,y)\big|_{\partial\Omega}$, $i = 0,...,n$. Besides, $\varphi_i(x,y)\big|_{\partial\Omega} < \infty$, $i = 0,...,n$. According to statement 3.1. $\delta^*{}_k(x,y)\big|_{\partial\Omega} = 0$, $k = 1,...,3$.

It follows that $\left(\sum_{i=0}^{n}\sum_{k=0}^{3} \tilde{c}_{i,k}\psi_i^k + \sum_{i=n+1}^{N} c_i\varphi_i\right)\Big|_{\partial\Omega} = \sum_{i=0}^{n} \tilde{c}_{i,0}\psi_i^0\Big|_{\partial\Omega}$.

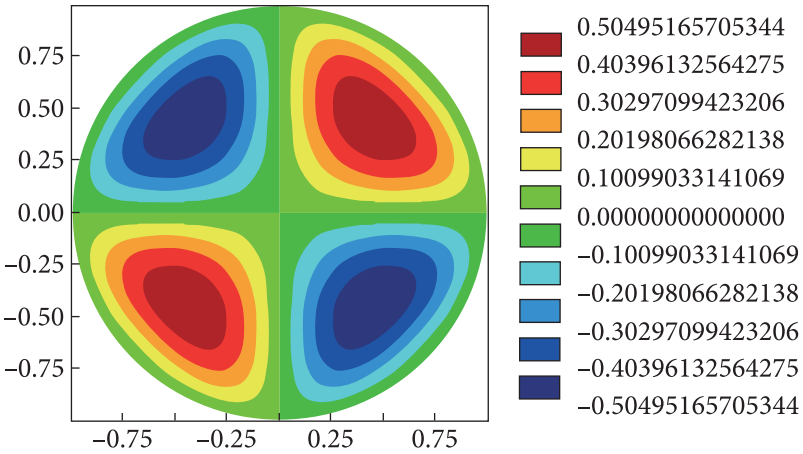

Fig. 3.3. Graph of the analytical solution of the boundary value problem (3.11) in the form of lines of constant level on the plane xOy

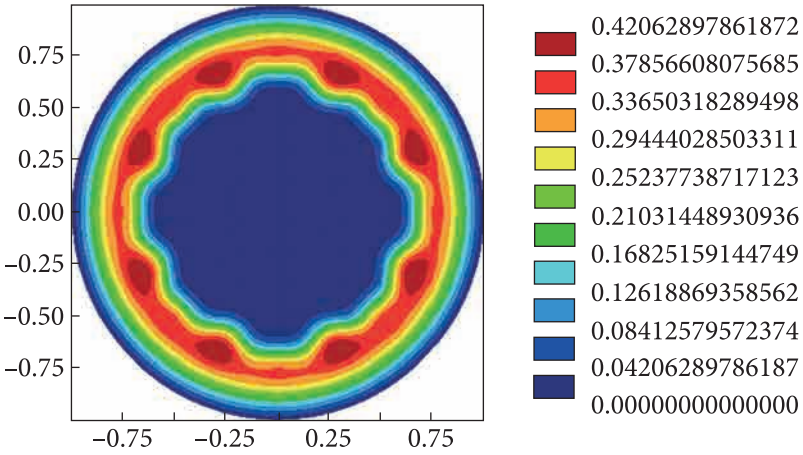

Fig. 3.4. Graph of function $\delta^*(x,y)$ for the boundary value problem (3.11) in the form of lines of constant level on the plane xOy

From the condition, $\left(\sum_{i=0}^{n}\sum_{k=0}^{3}\tilde{c}_{i,k}\psi_i^k+\sum_{i=n+1}^{N}c_i\varphi_i\right)\Big|_{\partial\Omega}=0$ it turns out that $\sum_{i=0}^{n}\tilde{c}_{i,0}\psi_i^0\Big|_{\partial\Omega}=0$. Since the function $\psi^0{}_i(x,y)\big|_{\partial\Omega}>0$, then $\tilde{c}_{i,0}=0,\quad i=0,...,n$. Thus, the functions of the form $\left\{\sum_{i=0}^{n}\sum_{k=1}^{3}\tilde{c}_{i,k}\psi_i^k+\sum_{i=n+1}^{N}c_i\varphi_i\right\}$ satisfy the homoge neous Dirichlet boundary condition.

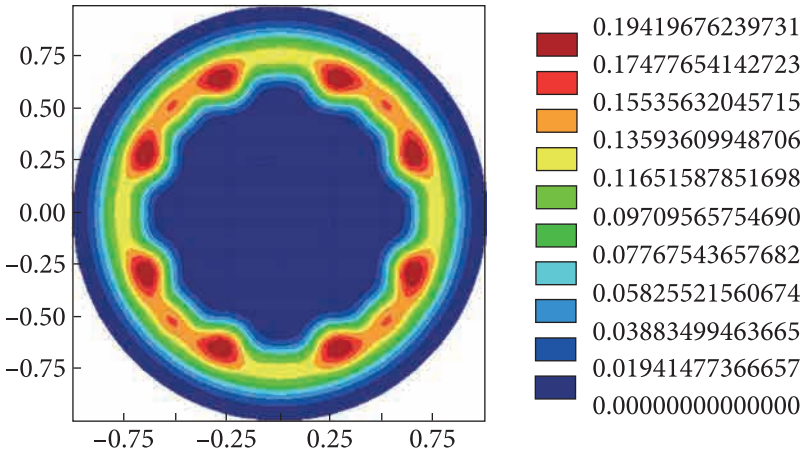

Fig. 3.5. Graph of function $\delta_2^*(x, y)$ for the boundary value problem (3.11) in the form of lines of constant level on the plane xOy

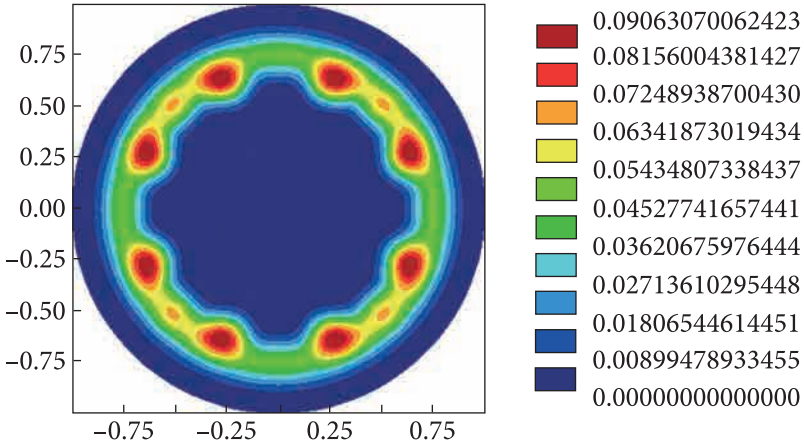

Fig. 3.6. Graph of function $\delta_3^*(x, y)$ for the boundary value problem (3.11) in the form of lines of constant level on the plane xOy

The given method is considered in the following example:

$$\begin{cases} \Delta u = 25x^2 \sin(5xy)(x^2 + y^2 - 1) - 40xy\cos(5xy) - 4\sin(5xy) + \\ +25y^2 \sin(5xy)(x^2 + y^2 - 1); \\ u\Big|_{x^2+y^2=1} = 0. \end{cases} \tag{3.11}$$

The analytical solution of this problem is a function

$$u = \sin(5xy)(1 - x^2 - y^2). \tag{3.12}$$

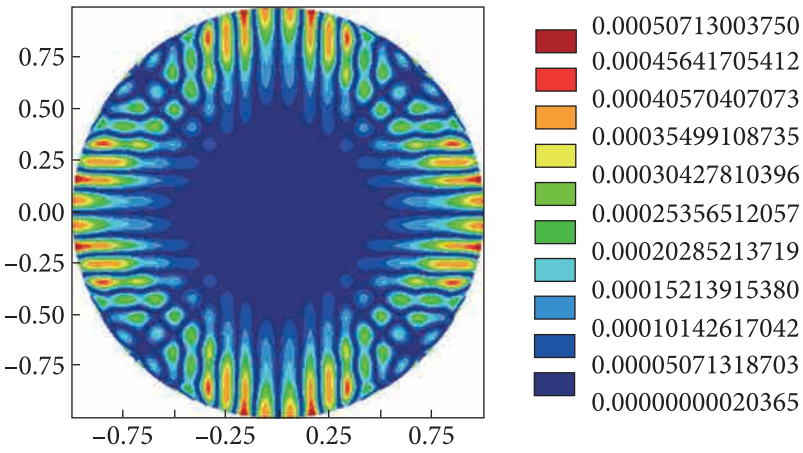

Fig. 3.7. Graph of the function of the difference modulus of the analytical solution of the problem (3.11) and the approximation problem solution of the function (3.12) by the method of least squares

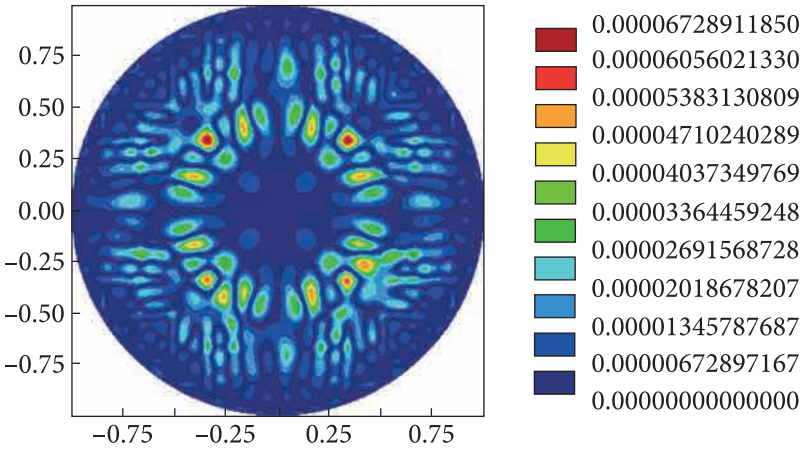

Fig. 3.8. Graph of the function of the difference modulus of the analytical and numerical solution of the problem (3.11) with the involvement of the given approach by the least squares method

Fig. 3.3 shows the analytical solution of the problem (3.11).

Fig. (3.4—3.6) show graphs of functions $\delta^*_k(x,y)$, $k=1,2,3$ for the boundary value problem (3.11). Fig. 3.7, and 3.8 show the results of numerical calculations using the least squares method for a grid of 19×19 B-splines constructed for a square $[-1,1]\times[-1,1]$.

3.3. Software description

To solve boundary value problems using the method of construction of boundary basic elements proposed in the chapter, programs «Boundary basis elements problem 1D» and «Boundary basis elements problem 2D» have been developed.

These programs are written in the language C++ using MFC libraries and consist of the following modules:

- input information processing module;
- a module of separation of «boundary» and «internal» elements of the basis;
- basic elements formation module;
- module for forming a system of linear equations;
- integral calculation module;
- module for solving a system of linear equations;
- results visualization module.

In the basic elements formation module basic splines of the 3rd and 5th orders are realized as indefinite components of the solution structure [1,10, 28, 44]. Standard basic splines are used as internal basic elements, and boundary basic elements are formed using the approach proposed in this chapter.

In the module for forming a system of linear equations, the matrix of the system of linear equations is formed using the least squares method and the Bubnov — Galerkin method [42, 43].

The Gauss method [14] is realized in the integral calculation module on k points where k =1, 2, ..., 10 In the module for solving the system of linear equations, the Gauss method with the choice of the principal element over the whole matrix and the Seidel method of the system of linear equations solution are implemented [14].

When solving boundary value problems using variational methods such as the least squares method, the Ritz method, and others, it is necessary to find the elements of the system of linear equations matrix that are integrals. In these integrals, the subintegral function depends on the basic elements and the operator of the boundary value problem. When using standard B-splines as basic elements, for differential equations, the operator of which is a linear combination of the function itself and its various derivatives, the elements of the system of linear equations matrix will be repeated and can be calculated accurately. Therefore, the use of a basis consisting of standard B-splines and boundary basic elements reduces the counting time and reduces the accumulation of errors.

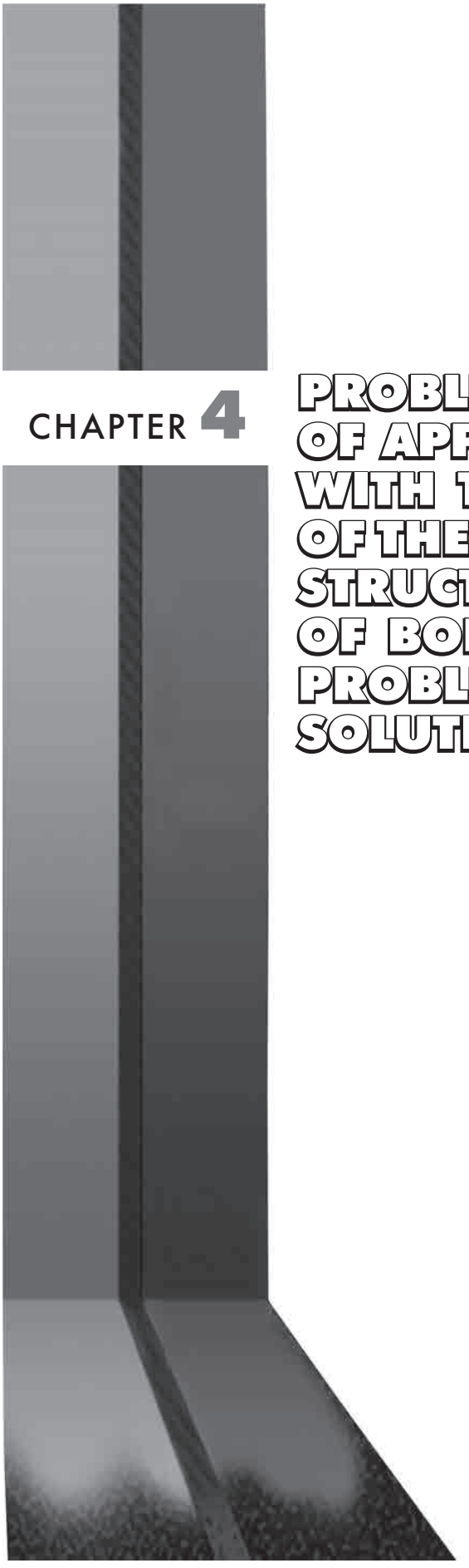

CHAPTER 4

PROBLEMS OF APPROXIMATION WITH THE USE OF THE DEVELOPED STRUCTURES OF BORDER PROBLEMS SOLUTIONS

This chapter presents the results of numerical calculations of test and model boundary value problems using the proposed constructive means of structural methods and developed approaches to solving boundary value problems in areas of complex shape, also shows solutions of approximation problems using different solution structures.

4.1. Solution structures usage for functions approximation

4.1.1. Approximation of smooth function $f(x, y) = x, y$

The problem of approximation of the function $f(x,y)=xy$ (Fig. 4.1) is solved by the least squares method for two domains $\Omega_1=[0,1]\times[0,1]$ and $\Omega_2=[-1,1]\times[-1,1]$ by using the structure $f(x,y)=\omega(x,y)P_k(x,y)$, where $\omega(x,y)=$ $=x\wedge_0 y$, $P_k(x,y)=\sum_{i=1}^{k}c_i\varphi_i(x,y)$, $\{\varphi_i(x,y)\}$ — cubic B-splines. In the domain, Ω_1 we take $k=81$, in the domain Ω_2 suppose $k=169$.

Fig. 4.2 and 4.3 show graphs of the functions of the difference modulus between the solutions of the approximation problems and the function $f(x,y)=xy$ in domains $\Omega_1=[0,1]\times[0,1]$ and $\Omega_2=[-1,1]\times[-1,1]$.

The analysis of the figures shows that when the level lines of the smooth function in the approximation domain form the input angle, the approximation properties of the sheaf of functions $\omega(x,y)P_k(x,y)$ are significantly reduced.

4.1. 2. Approximation of the function $f(x, y) = f_{11}(x, y)\, f_{12}(x, y)$

The approximation of the function $f(x,y)=f_{11}(x,y)f_{12}(x,y)$ (Fig. 4.4) in the domain $\Omega=(-1,1)\times(-1,1)/(-1,0)\times(-1,0)$,

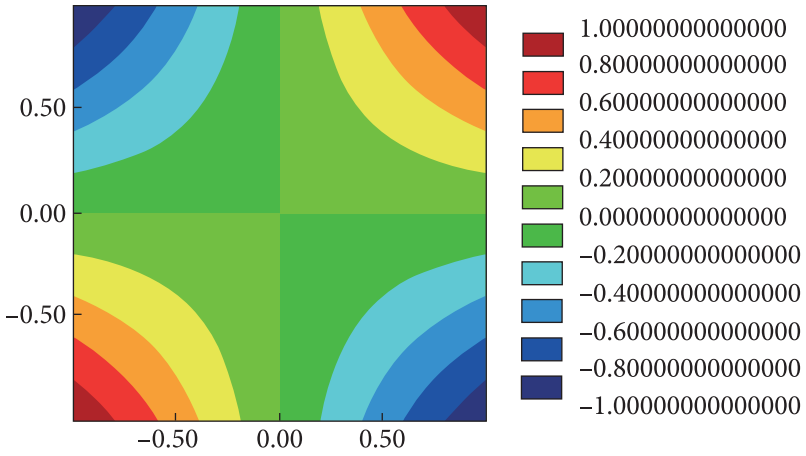

Fig. 4.1. Graph of the function $f(x,y)=xy$ in the form of lines of constant level on the plane xOy

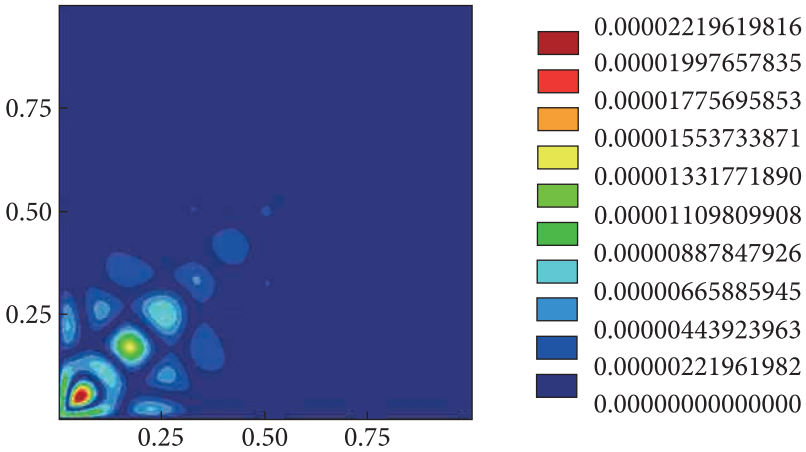

Fig. 4.2. Graph of the difference modulus between the function $f(x,y)=xy$ and the solution of the approximation problem in the domain Ω_1 in the form of lines of constant level on the plane xOy

where

$$f_{11}(x,y)=\begin{cases}x-y^3, & y\geq 0,\\ x, & y<0;\end{cases}\qquad f_{12}(x,y)=\begin{cases}y-x^3, & x\geq 0,\\ y, & x<0\end{cases}$$

is considered.

The solution of this problem was obtained using the least squares method in two ways. In the first case, the structure $u(x,y)=\omega(x,y)P_k(x,y)$ was used, where $\omega(x,y)=x\vee_0 y$, $P_k(x,y)=\sum_{i=1}^{k}c_i\varphi_i(x,y)$, $k=169$, $\{\varphi_i(x,y)\}$ — cubic

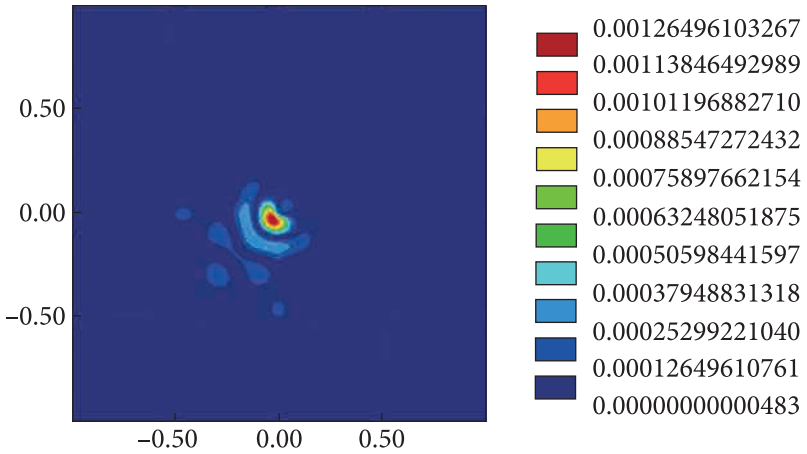

Fig. 4.3. Graph of the difference modulus between the function $f(x,y)=xy$ and the solution of the approximation problem in the domain Ω_2 in the form of lines of constant level on the plane xOy

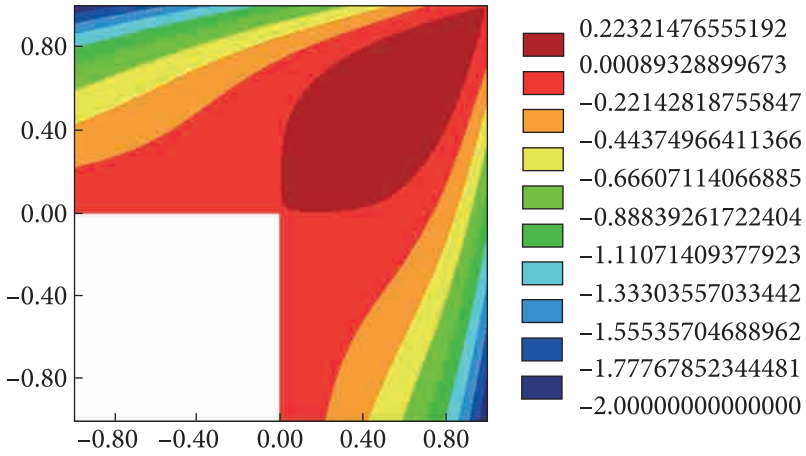

Fig. 4.4. Graph of the function $f(x,y)=f_{11}(x,y)f_{12}(x,y)$ in the form of lines of constant level on the plane xOy

B-splines. The graph of the difference modulus of the solution of the approximation problem and the function $f(x,y)=f_{11}(x,y)f_{12}(x,y)$ is shown in Fig. 4.5.

In the second case, the structure

$$f(x,y)=\omega_1(x,y)P_{1,k}(x,y)+\omega_2(x,y)P_{2,k}(x,y)$$

is used, where $\omega_1(x,y)=xy$,

$$\omega_2(x,y)=f_{21}(x,y)f_{22}(x,y),\ f_{11}(x,y)=\begin{cases}x+y^3, & y\geq 0,\\ x, & y<0,\end{cases}\quad f_{12}(x,y)=\begin{cases}y+x^3, & x\geq 0,\\ y, & x<0,\end{cases}$$

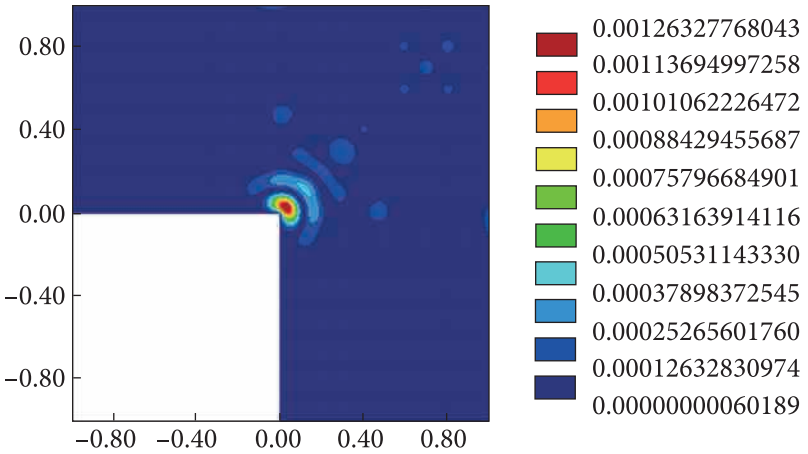

Fig. 4.5. Graph of the difference modulus between the function $f(x,y)=f_{11}(x,y)f_{12}(x,y)$ and the approximation problem solution involving the structure $u(x,y)=\omega(x,y)P_k(x,y)$ in the form of lines of constant level on the plane xOy

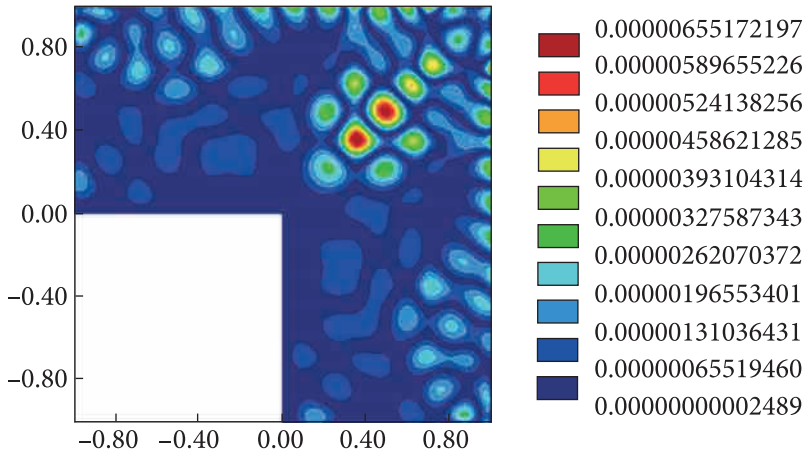

Fig. 4.6. Graph of the difference modulus between the function $f(x,y)=f_{11}(x,y)f_{12}(x,y)$ and the approximation problem solution involving the structure $f(x,y)=\omega_1(x,y)P_{1,k}(x,y)+\omega_2(x,y)P_{2,k}(x,y)$ in the form of lines of constant level on the plane xOy

$P_{1,k}(x,y)=\sum_{i=1}^{k_1}c_{l,i}\varphi_i(x,y)$, $k_1+k_2=162$, $\{\varphi_i(x,y)\}$ — cubic B-splines. A graph of the difference modulus function of the solution of the approximation problem and the function $f(x,y)=f_{11}(x,y)f_{12}(x,y)$ is shown in Fig. 4.6.

Analysis of the figures shows that for this problem the structure $f(x,y)=\omega_1(x,y)P_{1,k}(x,y)+\omega_2(x,y)P_{2,k}(x,y)$ has a much higher approximation capacity.

4.2. Implication of structures for analysis of boundary value problems solutions approximation ability

4.2.1. A model example of a boundary value problem

The following boundary value problem in the domain $\Omega = (0,1) \times (0,1)$ is considered:

$$\begin{cases} \Delta u(x,y) = -2\pi^2 \sin(\pi x)\sin(\pi y), \quad (x,y) \in \Omega, \\ u(x,y)\big|_{\partial\Omega} = 0. \end{cases}$$

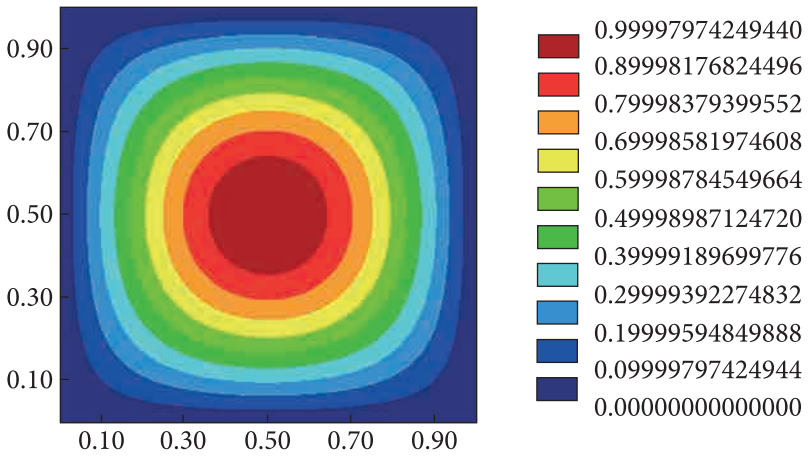

Fig. 4.7. Graph of the function $u(x,y) = \sin(\pi x)\sin(\pi y)$ in the form of lines of constant level on the plane xOy

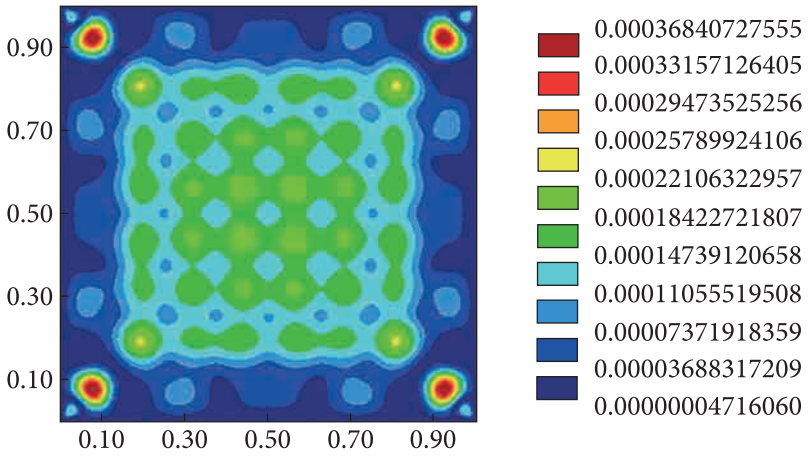

Fig. 4.8. Graph of the function of the difference modulus of the analytical and numerical solution using the structure $u(x,y) = \omega_1(x,y)P_k(x,y)$ in the form of lines of constant level on the plane xOy

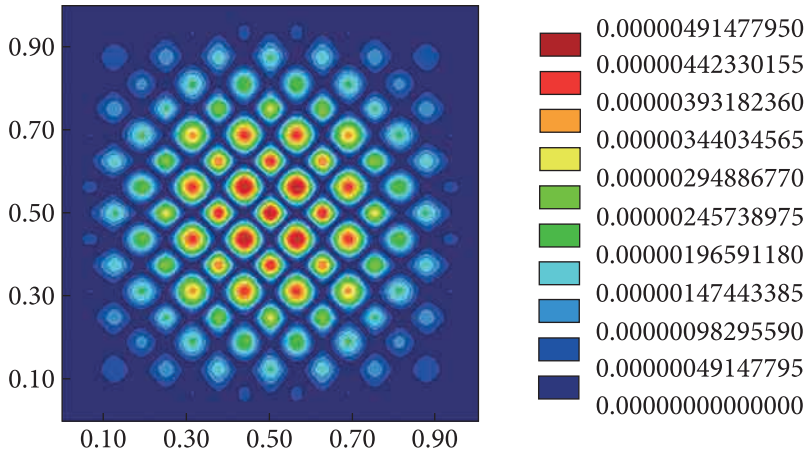

Fig. 4.9. Graph of the function of the difference modulus of the analytical and numerical solution using the structure $u(x,y)=\omega_2(x,y)P_k(x,y)$ in the form of lines of constant level on the plane xOy

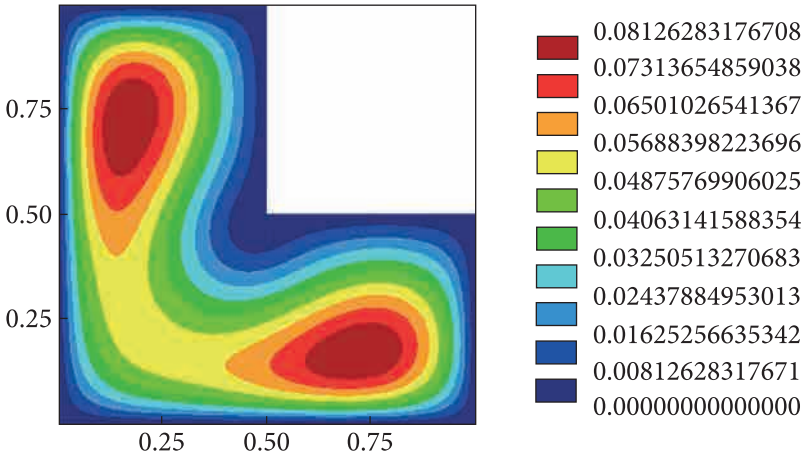

Fig. 4.10. Graph of the function $f_1(x,y)$ in the form of lines of constant level on the plane xOy

Analytical solution of this problem — $u(x,y)=\sin(\pi x)\sin(\pi y)$ (Fig. 4.7).

The solution of this problem was obtained using the least squares method and the structure $u(x,y)=\omega(x,y)P_k(x,y)$, where $P_k(x,y)=\sum_{i=1}^{k}c_i\varphi_i(x,y)$, $k=121$, $\{\varphi_i(x,y)\}$ — cubic B-splines.

$\omega_1(x,y)=(x(1-x))\wedge_0(y(1-y))$ and $\omega_2(x,y)=xy(1-x)(1-y)$ are used as a function of $\omega(x,y)$.

Fig. 4.8, and 4.9 show graphs of the functions of the difference modulus of analytical and numerical solutions for the weight functions $\omega_1(x,y)$ (Fig. 4.8) and $\omega_2(x,y)$ (Fig. 4.9).

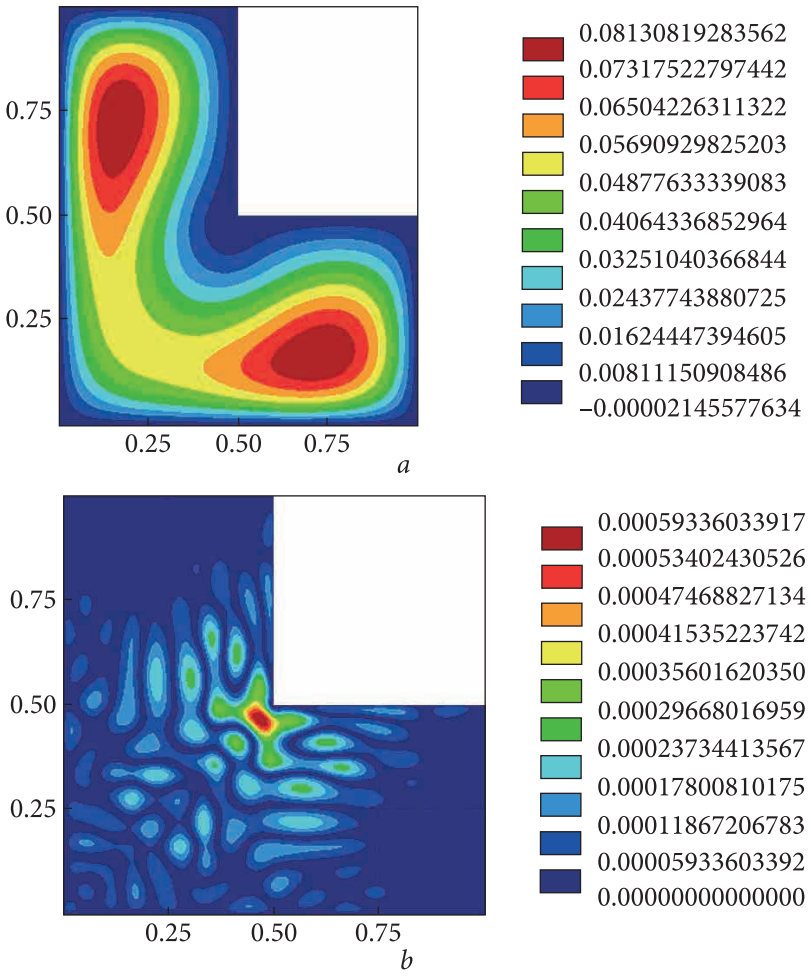

Fig. 4.11. Graphs of the functions: *a* — the approximation problem solution using the structure $f(x,y)=\omega_1(x,y)P_1(x,y)+\omega_2(x,y)P_2(x,y)$; *b* — the difference modulus of the function $f_1(x,y)$ and the approximation problem solution

The analysis of the figures shows that for this problem the structure of the solution $u(x,y)=\omega(x,y)P_k(x,y)$ when using the function $\omega_2(x,y)$ has a much higher approximation capacity.

4.2.2. Approximation of a function from the system of R-operations R^k

The problem of approximation of the function

$$f_k(x,y)=\left((0.5-x)\overset{k}{\vee}(0.5-y)\right)\overset{k}{\wedge}\left(\left(x(1-x)\right)\overset{k}{\wedge}\left(y(1-y)\right)\right)$$

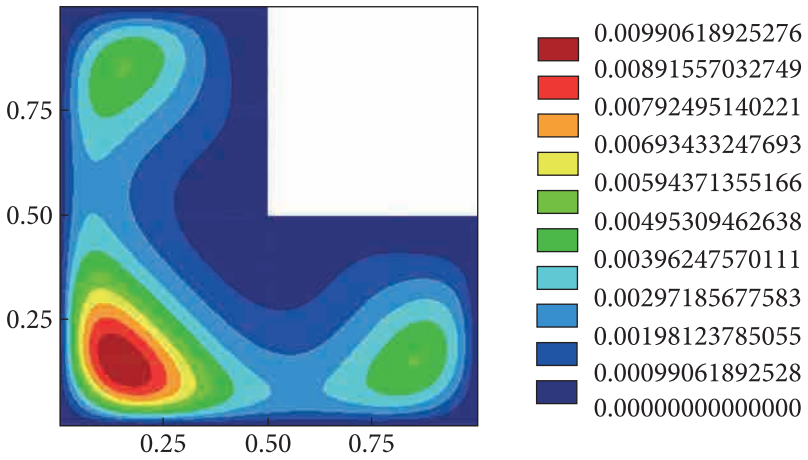

Fig. 4.12. Graph of the function $f_2(x, y)$ in the form of lines of constant level on the plane xOy

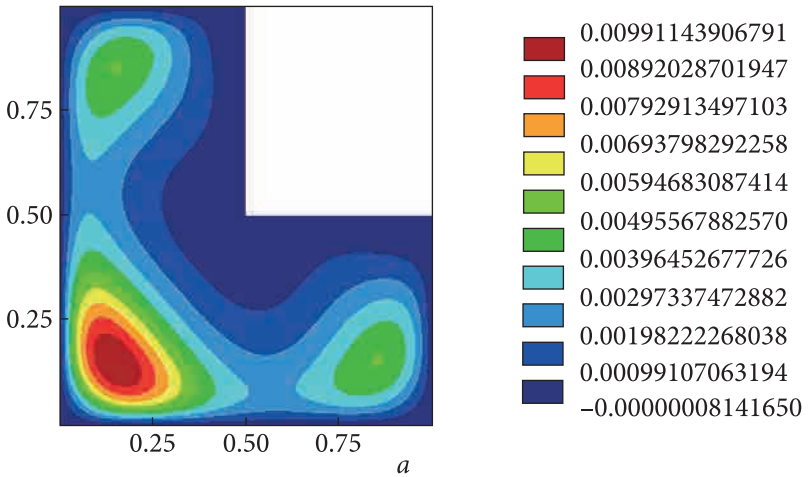

a

Fig. 4.13. Graphs of the functions: *a* — the approximation problem solution using the structure $f(x, y) = \omega_1(x, y)P_1(x, y) + \omega_2(x, y)P_2(x, y)$; *b* — the difference modulus of the function $f_2(x, y)$ and the approximation problem solution (see also page 99)

is considered. The solution structure is be taken in the form

$$f(x, y) = \omega_1(x, y)P_{1,k}(x, y) + \omega_2(x, y)P_{2,k}(x, y),$$

where

$$P_{1,k}(x, y) = \sum_{i=1}^{k_1} c_{l,i}\varphi_i(x, y),\ k_1 + k_2 = 144,\ \{\varphi_i(x, y)\} \text{ — cubic B-splines,}$$

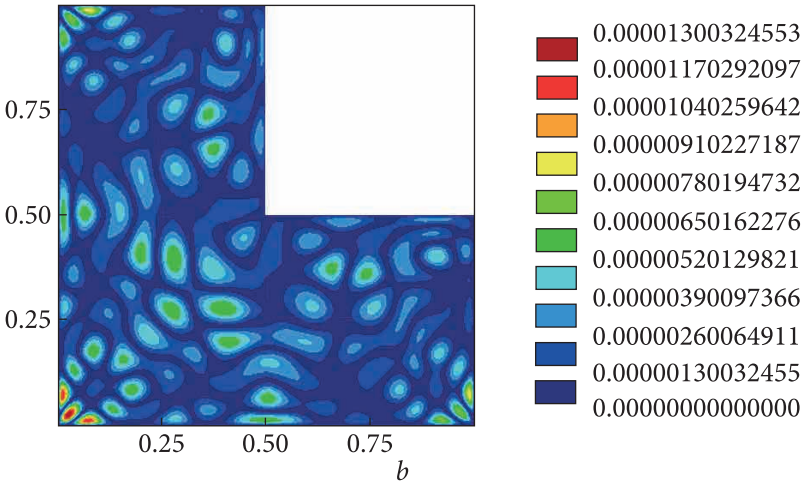

End of Fig. 4.13.

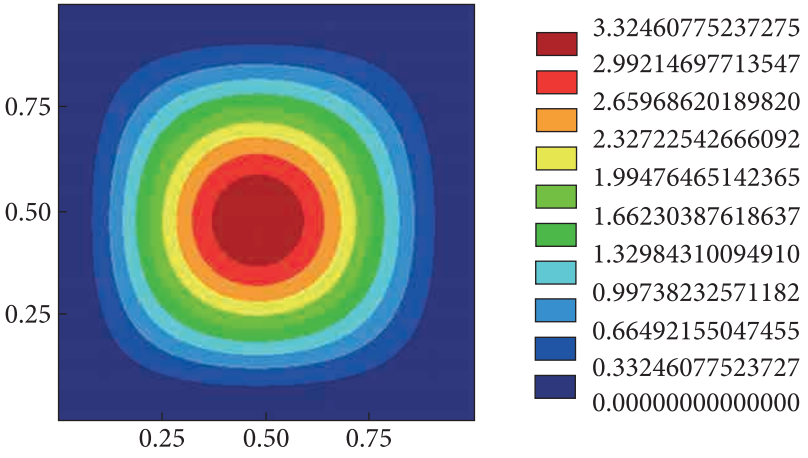

Fig. 4.14. Graphs of the function $u(x,y)=1000\sin^2(x)\sin^2(y)(xy-x-y+1)^2$ in the form of lines of constant level on the plane xOy

$$\omega_1(x,y)=x(1-x)y(1-y)f_1(0.5-x,0.5-y)\text{'}$$
$$\omega_2(x,y)=x(1-x)y(1-y)f_2(0.5-x,0.5-y),$$
$$f_1(x,y)=\frac{x^2|x|+x^3+y^2|y|+y^3}{2}-0{,}1xy,$$
$$f_2(x,y)=\frac{x^2|x|+x^3+y^2|y|+y^3}{2}-0{,}2xy.$$

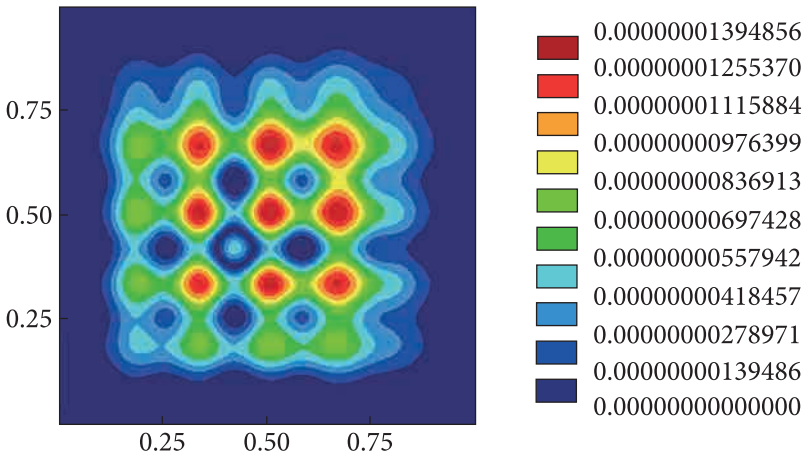

Fig. 4.15. Graph of the function of the difference modulus of the analytical and numerical solution in the form of lines of constant level on the plane xOy

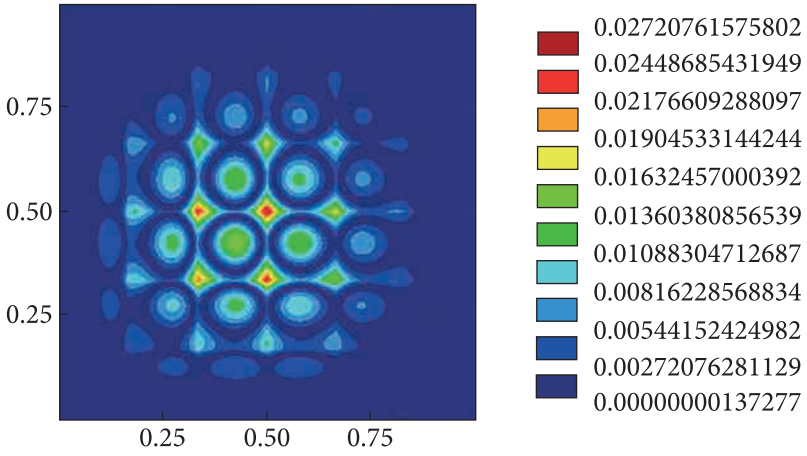

Fig. 4.16. Graph of the modulus of discrepancy of a numerical solution in the form of lines of constant level on a plane xOy

Fig. 4.10 and 4.12 show the graphs of functions $f_1(x,y)$ and $f_2(x,y)$, respectively. Fig. 4.11 and 4.13 show the results of numerical experiments.

The analysis of the figures shows that the structure $f(x,y) = \omega_1(x,y)P_1(x,y) + \omega_2(x,y)P_2(x,y)$ has a high approximation capacity also for functions in which the curves formed by the zeros of these functions do not extend inside the area.

4.2.3. Test boundary value problem that has an analytical solution

The following test boundary value problem in the domain $\Omega = (0,1)\times(0,1)$ is considered:

$$\begin{cases}
\Delta\Delta u(x,y) = 8000\sin^2(x)\sin^2(y) + 8000\cos^2(x)\sin^2(y)(x-1)^2 + \\
+ 24\,000\sin^2(x)\cos^2(y)(x-1)^2 - 32000\sin^2(x)\sin^2(y)(x-1)^2 + \\
+24\,000\cos^2(x)\sin^2(y)(y-1)^2 + 8000\sin^2(x)\cos^2(y)(y-1)^2 - \\
-32\,000\sin^2(x)\sin^2(y)(y-1)^2 + 16\,000\cos(x)\sin(x)\sin^2(y)(2x-2) + \\
+16\,000\sin^2(x)\cos(y)\sin(y)(2y-2)^2 + 8000\cos^2(x)\cos^2(y)(x-1)^2(y-1)^2 - \\
-16\,000\cos^2(x)\sin^2(y)(x-1)^2(y-1)^2 - 16\,000\sin^2(x)\cos^2(y)(x-1)^2(y-1)^2 + \\
+24\,000\sin^2(x)\sin^2(y)(x-1)^2(y-1)^2 + \\
+16\,000\cos(x)\sin(x)\cos^2(y)(2x-2)(y-1)^2 - \\
-48\,000\cos(x)\sin(x)\sin^2(y)(2x-2)(y-1)^2 + \\
+16\,000\cos^2(x)\cos(y)\sin(y)(2y-2)(x-1)^2 - \\
-48\,000\sin^2(x)\cos(y)\sin(y)(2y-2)(x-1)^2 + \\
+32\,000\cos(x)\sin(x)\cos(y)\sin(y)(2y-2)(2x-1); \\
u(x,y)\big|_{\partial\Omega} = 0; \\
\left.\dfrac{\partial u(x,y)}{\partial n}\right|_{\partial\Omega} = 0.
\end{cases}$$

Fig. 4.14. show the analytical solution of this problem is the function $u(x,y) = 1000\sin^2(x)\sin^2(y)(xy - x - y + 1)^2$.

The solution of this problem was obtained using the least squares method and the structure $u(x,y) = \omega^2(x,y)P_k(x,y)$, where $P_k(x,y) = \sum_{i=1}^{k} c_i\varphi_i(x,y)$, $k = 121$, $\{\varphi_i(x,y)\}$ — B-splines of the fifth order, $\omega(x,y) = xy(1-x)(1-y)$.

Fig. 4.15 shows the function of the difference modulus of the numerical and analytical solution. Fig. 4.16 shows the discrepancy of the numerical solution, where the discrepancy is the difference between the problem operator, which is applied to the numerical solution, and the right side of the equation.

4.2.4. Implication of boundary basic elements to solve boundary value problems

The following boundary value problem on the segment $\left[0,1\right]$ is considered:

$$\begin{cases} f''(x) = -\pi^2 \sin(\pi x), \quad x \in (0,1), \\ f(x)\big|_0 = 0, \\ f(x)\big|_1 = 0. \end{cases}$$

Analytical solution of this problem — $f(x) = \sin(\pi x)$.

To solve this, the least squares method and the Bubnov — Galerkin method [40, 41] are applied for a basis with boundary basic elements.

The problem of the function $f(x) = \sin(\pi x)$ approximation using the least squares method for a basis with boundary basic elements and a standard basis of a cubic spline is solved.

Fig. 4.17—4.22 show the results of numerical experiments for different numbers of basic elements.

The analysis of the figures shows that for this problem, the boundary basic elements do not impair the approximation ability of the B-splines when reducing the diameter of the carriers of the boundary basic elements.

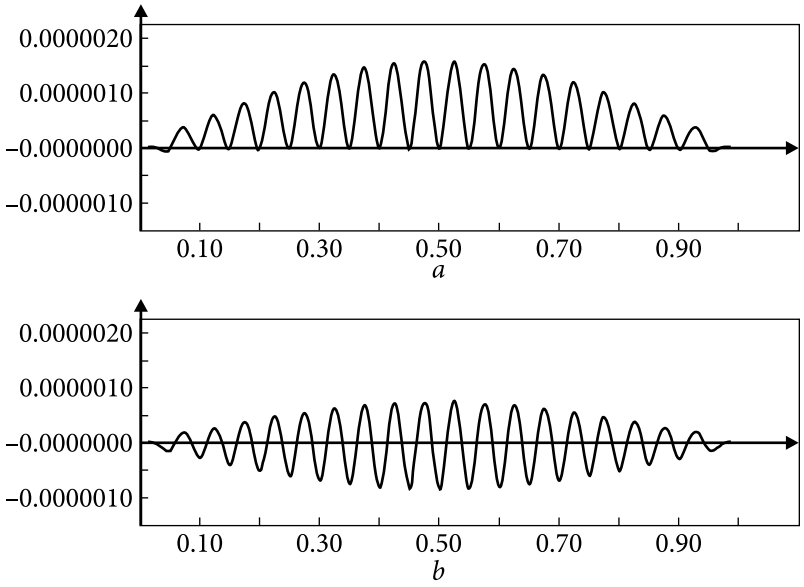

Fig. 4.17. Graphs of the different functions of the analytical and numerical solutions of the boundary value problem obtained using 21 basic elements: *a* — by the least squares method; *b* — by the Bubnov — Galerkin method

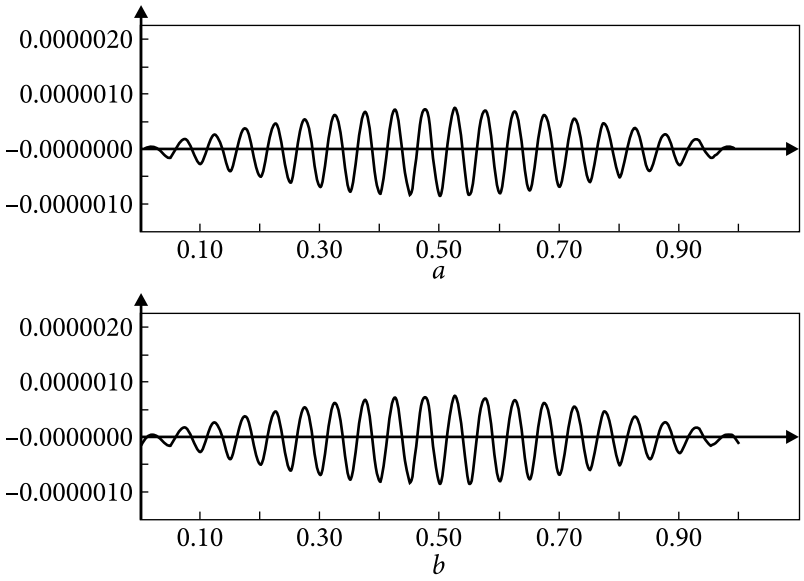

Fig. 4.18. Graphs of the difference between the function $f(x) = \sin(\pi x)$ and the approximation problem solutions using: *a* — 21 basic elements, which include boundary basic elements; *b* — 23 B-splines

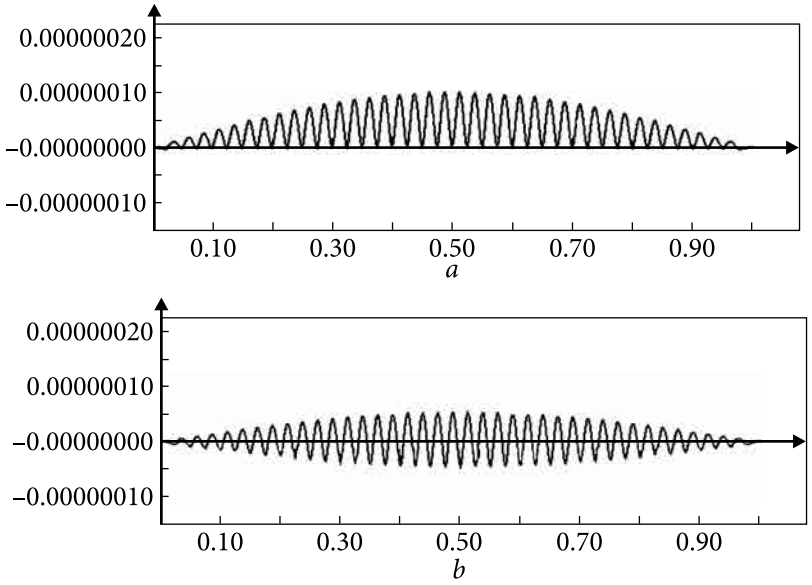

Fig. 4.19. Graphs of the difference functions of the analytical and numerical solutions of the boundary value problem obtained using 41 basic elements: *a* — by the least squares method; *b* — by the Bubnov — Galerkin method

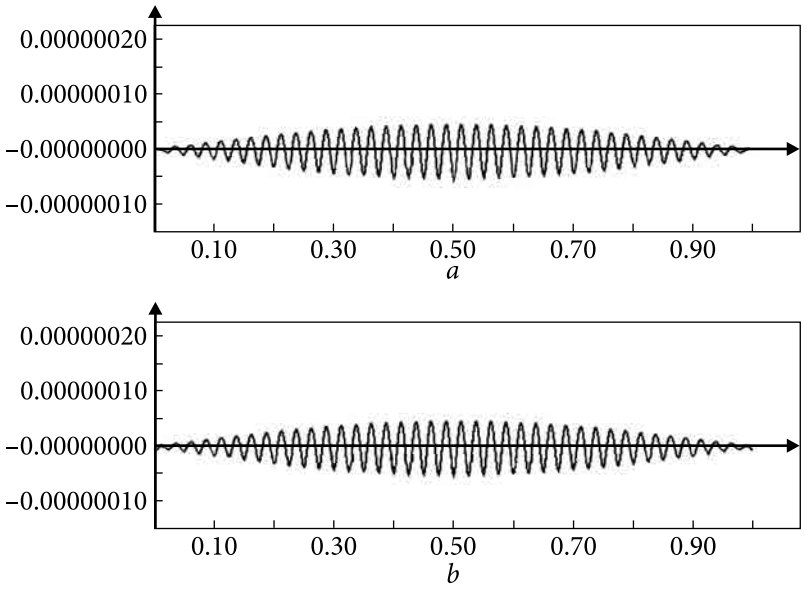

Fig. 4.20. Graphs of the difference between the function $f(x) = \sin(\pi x)$ and the approximation problem solutions using: *a* — 41 basic elements, which include boundary basic elements; *b* — 43 B-splines

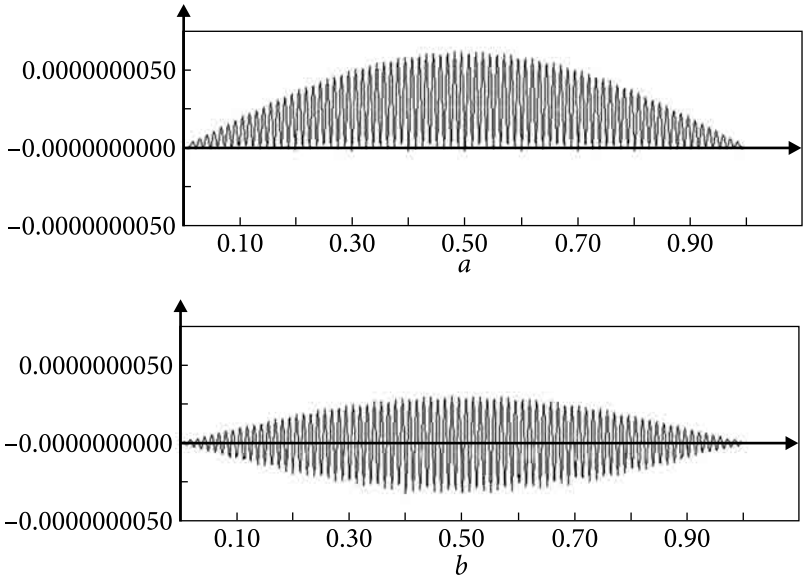

Fig. 4.21. Graphs of the difference functions of the analytical and numerical solutions of the boundary value problem obtained using 81 basic elements: *a* — by the least squares method; *b* — by the Bubnov — Galerkin method

4.3. Examples of some boundary value problems solving

4.3.1. Torsion of a square prism

To solve the square prism torsion problem, it is necessary to solve the following boundary value problem in some domain Ω. Domain Ω has the form $\Omega = (0,1)\times(0,1)$.

$$\begin{cases} \Delta u(x,y) = -2, \quad (x,y) \in \Omega; \\ u(x,y)\big|_{\partial\Omega} = 0. \end{cases}$$

Fig. 4.23 shows the analytical solution of this problem, which has the form [17]

$$u(x,y) = x(1-x) - \frac{8}{\pi^3}\sum_{i=1}^{\infty} \frac{ch\left(\left(2i-1\right)\pi\left(y-0.5\right)\right)\sin(2i-1)\pi x}{(2i-1)^3 ch\left(\dfrac{2i-1}{2}\pi\right)}.$$

To solve this problem, the least squares method and the structure $u(x,y) = \omega(x,y)P_k(x,y)$ were used, where $P_k(x,y) = \sum_{i=1}^{k} c_i\varphi_i(x,y)$, $k = 81$, $\{\varphi_i(x,y)\}$ — cubic B-splines.

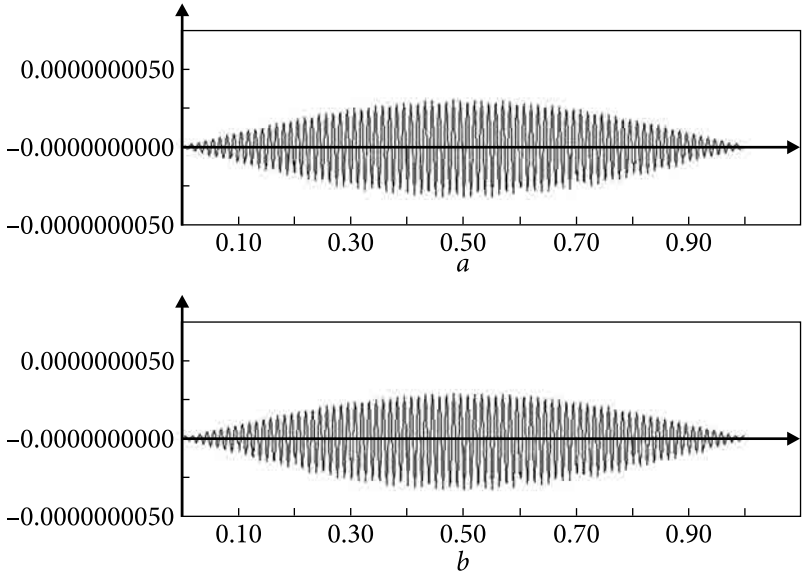

Fig. 4.22. Graphs of the difference between the function $f(x) = \sin(\pi x)$ and the approximation problem solutions using: *a* — 81 basic elements, which include boundary basic elements; *b* — 83 B-splines

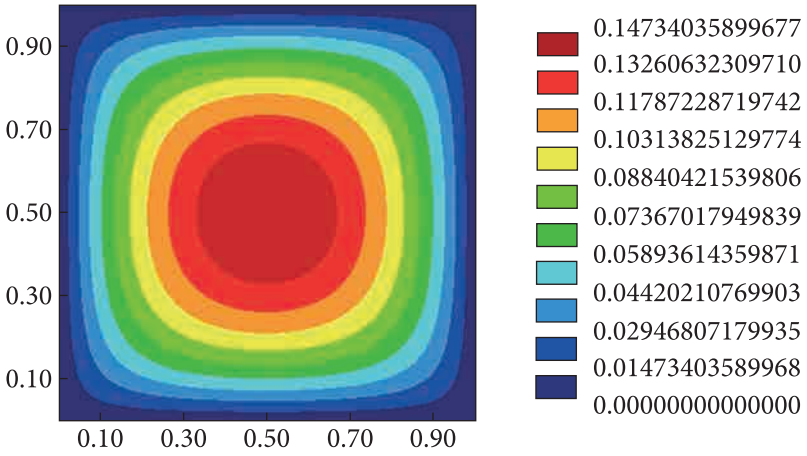

Fig. 4.23. Graph of a function that is an analytical solution of the square prism torsion problem in the form of lines of constant level on the plane xOy

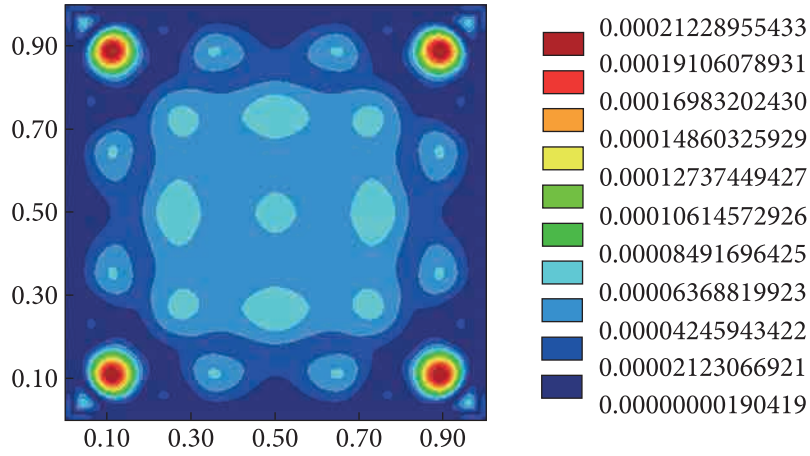

Fig. 4.24. Graph of the function of the difference modulus of the analytical and numerical solution using the structure $u(x,y)=\omega_1(x,y)P_k(x,y)$ in the form of lines of constant level on the plane xOy

$\omega_1(x,y)=\big(x(1-x)\big)\wedge_0\big(y(1-y)\big)$ and $\omega_2(x,y)=xy(1-x)(1-y)$ were used as a function $\omega(x,y)$. Fig. 4.24, and 4.25 show graphs of functions of difference moduli of the analytical and numerical solutions for weight functions $\omega_1(x,y)$ (Fig. 4.24) and $\omega_2(x,y)$ (Fig. 4.25).

The analytical solution of the problem is a function of class $C^2(\Omega)\cap.$ $\cap C^1(\bar{\Omega})$.The figures analysis shows that for this problem the use of a smooth

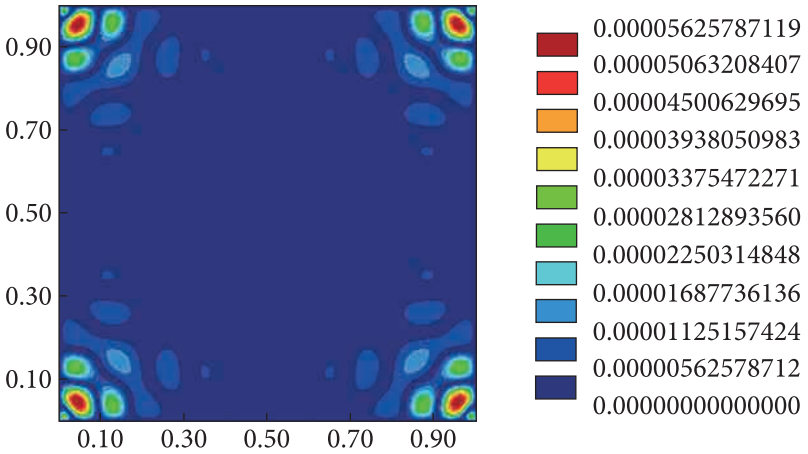

Fig. 4.25. Graph of the function of the difference modulus of the analytical and numerical solution using the structure $u(x,y)=\omega_2(x,y)P_k(x,y)$ in the form of lines of constant level on the plane xOy

weight function leads to a more accurate result than the use of a non-smooth weight function.

4.3.2. Solution of a real practical problem

The design element of the retention compartment model cross-section is considered (Fig. 4.26). The retention compartment is given in the form of a cylinder with stiffeners. A model cross-section of the retention compartment is constructed (Fig. 4.27).

The radius of the retention compartment and the wall thickness are characterized by the values r_2, and r_3. The stiffener thickness is characterized by values r_1,r_2,r_3, and r_4. The stiffener width is described by the angle α.

First, normalized equations of two cylinders are constructed.

For the first cylinder: $f_1(x,y)=r_3-\sqrt{x^2-y^2}$, $f_2(x,y)=\sqrt{x^2-y^2}-r_2$.

For the second cylinder: $f_3(x,y)=r_4-\sqrt{x^2-y^2}$, $f_4(x,y)=r_3-\sqrt{x^2-y^2}-r_1$.

Then the equations of the first and second cylinders will look like $\omega_1(x,y)=f_1\wedge f_2$ and $\omega_2(x,y)=f_3\wedge f_4$, respectively.

Next, a normalized equation of a sector with an angle α is constructed:

$$f_5(x,y)=\frac{y-kx}{\sqrt{k^2+1}},\ f_6(x,y)=\frac{y+kx}{\sqrt{k^2+1}},$$

where

$$k=tg\left(\frac{\pi-\alpha}{2}\right)\ ,\omega_3(x,y)=f_5\wedge f_6\ .$$

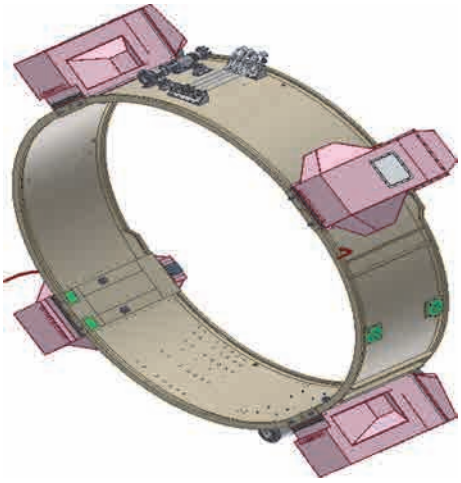

Fig. 4.26. Retention compartment

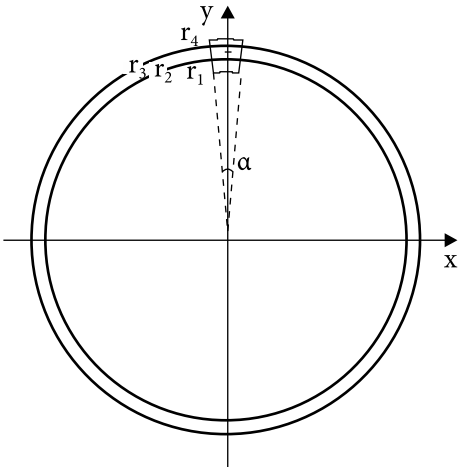

Fig. 4.27. Model cross-section of the retention compartment with one stiffener

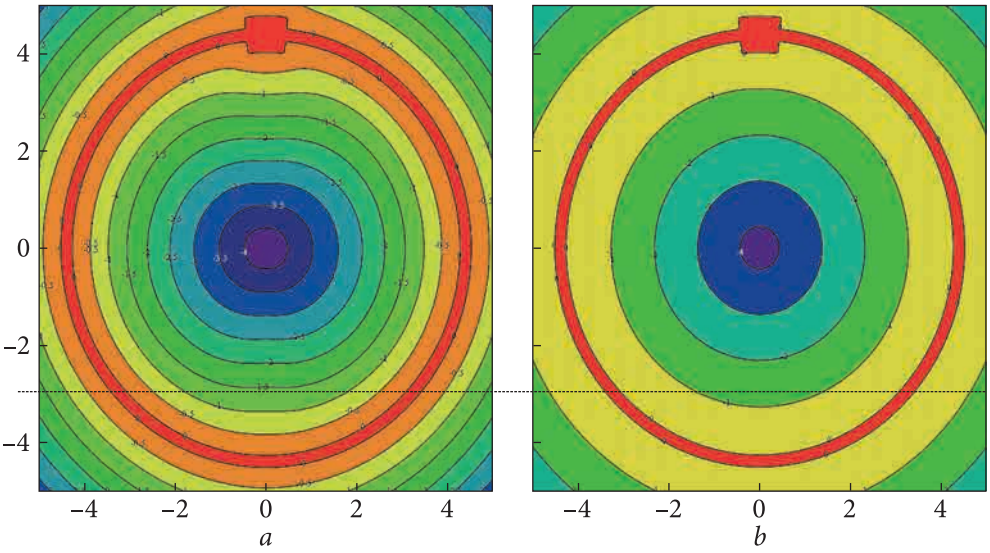

Fig. 4.28. Equation of the model cross-section of the retention compartment with one stiffener normalized up to the 9th order, at a — $n=10$ and $k=10$ and at b — $n=1$ and $k=10$

And later, a normalized equation for one stiffener is constructed

$$\omega_4(x,y)=\omega_2\wedge\omega_3.$$

Then the equation of the model cross-section of the retention compartment with one stiffener will have the form X ω(x, y) = $\omega_1\vee\omega_4$. The graph of this func-

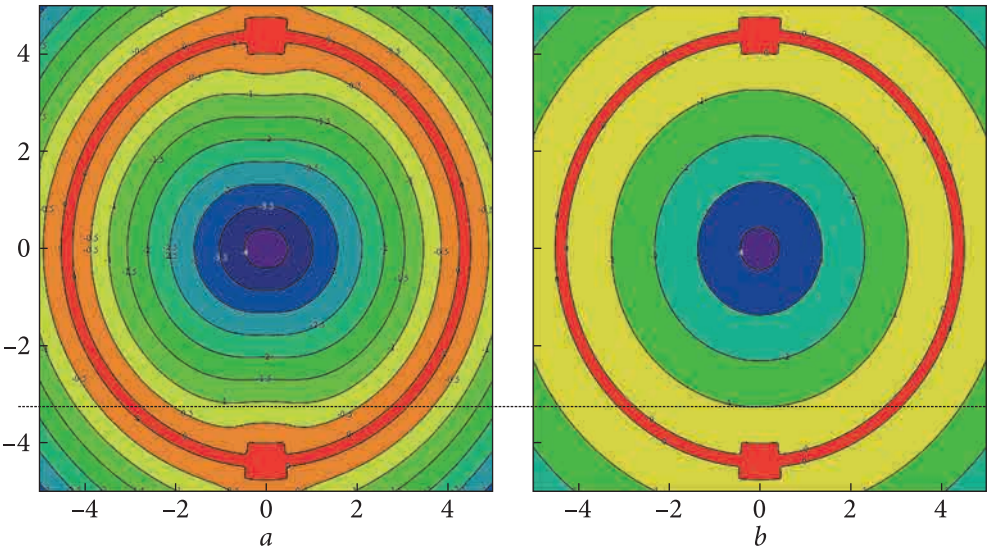

Fig. 4.29. Equation of the model cross-section of the retention compartment with two stiffeners normalized up to the 9th order, at: a — $n=10$, $k=10$, b — $n=1$, $k=10$

tion using the developed system of R-operations (2.22) at different values of parameters n and k is shown in Fig. 4.28.

A symmetrical structure with two stiffeners placed opposite each other is considered.

The equation of the model cross-section of the retention compartment with two stiffeners will have the form $\omega(x,y)=(f_1\wedge f_2)\vee\left(\left(f_3\wedge f_4\right)\wedge\left(f_7\wedge f_8\right)\right)$, where

$$f_7(x,y)=\frac{|y|-k|x|}{\sqrt{k^2+1}}\ ,\ f_8(x,y)=\frac{|y|+k|x|}{\sqrt{k^2+1}}\ ,$$

where

$$k=tg\left(\frac{\pi-\alpha}{2}\right).$$

The graph of this function using the developed system of R-operations (2.22) at different values of the parameters n and k is shown in Fig. 4.29.

Thus, a new system of parametric R-operations, which was developed in Chapter 2, is processed on the real problem.

Numerical calculations of test and model problems showed the effectiveness of new constructive tools of structural methods and approaches to solve boundary value problems.

CHAPTER 5

MATHEMATICAL AND COMPUTER MODELING OF HYDRODYNAMIC FIELDS

Nowadays, the most common method of mathematical modeling of hydrodynamics problems in technical objects is based on the numerical solution of the system of Navier—Stokes differential equations in partial derivatives, which describe the motion of a viscous Newtonian fluid. In this chapter, variational methods are used together with structural ones to solve boundary value problems of hydrodynamics, and the results obtained in the previous chapters are used as well.

5.1. Mathematical modeling of hydrodynamic processes using the R-function method for flat channels

In the two-dimensional case, the calculation of flows can be performed based on equations for the function of stream and vortex, as well as based on the Poisson equation for static pressure [65—67]. Also, in the two-dimensional case, the vortex equation can be excluded from the system, and the system of Navier — Stokes equations can be reduced to a sequence of equations for the stream function and static pressure [11—13, 65—67].

5.1.1. Problem statement for the velocity field

The flat steady flow of a viscous incompressible fluid is described by a system of Navier—Stokes equations [70]

$$V_x \frac{\partial V_x}{\partial x} + V_y \frac{\partial V_x}{\partial y} + \frac{\partial P}{\partial x} - \frac{1}{\mathrm{Re}} \Delta V_x = 0, \tag{5.1}$$

$$V_x \frac{\partial V_y}{\partial x} + V_y \frac{\partial V_y}{\partial y} + \frac{\partial P}{\partial y} - \frac{1}{\mathrm{Re}} \Delta V_y = 0, \tag{5.2}$$

$$\frac{\partial V_x}{\partial x} + \frac{\partial V_y}{\partial y} = 0, \tag{5.3}$$

where (5.1), (5.2) — equation of motion, (5.3) — the equation

of continuity of motion, Re — Reynolds number, (V_r, V_z) — velocity vector, P — static pressure.

The system of equations (5.1)—(5.3) can be reduced using the stream function ψ, which is determined from the relations $V_x = \frac{\partial \psi}{\partial y}$, $V_y = -\frac{\partial \psi}{\partial x}$, to the nonlinear differential equation in partial derivatives of the 4th order concerning the stream function ψ [70]:

$$\frac{1}{\mathrm{Re}} \Delta\Delta\psi - \frac{\partial \psi}{\partial y} \cdot \frac{\partial \Delta\psi}{\partial x} + \frac{\partial \psi}{\partial x} \cdot \frac{\partial \Delta\psi}{\partial y} = 0. \qquad (5.4)$$

To describe the motion of a viscous incompressible fluid in the channel, in addition to the differential equation, boundary conditions are required. Suppose the problem is to be solved in an area Ω, for which $\partial\Omega$ — its border. Regions of the area borders may correspond to the solid walls of the channel, the entrance to the channel, and the exit from it. The boundary conditions for equation (5.4) follow from the adhesion condition on a solid wall and given velocity at the entrance (exit).

On the region of the border Γ_{sw}, corresponding to the solid wall, we have the adhesion condition $\left(V_x = \frac{\partial \psi}{\partial y} = 0, \quad V_y = -\frac{\partial \psi}{\partial x} = 0 \right)$, from which it follows that on Γ_{sw}: $\frac{\partial \psi}{\partial \tau} = (\nabla\psi, \vec{\tau}) = 0$, $\frac{\partial \psi}{\partial n} = (\nabla\psi, \vec{n}) = 0$, where $\vec{\tau}$ — tangent vector to Γ_{sw}, $\vec{n}$ — normal vector to Γ_{sw}. Since $\frac{\partial \psi}{\partial \tau} = 0$ on Γ_{sw}, then along the curve, Γ_{sw} the stream function does not change, i.e. $\psi = const$ on Γ_{sw}.

The velocity distribution, which determines the steam function, is set at the entrance to the channel. If the velocity distribution at the exit is known (for example, the stationary laminar Poiseuille flow), then it can also be set.

5.1.2. Problem statement for the static pressure field

From the system of Navier — Stokes equations (5.1—5.2), after differentiation of (5.1) by x, and (5.2) by y, we have

$$\left(\frac{\partial V_x}{\partial x}\right)^2 + V_x \frac{\partial^2 V_x}{\partial x^2} + \frac{\partial V_y}{\partial x}\frac{\partial V_x}{\partial y} + V_y \frac{\partial^2 V_x}{\partial y \partial x} + \frac{\partial^2 P}{\partial x^2} - \frac{1}{\mathrm{Re}}\left(\frac{\partial^3 V_x}{\partial x^3} + \frac{\partial^3 V_x}{\partial y^2 \partial x}\right) = 0,$$

$$\frac{\partial V_x}{\partial y}\frac{\partial V_y}{\partial x} + V_x \frac{\partial^2 V_y}{\partial x \partial y} + \left(\frac{\partial V_y}{\partial y}\right)^2 + V_y \frac{\partial^2 V_y}{\partial y^2} + \frac{\partial^2 P}{\partial y^2} - \frac{1}{\mathrm{Re}}\left(\frac{\partial^3 V_y}{\partial x^2 \partial y} + \frac{\partial^3 V_y}{\partial y^3}\right) = 0.$$

If we add these two equations and add similar terms, taking into account (5.3), we obtain

$$\Delta P = 2\left(\frac{\partial V_x}{\partial x}\frac{\partial V_y}{\partial y} - \frac{\partial V_y}{\partial x}\frac{\partial V_x}{\partial y}\right)$$

This equation can be rewritten concerning the stream function ψ as follows:

$$\Delta P = 2\left(\frac{\partial^2 \psi}{\partial x^2}\frac{\partial^2 \psi}{\partial y^2} - \left(\frac{\partial^2 \psi}{\partial x \partial y}\right)^2\right). \tag{5.5}$$

The boundary conditions for this equation are considered. From Navier—Stokes equations (5.1)—(5.2) we have:

$$\frac{\partial P}{\partial x} = \left(\frac{1}{\mathrm{Re}}\Delta V_x - V_x\frac{\partial V_x}{\partial x} - V_y\frac{\partial V_x}{\partial y}\right),$$

$$\frac{\partial P}{\partial y} = \left(\frac{1}{\mathrm{Re}}\Delta V_y - V_x\frac{\partial V_y}{\partial x} - V_y\frac{\partial V_y}{\partial y}\right).$$

From $\frac{\partial P}{\partial n} = \left(\nabla P, \vec{n}\right)$, then on Γ_{sw}, taking into account the adhesion condition ($V_x = 0$, $V_y = 0$), we obtain:

$$\frac{\partial P}{\partial n} = \left(\left(\frac{1}{\mathrm{Re}}\Delta V_x, \frac{1}{\mathrm{Re}}\Delta V_y\right), \vec{n}\right) = \frac{1}{\mathrm{Re}}\Delta((V_x, V_y), \vec{n}) = \frac{1}{\mathrm{Re}}\Delta V_n,$$

where V_n — projection of the velocity vector on the normal vector $\vec{n}$ to Γ_{sw}.

Suppose that Γ_{sw} (solid wall) is described by the equation $sw(x, y) = 0$, where $sw(x, y)$ is a function normalized up to the first order, i.e.

$$\left.\frac{\partial sw(x,y)}{\partial n}\right|_{\Gamma_{sw}} = 1,$$

where $\vec{n}$ — normal vector to Γ_{sw}. Then

$$V_n = \frac{\partial \psi}{\partial y}\frac{\partial sw}{\partial x} - \frac{\partial \psi}{\partial x}\frac{\partial sw}{\partial y}.$$

Thus, on Γ_{sw}

$$\frac{\partial P}{\partial n} = \frac{1}{\mathrm{Re}}\Delta\left(\frac{\partial \psi}{\partial y}\frac{\partial sw}{\partial x} - \frac{\partial \psi}{\partial x}\frac{\partial sw}{\partial y}\right). \tag{5.6}$$

In some approximation, it can be assumed that the normal component of the velocity to the solid wall in some parts of the boundary layer is missing.

Then

$$\frac{\partial P}{\partial n} = \frac{1}{\mathrm{Re}} \Delta V_n = 0 . \tag{5.7}$$

The boundary conditions at the entrance and exit to the channel are written down. The region of the border that corresponds to the entrance is denoted as Γ_{si}, and the region of the border that corresponds to the exit is denoted as Γ_{so}.

Suppose that Γ_{si} is described by the equation $si(x, y) = 0$, where $si(x, y)$ — function normalized up to the first order.

A derivative of the function P is considered on the region of the border Γ_{si},

$$\frac{\partial P}{\partial n} = \left(\left(\left(\frac{1}{\mathrm{Re}} \Delta V_x - V_x \frac{\partial V_x}{\partial x} - V_y \frac{\partial V_x}{\partial y} \right), \left(\frac{1}{\mathrm{Re}} \Delta V_y - V_x \frac{\partial V_y}{\partial x} - V_y \frac{\partial V_y}{\partial y} \right) \right), \vec{n} \right) =$$

$$= \left(\frac{1}{\mathrm{Re}} \left(\Delta V_x, \Delta V_y \right) - V_x \left(\frac{\partial V_x}{\partial x}, \frac{\partial V_y}{\partial x} \right) - V_y \left(\frac{\partial V_x}{\partial y}, \frac{\partial V_y}{\partial y} \right), \vec{n} \right) =$$

$$= \frac{1}{\mathrm{Re}} \Delta V_n - V_x \frac{\partial V_n}{\partial x} - V_y \frac{\partial V_n}{\partial y},$$

where V_n — projection of the velocity vector on the normal vector $\vec{n}$ to Γ_{si}.

Since on Γ_{si} $V_n = \frac{\partial \psi}{\partial y} \frac{\partial si}{\partial x} - \frac{\partial \psi}{\partial x} \frac{\partial si}{\partial y}$, then on Γ_{si} $so(x, y) = 0$.

$$\frac{\partial P}{\partial n} = \frac{1}{\mathrm{Re}} \Delta \left(\frac{\partial \psi}{\partial y} \frac{\partial si}{\partial x} - \frac{\partial \psi}{\partial x} \frac{\partial si}{\partial y} \right) - \frac{\partial \psi}{\partial y} \frac{\partial \left(\frac{\partial \psi}{\partial y} \frac{\partial si}{\partial x} - \frac{\partial \psi}{\partial x} \frac{\partial si}{\partial y} \right)}{\partial x} +$$

$$+ \frac{\partial \psi}{\partial x} \frac{\partial \left(\frac{\partial \psi}{\partial y} \frac{\partial si}{\partial x} - \frac{\partial \psi}{\partial x} \frac{\partial si}{\partial y} \right)}{\partial y}. \tag{5.8}$$

Suppose that Γ_{so} is described by the equation $so(x, y) = 0$, where $so(x, y)$ — function normalized up to the first order. Then, similarly, we have on Γ_{so}

$$\frac{\partial P}{\partial n} = \frac{1}{\mathrm{Re}} \Delta \left(\frac{\partial \psi}{\partial y} \frac{\partial so}{\partial x} - \frac{\partial \psi}{\partial x} \frac{\partial so}{\partial y} \right) - \frac{\partial \psi}{\partial y} \frac{\partial \left(\frac{\partial \psi}{\partial y} \frac{\partial so}{\partial x} - \frac{\partial \psi}{\partial x} \frac{\partial so}{\partial y} \right)}{\partial x} +$$

$$+ \frac{\partial \psi}{\partial x} \frac{\partial \left(\frac{\partial \psi}{\partial y} \frac{\partial so}{\partial x} - \frac{\partial \psi}{\partial x} \frac{\partial so}{\partial y} \right)}{\partial y}. \tag{5.9}$$

5.1.3. Implementation examples

Problem 1. Calculation of hydrodynamic heat generators. A hydrodynamic heat generator, which is an axisymmetric structure — a cylindrical tube (housing) with a «garland» located inside the axis, consisting of cones, which in our case are designed to convert the energy of the fluid motion into heat, is considered. The scheme of such a generator is given in Fig. 5.1. Development and numerical implementation of a mathematical model of the working body flow through the generator (left — right) will allow us to perform a quantitative assessment of hydrodynamic heating of the fluid due to dissipated energy because of hydraulic pulsations, reverse flows, and reversible motion.

Problem statement. It is necessary to find the solution of equation (5.4) in the area Ω (Fig. 5.2), for which $\partial\Omega = \Gamma_1 \cup \Gamma_2 \cup \Gamma_3 \cup \Gamma_4 \cup \Gamma_5$ — its border. In this case Γ_4 is the entrance to the channel, Γ_5 — exit from the channel, Γ_1, Γ_2, Γ_3 — solid walls.

Based on the physical formulation of the problem, the boundary conditions are as follows:

$$\Gamma_1:\ \psi = \frac{a}{3},\quad \frac{\partial\psi}{\partial n} = 0;$$

$$\Gamma_2:\ \psi = -\frac{a}{3},\quad \frac{\partial\psi}{\partial n} = 0;\ \Gamma_3:\ \psi = 0,\quad \frac{\partial\psi}{\partial n} = 0;$$

$$\Gamma_4:\ \psi = y - \frac{4y^3}{3a^2},\quad \frac{\partial\psi}{\partial n} = 0;\ \Gamma_5:\ \psi = y - \frac{4y^3}{3a^2},\quad \frac{\partial\psi}{\partial n} = 0.$$

The area Ω is described by inequality $\omega(x, y) \geq 0$. A function $\omega(x, y)$ is constructed using R-operations [48].

For the area, Ω the function $\omega(x, y)$ has the form of

$$\omega = \left(f_1 \wedge_0 f_2\right) \wedge_0 \left(f_3 \wedge_0 f_4 \wedge_0 f_5\right) \wedge_0 \left(f_6 \wedge_0 f_7 \wedge_0 f_8\right) \wedge_0$$
$$\wedge_0 \left(f_9 \wedge_0 f_{10} \wedge_0 f_{11}\right) \wedge_0 \left(f_{12} \wedge_0 f_{13} \wedge_0 f_{14}\right) \wedge_0 \left(f_{15} \wedge_0 f_{16} \wedge_0 f_{17}\right),$$

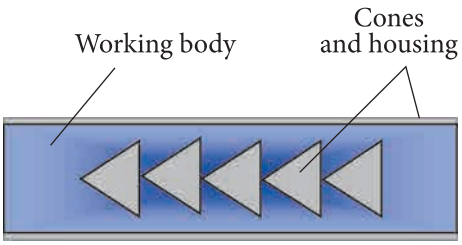

Fig. 5.1. Heat generator scheme

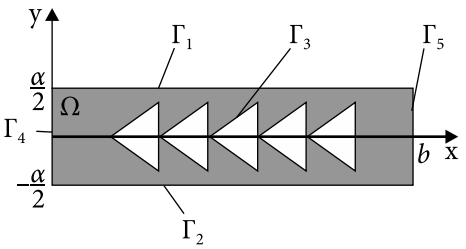

Fig. 5.2. Area of the problem solution

where

$$x \wedge_0 y = x + y - \sqrt{x^2 + y^2} \text{ — R-conjunction;}$$

$$x \wedge_0 y = x + y + \sqrt{x^2 + y^2} \text{ — R-disjunction;}$$

$$f_1 = x(b - x) / b;$$

$$f_2 = \left(y + \frac{a}{2} \right) \left(\frac{a}{2} - y \right) / a;$$

$$f_3 = x - c - d\frac{\sqrt{3}}{2};$$

$$f_4 = -\left(y + \frac{d}{2} \right) \frac{2}{d} + \left(x - c - d\frac{\sqrt{3}}{2} \right) \left(-\frac{2}{\sqrt{3}d} \right);$$

$$f_5 = \left(y - \frac{d}{2} \right) \frac{2}{d} + \left(x - c - d\frac{\sqrt{3}}{2} \right) \left(-\frac{2}{\sqrt{3}d} \right);$$

$$f_6 = x - c - d\sqrt{3} - h;$$

$$f_7 = -\left(y + \frac{d}{2} \right) \frac{2}{d} + \left(x - c - d\sqrt{3} - h \right) \left(-\frac{2}{\sqrt{3}d} \right);$$

$$f_8 = \left(y - \frac{d}{2} \right) \frac{2}{d} + (x - c - d\sqrt{3} - h) \left(-\frac{2}{\sqrt{3}d} \right);$$

$$f_9 = x - c - d\frac{3\sqrt{3}}{2} - 2h;$$

$$f_{10} = -\left(y + \frac{d}{2} \right) \frac{2}{d} + \left(x - c - d\frac{3\sqrt{3}}{2} - 2h \right) \left(-\frac{2}{\sqrt{3}d} \right);$$

$$f_{11} = \left(y - \frac{d}{2} \right) \frac{2}{d} + \left(x - c - d\frac{3\sqrt{3}}{2} - 2h \right) \left(-\frac{2}{\sqrt{3}d} \right);$$

$$f_{12} = x - c - d\frac{4\sqrt{3}}{2} - 3h;$$

$$f_{13} = -\left(y + \frac{d}{2} \right) \frac{2}{d} + \left(x - c - d\frac{4\sqrt{3}}{2} - 3h \right) \left(-\frac{2}{\sqrt{3}d} \right);$$

Fig. 5.3. Function $\omega(x, y)$

Fig. 5.4. Function $\psi_0(x, y)$

$$f_{14} = \left(y - \frac{d}{2}\right)\frac{2}{d} + \left(x - c - d\frac{4\sqrt{3}}{2} - 3h\right)\left(-\frac{2}{\sqrt{3}d}\right);\ f_{15} = x - c - d\frac{5\sqrt{3}}{2} - 4h;$$

$$f_{16} = -\left(y + \frac{d}{2}\right)\frac{2}{d} + \left(x - c - d\frac{5\sqrt{3}}{2} - 4h\right)\left(-\frac{2}{\sqrt{3}d}\right);$$

$$f_{17} = \left(y - \frac{d}{2}\right)\frac{2}{d} + \left(x - c - d\frac{5\sqrt{3}}{2} - 4h\right)\left(-\frac{2}{\sqrt{3}d}\right);$$

b — channel length; a — channel width; d — the length of the triangle side; c — indentation of the 1st triangle from the beginning; h — the distance between the triangles.

Fig. 5.3 shows the function $\omega(x, y)$ in the form of isolines.

The solution of the boundary value problem for equation (5.4) with the corresponding boundary conditions will be sought in the form $\psi = \psi_1 + \psi_0$, where ψ_0 is a function that meets the inhomogeneous boundary conditions of the problem; ψ_1 is a function with zero Dirichlet and Neumann boundary conditions.

The solution structure for a function ψ_1 has the form

$$\psi_1 = \omega^2 P,$$

where P — undefined structure component. For the problem under consideration, the undefined component P is written in the form $P(x, y) = \sum_{i=1}^{k} c_i \varphi_i(x, y)$, where $\{\varphi_i(x, y)\}$ — B-splines of the fifth order, $\{c_i\}, i = 1, \ldots, k$ — constants that need to be defined [30, 31, 65—69].

Function ψ_0: $\psi_0\big|_{\Gamma_i} = \Psi_i$, $\frac{\partial \psi_0}{\partial n}\Big|_{\Gamma_i} = 0$, i = 1,..., 5 will be constructed using the gluing formula [43] $\psi_0 = \dfrac{\sum_{i=1}^{5} \frac{\Psi_i}{w_i^2}}{\sum_{i=1}^{5} \frac{1}{w_i^2}}$, where

$$\Psi_1 = \frac{a}{3}, \Psi_2 = -\frac{a}{3}, \Psi_3 = 0, \Psi_4 = y - \frac{4y^3}{3a^2}, \Psi_5 = y - \frac{4y^3}{3a^2},$$

$$w_1 = \frac{a}{2} - y, \; w_2 = y - \frac{a}{2},$$

$$w_3 = \left(f_3 \wedge_0 f_4 \wedge_0 f_5\right) \wedge_0 \left(f_6 \wedge_0 f_7 \wedge_0 f_8\right) \wedge_0 \left(f_9 \wedge_0 f_{10} \wedge_0 f_{11}\right) \wedge_0$$
$$\wedge_0 \left(f_{12} \wedge_0 f_{13} \wedge_0 f_{14}\right) \wedge_0 \left(f_{15} \wedge_0 f_{16} \wedge_0 f_{17}\right), w_4 = x, w_4 = b - x.$$

Fig. 5.4 shows the function $\psi_0(x, y)$ that accurately meets all the boundary conditions. As to functions ψ_1 and ψ_0, equation (5.4) has the form

$$\frac{1}{\mathrm{Re}}\Delta\Delta\psi_1 - \left\{\frac{\partial\psi_1}{\partial y}\cdot\frac{\partial\Delta\psi_1}{\partial x} - \frac{\partial\psi_1}{\partial x}\cdot\frac{\partial\Delta\psi_1}{\partial y}\right\} - \frac{\partial\psi_1}{\partial y}\cdot\frac{\partial\Delta\psi_0}{\partial x} -$$
$$-\frac{\partial\psi_0}{\partial y}\cdot\frac{\partial\Delta\psi_1}{\partial x} + \frac{\partial\psi_1}{\partial x}\cdot\frac{\partial\Delta\psi_0}{\partial y} + \frac{\partial\psi_0}{\partial x}\cdot\frac{\partial\Delta\psi_1}{\partial y} = -\frac{1}{\mathrm{Re}}\Delta\Delta\psi_0 + \qquad (5.10)$$
$$+\frac{\partial\psi_0}{\partial y}\cdot\frac{\partial\Delta\psi_0}{\partial x} - \frac{\partial\psi_0}{\partial x}\cdot\frac{\partial\Delta\psi_0}{\partial y}.$$

The linearization process according to Newton — Kantorovich is applied to equation (5.10). The sequence of approximations $\{\psi_n\}_{n=1}^{N}$ to the solution ψ_1 is considered. To do this, the function $\psi_{n+1} = \psi_n + \delta\psi_n$ is substituted in equation (5.10) instead of the function ψ_1. The following equation is obtained

$$\frac{1}{\mathrm{Re}}\Delta\Delta\left(\psi_n + \delta\psi_n\right) - \left\{\frac{\partial\left(\psi_n + \delta\psi_n\right)}{\partial y}\cdot\frac{\partial\Delta\left(\psi_n + \delta\psi_n\right)}{\partial x} - \frac{\partial\left(\psi_n + \delta\psi_n\right)}{\partial x}\cdot\frac{\partial\Delta\left(\psi_n + \delta\psi_n\right)}{\partial y}\right\} -$$
$$-\frac{\partial\left(\psi_n + \delta\psi_n\right)}{\partial y}\cdot\frac{\partial\Delta\psi_0}{\partial x} - \frac{\partial\psi_0}{\partial y}\cdot\frac{\partial\Delta\left(\psi_n + \delta\psi_n\right)}{\partial x} + \frac{\partial\left(\psi_n + \delta\psi_n\right)}{\partial x}\cdot\frac{\partial\Delta\psi_0}{\partial y} +$$
$$+\frac{\partial\psi_0}{\partial x}\cdot\frac{\partial\Delta\left(\psi_n + \delta\psi_n\right)}{\partial y} = -\frac{1}{\mathrm{Re}}\Delta\Delta\psi_0 + \frac{\partial\psi_0}{\partial y}\cdot\frac{\partial\Delta\psi_0}{\partial x} - \frac{\partial\psi_0}{\partial x}\cdot\frac{\partial\Delta\psi_0}{\partial y}.$$

The brackets are opened, neglecting the terms of the second order of smallness and given that $\delta\psi_n = \psi_{n+1} - \psi_n$. A sequence of linear equations is obtained

$$\frac{1}{\mathrm{Re}}\Delta\Delta\psi_{n+1} - \left\{\frac{\partial\psi_n}{\partial y}\cdot\frac{\partial\Delta\psi_{n+1}}{\partial x} + \frac{\partial\psi_{n+1}}{\partial y}\cdot\frac{\partial\Delta\psi_n}{\partial x} - \frac{\partial\psi_n}{\partial x}\cdot\frac{\partial\Delta\psi_{n+1}}{\partial y} - \frac{\partial\psi_{n+1}}{\partial x}\cdot\frac{\partial\Delta\psi_n}{\partial y}\right\} -$$
$$-\frac{\partial\psi_{n+1}}{\partial y}\cdot\frac{\partial\Delta\psi_0}{\partial x} - \frac{\partial\psi_0}{\partial y}\cdot\frac{\partial\Delta\psi_{n+1}}{\partial x} + \frac{\partial\psi_{n+1}}{\partial x}\cdot\frac{\partial\Delta\psi_0}{\partial y} + \frac{\partial\psi_0}{\partial x}\cdot\frac{\partial\Delta\psi_{n+1}}{\partial y} = -\frac{1}{\mathrm{Re}}\Delta\Delta\psi_0 +$$
$$+\frac{\partial\psi_0}{\partial y}\cdot\frac{\partial\Delta\psi_0}{\partial x} - \frac{\partial\psi_0}{\partial x}\cdot\frac{\partial\Delta\psi_0}{\partial y} - \frac{\partial\psi_n}{\partial y}\cdot\frac{\partial\Delta\psi_n}{\partial x} + \frac{\partial\psi_n}{\partial x}\cdot\frac{\partial\Delta\psi_n}{\partial y}. \qquad (5.11)$$

Fig. 5.5. The function of the velocity modulus (Re = 200)

Fig. 5.6. The stream function (Re = 200)

Fig. 5.5 and 5.6 show the results of a computational experiment, with the flow of one element of the heat generator. Fig. 5.5 shows the function of the velocity modulus at Re = 200. Fig. 5.6 shows the steam function at Re = 200.

Numerical implementation of the mathematical model of the working body flow on the generator gives a method of obtaining a quantitative estimate of the hydrodynamic heating of the fluid due to hydraulic pulsations, reverse flows, and reversible motion. The corresponding computational algorithm for finding the dissipated energy and the liquid heating in the channel is implemented by a single software package. The versatility of the method and program allows us to conduct multiparameter numerical experiments for different heat generators.

The authors gave an example of a computational experiment at small values of Re = 200.

The methodology of achieving the expected thermal effects and methods of further optimization of real designs of heat generators is a separate, even more, complex problem, which is not considered in this monograph.

But this example proves that the proposed approach for quantitative assessment of the impact of the effects of excess energy generation can be successfully used both in the development of new designs of heat generators and in the modernization of the existing ones.

Problem 2. Calculation of hydrodynamic characteristics of the flow in the channel with ledge.

The following problem statement is considered: to find the distributions of the velocity field and the pressure field in the flow when it flows through a flat model channel with a ledge (Fig. 5.7).

It is necessary to solve the equation for the stream function first, then the Poisson equation for the function P in the area shown in Fig. 5.7. This area is described by the equation $\omega(x, y) = 0$, the function $\omega(x, y)$ is given in Fig. 5.8.

The structure of the solution of the equation for the stream function with the corresponding boundary conditions has a form $\psi = \psi_1 + \psi_0$, where ψ_0 meets all the boundary conditions of the problem

$$\psi_0 = \frac{\sum_{i=1}^{3} \frac{\Psi_i}{w_i^2}}{\sum_{i=1}^{3} \frac{1}{w_i^2}},$$

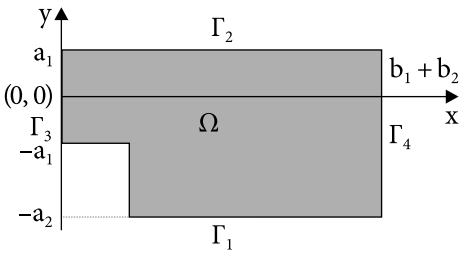

Fig. 5.7. Area Ω — model channel

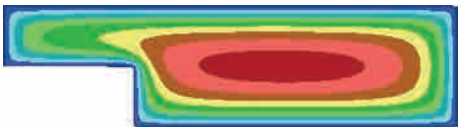

Fig. 5.8. The function $\omega(x, y)$

where Ψ — the values function given in the border regions described by the equation $w_i = 0$. Here

$$\Psi_1 = -\frac{2a_1}{3},\ w_1 = \left(\left(f_3 \vee_0 f_4\right) \wedge_0 f_5\right),$$

$$\Psi_2 = \frac{2a_1}{3},\ w_2 = a_1 - y,\ \Psi_3 = y - \frac{y^3}{3a_1^2},\ w_3 = x.$$

Thus,

$$\psi_0\Big|_{\Gamma_i} = \Psi_i,\ \frac{\partial \psi_0}{\partial n}\Big|_{\Gamma_i} = 0,\ i = 1,2,3,$$

where ψ_1 — an unknown function with zero Dirichlet and Neumann boundary conditions, which has the form $\psi_1 = \omega_1^2 P_1$. Here $P_1 = \sum_{i=1}^{N} A_i \zeta_i$, where P_1 — undefined structure component, A_i — constants that need to be defined, ζ_i — special functions that form the basis in the Hilbert space in which the solution is sought;

$$\omega_1 = f_1 \wedge_0 \left(\left(f_3 \vee_0 f_4\right) \wedge_0 f_5\right) \wedge_0 f_6,$$

where $\wedge_0 (x, y) = x + y - \sqrt{x^2 + y^2}$ — R-conjunction; $\vee_0 (x, y) = x +$ $+ y + \sqrt{x^2 + y^2}$ — R-disjunction; $f_1 = x$; $f_2 = x(b_1 + \ + b_2 - x)/(b_1 + b_2)$; $f_3 = y + a_1$; $f_4 = x - b_1$; $f_5 = y + a_2$; $f_6 = a_1 - y$.

The problem is solved by the least squares method. Next, Poisson's equation concerning the function P in area Ω is solved.

The boundary conditions for Poisson's equation are considered.

On the solid walls, Γ_1 and Γ_2 the boundary condition $\frac{\partial P}{\partial n} = 0$ is used. At the entrance to channel Γ_3, the boundary condition $\frac{\partial P}{\partial n} = const$ is used. At the exit from channel Γ_4, the boundary condition $P = const$ is used.

The structure of the solution for Poisson's equation with the corresponding boundary conditions has the form

$$P = P_2\omega_2 - \omega\left(\frac{\partial\omega_1}{\partial x}\frac{\partial(P_2\omega_2)}{\partial x} + \frac{\partial\omega_1}{\partial y}\frac{\partial(P_2\omega_2)}{\partial y}\right) - \omega\phi + \omega_1^{\,2}\omega_2 P_3 + C,$$

where $\omega_1 = f_1 \wedge_0 \left(\left(f_3 \vee_0 f_4\right) \wedge_0 f_5\right) \wedge_0 f_6$; $\omega = f_2 \wedge_0 \left(\left(f_3 \vee_0 f_4\right) \wedge_0 f_5\right) \wedge_0 f_6$;

$\omega_2 = (b_1 + b_2 - x)$; $P_2 = \sum_{i=1}^{N} C_i\zeta_i$; $P_3 = \sum_{i=1}^{N} D_i\zeta_i$; C_i, D_i — constants that need to be defined; C — the value of static pressure at the exit (the constant is set based on the physical problem statement, in our case $C = 1$); φ — function, which value in the regions of the area border coincides with the derivative normal to the function P in the corresponding border regions on which the following Neumann condition is given:

$$\varphi = \frac{\sum_{i=1}^{3} \frac{\varphi_i}{w_i}}{\sum_{i=1}^{3} \frac{1}{w_i}}.$$

This function is based on the gluing formula. Here φ_i — the value of the Neumann condition is given in the regions of the border Γ_i

$$\varphi_i = 0,\ i = 1, 2,\ \varphi_3 = \frac{8}{\mathrm{Re}\,a^2}.$$

Then the least squares method is used.

Fig. 5.9—5.19 show the results of computational experiments: stream functions, velocity modulus functions, and static flow pressure during its flow through the model element of the rotary-cavitation dispersant. Computational experiments were performed on a grid of 40 × 40 splines of the 5th order. The number of iterations — is 9.

It should be noted that the given solution of the problem included the solution of Poisson's equation for the function P. This approach opens up additional opportunities for the analysis of not only the pressure fields in the fluid flow. In particular, the determination of the numbers Re, at which the formed in the flow pressure drop zones to the level of pressures of saturated vapors of the flowing liquid, or lower, makes it possible to determine the conditions of the beginning of cavitation. This is very important when creating a variety of hydraulic and process equipment.

Problem 3. The problem of fluid flow between two parallel plates. The test problem of stationary fluid flow between two parallel plates is considered. It is

Fig. 5.9. Stream function (Re = 250)

Fig. 5.10. Velocity modulus function (Re = 250)

Fig. 5.11. Static pressure function (Re = 250)

Fig 5.12. Stream function (Re = 600)

Fig. 5.13. Velocity modulus function (Re = 600)

Fig. 5.14. Static pressure function (Re = 600)

Fig. 5.15. Stream function (Re = 500)

Fig. 5.16. Velocity modulus function (Re = 500)

Fig. 5.17. Stream function (Re = 400)

Fig. 5.18. Velocity modulus function (Re = 400)

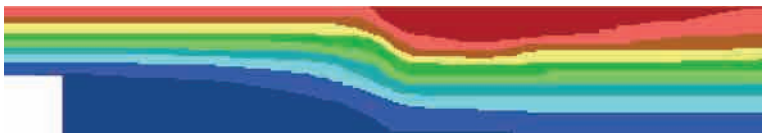

Fig. 5.19. Stream function (Re = 2000)

necessary to find the steam function for this problem. To do this, the boundary value problem for equation (5.4) in the area Ω (Fig. 5.20), for which the border $\partial\Omega = \Gamma_1 \cup \Gamma_2 \cup \Gamma_3 \cup \Gamma_4$ is solved. In our case Γ_1 — entrance to the channel, Γ_2 — exit from the channel, Γ_3, Γ_4 — solid walls.

We set the following boundary conditions for area Ω: on Γ_1 and Γ_2 — $\psi = \frac{y^2}{2} - \frac{y^3}{3} - \frac{1}{12}$ (parabolic Poiseuille velocity profile), $\frac{\partial\psi}{\partial n} = 0$; on Γ_3 — $\psi = -\frac{1}{12}, \frac{\partial\psi}{\partial n} = 0$; on Γ_4 $-\psi = \frac{1}{12}, \frac{\partial\psi}{\partial n} = 0$.

The solution of the boundary value problem for equation (5.4) with the corresponding boundary conditions will be sought in the form $\psi = \psi_1 + \psi_0$, where is a function that meets the inhomogeneous boundary conditions of the problem, ψ_1 — a function with zero Dirichlet and Neumann boundary

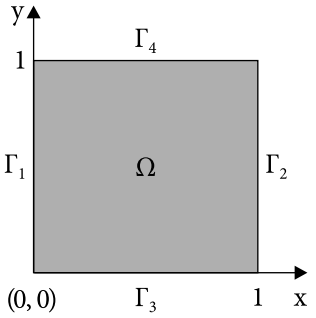

Fig. 5.20. Area Ω

conditions. The structure of the solution of the function ψ_1 has the form $\psi_1 = \omega^2 P_k$, where P_k — undefined structure component, ω: $\omega(x,y) > 0$, $(x,y) \in \Omega$, $\omega(x,y)\big|_{\partial\Omega} = 0$. The function ω can be taken as $\omega(x,y) = xy(1-x)(1-y)$. The function

$$\psi_0(x,y) = \frac{y^2}{2} - \frac{y^3}{3} - \frac{1}{12} +$$

$$+ \alpha\left(x^4 - 2x^3 + x^2\right)\left(y^5 - 2.5y^4 + 2y^3 - 0.5y^2\right)$$

is taken as a function that satisfies the inhomogeneous conditions of the problem.

For this problem, the undefined component is introduced as $P_k(x,y) = \sum_{i=1}^{k} c_i \phi_i(x,y)$, $k = 121$, $\{\varphi_i(x,y)\}$ — B-splines of the fifth order.

The analytical solution of the problem is the function $\psi(x,y) = \frac{y^2}{2} - \frac{y^3}{3} - \frac{1}{12}$ (Fig. 5.21).

For functions ψ_1 and ψ_0, equation (5.4) has the form

$$\frac{1}{\mathrm{Re}}\Delta\Delta\psi_1 - \left\{\frac{\partial\psi_1}{\partial y}\cdot\frac{\partial\Delta\psi_1}{\partial x} - \frac{\partial\psi_1}{\partial x}\cdot\frac{\partial\Delta\psi_1}{\partial y}\right\} - \frac{\partial\psi_1}{\partial y}\cdot\frac{\partial\Delta\psi_0}{\partial x} - \frac{\partial\psi_0}{\partial y}\cdot\frac{\partial\Delta\psi_1}{\partial x} +$$

$$+ \frac{\partial\psi_1}{\partial x}\cdot\frac{\partial\Delta\psi_0}{\partial y} + \frac{\partial\psi_0}{\partial x}\cdot\frac{\partial\Delta\psi_1}{\partial y} = -\frac{1}{\mathrm{Re}}\Delta\Delta\psi_0 + \frac{\partial\psi_0}{\partial y}\cdot\frac{\partial\Delta\psi_0}{\partial x} - \frac{\partial\psi_0}{\partial x}\cdot\frac{\partial\Delta\psi_0}{\partial y}. \quad (5.12)$$

The process of linearization according to Newton — Kantorovich is applied to equation (5.12). The sequence of approximations $\{\psi_n\}_{n=1}^{N}$ to the solution ψ_1 is considered. To do this, the function $\delta\psi_n = \psi_{n+1} - \psi_n$ is substituted in equation (5.10) instead of the function ψ_1. The following equation is obtained

$$\frac{1}{\mathrm{Re}}\Delta\Delta\left(\psi_n + \delta\psi_n\right) - \left\{\frac{\partial\left(\psi_n + \delta\psi_n\right)}{\partial y}\cdot\frac{\partial\Delta\left(\psi_n + \delta\psi_n\right)}{\partial x} - \frac{\partial\left(\psi_n + \delta\psi_n\right)}{\partial x}\cdot\frac{\partial\Delta\left(\psi_n + \delta\psi_n\right)}{\partial y}\right\} -$$

$$- \frac{\partial\left(\psi_n + \delta\psi_n\right)}{\partial y}\cdot\frac{\partial\Delta\psi_0}{\partial x} - \frac{\partial\psi_0}{\partial y}\cdot\frac{\partial\Delta\left(\psi_n + \delta\psi_n\right)}{\partial x} + \frac{\partial\left(\psi_n + \delta\psi_n\right)}{\partial x}\cdot\frac{\partial\Delta\psi_0}{\partial y} +$$

$$+ \frac{\partial\psi_0}{\partial x}\cdot\frac{\partial\Delta\left(\psi_n + \delta\psi_n\right)}{\partial y} = -\frac{1}{\mathrm{Re}}\Delta\Delta\psi_0 + \frac{\partial\psi_0}{\partial y}\cdot\frac{\partial\Delta\psi_0}{\partial x} - \frac{\partial\psi_0}{\partial x}\cdot\frac{\partial\Delta\psi_0}{\partial y}.$$

The brackets are opened, neglecting the terms of the second order of smallness and given that $\delta\psi_n = \psi_{n+1} - \psi_n$. A sequence of linear equations is obtained

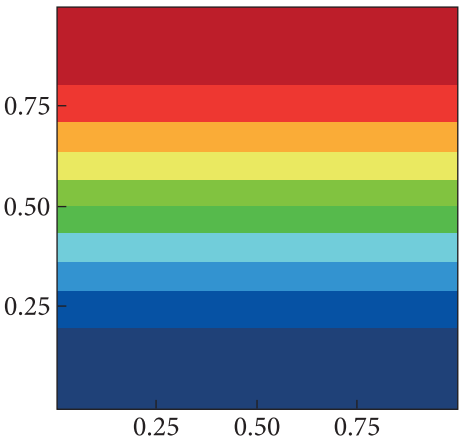

Fig. 5.21. Graph of the function $\psi(x,y)=\frac{y^2}{2}-\frac{y^3}{3}-\frac{1}{12}$

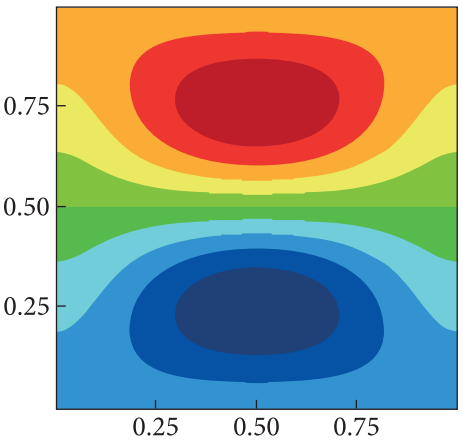

Fig. 5.22. Graph of the function $\psi_0(x,y)$ at α= 200

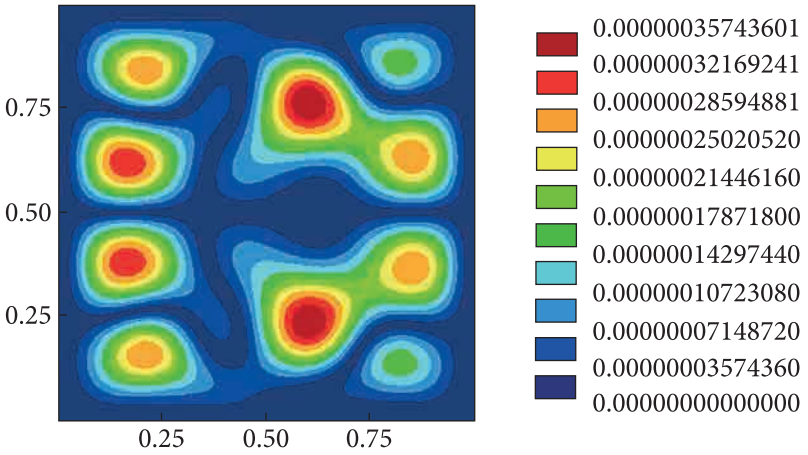

Fig. 5.23. Graph of the function of the difference modulus of numerical and analytical solutions

$$\frac{1}{\mathrm{Re}}\Delta\Delta\psi_{n+1}-\left\{\frac{\partial\psi_n}{\partial y}\cdot\frac{\partial\Delta\psi_{n+1}}{\partial x}+\frac{\partial\psi_{n+1}}{\partial y}\cdot\frac{\partial\Delta\psi_n}{\partial x}-\frac{\partial\psi_n}{\partial x}\cdot\frac{\partial\Delta\psi_{n+1}}{\partial y}-\frac{\partial\psi_{n+1}}{\partial x}\cdot\frac{\partial\Delta\psi_n}{\partial y}\right\}-$$
$$-\frac{\partial\psi_{n+1}}{\partial y}\cdot\frac{\partial\Delta\psi_0}{\partial x}-\frac{\partial\psi_0}{\partial y}\cdot\frac{\partial\Delta\psi_{n+1}}{\partial x}+\frac{\partial\psi_{n+1}}{\partial x}\cdot\frac{\partial\Delta\psi_0}{\partial y}+\frac{\partial\psi_0}{\partial x}\cdot\frac{\partial\Delta\psi_{n+1}}{\partial y}=-\frac{1}{\mathrm{Re}}\Delta\Delta\psi_0+$$
$$+\frac{\partial\psi_0}{\partial y}\cdot\frac{\partial\Delta\psi_0}{\partial x}-\frac{\partial\psi_0}{\partial x}\cdot\frac{\partial\Delta\psi_0}{\partial y}-\frac{\partial\psi_n}{\partial y}\cdot\frac{\partial\Delta\psi_n}{\partial x}+\frac{\partial\psi_n}{\partial x}\cdot\frac{\partial\Delta\psi_n}{\partial y}. \qquad (5.13)$$

Figs 5.22, 5.23 show the graphs of the function $\psi_0(x,y)$ at α =200 and the difference modulus of the analytical solution and the numerical solution

(2 iterations) obtained using the least squares method in the form of constant level lines on the plane xOy.

Problem 4. The liquid flow around the cylinder located between the two plates. Problem statement. It is needed to find the distribution of the velocity field and the pressure field in the flow when the fluid is flowing around the cylinder located between the two plates. To do this, it is needed to consistently solve equation (5.4) in the area Ω, and then equation (5.5) for the function P in the area Ω. The area Ω is shown in Fig. 5.24, for which the border — $\partial\Omega = \Gamma_1 \cup \Gamma_2 \cup \Gamma_3 \cup \Gamma_4 \cup \Gamma_5$. In this case Γ_1, Γ_2, Γ_3 — solid walls, Γ_4 — entrance to the channel, Γ_5 — exit from the channel.

We set the following boundary conditions for the area Ω: on Γ_1 — $\psi = \frac{a}{3}, \frac{\partial\psi}{\partial n} = 0$; on Γ_2 $-\psi = -\frac{a}{3}$, $\frac{\partial\psi}{\partial n} = 0$; on Γ_3 $-$ $\psi = 0$, $\frac{\partial\psi}{\partial n} = 0$; on Γ_4 and Γ_5 $-$ $\psi = 2\frac{y^2}{a} - \frac{4}{3}\frac{y^3}{a^2} - \frac{a}{3}$ (parabolic Poiseuille velocity profile), $\frac{\partial\psi}{\partial n} = 0$.

The solution of the boundary value problem for equation (5.4) with the corresponding boundary conditions is sought in the form $\psi = \psi_1 + \psi_0$ [12,13, 63—69], where ψ_0 — a function that satisfies the inhomogeneous boundary conditions of the problem, ψ_1 — a function with zero Dirichlet and Neumann boundary conditions. The structure of the solution for the function ψ_1 has the form $\psi_1 = \omega_1^2 P_{1,k}$, where $P_{1,k}$ — undefined structure component, $\omega_1 = x(b-x)$ $y(a-y)\left(\left(x-d\right)^2 + \left(y-a/2\right)^2 - r^2\right)$, a — channel width, b — channel length, r — radius of flow around the cylinder, d — the distance from the center of the cylinder to the entrance to the channel.

The undefined component is written for the considered problem in the form $P_{1,k}(x,y) = \sum_{i=1}^{k} c_{1,i}\phi_i(x,y)$, where $\{\varphi_i(x,y)\}$ — B-splines of the fifth order, $\{c_{1i}\}$, $i = 1, ..., k$— constants that need to be defined.

Function ψ_0, which meets the boundary conditions of the problem, is taken in the form

$$\psi_0 = \frac{\Psi_1 w_2^2}{w_1^2 + w_2^2}, \text{ where } \Psi_1 = 2\frac{y^2}{a} - \frac{4}{3}\frac{y^3}{a^2} - \frac{a}{3}, w_1 = x(b-x)y(a-y),$$

$$w_2 = \left(x-d\right)^2 + \left(y-a/2\right)^2 - r^2.$$

The problem is solved by the least squares method. Next, equation (5.5) for the function P is solved in the area Ω. The boundary conditions for equation (5.5) are considered. On the regions of the border Γ_1, Γ_2, Γ_3 the boundary condition $\frac{\partial P}{\partial n} = 0$ is used.

For regions of the border Γ_4 and Γ_5, we have parabolic velocity profiles. Based on this, on Γ_4 and Γ_5, the tangent component of velocity is $V_y = 0$, and also $V_y = 0$ in some volume after the entrance and before the exit.

The Neumann condition is written for Γ_4, given that

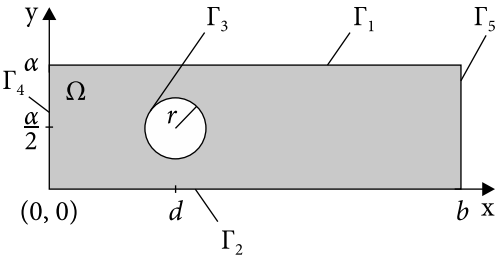

Fig. 5.24. Area Ω of the problem solution

$$V_n = -V_x,\ \frac{\partial P}{\partial n} = -\frac{1}{\mathrm{Re}}\Delta V_x + V_x\frac{\partial V_x}{\partial x} + V_y\frac{\partial V_x}{\partial y}.$$

This condition for the problem under consideration can be simplified. Since on Γ_4 we have a parabolic velocity profile, then $\frac{1}{\mathrm{Re}}\Delta V_x = m$, where m — some constant, which is determined from the boundary condition.

Consider

$$V_x\frac{\partial V_x}{\partial x} + V_y\frac{\partial V_x}{\partial y} = \left(\left(V_x, V_y\right), \nabla V_x\right) = \left(\left(V_x, V_y\right), l\vec{\tau}\right) = V_y = 0,$$

where l — some constant. Then

$$\frac{\partial P}{\partial n} = m. \tag{5.14}$$

A tangential derivative to the function P on Γ_5 is considered

$$\frac{\partial P}{\partial \tau} = \frac{\partial P}{\partial y} = \left(\frac{1}{\mathrm{Re}}\Delta V_y - V_x\frac{\partial V_y}{\partial x} - V_y\frac{\partial V_y}{\partial y}\right).$$

Since $V_y = 0$ not only at the exit from Γ_5 directly but also in some volume before the exit $\frac{\partial V_y}{\partial x} = 0, \frac{\partial V_y}{\partial y} = 0, \Delta V_y = 0$. So, $\frac{\partial P}{\partial \tau} = 0$.

The Dirichlet boundary condition is set by some constant ($\frac{\partial P}{\partial \tau} = 0$) at the exit since Neumann's condition on the whole border does not give an unambiguous solution of Poisson's equation (only to the nearest constant). Thus, the total flow energy is set and we obtain an unambiguous solution.

The structure of the solution for equation (5.5) with the corresponding boundary conditions has the form

$$P = P_{2,k}\omega_2 - \omega\left(\frac{\partial \omega_1}{\partial x}\frac{\partial (P_{2,k}\omega_2)}{\partial x} + \frac{\partial \omega_1}{\partial y}\frac{\partial (P_{2,k}\omega_2)}{\partial y}\right) - \omega\phi + \omega_1^{\,2}\omega_2 P_{3,k} + C,$$

where ω, ω_1, ω_2 — normalized functions that describe the entire border of the area, the border of the area without region Γ_5 and border region Γ_5 respectively; φ — function: $\varphi\big|_{\Gamma_i} = \dfrac{\partial P}{\partial n}\Big|_{\Gamma_i}$, i=1, 2, 3, 4; $P_{1,k}(x,y)$, $P_{2,k}(x,y)$ — undefined structure components; C — the value of static pressure at the exit.

For such a problem functions ω, ω_1, ω_2 are constructed in the form

$$\omega_1 = \left(f_1 \overset{\alpha}{\wedge_0} f_2 \right) \overset{\alpha}{\wedge_0} \left(f_3 \right), \ \omega = \left(f_2 \overset{\alpha}{\wedge_0} f_4 \right) \overset{\alpha}{\wedge_0} \left(f_3 \right), \ \omega_2 = (b - x),$$

where

$$f_1 = x \quad f_2 = \left(y - \frac{y^2}{a} \right), \ f_3 = \left(\left(x - d \right)^2 + \left(y - a/2 \right)^2 - r^2 \right) / 2r, \ f_4 = x(b-x)/b,$$

$$x \overset{\alpha}{\wedge_0} y = x + y - \sqrt{x^2 + y^2 + \alpha_k(x,y)},$$

$$\alpha_k(x,y) = \begin{cases} \overline{b}\left(1 - \left(\dfrac{x}{\overline{a}} \right)^2 - \left(\dfrac{y}{\overline{a}} \right)^2 \right)^{k+1}, & x^2 + y^2 < \overline{a}^2, \\ 0, \quad x^2 + y^2 \geq \overline{a}^2. \end{cases}$$

Undefined components are given in the form $P_{l,k}(x,y) = \sum_{i=1}^{k} c_{l,i} \phi_i(x,y)$,

where $l = 1,2$, $\{\varphi_i(x,y)\}$ — B-splines of the fifth order, $\{c_{l,i}\}$, $i = 1,\ldots, k$, $l = 1, 2$ — constants that need to be defined.

Function φ: $\varphi\big|_{\Gamma_i} = \dfrac{\partial P}{\partial n}\Big|_{\Gamma_i}$, i = 1, 2, 3, 4 is constructed using the gluing formula [43]

$$\varphi = \sum_{i=1}^{4} \frac{\phi_i}{\overline{w}_i} \Bigg/ \sum_{i=1}^{4} \frac{1}{\overline{w}_i},$$

where

$$\varphi_i = 0, \ i = 1,2,3, \ \varphi_4 = \frac{8}{\mathrm{Re}\, a^2}, \ \overline{w}_1 = a - y, \ \overline{w}_2 = y,$$

$$\overline{w}_3 = \left(\left(x - d \right)^2 + \left(y - a/2 \right)^2 - r^2 \right) / 2r, \ \overline{w}_4 = x.$$

Next, the least squares method is applied.

The following parameters were chosen for numerical calculations:

$$a = 1, \ b = 4, \ d = 1, \ r = 0.25, \ \overline{a} = 0.01, \ \overline{b} = 1.312 \times 10^{-5}, \ k = 3, \ C = 0.$$

Fig. 5.25—5.31 show graphs of functions in the form of lines of constant level on the plane *xOy* for different values of the number Re, which are based on the results of computational experiments.

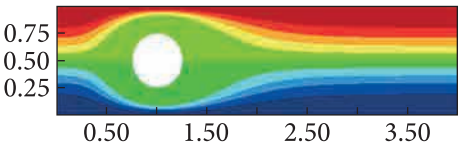

Fig. 5.25. Graph of the function ψ_0

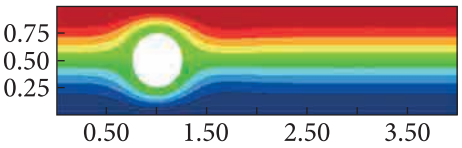

Fig. 5.26. Graph of the flow function (Re = 10)

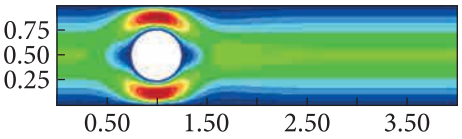

Fig. 5.27. Graph of the velocity modulus function (Re = 10)

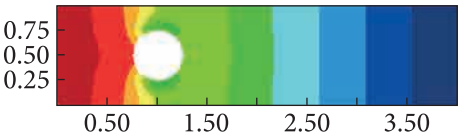

Fig. 5.28. Graph of static pressure function (Re = 10)

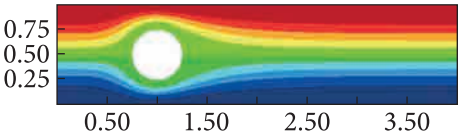

Fig. 5.29. Graph of the flow function (Re = 50)

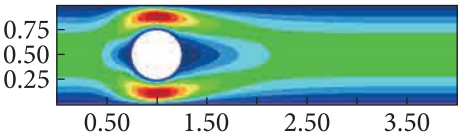

Fig. 5.30. Graph of the velocity modulus function (Re = 50)

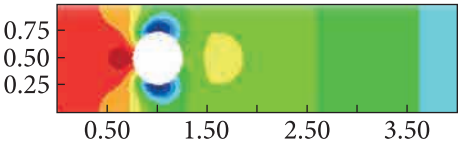

Fig. 5.31. Graph of static pressure function (Re = 50)

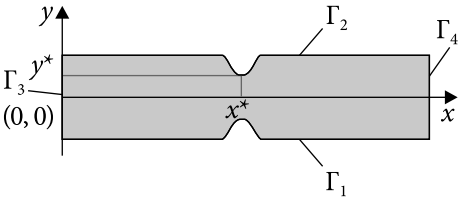

Fig. 5.32. Area Ω

Computational experiments were performed on a 32 × 32 grid of spline of the 5th order. For these problems, convergence was observed at 4 iterations (the maximum difference modulus of the solutions obtained at the 4th and 5th iterations was $\varepsilon < 10^{-4}$).

Problem 5. Numerical modeling of hydrodynamics and heat transfer in the «crack — fluid» system. Computer modeling of filtration processes is widely used in the oil and gas industry. Determination of the rate of fluids (oil, gas, or process fluids in fractured-porous reservoirs) filtration allows significant increase in the efficiency of technologies for the intensification of hydrocarbon production, to optimize the modes of technological processes machining. Darcy's law of filtration in a porous medium determines the relation between the pressure drop and the filtration rate. But when it comes to non-isothermal filtration with a possible chemical interaction of fluids with the mineral part of

the seam, the question of researching such processes at the level of elementary structures — pores or cracks in the rock — arises.

Numerous studies have been carried out on the example of a flat channel simulating an extended crack with a narrowing, in which the pressure in the fluid flow decreases with a local increase in movement speed [31]. To study the process of pore space heating, a related problem is solved in the following formulation: a hydrodynamic problem in the channel and a problem of thermal conduction in the rock.

Using the developed method of mathematical modeling of the viscous incompressible fluid movement in channels of a complex shape with the R-function method [67—69], the problem of steady-state fluid motion in the channel, the area of which is shown in Fig. 5.31, is solved. The area boundary is $\partial\Omega = \Gamma_1 \cup \Gamma_2 \cup \Gamma_3 \cup \Gamma_4$, where Γ_3 is the channel entrance, Γ_4 — exit from the channel, Γ_1, Γ_2 — solid walls.

Regions of the border Γ_i are described by equations $f_i = 0$, where

$$f_1 = \frac{-y - \left(a - y^*\right) e^{-x^*\left(x - x^*\right)^2} + a}{\sqrt{1 + \left(a - y^*\right)^2 4x^{*2}\left(x - x^*\right)^2 e^{-2x^*\left(x - x^*\right)^2}}};$$

$$f_2 = \frac{y - \left(a - y^*\right) e^{-x^*\left(x - x^*\right)^2} + a}{\sqrt{1 + \left(a - y^*\right)^2 4x^{*2}\left(x - x^*\right)^2 e^{-2x^*\left(x - x^*\right)^2}}};$$

$f_3 = x$; $f_4 = b - x$; a — half the width of the channel entrance; b — channel length; x^* — point of minimum channel width; y^* — half of the minimum channel width.

The plane stationary motion of a viscous incompressible fluid is described by the system of Navier — Stokes equations, which is reduced to a nonlinear differential equation in partial derivatives of the 4th order concerning the stream function ψ (5.4).

Boundary conditions must be set to describe the fluid movement in the channel. Boundary conditions that are included in the model take into account the increase in the permeability of the rock under the influence of hydrogen. Experimental data show that in seam conditions, the flow rate of working gases with hydrogen is 10 times higher than without hydrogen. In dimensionless form, this corresponds to Reynolds numbers of 1 (without hydrogen) and 10 (with activated hydrogen).

According to [67—69], the boundary value problem for equation (5.4) with the corresponding boundary conditions is sought in the form $\psi = \psi_1 + \psi_0$, where

Fig. 5.33. Stream function Re = 1 (without hydrogen)

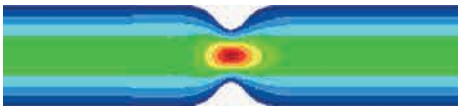

Fig. 5.34. Velocity modulus function Re = 1 (without hydrogen)

Fig. 5.35. Stream function Re = 10 (with hydrogen)

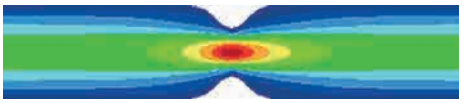

Fig. 5.36. Velocity modulus function Re = 10 (with hydrogen)

Ψ_0 is a function that satisfies the heterogeneous boundary conditions of the problem, ψ_1 is a function with zero Dirichlet and Neumann boundary conditions. The solution structure for the function has the form $\psi_1 = \omega_1^2 P_{1,k}$, where $P_{1,k}$ is the undefined component of the structure, $\omega_1(x,y) = (f_1 \wedge f_2) \wedge f_3$.

For the problem under consideration, the functions ω, ω_1, ω_2, describing the entire area border, the area border without a region, and the border region, respectively, are constructed in the form

$$\omega_1 = \left(f_1 \overset{\alpha}{\wedge_0} f_2 \right) \overset{\alpha}{\wedge_0} (f_3), \ \omega = \left(f_1 \overset{\alpha}{\wedge_0} f_2 \right) \overset{\alpha}{\wedge_0} \left(f_3 \overset{\alpha}{\wedge_0} f_4 \right), \ \omega_2 = (b - x),$$

where the conjunction is determined by the formula

$$x \overset{\alpha}{\wedge_0} y = x + y - \sqrt{x^2 + y^2 + \alpha_k(x,y)},$$

$$\alpha_k(x,y) = \begin{cases} \overline{b}\left(1 - \left(\frac{x}{\overline{a}}\right)^2 - \left(\frac{y}{\overline{a}}\right)^2\right)^{k+1}, & x^2 + y^2 < \overline{a}^2, \\ 0, & x^2 + y^2 \geq \overline{a}^2. \end{cases}$$

The unknown components of the structure have the form $P_{l,k}(x,y) = \sum_{i=1}^{k} c_{l,i} \phi_i(x,y)$, where $l = 1,2$, $\{\varphi_i(x,y)\}$ — B-splines of the fifth order, $\{c_{l,i}\}$, $i = 1, ..., k$, $l = 1,2$ — constants to be defined.

Function φ: $\varphi\big|_{\Gamma_i} = \left.\frac{\partial P}{\partial n}\right|_{\Gamma_i}$, $i = 1, 2, 3, 4$ will be constructed using the gluing formula $\varphi = \sum_{i=1}^{3} \frac{\phi_i}{f_i} \Big/ \sum_{i=1}^{3} \frac{1}{f_i}$, where $\varphi_i = 0$, $i = 1,2$, $\varphi_3 = \frac{8}{\mathrm{Re} a^2}$.

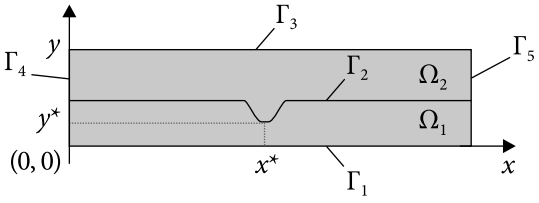

Fig. 5.37. Area of the problem solution

The solution is sought with the least squares method.

The following parameters were chosen for numerical calculations: $a = 1, b = 10, d = 1,\ x^* = 5,\ y^* = 0{,}5,\ \overline{a} = 0.01,\ \overline{b} = 1.312 \times 10^{-5},\ k = 3,\ C = 0.$

Fig. 5.33—5.36 show graphs of the stream and velocity modulus functions in the form of constant level lines on the plane xOy for Reynolds numbers 1 and 10. Computational experiments were performed on a grid of 32 × 32 splines of the 5th order. For these problems, convergence was achieved with 4 iterations (the maximum difference modulus of the solutions obtained at the 4th and 5th iterations, was $\varepsilon < 10^{-4}$).

Having solved the problem of fluid flow, it is necessary to solve the related problem of thermal conductivity in the prepared space [31]. Since the problem statement is symmetrical, it is enough to consider half of the area of the crack shown in Fig. 5.37.

Problem statement. To find the function T from the system [31]:

$$\begin{cases} \dfrac{\partial T_1}{\partial t} + \dfrac{\partial \psi}{\partial y}\dfrac{\partial T_1}{\partial x} - \dfrac{\partial \psi}{\partial x}\dfrac{\partial T_1}{\partial y} = \alpha_1 \Delta T_1, \quad x \in \Omega_1, \\ \dfrac{\partial T_2}{\partial t} = \alpha_2 \Delta T_2, \quad x \in \Omega_2. \end{cases}$$

the boundary conditions for this problem are considered as follows. On Γ_1: $\dfrac{\partial T_1}{\partial n} = 0$ (symmetry condition). On Γ_2: $\dfrac{\partial T_1}{\partial n_1} = -\dfrac{\partial T_2}{\partial n_2} = \lambda\left(T_2 - T_1\right)$. On Γ_3: $\dfrac{\partial^2 T_2}{\partial n^2} = \dfrac{1}{\alpha_2}\dfrac{\partial T_2}{\partial t}$ (condition at infinity). On Γ_4: $\dfrac{\partial T_1}{\partial n} = 0$, $\dfrac{\partial T_2}{\partial n} = 0$. On Γ_5: $\dfrac{\partial T_1}{\partial n} = 0$, $\dfrac{\partial T_2}{\partial n} = 0$.

To solve these equations the finite difference method is used, the scheme — «classics» [28]. The sought functions T_1 and T_2 are replaced by grid functions ${T_1}^n{}_{i,j}$ and ${T_2}^n{}_{i,j}$. The «classics» scheme consists of two consecutive passages throughout the calculation area. At the first passage of magnitude ${T_1}^{n+1}{}_{i,j}$ and ${T_2}^{n+1}{}_{i,j}$ are calculated at the grid nodes, where $(i + j + n)$ — an even number according to the schemes:

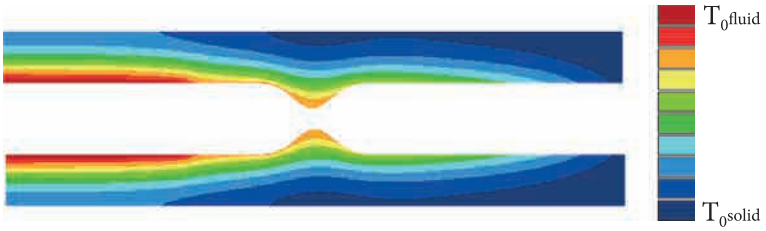

Fig. 5.38. Temperature distribution in the rock during the flow of working gases without hydrogen (Re = 1)

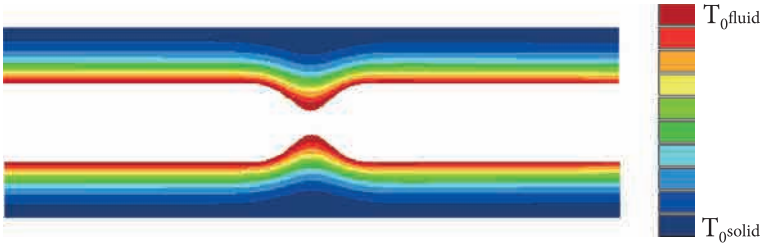

Fig. 5.39. Temperature distribution in the rock during the flow of working gases with hydrogen (Re = 10)

$$\frac{T_1{}^{n+1}{}_{i,j}-T_1{}^{n}{}_{i,j}}{\Delta t}+\frac{\overline{\delta}_x T_1{}^{n}{}_{i,j}}{\Delta x}\frac{\partial\psi}{\partial y}\bigg|_{i,j}-\frac{\overline{\delta}_y T_1{}^{n}{}_{i,j}}{\Delta y}\frac{\partial\psi}{\partial x}\bigg|_{i,j}=\alpha_2\left(\frac{\delta_x^2 T_1{}^{n}{}_{i,j}}{\Delta x^2}+\frac{\delta_y^2 T_1{}^{n}{}_{i,j}}{\Delta y^2}\right),$$

$$\frac{T_2{}^{n+1}{}_{i,j}-T_2{}^{n}{}_{i,j}}{\Delta t}=\alpha_2\left(\frac{\delta_x^2 T_2{}^{n}{}_{i,j}}{\Delta x^2}+\frac{\delta_y^2 T_2{}^{n}{}_{i,j}}{\Delta y^2}\right).$$

In the second passage, the values $T_1{}^{n+1}{}_{i,j}$ and $T_2{}^{n+1}{}_{i,j}$ are calculated at those grid nodes where $(i+j+n)$ — an odd number is according to the schemes:

$$\frac{T_1{}^{n+1}{}_{i,j}-T_1{}^{n}{}_{i,j}}{\Delta t}+\frac{\overline{\delta}_x T_1{}^{n+1}{}_{i,j}}{\Delta x}\frac{\partial\psi}{\partial y}\bigg|_{i,j}-\frac{\overline{\delta}_y T_1{}^{n+1}{}_{i,j}}{\Delta y}\frac{\partial\psi}{\partial x}\bigg|_{i,j}=\alpha_2\left(\frac{\delta_x^2 T_1{}^{n+1}{}_{i,j}}{\Delta x^2}+\frac{\delta_y^2 T_1{}^{n+1}{}_{i,j}}{\Delta y^2}\right),$$

$$\frac{T_2{}^{n+1}{}_{i,j}-T_2{}^{n}{}_{i,j}}{\Delta t}=\alpha_2\left(\frac{\delta_x^2 T_2{}^{n+1}{}_{i,j}}{\Delta x^2}+\frac{\delta_y^2 T_2{}^{n+1}{}_{i,j}}{\Delta y^2}\right).$$

This scheme is stable [31]. The approximation error is $O(\Delta t,(\Delta x)^2,(\Delta y)^2)$.

Fig. 5.38 and 5.39 show the distribution of the temperature function T_2 in the rock forming the crack, the function ψ is the solution of the boundary value problem for the differential equation (5.5) when Re = 1 and Re = 10.

The obtained results of computer modeling clearly explain the increase in the efficiency of thermobaric and chemical treatment in the presence of hydrogen in the working gases. At the same time, due to the increase in the filtration rate, during the same time, hot gases with hydrogen manage to penetrate further into the bottom hole zone, transferring and spending heat mainly on a uniform and intensive heating of the inner surface of cracks and combatants at a greater distance from the wellbore. After all, such a process more effectively realizes the thermochemical potential and contributes to the effective cleaning of the bottom hole formation zone. In the absence of hydrogen, the thermal potential of the working gases is used more for heating the rock near the wellbore and less for the intrapore space.

The results of theoretical and experimental studies confirm the decisive role of hydrogen as an activator of the processes of diffusion and filtration of fluids in the pore space of rock in the technology of complex hydrogen thermobaric and chemical effect on the bottom hole zone of productive horizons with the aim of stimulation the production of oil, gas, gas condensate.

5.2. Mathematical modeling of viscous incompressible fluid flow along axisymmetric channels of the complex cross-section using the R-function method

A large number of elements of hydraulic automation, hydraulics, fuel systems, technological devices, etc., are axisymmetric structures with channels of the complex cross-section. Therefore, the statement of the problem of mathematical modeling of the viscous incompressible fluid flow in axisymmetric channels of the complex cross-section using the R-function method is a very relevant problem. Moreover, the accuracy of the channel geometry description can significantly affect not only the efficiency of hydraulic devices but also their performance in general. Next, the problem statement to determine the velocity and pressure fields is considered.

5.2.1. Problem statement for the velocity field

The problem of the determination of the fluid flow velocity field in an axisymmetric channel is considered. The motion of a viscous incompressible fluid is described by a system of Navier — Stokes equations, which in cylindrical coordinates has the form [55]:

$$\frac{\partial v_r}{\partial t}+v_r\frac{\partial v_r}{\partial r}+\frac{v_\varphi}{r}\frac{\partial v_r}{\partial \varphi}+v_z\frac{\partial v_r}{\partial z}-\frac{v_\varphi^2}{r}=-\frac{1}{\rho}\frac{\partial p}{\partial r}+\nu\left(\Delta v_r-\frac{v_r}{r^2}-\frac{2}{r^2}\frac{\partial \nu\varphi}{\partial \varphi}\right), \quad (5.15)$$

$$\frac{\partial v_\varphi}{\partial t}+v_r\frac{\partial v_\varphi}{\partial r}+\frac{v_\varphi}{r}\frac{\partial v_\varphi}{\partial \varphi}+v_z\frac{\partial v_\varphi}{\partial z}+\frac{v_r v_\varphi}{r}=-\frac{1}{\rho r}\frac{\partial p}{\partial \varphi}+\nu\left(\Delta v_\varphi-\frac{v_\varphi}{r^2}+\frac{2}{r^2}\frac{\partial v_r}{\partial \varphi}\right), \quad (5.16)$$

$$\frac{\partial v_z}{\partial t}+v_r\frac{\partial v_z}{\partial r}+\frac{v_\varphi}{r}\frac{\partial v_z}{\partial \varphi}+v_z\frac{\partial v_z}{\partial z}=-\frac{1}{\rho}\frac{\partial p}{\partial z}+\nu\Delta v_z, \tag{5.17}$$

$$\frac{1}{r}\frac{\partial\left(rv_r\right)}{\partial r}+\frac{1}{r}\frac{\partial v_\varphi}{\partial \varphi}+\frac{\partial v_z}{\partial z}=0, \tag{5.18}$$

where (5.15)—(5.17) are the Navier — Stokes equations, (5.18) is the equation of motion continuity, and the operator Δ is determined by the formula:

$$\Delta=\frac{1}{r}\frac{\partial}{\partial r}\left(r\frac{\partial}{\partial r}\right)+\frac{1}{r^2}\frac{\partial^2}{\partial \varphi^2}+\frac{\partial^2}{\partial z^2}.$$

For the stationary and axisymmetric case, this system of equations in dimensionless form is transformed into:

$$v_r\frac{\partial v_r}{\partial r}+v_z\frac{\partial v_r}{\partial z}=-\frac{\partial p}{\partial r}+\frac{1}{\mathrm{Re}}\left(\frac{1}{r}\frac{\partial}{\partial r}\left(r\frac{\partial v_r}{\partial r}\right)+\frac{\partial^2 v_r}{\partial z^2}-\frac{v_r}{r^2}\right), \tag{5.19}$$

$$v_r\frac{\partial v_z}{\partial r}+v_z\frac{\partial v_z}{\partial z}=-\frac{\partial p}{\partial z}+\frac{1}{\mathrm{Re}}\left(\frac{1}{r}\frac{\partial}{\partial r}\left(r\frac{\partial v_z}{\partial r}\right)+\frac{\partial^2 v_z}{\partial z^2}\right), \tag{5.20}$$

$$\frac{1}{r}\frac{\partial\left(rv_r\right)}{\partial r}+\frac{\partial v_z}{\partial z}=0, \tag{5.21}$$

where Re — Reynolds number, (v_r, v_z) — velocity vector, P — static pressure.

Equation (5.19) is differentiated by z, and (5.20) — by r, and the second equation is subtracted from the first one, excluding terms with the pressure p. The stream function is introduced using relations $v_z=\frac{1}{r}\frac{\partial\psi}{\partial r}, v_r=-\frac{1}{r}\frac{\partial\psi}{\partial z}$.

As a result of the transformations, the following nonlinear equation of the 4th order concerning the stream function ψ is obtained:

$$\begin{aligned}&-\frac{3}{r^4}\frac{\partial\psi}{\partial z}\frac{\partial\psi}{\partial r}+\frac{3}{r^3}\frac{\partial\psi}{\partial z}\frac{\partial^2\psi}{\partial r^2}+\frac{2}{r^3}\frac{\partial\psi}{\partial z}\frac{\partial^2\psi}{\partial r^2}-\frac{1}{r^3}\frac{\partial\psi}{\partial r}\frac{\partial^2\psi}{\partial r\partial z}-\\&-\frac{1}{r^2}\frac{\partial\psi}{\partial z}\frac{\partial^3\psi}{\partial r^3}-\frac{1}{r^2}\frac{\partial\psi}{\partial z}\frac{\partial^3\psi}{\partial r\partial z^2}+\frac{1}{r^2}\frac{\partial\psi}{\partial r}\frac{\partial^3\psi}{\partial r^2\partial z}+\frac{1}{r^2}\frac{\partial\psi}{\partial r}\frac{\partial^3\psi}{\partial z^3}+\\&+\frac{1}{\mathrm{Re}}\left(-\frac{1}{r}\frac{\partial^4\psi}{\partial r^4}-\frac{2}{r}\frac{\partial^4\psi}{\partial r^2\partial z^2}-\frac{1}{r}\frac{\partial^4\psi}{\partial z^4}+\frac{2}{r^2}\frac{\partial^3\psi}{\partial r^3}+\frac{2}{r^2}\frac{\partial^3\psi}{\partial r\partial z^2}-\frac{3}{r^3}\frac{\partial^2\psi}{\partial r^2}+\frac{3}{r^4}\frac{\partial\psi}{\partial r}\right)=0.\end{aligned} \tag{5.22}$$

Boundary conditions must be set to describe the motion of a viscous incompressible fluid in an axisymmetric channel. Suppose the problem is solved in the area Ω, for which $\partial\Omega$ — its borders. The border regions may correspond to the solid walls of the channel, the entrance, and exit to the channel, and the axis of symmetry. The boundary conditions for equation (5.22) follow from the condition of adhesion on a solid wall, the velocity at the entrance (exit), and the condition of impermeability on the axis of symmetry.

On the region of the border Γ_{sw}, which corresponds to the solid wall, we have the adhesion condition — $v_r = -\frac{1}{r}\frac{\partial\psi}{\partial z} = 0, \quad v_z = \frac{1}{r}\frac{\partial\psi}{\partial r} = 0$, from which it follows that on Γ_{sw}

$$\frac{\partial\psi}{\partial\tau} = \left(\nabla\psi, \vec{\tau}\right) = 0, \; \frac{\partial\psi}{\partial n} = \left(\nabla\psi, \vec{n}\right) = 0,$$

where $\vec{\tau}$ — tangent vector to Γ_{sw}, $\vec{n}$ — normal vector to Γ_{sw}. Since $\frac{\partial\psi}{\partial\tau} = 0$ on Γ_{sw}, then along the curve Γ_{sw}, the stream function does not change, i.e. $\psi = const$ on Γ_{sw}.

The impermeability condition on the axis of symmetry means that

$$v_r = -\frac{1}{r}\frac{\partial\psi}{\partial z} = 0, \; v_z = \frac{1}{r}\frac{\partial\psi}{\partial r} = f(z),$$

where $f(z)$ — some function. It follows from here $\frac{\partial\psi}{\partial r} = rf(z)\Big|_{r=0} = 0, \; \frac{\partial\psi}{\partial z} = 0$. Since $\frac{\partial\psi}{\partial z} = 0$, then on the axis of symmetry Ψ = *const*.

The velocity distribution, which determines the stream function, is set at the entrance to the channel. The boundary conditions will be considered in more detail on the example of fluid flow through the model channel of the hydro vortex nozzle. If the velocity distribution at the exit is known (for example, the stationary laminar flow of Poiseuille), then it can also be set.

The solution of the boundary value problem for equation (5.22) with the corresponding boundary conditions will be sought in the form $\Psi = \Psi_1 + \Psi_0$, where Ψ_1 — the function with zero Dirichlet and Neumann boundary conditions, Ψ_0 — function that meets all the inhomogeneous boundary conditions of the problem.

For functions ψ_1 and ψ_0 equation (5.22) has the form:

$$\frac{1}{\mathrm{Re}}\left(-\frac{1}{r}\frac{\partial^4\psi_1}{\partial r^4} - \frac{2}{r}\frac{\partial^4\psi_1}{\partial z^2\partial r^2} - \frac{1}{r}\frac{\partial^4\psi_1}{\partial z^4} + \frac{2}{r^2}\frac{\partial^3\psi_1}{\partial r^3} + \frac{2}{r^2}\frac{\partial^3\psi_1}{\partial z^2\partial r} - \frac{3}{r^3}\frac{\partial^2\psi_1}{\partial r^2} + \frac{3}{r^4}\frac{\partial\psi_1}{\partial r}\right) -$$

$$-\frac{1}{r^2}\frac{\partial\psi_1}{\partial z}\frac{\partial^3\psi_1}{\partial z^2\partial r}-\frac{1}{r^2}\frac{\partial\psi_1}{\partial z}\frac{\partial^3\psi_1}{\partial r^3}+\frac{2}{r^3}\frac{\partial\psi_1}{\partial z}\frac{\partial^2\psi_1}{\partial z^2}+\frac{3}{r^3}\frac{\partial\psi_1}{\partial z}\frac{\partial^2\psi_1}{\partial r^2}-$$

$$-\frac{3}{r^4}\frac{\partial\psi_1}{\partial z}\frac{\partial\psi_1}{\partial r}+\frac{1}{r^2}\frac{\partial\psi_1}{\partial r}\frac{\partial^3\psi_1}{\partial z^3}+\frac{1}{r^2}\frac{\partial\psi_1}{\partial r}\frac{\partial^3\psi_1}{\partial r^2\partial z}-\frac{1}{r^3}\frac{\partial\psi_1}{\partial r}\frac{\partial^2\psi_1}{\partial r\partial z}-$$

$$-\frac{1}{r^2}\left(\frac{\partial\psi_1}{\partial z}\frac{\partial^3\psi_0}{\partial z^2\partial r}+\frac{\partial\psi_0}{\partial z}\frac{\partial^3\psi_1}{\partial z^2\partial r}\right)-\frac{1}{r^2}\left(\frac{\partial\psi_1}{\partial z}\frac{\partial^3\psi_0}{\partial r^3}+\frac{\partial\psi_0}{\partial z}\frac{\partial^3\psi_1}{\partial r^3}\right)+$$

$$+\frac{2}{r^3}\left(\frac{\partial\psi_1}{\partial z}\frac{\partial^2\psi_0}{\partial z^2}+\frac{\partial\psi_0}{\partial z}\frac{\partial^2\psi_1}{\partial z^2}\right)+\frac{3}{r^3}\left(\frac{\partial\psi_1}{\partial z}\frac{\partial^2\psi_0}{\partial r^2}+\frac{\partial\psi_0}{\partial z}\frac{\partial^2\psi_1}{\partial r^2}\right)-$$

$$-\frac{3}{r^4}\left(\frac{\partial\psi_1}{\partial z}\frac{\partial\psi_0}{\partial r}+\frac{\partial\psi_0}{\partial z}\frac{\partial\psi_1}{\partial r}\right)+\frac{1}{r^2}\left(\frac{\partial\psi_1}{\partial r}\frac{\partial^3\psi_0}{\partial z^3}+\frac{\partial\psi_0}{\partial r}\frac{\partial^3\psi_1}{\partial z^3}\right)+$$

$$+\frac{1}{r^2}\left(\frac{\partial\psi_1}{\partial r}\frac{\partial^3\psi_0}{\partial r^2\partial z}+\frac{\partial\psi_0}{\partial r}\frac{\partial^3\psi_1}{\partial r^2\partial z}\right)-\frac{1}{r^3}\left(\frac{\partial\psi_1}{\partial r}\frac{\partial^2\psi_0}{\partial r\partial z}+\frac{\partial\psi_0}{\partial r}\frac{\partial^2\psi_1}{\partial r\partial z}\right)=$$

$$=-\frac{1}{\mathrm{Re}}\left(-\frac{1}{r}\frac{\partial^4\psi_0}{\partial r^4}-\frac{2}{r}\frac{\partial^4\psi_0}{\partial z^2\partial r^2}-\frac{1}{r}\frac{\partial^4\psi_0}{\partial z^4}+\frac{2}{r^2}\frac{\partial^3\psi_0}{\partial r^3}+\frac{2}{r^2}\frac{\partial^3\psi_0}{\partial z^2\partial r}-\frac{3}{r^3}\frac{\partial^2\psi_0}{\partial r^2}+\frac{3}{r^4}\frac{\partial\psi_0}{\partial r}\right)+$$

$$+\frac{1}{r^2}\frac{\partial\psi_0}{\partial z}\frac{\partial^3\psi_0}{\partial z^2\partial r}+\frac{1}{r^2}\frac{\partial\psi_0}{\partial z}\frac{\partial^3\psi_0}{\partial r^3}-\frac{2}{r^3}\frac{\partial\psi_0}{\partial z}\frac{\partial^2\psi_0}{\partial z^2}-\frac{3}{r^3}\frac{\partial\psi_0}{\partial z}\frac{\partial^2\psi_0}{\partial r^2}+$$

$$+\frac{3}{r^4}\frac{\partial\psi_0}{\partial z}\frac{\partial\psi_0}{\partial r}-\frac{1}{r^2}\frac{\partial\psi_0}{\partial r}\frac{\partial^3\psi_0}{\partial z^3}-\frac{1}{r^2}\frac{\partial\psi_0}{\partial r}\frac{\partial^3\psi_0}{\partial r^2\partial z}+\frac{1}{r^3}\frac{\partial\psi_0}{\partial r}\frac{\partial^2\psi_0}{\partial r\partial z}. \qquad (5.23)$$

After applying the Newton — Kantorovich linearization process similarly to the flat case, a sequence of linear equations is obtained

$$\frac{1}{\mathrm{Re}}\left(-\frac{1}{r}\frac{\partial^4\psi_{n+1}}{\partial r^4}-\frac{2}{r}\frac{\partial^4\psi_{n+1}}{\partial z^2\partial r^2}-\frac{1}{r}\frac{\partial^4\psi_{n+1}}{\partial z^4}+\frac{2}{r^2}\frac{\partial^3\psi_{n+1}}{\partial r^3}\right.$$

$$\left.+\frac{2}{r^2}\frac{\partial^3\psi_{n+1}}{\partial z^2\partial r}-\frac{3}{r^3}\frac{\partial^2\psi_{n+1}}{\partial r^2}+\frac{3}{r^4}\frac{\partial\psi_{n+1}}{\partial r}\right)-$$

$$-\frac{1}{r^2}\frac{\partial\psi_{n+1}}{\partial z}\frac{\partial^3\psi_n}{\partial z^2\partial r}-\frac{1}{r^2}\frac{\partial\psi_n}{\partial z}\frac{\partial^3\psi_{n+1}}{\partial z^2\partial r}-\frac{1}{r^2}\frac{\partial\psi_{n+1}}{\partial z}\frac{\partial^3\psi_n}{\partial r^3}-\frac{1}{r^2}\frac{\partial\psi_n}{\partial z}\frac{\partial^3\psi_{n+1}}{\partial r^3}+$$

$$+\frac{2}{r^3}\frac{\partial\psi_{n+1}}{\partial z}\frac{\partial^2\psi_n}{\partial z^2}+\frac{2}{r^3}\frac{\partial\psi_n}{\partial z}\frac{\partial^2\psi_{n+1}}{\partial z^2}+\frac{3}{r^3}\frac{\partial\psi_n}{\partial z}\frac{\partial^2\psi_{n+1}}{\partial r^2}+\frac{3}{r^3}\frac{\partial\psi_{n+1}}{\partial z}\frac{\partial^2\psi_n}{\partial r^2}-$$

$$-\frac{3}{r^4}\frac{\partial\psi_n}{\partial z}\frac{\partial\psi_{n+1}}{\partial r}-\frac{3}{r^4}\frac{\partial\psi_{n+1}}{\partial z}\frac{\partial\psi_n}{\partial r}+\frac{1}{r^2}\frac{\partial\psi_{n+1}}{\partial r}\frac{\partial^3\psi_n}{\partial z^3}+\frac{1}{r^2}\frac{\partial\psi_n}{\partial r}\frac{\partial^3\psi_{n+1}}{\partial z^3}+$$

$$+\frac{1}{r^2}\frac{\partial\psi_n}{\partial r}\frac{\partial^3\psi_{n+1}}{\partial r^2\partial z}+\frac{1}{r^2}\frac{\partial\psi_{n+1}}{\partial r}\frac{\partial^3\psi_n}{\partial r^2\partial z}-\frac{1}{r^3}\frac{\partial\psi_n}{\partial r}\frac{\partial^2\psi_{n+1}}{\partial r\partial z}-\frac{1}{r^3}\frac{\partial\psi_{n+1}}{\partial r}\frac{\partial^2\psi_n}{\partial r\partial z}-$$

$$-\frac{1}{r^2}\left(\frac{\partial\psi_{n+1}}{\partial z}\frac{\partial^3\psi_0}{\partial z^2\partial r}+\frac{\partial\psi_0}{\partial z}\frac{\partial^3\psi_{n+1}}{\partial z^2\partial r}\right)-\frac{1}{r^2}\left(\frac{\partial\psi_{n+1}}{\partial z}\frac{\partial^3\psi_0}{\partial r^3}+\frac{\partial\psi_0}{\partial z}\frac{\partial^3\psi_{n+1}}{\partial r^3}\right)+$$

$$+\frac{2}{r^3}\left(\frac{\partial\psi_{n+1}}{\partial z}\frac{\partial^2\psi_0}{\partial z^2}+\frac{\partial\psi_0}{\partial z}\frac{\partial^2\psi_{n+1}}{\partial z^2}\right)+\frac{3}{r^3}\left(\frac{\partial\psi_{n+1}}{\partial z}\frac{\partial^2\psi_0}{\partial r^2}+\frac{\partial\psi_0}{\partial z}\frac{\partial^2\psi_{n+1}}{\partial r^2}\right)-$$

$$-\frac{3}{r^4}\left(\frac{\partial\psi_{n+1}}{\partial z}\frac{\partial\psi_0}{\partial r}+\frac{\partial\psi_0}{\partial z}\frac{\partial\psi_{n+1}}{\partial r}\right)+\frac{1}{r^2}\left(\frac{\partial\psi_{n+1}}{\partial r}\frac{\partial^3\psi_0}{\partial z^3}+\frac{\partial\psi_0}{\partial r}\frac{\partial^3\psi_{n+1}}{\partial z^3}\right)+$$

$$+\frac{1}{r^2}\left(\frac{\partial\psi_{n+1}}{\partial r}\frac{\partial^3\psi_0}{\partial r^2\partial z}+\frac{\partial\psi_0}{\partial r}\frac{\partial^3\psi_{n+1}}{\partial r^2\partial z}\right)-\frac{1}{r^3}\left(\frac{\partial\psi_{n+1}}{\partial r}\frac{\partial^2\psi_0}{\partial r\partial z}+\frac{\partial\psi_0}{\partial r}\frac{\partial^2\psi_{n+1}}{\partial r\partial z}\right)=$$

$$=-\frac{1}{\mathrm{Re}}\left(-\frac{1}{r}\frac{\partial^4\psi_0}{\partial r^4}-\frac{2}{r}\frac{\partial^4\psi_0}{\partial z^2\partial r^2}-\frac{1}{r}\frac{\partial^4\psi_0}{\partial z^4}+\frac{2}{r^2}\frac{\partial^3\psi_0}{\partial r^3}+\frac{2}{r^2}\frac{\partial^3\psi_0}{\partial z^2\partial r}-\frac{3}{r^3}\frac{\partial^2\psi_0}{\partial r^2}+\right.$$

$$\left.+\frac{3}{r^4}\frac{\partial\psi_0}{\partial r}\right)+\frac{1}{r^2}\frac{\partial\psi_0}{\partial z}\frac{\partial^3\psi_0}{\partial z^2\partial r}+\frac{1}{r^2}\frac{\partial\psi_0}{\partial z}\frac{\partial^3\psi_0}{\partial r^3}-\frac{2}{r^3}\frac{\partial\psi_0}{\partial z}\frac{\partial^2\psi_0}{\partial z^2}-\frac{3}{r^3}\frac{\partial\psi_0}{\partial z}\frac{\partial^2\psi_0}{\partial r^2}+$$

$$+\frac{3}{r^4}\frac{\partial\psi_0}{\partial z}\frac{\partial\psi_0}{\partial r}-\frac{1}{r^2}\frac{\partial\psi_0}{\partial r}\frac{\partial^3\psi_0}{\partial z^3}-\frac{1}{r^2}\frac{\partial\psi_0}{\partial r}\frac{\partial^3\psi_0}{\partial r^2\partial z}+\frac{1}{r^3}\frac{\partial\psi_0}{\partial r}\frac{\partial^2\psi_0}{\partial r\partial z}-$$

$$-\frac{1}{r^2}\frac{\partial\psi_n}{\partial z}\frac{\partial^3\psi_n}{\partial z^2\partial r}-\frac{1}{r^2}\frac{\partial\psi_n}{\partial z}\frac{\partial^3\psi_n}{\partial r^3}+\frac{2}{r^3}\frac{\partial\psi_n}{\partial z}\frac{\partial^2\psi_n}{\partial z^2}+\frac{3}{r^3}\frac{\partial\psi_n}{\partial z}\frac{\partial^2\psi_n}{\partial r^2}-$$

$$-\frac{3}{r^4}\frac{\partial\psi_n}{\partial z}\frac{\partial\psi_n}{\partial r}+\frac{1}{r^2}\frac{\partial\psi_n}{\partial r}\frac{\partial^3\psi_n}{\partial z^3}+\frac{1}{r^2}\frac{\partial\psi_n}{\partial r}\frac{\partial^3\psi_n}{\partial r^2\partial z}-\frac{1}{r^3}\frac{\partial\psi_n}{\partial r}\frac{\partial^2\psi_n}{\partial r\partial z}. \qquad (5.24)$$

Thus, the nonlinear equations concerning the stream function are reduced to a sequence of linear differential equations of the 4th order.

5.2.2. Problem statement for the static pressure field

The problem of the static pressure determination in the fluid flow flowing through the axisymmetric channel is considered. After finding the solution of the equation for the steam function, the static pressure function can be determined from Poisson's equation [11, 13], the right part of which is expressed in terms of the derivatives of the stream function

$$\frac{\partial^2 p}{\partial z^2}+\frac{\partial^2 p}{\partial r^2}+\frac{1}{r}\frac{\partial p}{\partial r}=\frac{2}{r^2}\left[\frac{\partial^2\psi}{\partial z^2}\left(\frac{\partial^2\psi}{\partial r^2}-\frac{1}{r}\frac{\partial\psi}{\partial r}\right)-\frac{1}{r^2}\left(\frac{\partial\psi}{\partial z}\right)^2+\frac{\partial^2\psi}{\partial z\partial r}\left(\frac{1}{r}\frac{\partial\psi}{\partial z}-\frac{\partial^2\psi}{\partial z\partial r}\right)\right]. \qquad (5.25)$$

The boundary conditions for this equation are considered. From the Navier — Stokes equations (5.19), (5.20)

$$\frac{\partial}{\partial r} = -v_r \frac{\partial v_r}{\partial r} - v_z \frac{\partial v_r}{\partial z} + \frac{1}{\mathrm{Re}}\left(\frac{1}{r}\frac{\partial}{\partial r}\left(r\frac{\partial v_r}{\partial r}\right) + \frac{\partial\, v_r}{\partial z^2} - \frac{v_r}{r^2}\right),$$

$$\frac{\partial p}{\partial z} = -v_r \frac{\partial v_z}{\partial r} - v_z \frac{\partial v_z}{\partial z} + \frac{1}{\mathrm{Re}}\left(\frac{1}{r}\frac{\partial}{\partial r}\left(r\frac{\partial v_z}{\partial r}\right) + \frac{\partial^2 v_z}{\partial z^2}\right).$$

From $\frac{\partial p}{\partial n} = \left(\nabla p, \vec{n}\right)$, then on Γ_{sw}, taking into account the adhesion condition ($v_r = 0$, $v_z = 0$), we have

$$\frac{\partial P}{\partial n} = \left(\left(\frac{1}{\mathrm{Re}}\Delta v_r, \frac{1}{\mathrm{Re}}\Delta v_z\right), \vec{n}\right) = \frac{1}{\mathrm{Re}}\Delta((v_r, v_z), \vec{n}) = \frac{1}{\mathrm{Re}}\Delta v_n,$$

where v_n — projection of the velocity vector on the normal vector $\vec{n}$ to Γ_{sw}.

Suppose that Γ_{sw} (solid wall) is described by the equation $sw(r,z) = 0$, where $sw(r,z)$ — function normalized up to the first order, i.e. $\left.\frac{\partial sw(r,z)}{\partial n}\right|_{\Gamma_{sw}} = 1$, where $\vec{n}$ — normal vector to Γ_{sw}. Then

$$v_n = \left(\vec{v}, \vec{n}\right) = \frac{1}{r}\frac{\partial \psi}{\partial r}\frac{\partial s}{\partial z} - \frac{1}{r}\frac{\partial \psi}{\partial z}\frac{\partial s}{\partial r}.$$

So,

$$\frac{\partial p}{\partial n} = \frac{1}{\mathrm{Re}}\Delta\left(\frac{1}{r}\frac{\partial \psi}{\partial r}\frac{\partial s}{\partial z} - \frac{1}{r}\frac{\partial \psi}{\partial z}\frac{\partial s}{\partial r}\right).$$

In some approximation, it is possible to assume that the normal component of the velocity to the solid wall in some parts of the border layer is missing.

Then

$$\frac{\partial p}{\partial n} = \frac{1}{\mathrm{Re}}\Delta v_n = 0.$$

Suppose that Γ_{sym} — the region of the border of the area that lies on the axis of symmetry Oz. Given the condition of impermeability on the axis of symmetry ($v_r = 0$), we have

$$\frac{\partial p}{\partial n} = -\frac{\partial p}{\partial r} = -\frac{1}{\mathrm{Re}}\left(\frac{1}{r}\frac{\partial}{\partial r}\left(r\frac{\partial v_r}{\partial r}\right) + \frac{\partial^2 v_r}{\partial z^2}\right) = -\frac{1}{\mathrm{Re}}\left(\frac{\partial^2 v_r}{\partial r^2} + \frac{\partial^2 v_r}{\partial z^2} + \frac{1}{r}\frac{\partial v_r}{\partial r}\right) \text{ on } \Gamma_{sym}.$$

Function $\frac{\partial p}{\partial r}$ on the axis of symmetry ($r = 0$) is considered. Suppose that $\left.\frac{\partial p}{\partial r}\right|_{r=0} = f(z)$.

A new function $\tilde{p}(r,z)$ is built as follows: $\tilde{p}(r,z)=\begin{cases} p(r,z) & r\geq 0, \\ p(-r,z) & r<0 \end{cases}$. The function $\tilde{p}(r,z)$ is a projection of the static pressure function on a plane passing through the center of symmetry. Consider

$$\frac{\partial\tilde{p}(r,z)}{\partial r}=\begin{cases} \dfrac{\partial p(r,z)}{\partial r}, & r\geq 0, \\ -\dfrac{\partial p(-r,z)}{\partial r}, & r<0. \end{cases}$$

Then on the axis of symmetry, we have

$$\left.\frac{\partial\tilde{p}}{\partial r}\right|_{r\to+0}=f(z) \text{ and } \left.\frac{\partial\tilde{p}}{\partial r}\right|_{r\to-0}=-f(z).$$

Due to the smoothness of the static pressure field $f(z)=0$. Therefore $\frac{\partial p}{\partial r}=0$. So, on the axis of symmetry

$$\frac{\partial p}{\partial n}=0. \tag{5.26}$$

The boundary conditions at the entrance and exit to the channel are written down. The region of the border that corresponds to the entrance is denoted as Γ_{si}; the region of the border that corresponds to the exit is denoted as Γ_{so}.

Suppose that Γ_{si} is described by the equation

$$z=c_1,$$

where c_1 — some constant.

The normal derivative of the function p is considered on the region of the border Γ_{si}

$$\frac{\partial p}{\partial n}=-\frac{\partial p}{\partial z}=-\left(-\nu_r\frac{\partial v_z}{\partial r}-\nu_z\frac{\partial v_z}{\partial z}+\frac{1}{\mathrm{Re}}\left(\frac{\partial^2 v_z}{\partial r^2}+\frac{\partial^2 v_z}{\partial z^2}+\frac{1}{r}\frac{\partial v_z}{\partial r}\right)\right)=$$

$$=-\frac{\partial p}{\partial z}=-\left(\frac{1}{r}\frac{\partial\psi}{\partial z}\frac{\partial}{\partial r}\left(\frac{1}{r}\frac{\partial\psi}{\partial r}\right)-\frac{1}{r}\frac{\partial\psi}{\partial r}\frac{\partial}{\partial z}\left(\frac{1}{r}\frac{\partial\psi}{\partial r}\right)+\right.$$

$$\left.+\frac{1}{\mathrm{Re}}\left(\frac{\partial^2}{\partial r^2}\left(\frac{1}{r}\frac{\partial\psi}{\partial r}\right)+\frac{\partial^2}{\partial z^2}\left(\frac{1}{r}\frac{\partial\psi}{\partial r}\right)+\frac{1}{r}\frac{\partial}{\partial r}\left(\frac{1}{r}\frac{\partial\psi}{\partial r}\right)\right)\right).$$

For the case of the parabolic Poiseuille velocity profile, the function ψ is a polynomial of 4th degree for r, so $\frac{\partial p}{\partial n}=m$, where m — some constant, which is determined from the boundary condition.

Suppose that Γ_{so} is described by the equation z = *c2*, where c_2 — some constant. For the case of the parabolic Poiseuille velocity profile $\frac{\partial p}{\partial n} = -m$, where Γ_{so}.

A tangent derivative for the function p is considered on the region of the boundary Γ_{so}.

$$\frac{\partial p}{\partial \tau} = \frac{\partial p}{\partial r} = \left(-v_r \frac{\partial v_r}{\partial r} - v_z \frac{\partial v_r}{\partial z} + \frac{1}{\mathrm{Re}} \left(\frac{\partial^2 v_r}{\partial r^2} + \frac{\partial^2 v_r}{\partial z^2} + \frac{1}{r} \frac{\partial v_r}{\partial r} - \frac{v_r}{r^2} \right) \right) =$$

$$= \left(-\frac{1}{r} \frac{\partial \psi}{\partial z} \frac{\partial}{\partial r} \left(\frac{1}{r} \frac{\partial \psi}{\partial z} \right) + \frac{1}{r} \frac{\partial \psi}{\partial r} \frac{\partial}{\partial z} \left(\frac{1}{r} \frac{\partial \psi}{\partial z} \right) + \right.$$

$$\left. + \frac{1}{\mathrm{Re}} \left(-\frac{\partial^2}{\partial r^2} \left(\frac{1}{r} \frac{\partial \psi}{\partial z} \right) - \frac{\partial^2}{\partial z^2} \left(\frac{1}{r} \frac{\partial \psi}{\partial z} \right) - \frac{1}{r} \frac{\partial}{\partial r} \left(\frac{1}{r} \frac{\partial \psi}{\partial z} \right) + \frac{1}{r^3} \frac{\partial \psi}{\partial z} \right) \right).$$

For the case of the parabolic Poiseuille velocity profile, we have

$$\frac{\partial p}{\partial \tau} = 0 \Rightarrow p = const.$$

5.2.3. Mathematical modeling of hydrodynamic processes in the model channel of the hydro vortex nozzle

The nozzle is a technical device designed for spraying liquids, various types of emulsions, and suspensions. The quality of spraying is characterized by the drops dispersion, the opening angle of the drip torch, and its filling uniformity. For many technical devices, these parameters are critical. In ramjet-type nozzles, improved dispersion is usually achieved by reducing the exit holes and increasing the entrance pressures. Such requirements cannot always be met, in particular, when spraying liquids of high viscosity, and fuel suspensions with the presence of a solid phase. Moreover, modern chemical and energy technologies require nozzles not only to spray well but also to mix several liquids with their hydromechanical treatment. Next, we will consider the problem of using the structural R-function method to create just such an efficient nozzle with the possibility of hydro cavitation treatment of sprayed liquids.

Problem statement. It is needed to solve the interconnected boundary value problem. To do this, the boundary value problem for equation (5.4) is solved first, and then — the boundary value problem for equation (5.5) for function p in the area Ω, which is shown for the model channel of the hydro vortex nozzle in Fig. 5.40. Function $\omega(r,z)$, which describes the area Ω, is shown in Fig. 5.41.

The following boundary conditions are set for the area Ω: on Γ_1 — $\psi = 0, \frac{\partial \psi}{\partial n} = 0$; on Γ_2 — $\psi = \frac{a_1^2}{4}$, $\frac{\partial \psi}{\partial n} = 0$; on Γ_3 — $\psi = \frac{r^2}{2} - \frac{r^4}{4a_1^2}$ (parabolic (Poiseuille velocity profile), $\frac{\partial \psi}{\partial n} = 0$.

The solution of the boundary value problem for equation (5.4) with the corresponding boundary conditions is sought in the form $\psi = \psi_1 + \psi_0$, where ψ_1 — function with zero Dirichlet and Neumann boundary conditions, ψ_0 — a function that meets all the inhomogeneous boundary conditions of the problem. The solution structure for the function ψ_1 has the form $\psi_1 = \omega_1^2 P_1$, where P_1 — undefined structure component, ω_1 a — function that describes the border section of an area ($\Gamma_1 \cup \Gamma_2 \cup \Gamma_3$).

The undefined solution structure component is set in the form $P_1(x, y) = \sum_{i=1}^{k} c_i \varphi_i(r, z)$, where $\{\varphi_i(r,z)\}$ — B-splines of the fifth order, $\{c_i\}, i = 1,...,k$ — constants need to be defined.

For the problem under consideration, a function ω_1 is constructed as

$$\omega_1 = \left(f_1 \wedge_0 f_2 \right) \vee_0 \left(f_3 \wedge_0 f_4 \right) \vee_0 \left(f_5 \right),$$

where $f_1 = z(b_1 + b_2 - z)/(b_1 + b_2)$ $f_2 = r(a_1 - r)/a_1$, $f_3 = (z - b_1)$, $f_4 = r(a_2 - r)/a_2$, $f_5 = \left(r_0^2 - \left(z - b_1 \right)^2 - \left(r - c \right)^2 \right)/(2r_0)$, a_1 — radius of an entrance to the nozzle, — radius of an exit from the nozzle, $b_1 + b_2$ — nozzle length, b_1 — the distance between the center of the torus and the entrance along the axis *Oz*, *c* — the distance between the center of the torus and the axis of symmetry along the axis *Or*, r_0 — radius of the circle.

Function ψ_0: $\psi_0\big|_{\Gamma_i} = \Psi_i$, $\frac{\partial \psi_0}{\partial n}\Big|_{\Gamma_i} = 0$, $i = 1,2,3$ is built using the gluing formula

$$\psi_0 = \sum_{i=1}^{3} \frac{\Psi_i}{w_i^2} \Bigg/ \sum_{i=1}^{3} \frac{1}{w_i^2},$$

where

$$\Psi_1 = 0,\ \Psi_2 = \frac{a_1^2}{4},\ \Psi_3 = \frac{r^2}{2} - \frac{r^4}{4a_1^2},\ w_1 = r,\ w_3 = z,$$

$$w_2 = \left(\left(z - b_1 \right) \overset{\alpha}{\wedge}_0 \left(a_2 - r \right) \overset{\alpha}{\vee}_0 \left(a_1 - r \right) \overset{\alpha}{\vee}_0 \left(r_0^2 - \left(z - b_1 \right)^2 - \left(r - c \right)^2 \right) \right).$$

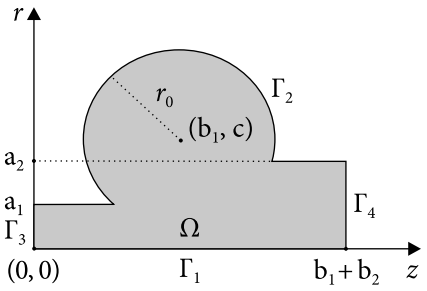

Fig. 5.40. Area Ω

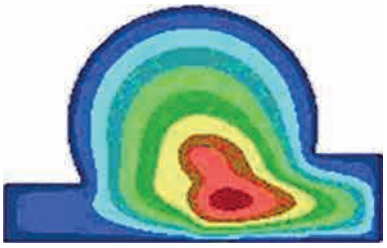

Fig. 5.41. Graph of function ω(r, *z*)

Fig. 5.42. Graph of the velocity modulus function (Re = 200)

Fig. 5.43. Graph of the static pressure function (Re = 200)

The problem is solved by the least squares method.

Next, equation (5.5) is solved for the function *p* in the area Ω. The boundary conditions for this boundary value problem are considered.

On (Γ_2) and on the axis of symmetry (Γ_1), the boundary condition $\frac{\partial p}{\partial n} = 0$ is used. At the entrance to the channel (Γ_4), the boundary condition $\frac{\partial p}{\partial n} = const$ is used.

At the exit from the channel (Γ_5), the boundary condition $P = const$ is used.

The structure of the solution for equation (5.5) with the corresponding boundary conditions has the form

$$p = P_{2,k}\omega_2 - \omega\left(\frac{\partial\omega_1}{\partial x}\frac{\partial(P_{2,k}\omega_2)}{\partial x} + \frac{\partial\omega_1}{\partial y}\frac{\partial(P_{2,k}\omega_2)}{\partial y}\right) - \omega\varphi + \omega_1^{\,2}\omega_2 P_{3,k} + C\,,$$

Fig. 5.44. Hydro cavitation nozzles

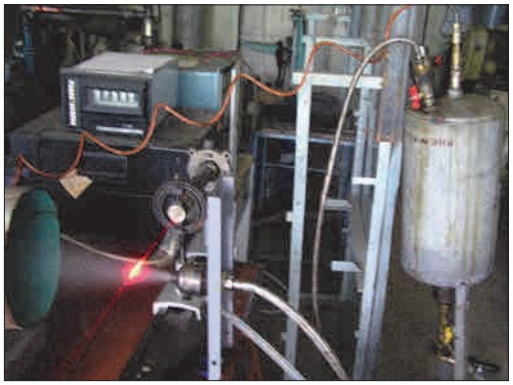

Fig. 5.45. Laboratory studies of the quality of nozzle spraying using a laser

Fig. 5.46. Semi-industrial tests of the nozzle when burning composite fuel in a boiler with a capacity of 1 ton of steam per hour

where ω, ω_1, ω_2 — normalized functions that describe the entire border of the area ω, the border of the area without taking into account the region $\Gamma_4 - \omega_1$ and a region of the border $\Gamma_4 - \omega_2$; function φ: $\varphi\big|_{\Gamma_i} = \left.\dfrac{\partial P}{\partial n}\right|_{\Gamma_i}$, $i = 1,2,3$; $P_{1,k}(x,y)$, $P_{2,k}(x,y)$ — undefined structure components; C the value of static pressure at the exit.

For the problem under consideration, functions ω, ω_1, ω_2 are constructed as follows:

$$\omega_1 = \left(f_1 \wedge_0 f_2\right) \vee_0 \left(f_3 \wedge_0 f_4\right) \vee_0 \left(f_5\right), \quad \omega = \left(f_1 \wedge_0 f_2\right) \vee_0 \left(f_7 \wedge_0 f_4\right) \vee_0 \left(f_5\right),$$

$$\omega_2 = (b_1 + b_2 - z),$$

where $f_7 = (z - b_1)(b_1 + b_2 - z)/b_2$.

Undefined components are given in the form $P_{l,k}(r,z) = \sum_{i=1}^{k} c_{l,i}\varphi_i(r,z)$, where $l = 1,2$, $\{\varphi_i(r,z)\}$ — B-splines of the fifth order, $\{c_{l,i}\}$ — undefined constants.

Function φ: $\varphi\big|_{\Gamma_i} = \left.\frac{\partial P}{\partial n}\right|_{\Gamma_i}$, i = 1,2,3 is constructed using the gluing formula

$$\varphi = \sum_{i=1}^{3} \frac{\varphi_i}{w_i} \Big/ \sum_{i=1}^{3} \frac{1}{w_i},$$

where φ_1=0, φ_2 = 0, $\varphi_3 = \frac{4}{\mathrm{Re}\, a_1^{\,2}}$.

Next, the least squares method is used.

Fig. 5.42, and 5.43 show graphs of functions in the form of lines of constant level on the plane *rOz*, which are constructed according to the results of computational experiments. The results of computational experiments were performed on a grid of 40 × 40 splines of the 5th order, the number of iterations — 9. The calculations were performed in the system POLE [65—69].

Mathematical modeling of liquid flow in channels of complex shape, according to the algorithm described above, allows to improve existing designs of nozzles for different purposes and create new ones. Analysis of the results of numerical simulation of velocity and pressure fields at different Reynolds numbers allows the selection of the optimal geometry of the nozzles channels, which achieves the expected performance [30—33].

Fig. 5.44 shows the current samples of nozzles for the combustion of different types of composite fuel created according to the developed methodology. All these nozzles carry out simultaneous mixing, hydro cavitation processing, and high-quality spraying of composite fuels.

Experimental laboratory (Fig. 5.45) and semi-industrial (Fig. 5.46) studies have proved the high quality of the nozzles.

Studies have shown that the use of nozzles can not only solve the problem of disposal of liquid and moisture-containing waste, in particular, sludge from municipal treatment plants, concentrated residues of waste hydraulic fracturing oil and gas wells, phenolic effluents, but also save up to 10% of hydrocarbons during the production of heat and electricity [29, 34, 71].

REFERENCES

1. Ahlberg J.H., Nilson E.N., Walsh J.L. The Theory of Splines and Their Applications Mathematics in science and engineering: a series of monographs and textbooks. Vol. 38. 319 p.
2. Aminov Yu.A. Differencialnaya geometriya i topologiya krivyh. Moscow: Nauka, 1987. 160 p. [in Russian].
3. Ahiezer N.I. Lekcii po teorii approksimacii. Moscow: Nauka, 1965. 408 p. [in Russian].
4. Baranov I.A. Bazis kraevyh zadach s granichnymi usloviyami shirokogo klassa dlya ispolzovaniya variacionnyh metodov. *Visnyk KhNU. Seriia* «Matematychne modeliuvannia. Informatsiini tekhnolohii. Avtomatyzovani systemy upravlinnia». Kharkiv: KhNU, 2011. No. 977: 25—34 [in Russian].
5. Baranov I.A. Metod postroeniya bazisa kraevyh zadach differencialnyh uravnenij dlya primeneniya variacionnyh metodov. *Kompyuternaya matematika*. Kyiv: In-t kibernetiki im. V.M. Glushkova NAN Ukrainy, 2011. No. 1: 122—129 [in Russian].
6. Baranov I.A. Metod postroeniya bazisa kraevoj zadachi Dirihle dlya ispolzovaniya variacionnyh metodov. *Visnyk Kharkivskoho natsionalnoho universytetu im. V.N. Karazina. Seriia «Matematychne modeliuvannia. Informatsiini tekhnolohii. Avtomatyzovani systemy upravlinnia»*. Kharkiv: KhNU, 2016. Vyp. 31: 9—18 [in Russian].
7. Baranov I.A. Postroenie bazisa smeshannoj kraevoj zadachi dlya primeneniya variacionnyh metodov. *Visnyk Kharkivskoho natsionalnoho universytetu im. V.N. Karazina. Seriia «Matematychne modeliuvannia. Informatsiini tekhnolohii. Avtomatyzovani systemy upravlinnia»*. Kharkiv: KhNU, 2010: 5—12 [in Russian].
8. Baranov I.A. Novye R-operacii razlichnogo klassa gladkosti dlya postroeniya bazisov kraevyh zadach. *Vestnik Zaporozhskogo nacionalnogo universiteta, seriya fiziko-matematicheskie nauki.* Zaporizhzhia: ZNU, 2011. No. 2: 13—28 [in Russian].
9. Baranov I.A. Postroenie bazisa smeshannoj kraevoj zadachi dlya primeneniya variacionnyh metodov. Tez. dokl. konf.

molodyh uchenyh i specialistov. *Sovre-mennye problemy mashinostroeniya.* Kharkiv: IPMash NAN Ukrainy, 2010. P. 25 [in Russian].
10. Baranov I.A. Postroenie gladkih bazisov kraevoj zadachi Dirihle dlya oblastej s negladkoj granicej. *Vestnik Zaporozhskogo nacionalno*go *universiteta, seriya fiziko-matematicheskie nauki.* Zaporizhzhia: ZNU, 2012. No. 1: 19—38 [in Russian].
11. Baranov I.A. Primenenie metoda R-funkcij dlya rascheta polej skorosti i davleniya v potoke vyazkoj neszhimaemoj zhidkosti. Tez. dokl. konf. molodyh uchenyh i specialistov. *Sovremennye problemy mashinostroeniya*. Kharkiv: IPMash NAN Ukrainy, 2008. P. 20 [in Russian].
12. Baranov I.A., Kravchenko O.V., Suvorova I.G. Metod R-funkcij dlya rascheta vzaimosvyazannyh polej v gidropotokah. *Visnyk Kharkivskoho natsionalnoho universytetu. Seriia «Matematychne modeliuvannia. Informatsiini tekhnolohii. Avtomatyzovani systemy upravlinnia»*. Kharkiv: KhNU, 2007. No. 780: 9—18 [in Russian].
13. Baranov I.A., Kravchenko O.V., Suvorova I.G. Raschet gidrodinamicheskih harakteristik potoka vyazkoj neszhimaemoj zhidkosti metodom R-funkcij. *Visnyk Kharkivskoho natsionalnoho universytetu. Seriia «Matematychne modeliuvannia. Informatsiini tekhnolohii. Avtomatyzovani systemy upravlinnia».* Kharkiv: KhNU, 2008. No. 809: 9—19 [in Russian].
14. Bahvalov N.S., Zhidkov N.P., Kobelkov G.M. Chislennye metody. Moscow: Binom, 2003. 632 p. [in Russian].
15. Eremenko Yu.S. Metody konechnyh elementov v mekhanike deformiruemyh tel. Kharkiv: Osnova, 1991. 272 p. [in Russian].
16. Harrik I. Yu. O priblizhenii funkcij, obrashchayushchihsya na granice oblasti v nul, funkciyami osobogo vida. *Mat. Sb.* 1955. Vol. 37(79). No. 2: 353—384 [in Russian].
17. Harrik I. Yu. O priblizhenii funkcij, obrashchayushchihsya vmeste s gradientom v nul na granice oblasti, funkciyami osobogo vida. *Mat. Sb.* 1959. Vol. 47(89). No. 2: 177—208 [in Russian].
18. Harrik I. Yu. O priblizhenii funkcij, obrashchayushchihsya na granice oblasti v nul vmeste s chastnymi proizvodnymi, funkciyami osobogo vida. *Sib. mat. zhurn.* 1963. Vol. IV. No. 2: 408—425 [in Russian].
19. Kantorovich L.V., Krylov V.I. Priblizhennye metody vysshego analiza. Moscow — Leningrad: Fizmatgiz, 1962. 708 p. [in Russian].
20. Kolmogorov A.N., Fomin S.V. Elementy teorii funkcij i funkcionalnogo analiza. Moscow: Nauka, 1989. 624 p. [in Russian].
21. Kolodyazhnyj V.M., Rvachev V.A. O priblizhenii v ravnomernoj metrike funkcij, udov-letvoryayushchih granichnomu usloviyu, funkciyami specialnogo vida. *DAN SSSR.* Vol. 222. No. 6. 1975: 1276—1278 [in Russian].
22. Kolodyazhnyj V.M., Rvachev V.A. K postroeniyu struktur reshenij kraevyh zadach. *Differencialnye uravneniya*. Vol. 13. No. 4. 1977: 646—653 [in Russian].
23. Kolodyazhnyj V.M., Rvachev V.A. O priblizhenii funkcij, udovletvoryayushchih granichnym usloviyam. *Teoreticheskie i prikladnye voprosy algebry i differencialnyh uravnenij.* Kyiv: In-t matematiki AN USSR, 1976: 49—53 [in Russian].

24. Kolodyazhnyj V.M. Strukturno-variacionnyj metod resheniya kraevyh zadach matematicheskoj fiziki. Kharkiv: KhAI, 1981. 92 p. [in Russian].
25. Kolodiazhnyi V.M., Rvachev V.A. Do pytannia pro vyznachennia approksymatsiinykh vlastyvostei strukturnykh rozviazkiv kraiovykh zadach. *Dopovidi NAN Ukrainy.* No. 11. 2003: 22—26 [in Ukrainian].
26. Kolodyazhnyj V.M., Lisina O.Yu. Bessetochnye metody v zadachah modelirovaniya fizicheskih processov. *Problemy mashinostroeniya*. 2010. Vol. 13. No. 3: 67—74 [in Russian].
27. Kolodyazhnyj V.M., Lisina O.Yu. Chislennye skhemy resheniya kraevyh zadach na osnove bessetochnyh metodov s ispolzovaniem RBF i ARBF. *Problemy mashinostroeniya*. 2010. Vol. 13. No. 4: 49—56 [in Russian].
28. Kornejchuk N.P. Splajny v teorii priblizheniya. Moscow: Nauka, 1984. 352 p. [in Russian].
29. Kravchenko Oleg, Homan Vitalii, Suvorova Iryna, Baranov Ihor. Refining the hydrocavitation technology for recycling hydraulic fracturing flowback water by using numerical simulation and physical modelling methods. *Procedia Environmental Science, Engineering and Management*. 2021. Vol. 8. No. 1: 283—292.
30. Kravchenko O.V., Suvorova I.G., Smirnov Ya.V., Holobcev S.S. Matematicheskoe i kompyuternoe modelirovanie kavitacionnyh potokov v slozhnopolostnyh kanalah. *Problemy mashinostroeniya*. 2007. Vol. 10. No. 3: 22—26 [in Russian].
31. Kravchenko O.V., Suvorova I.G., Baranov I.A., Veligotskiy D.A. Vliyanie vodoroda na techenie i teploobmen v sisteme «treschina gornoy porodyi — flyuid». *Intehrovani tekhnolohii ta enerhozberezhennia*. Kharkiv: NTU «KhPI». 2018. No. 3: 35—46 [in Russian].
32. Kravchenko O.V., Suvorova I.G., Baranov I.A. Povyshenie kachestva raspyla tekhnologicheskih zhidkostej v energeticheskih ustanovkah. *Vostochno-evropejskij zhurnal peredovyh tekhnologij*. 2009. No. 4/6(40): 34—38 [in Russian].
33. Kravchenko O.V., Suvorova I.G., Baranov I.A. Sovershenstvovanie processov i apparatov gidrokavitacionnoj aktivacii na osnove matematicheskogo i kompyuternogo modelirovaniya. *Zbirnyk naukovykh prats. Modeliuvannia ta informatsiini tekhnolohii*. Kyiv: In-t problem modeliuvannia v enerhetytsi im. H.Ie. Pukhova NAN Ukrainy, 2010. Vol. 3: 186—194 [in Russian].
34. Kravchenko O., Suvorova I., Baranov I., Goman V. Hydrocavitational activation in the technologies of production and combustion of composite fuels. *Eastern-European J. of Enterprise Technologies*. 2017. No. 4/5(88): 33—42.
35. Kurosh A.G. Kurs vysshej algebry Moscow: Nauka, 1968. 431 p. [in Russian].
36. Lytvyn O.M., Rvachev V.L. Interlinatsiia ta interfletatsiia funktsii i strukturnyi metod. *Matematychni metody y fiziko-mekhanichni polia*. 2007. Vol. 50. No. 4: 61—82 [in Ukrainian].
37. Lytvyn O.M., Nefiodorova I.V. Deiaki aspekty chyselnoi realizatsii metodu skinchennykh elementiv z optymalnym vyborom parametriv, bazysnykh funktsii ta koordynatnykh vuzliv elementiv. *Dopovidi NAN Ukrainy*. No. 4. 2009: 33—38 [in Ukrainian].
38. Lytvyn O.M., Rvachev V.L. Formula dlia mnohokutnykiv. *Dopovidi AN URSR*. Ser. A. 1971. No. 11: 973—976 [in Ukrainian].

39. Maksimenko-Sheiko K.V., Sheiko T.I. R-funkcii v matematicheskom modelirovanii geometricheskih obektov, obladayushchih simmetriej. *Kibernetika i sistemnyj analiz*. 2008. No. 6: 75—83 [in Russian].
40. Maksimenko-Sheiko K.V., Macevityi A.M., Shejko T.I. Konstruktivnye sredstva metoda R-funkcij dlya postroeniya primitivov v 3D. *Problemy mashinostroeniiya*. 2005. Vol. 8. No. 1: 59—65 [in Russian].
41. Maksimenko-Sheiko K.V. R-funkcii v matematicheskom modelirovanii geometricheskih obektov i fizicheskih polej. Kharkiv: IPMash NAN Ukrainy, 2009. 306 p. [in Russian].
42. Mihlin S.G. Chislennaya realizaciya variacionnyh metodov. Moscow: Nauka, 1966. 432 p. [in Russian].
43. Mihlin S.G. Variacionnye metody v matematicheskoj fizike. Moscow: Nauka, 1970. 512 p. [in Russian].
44. Rogers David F., Adams J. Alan. Mathematical elements for computer graphics. McGraw-Hill Publishing Company, 2001. 604 p.
45. Rvachev V.L., Goncharyuk I.V. Kruchenie sterzhnej slozhnogo profilya. Kharkiv: Kh. Politekhn. In-t, 1973. 104 p. [in Russian].
46. Rvachev V.L. Metody algebry logiki v matematicheskoj fizike. Kyiv: Nauk. dumka, 1974. 259 p. [in Russian].
47. Rvachev V.L., Slesarenko A.P. Algebra logiki i integralnye preobrazovaniya v kraevyh zadachah. Kyiv: Nauk. dumka, 1976. 288 p. [in Russian].
48. Rvachev V.L. Teoriya R-funkcij i nekotorye ee prilozheniya. Kyiv: Nauk. dumka, 1982. 552 p. [in Russian].
49. Rvachev V.A. Finitary solution of functional-differential equations and their application. *Adv. Math. Sci*. 1991. Vol. 45. No. 1(271): 77—103.
50. Rvachev V.L., Sheiko T.I. R-functions in boundary value problems in mechanics. *Applied Mechanics Reviews*. Vol. 48. No. 4. 1995: 151—188.
51. Rvachev V.L., Sheiko T.I., Shapiro V., Uickcr J.J. Implicit function modeling of solidification in metal casting. *Technical report, SAL 1996-4*. October 1996, Spatial automation laboratory, University of Wisconsin, Madison: 1—14.
52. Rvachev V.L., Sheiko T.I., Shapiro V. Interpolation Operators in the Theory of R-functions (Generalized Lagrangian & Hermitian Interpolation of Arbitrary Loci). *Proc. of the Int. conf. on operator theory and its appl. to sci. and industr. probl.* Winnipeg, 1998. P. 50.
53. Rvachev V.L., Sheiko T.I., Shapiro V. The R-function method in boundary-value problems with geometric and physical symmetry. *J. Math. Sci.* 1999. Vol. 97. No. 1: 3888—3899.
54. Rvachev V.L., Sheiko T.I., Shapiro V., Tsukanov I. On Completeness of RFM Solution Structures. *Computational Mech.* 25. 2000: 305—316.
55. Rvachev V.L., Sheiko T.I., Shapiro V., Tsukanov I. Transfinite Interpolation over Implicitly Defined Sets. *Computer Aided Geometric Design*. 2001. No. 18: 195—220.

56. Sheiko T.I. Ob uchete osobennostej v uglovyh tochkah i tochkah styka granichnyh uslovij v metode R-funkci. *Prikl. mekhanika.* 1982. No. 4: 95—102 [in Russian].
57. Slesarenko A.P., Temnikov A.V. Sovremennye priblizhennye analiticheskie metody resheniya zadach teploobmena. Samara: Samarskij politekhnicheskij institut, 1991. 91 p. [in Russian].
58. Slesarenko A.P. S-funkcii v obratnyh zadachah analiticheskoj geometrii i modelirovanii teplovyh processov. *Vostochno-Evropejskij zhurnal peredovyh tekhnologij.* 2011. No. 3/4(51): 41—46 [in Russian].
59. Slesarenko A.P. S-funkcii v obratnyh zadachah differencialnoj geometrii i upravlenii obrazovaniya form. *Vostochno-Evropejskij zhurnal peredovyh tekhnologij.* 2012. No. 1/4(55): 4—10 [in Russian].
60. Slesarenko A.P. S-funkcii v postroenii konservativnyh struktur resheniya geometricheskih obratnyh kraevyh zadach. *Vostochno-Evropejskij zhurnal peredovyh tekhnologij.* 2012. No. 2/4(56): 60—66 [in Russian].
61. Slesarenko A.P., Suvorova I.G., Kravchenko O.V., Baranov I.A. Nekotorye sistemy dostatochno polnyh funkcij, obladayushchih logicheskimi svojstvami. *Sbornik trudov konferencii Modelirovanie-2012.* Kyiv: In-t problem modelirovaniya v energetike im. G.E. Puhova NAN Ukrainy, 2012: 84—87 [in Russian].
62. Slesarenko A.P., Safonov N.A. Identifikaciya nelinejnoj nestacionarnoj zavisimosti moshchnosti istochnika energii ot temperatury na baze variacionno-strukturnogo i proekcionnyh metodov. *Problemy mashinostroeniya*. 2010. Vol. 13. No. 6: 58—63 [in Russian].
63. Suvorova I.G. Metod R-funkcij v issledovaniyah i raschetah fiziko-mekhanicheskih polej dlya zadach stroitelstva: avtoref. … dis. PhD (Tech.). Kharkiv, 1991. 21 p. [in Russian].
64. Suvorova I.G., Kravchenko O.V. Matematicheskoe modelirovanie potoka zhidkosti metodom R-funkcij. *Systemni tekhnolohii.* Dnipropetrovsk: DNVP «Systemni tekhnolohii», 2006. Vyp. 4 (45): 57—69 [in Russian].
65. Suvorova I.G., Shevchenko A.N. Avtomatizaciya raschetov metodom R-funkcij primenitelno k zadacham strojindustrii. Kyiv: Ucheb.-metod. kab. vyssh. obrazovaniya, 1991. 60 p. [in Russian].
66. Suvorova I.G. Kompyuternoe modelirovanie osesimmetrichnyh techenij zhidkosti v kanalah slozhnoj formy. *Vestnik NTU KhPI.* Kharkiv: NTU, 2004. No. 31: 141—148 [in Russian].
67. Suvorova I.G., Kravchenko O.V., Baranov I.A. Matematicheskoe i kompyuternoe modelirovanie osesimmetrichnyh techenij vyazkoj neszhimaemoj zhidkosti s ispolzovaniem metoda R-funkcij. *Matematicheskie metody i fiziko-mekhanicheskie polya*. 2011. Vol. 54. No. 2: 139—149 [in Russian].
68. Suvorova I.G., Kravchenko O.V., Baranov I.A. Metod R-funkcij dlya rascheta vzaimosvyazannyh polej v gidropotokah. Tez. dokl. 5-j nauch. shk.-konf. «*Aktualnye voprosy teplofiziki i fizicheskoj gidrogazodinamiki*». Alushta, 2007: 149—152 [in Russian].

69. Suvorova I.G., Kravchenko O.V., Baranov I.A. Primenenie metoda R-funkcij dlya rascheta gidrodinamicheskih harakteristik potoka v kanalah slozhnoj formy. Tez. dokl. 6-j nauch. mezhdunar. shk.-konf. «*Aktualnye voprosy teplofiziki i fizicheskoj gidrogazodinamiki*». Alushta, 2008: 201—206 [in Russian].
70. Suvorova I.G., Kravchenko O.V., Baranov I.A. Mathematical and computer modeling of axisymmetric flows of an incompressible viscous fluid by the method of R-functions. *J. of Mathematical Sciences.* Springer US, 2012. Vol. 184. No. 2: 165—180.
71. Suvorova Irina, Kravchenko Oleg, Veligotskiy Dmitriy, Goman Vitaliy. Theoretical Foundations of Optimising Processes in Energy Conversion Systems to Increase the Effectiveness and Ecological Safety of Their Functioning. *European J. of Sustainable Development*. 2019. Vol. 8. No. 5: 171—179. https://doi: 10.14207/ejsd.2019.v8n5p171
72. Suvorova Iryna, Kravchenko Oleg, Goman Vitalii, Baranov Ihor. Criteria for assessing the energy-ecological effectiveness of using the sludge of waste treatment plants as components of liquid composite fuels. *European J. of Sustainable Development*. 2020. Vol. 9. No. 4: 328—336. https://doi: 10.14207/ejsd.2020.v9n4p328
73. Zavyalov Yu.S., Kvasov B.I., Miroshnichenko V.L. Metody splajn-funkcij. Moscow: Nauka, 1980. 352 p. [in Russian].

AUTHORS

Igor Baranov (male), Ph.D., senior researcher of Nom-Traditional Energy Technologies Department of Pidgorny Institute for Mechanical Engineering Problems of the National Academy of Science of Ukraine, birthday 27.10.1984.
ORCID: 0000-0001-6367-8570

Oleg Kravchenko (male), Corresponding member of the NAS of Ukraine, Doctor of Technical Sciences, Head of Nom-Traditional Energy Technologies Department of Pidgorny Institute for Mechanical Engineering Problems of the National Academy of Science of Ukraine, senior researcher, birthday 04.10.1964.
ORCID: 0000-0003-0048-6744

Iryna Suvorova (female), Doctor of Technical Sciences, Professor, Leading researcher of Nom-Traditional Energy Technologies Department of Pidgorny Institute for Mechanical Engineering Problems of the National Academy of Science of Ukraine, birthday 23.04.1942.
ORCID: 0000-0003-0287-154X

Vitalii Goman (male), Ph.D., senior researcher of Nom-Traditional Energy Technologies Department of Pidgorny Institute for Mechanical Engineering Problems of the National Academy of Science of Ukraine, birthday 24.09.1987.
ORCID: 0000-0002-3422-0146

Dmytro Veligotskyi (male), Ph.D., senior researcher of Nom-Traditional Energy Technologies Department of Pidgorny Institute for Mechanical Engineering Problems of the National Academy of Science of Ukraine, birthday 17.04.1986.
ORCID: 0000-0001-9075-2051

У монографії викладено методи вирішення крайових задач для диференційних рівнянь у часткових похідних, які моделюють поля різної фізичної природи (деформаційні, силові, гідродинамічні, температурні). Представлено розвиток структурних методів для підвищення апроксимаційної здатності базисних функцій в околі кутових точок області вирішення крайових задач і також розробку локальних структур, що враховують крайові умови на межі області та стиковку зі стандартним базисом усередині області. Розвиток структурних методів на основі цих підходів значно розширює можливості моделювання фізико-механічних полів в областях складної форми для створення екологічних і економічних пристроїв у різних галузях виробництва.

Наукове видання

НАЦІОНАЛЬНА АКАДЕМІЯ НАУК УКРАЇНИ
ІНСТИТУТ ПРОБЛЕМ МАШИНОБУДУВАННЯ
ім. А.М. ПІДГОРНОГО НАН УКРАЇНИ

БАРАНОВ Ігор Андрійович, КРАВЧЕНКО Олег Вікторович,
СУВОРОВА Ірина Георгіївна, ГОМАН Віталій Олександрович,
ВЕЛІГОЦЬКИЙ Дмитро Олексійович

КОНСТРУКТИВНІ ЗАСОБИ ДЛЯ МАТЕМАТИЧНОГО ТА КОМП'ЮТЕРНОГО МОДЕЛЮВАННЯ ФІЗИКО-МЕХАНІЧНИХ ПОЛІВ У ОБЛАСТЯХ СКЛАДНОЇ ФОРМИ

Англійською мовою

Редактор-коректор *В.К. Рего*

Художнє оформлення *Є.О. Ільницького*
Технічне редагування *Т.М. Шендерович*
Виготовлення рисунків *О.В. Туровський*
Комп'ютерна верстка *С.В. Кубарєва*

Підп. до друку 09.10.2023. Формат 70 × 100/16. Гарн. Minion Pro.
Ум. друк. арк.12,68. Обл.-вид. арк. 11,63. Тираж 145 прим.
(у т. ч. 100 прим. за державні кошти). Зам. № 7058.

Видавець і виготовлювач Видавничий дім "Академперіодика" НАН України
01024, Київ, вул. Терещенківська, 4

Свідоцтво про внесення до Державного реєстру суб'єктів видавничої справи серії ДК № 544 від 27.07.2001 р.